UNIVERSITY OF ALBERTA

DRUG-DRUG INTERACTIONS OF METOPROLOL AND SOME SELECTED ANTIDEPRESSANTS INVESTIGATED *IN VITRO* AND *EX VIVO*

BY

PENNY D. COLBOURNE ©

A THESIS SUBMITTED TO THE FACULTY OF GRADUATE STUDIES AND RESEARCH IN PARTIAL FULFILLMENT OF THE REQUIREMENTS FOR THE DEGREE OF DOCTOR IN PHILOSOPHY

IN

PHARMACEUTICAL SCIENCES

(NEUROCHEMISTRY)

FACULTY OF PHARMACY AND PHARMACEUTICAL SCIENCES

AND

FACULTY OF MEDICINE AND DENTISTRY

(PSYCHIATRY)

EDMONTON, ALBERTA

FALL, 1999

National Library of Canada
Acquisitions and Bibliographic Services
395 Wellington Street
Ottawa ON K1A 0N4
Canada

Bibliothèque nationale du Canada
Acquisitions et services bibliographiques
395, rue Wellington
Ottawa ON K1A 0N4
Canada

Your file Votre référence

Our file Notre référence

The author has granted a non-exclusive licence allowing the National Library of Canada to reproduce, loan, distribute or sell copies of this thesis in microform, paper or electronic formats.

L'auteur a accordé une licence non exclusive permettant à la Bibliothèque nationale du Canada de reproduire, prêter, distribuer ou vendre des copies de cette thèse sous la forme de microfiche/film, de reproduction sur papier ou sur format électronique.

The author retains ownership of the copyright in this thesis. Neither the thesis nor substantial extracts from it may be printed or otherwise reproduced without the author's permission.

L'auteur conserve la propriété du droit d'auteur qui protège cette thèse. Ni la thèse ni des extraits substantiels de celle-ci ne doivent être imprimés ou autrement reproduits sans son autorisation.

0-612-46819-4

Canada

UNIVERSITY OF ALBERTA

LIBRARY RELEASE FORM

NAME OF AUTHOR: Penny D. Colbourne

TITLE OF THESIS: Drug-Drug Interactions of Metoprolol and Some Selected Antidepressants Investigated *In Vitro* and *Ex Vivo*.

DEGREE: Doctor of Philosophy

YEAR THIS DEGREE GRANTED: 1999

Permission is hereby granted to the University of Alberta Library to reproduce single copies of this thesis and to lend or sell such copies for private, scholarly, or scientific research purposes only.

The author reserves all other publication and other rights in association with the copyright in the thesis, and except as hereinbefore provided, neither the thesis nor any substantial portion thereof may be printed or otherwise reproduced in any material form whatever without the author's prior written permission.

Colbourne

136 Kirkwood Way

Edmonton, Alberta

T6L 6K5

Dated: October 1, 1999

UNIVERSITY OF ALBERTA

FACULTY OF GRADUATE STUDIES AND RESEARCH

The undersigned certify that they have read, and recommend to the Faculty of Graduate Studies and Research for acceptance, a thesis entitled Drug-Drug Interactions of Metoprolol Investigated *In Vitro* and *Ex Vivo* submitted by Penny D. Colbourne in partial fulfillment of the requirements for the degree of Doctor of Philosophy.

G.B. Baker (Supervisor)

R.T. Coutts (Co-Supervisor)

J.-M. Le Mellédo (Committee Member)

K.M. Hegadoren (Committee Member)

F.M. Pasutto (Committee Member)

A.J. Nazarali (External Examiner)

Dated: October 1, 1999

DEDICATION

To my husband Burn, for being there at the end of some very long days.

ABSTRACT

Metoprolol (MET) is a commonly prescribed β-adrenergic receptor antagonist (β-blocker) that undergoes extensive hepatic metabolism involving the cytochrome P450 (CYP) enzymes. Three main routes of metabolism are O-demethylation with subsequent oxidation to an acid metabolite, α-hydroxylation, and N-dealkylation with further oxidation to an acid metabolite. CYP2D6, and other as yet unidentified enzymes, have been implicated in the metabolism of MET. Due to the involvement of the CYP enzymes in the metabolism of MET, drug-drug interactions with other substrates and inhibitors of CYP enzymes is a concern in clinical situations.

The kinetics of metabolite formation were investigated with respect to the formation of O-desmethylmetoprolol (ODM), α-hydroxymetoprolol (HM) and N-dealkylmetoprolol (NDM) in human liver microsomes. It was determined that both the O-demethylation and the α-hydroxylation pathways were biphasic and that the N-dealkylation pathway involved at least three enzymes.

The potential of the antidepressants fluoxetine (FLU), desipramine (DMI), paroxetine (PAR) and fluvoxamine (FVX) to inhibit the metabolism of MET was investigated *in vitro* using human liver microsomes. The inhibitory potential was studied with respect to both the low and high affinity enzymes responsible for the O-demethylation of MET. The rank order of inhibiton of the high affinity enzyme was PAR>FLU>FVX>DMI. The rank order of inhibition of the low affinity enzyme was PAR>DMI>FVX>FLU.

Using human liver microsomes and microsomes from cells expressing individual CYP enzymes, CYP2D6 and CYP2E1 were implicated in the formation of ODM. These

studies also revealed that CYP2D6 and CYP3A4 were involved in the formation of HM and CYP2D6, CYP3A4 and CYP2C19 in the formation of NDM. Interestingly, CYP2D6 and CYP3A4 were also implicated in the formation of the acid metabolite of ODM.

Studies in rats showed that both DMI and FVX, but not FLU, inhibited the metabolism of MET. These results are interesting in that they demonstrate that, at least with respect to MET, the rat model does not mimic the inhibition situation seen using human liver microsomes.

ACKNOWLEDGEMENTS

To Dr. Baker and Dr. Coutts for giving me the opportunity to study under your direction. It is because of you that the Neurochemical Research Unit is a first-class research facility. I feel privileged to have been a part of it. I am always in awe of your vast knowledge, of which I can only aspire to. I thank my good fortune that fate lead me in your direction. I could not imagine doing this degree anywhere else.

To Dr. Le Mellédo, Dr. Hegadoren, Dr. Pasutto and Dr. Nazarali for giving up your valuable time so that I could accomplish my goals.

To Dr. Greenshaw for helping me make some sense out of statistics and to Dr. Holt for shedding some light on the darkness that was enzyme kinetics. To Rick Strel and Carolyn Kuefler for your technical expertise. I could not have done it without you.

To Gail, Jordyce and Kathryn, my thanks go far beyond your wealth of experience. I think it was your ability to make me laugh, at life and at myself, that I appreciate the most. You make the Unit a great place to work and although I am happy to be moving on, I will miss the everyday camaraderie. The staff of the Neurochemical Research Unit and my fellow students helped make this experience a very positive one. For that I am grateful.

To my friends and colleagues at Dynacare Kasper Medical Laboratories for taking an interest in my endeavors. I look forward to our continued association. To Adeline for granting me the flexibility I so desperately needed, and to Carol for allowing that to continue. Also to Dr. Kinnibugh for overlooking, on more than one occasion, my less than enthusiastic attitude.

To Ann and Yvette, it is through you that I know the value of true friendship.

To me parents, Max and Doreen Ryan, for taking pride in my accomplishments. It is because of you that I understand the value of hard work. To me sisters, Kerry and Lori, for always standing behind me, regardless of my decisions in life. To my family, both immediate and extended, it is through you that I learned the art of laughter.

To Burn for your support, your encouragement and your unwavering faith in my abilities.

TABLE OF CONTENTS

Chapter 1: Introduction ---- *1*

1.1 General Introduction ---- **2**

1.2 Drug Metabolism ---- **2**

1.2.1 Basic Concepts ---- 2

1.2.2 Cytochrome P450 Enzymes ---- 4

1.2.2.1 General Overview ---- 4

1.2.2.2 Catalytic Cycle of the CYP Enzyme System ---- 7

1.2.2.3 The Diversity of the CYP Enzymes ---- 10

1.2.2.4 Nomenclature Associated with CYP Enzymes ---- 10

1.2.2.5 Variations in Drug Metabolism ---- 12

1.2.2.6 Specific Features of Several CYP Enzymes, Including Comments on Species Variation ---- 15

1.2.2.6.1 CYP2B6 ---- 15

1.2.2.6.2 CYP2C19 ---- 18

1.2.2.6.3 CYP2D6 ---- 19

1.2.2.6.4 CYP2E1 ---- 24

1.2.2.6.5 CYP3A4 ---- 26

1.2.3 Alcohol Dehydrogenase and Aldehyde Dehydrogenase ---- 28

1.3 Enzyme Kinetics ---- **31**

1.4 Inhibition of Drug Metabolism ---- **38**

1.4.1 Mechanisms of Inhibition ---- 38

1.4.2 Competitive Inhibition ---- 40

1.4.3 Determining Inhibition Constants ---- 42

1.5 Comparison of *In Vitro* and *In Vivo* Data ---- 45

1.6 Clinical Implications of the Project Described in this Thesis ---- 49

1.6.1 Hypertension ---- 49

1.6.2 Depression ---- 52

1.6.3 Comorbidity ---- 54

1.6.4 Drug-Drug Interactions ---- 58

1.7 Metoprolol ---- 59

1.7.1 Pharmacokinetics of Metoprolol ---- 59

1.7.2 Relevant CYP Enzymes ---- 62

1.8 Putative Inhibitors of the Metabolism of Metoprolol ---- 69

1.9 Analytical Procedures ---- 71

1.9.1 General Principles of Chromatography ---- 71

1.9.2 High Performance Liquid Chromatography ---- 73

1.9.2.1 Theory (Partition Chromatography with UV Detection) ---- 73

1.9.2.2 Method Development ---- 75

1.9.3 Gas Chromatography ---- 78

1.9.3.1 Theory (Capillary Chromatography) ---- 78

1.9.3.2 Detectors ---- 81

1.9.3.2.1 Nitrogen-Phosphorus Detector ---- 81

1.9.3.2.2 Electron-Capture Detector ---- 81

1.9.3.2.3 Mass Spectrometry in the Electron Impact Mode ---- 82

1.9.4 Derivatization ---- 83

1.10 Thesis Objectives ---- 85

1.11 Materials ---- 85

1.11.1 Instrumentation ---- 85

1.11.1.2 High Performance Liquid Chromatograph ---- 85

1.11.1.2 Gas Chromatographs ---- 86

1.11.1.2.1 Nitrogen-Phosphorus Detector ---- 86

1.11.1.2.2 Electron-Capture Detector ---- 86

1.11.1.2.3 Mass Spectrometry Detector ---- 86

1.11.2 Microsomal Products ---- 87

1.11.2.1 Human Liver Microsomes ---- 87

1.11.2.2 Microsomes from cDNA-Expressed Cells ---- 88

1.11.3 Equipment ---- 88

1.11.3.1 Balance ---- 88

1.11.3.2 Centrifuges ---- 91

1.11.3.3 Filter Apparatus for Mobile Phase Preparation ---- 91

1.11.3.4 Glassware Cleaning ---- 91

1.11.3.5 pH Meter ---- 91

1.11.3.6 Tissue Homogenizer ---- 92

1.11.3.7 Vacuum Evaporator ---- 92

1.11.3.8 Vortex Mixer ---- 92

1.11.3.9 Vortex Shaker ---- 92

1.11.3.10 Waterbath ---- 92

1.11.3.11 Waterstill ---- 92

1.11.4 Chemicals and Reagents ---- 93

1.12 Solution Preparation ---- 95

1.12.1 0.1 M Potassium Phosphate Buffer (pH = 7.4) ---- 95

1.12.2 0.1 M Tris Buffer (pH = 7.5) ---- 95

1.12.3 NADPH Generating System ---- 95

1.12.4 1 N Perchloric Acid ---- 95

1.13 References ---- 97

Chapter 2: The Effect of the Antidepressants Desipramine, Fluoxetine and Fluvoxamine on the Metabolism of Metoprolol in Rat Tissue ---- 111

2.1 Introduction ---- 112

2.2 Animal Experiment ---- 114

2.3 Analysis of Metoprolol and O-Desmethylmetoprolol ---- 114

2.3.1 Assay Procedure ---- 114

2.3.2 Calibration Curves ---- 115

2.3.3 Assay Validation ---- 115

2.3.4 Instrumentation ---- 117

2.3.4.1 Gas Chromatography with Electron-Capture Detection ---- 117

2.3.4.2 Gas Chromatography with Mass Spectrometry Detection ---- 118

2.3.5 Statistical Analysis ---- 118

2.4 Results ---- 118

2.4.1 Assay Procedure ---- 118

2.4.2 Calibration Curves ---- 119

2.4.3 Assay Validation ---- 119

2.4.4 Confirmation of Structures of Derivatives ---- 124

2.4.5 Metoprolol Levels ---- 124

2.4.6 O-Desmethylmetoprolol Levels ---- 132

2.5 Discussion ---- 132

2.5.1 Assay Procedure ---- 132
2.5.2 Calibration Curves ---- 134
2.5.3 Assay Validation ---- 134
2.5.4 Confirmation of Structures of Derivatives ---- 135
2.5.5 Metoprolol Levels ---- 135
2.5.6 O-Desmethylmetoprolol Levels ---- 137
2.6 References ---- 138
Chapter 3: The Levels of the Antidepressants Desipramine, Fluoxetine and Fluvoxamine in Rat Tissue and the Effect of Metoprolol ---- 143
3.1 Introduction ---- 144
3.2 Animal Experiment ---- 145
3.3 Analysis of Fluoxetine, Norfluoxetine and Fluvoxamine ---- 146
3.3.1 Assay Procedure ---- 146
3.3.2 Calibration Curves ---- 146
3.3.3 Assay Validation ---- 148
3.3.4 Instrumentation ---- 148
3.4 Analysis of Desipramine ---- 149
3.4.1 Assay Procedure ---- 149
3.4.2 Calibration Curves ---- 150
3.4.3 Assay Validation ---- 150
3.4.4 Instrumentation ---- 152
3.4 Statistical Analysis ---- 153
3.5 Results ---- 153
3.6.1 Fluoxetine, Norfluoxetine and Fluvoxamine Analysis ---- 153

3.6.1.1 Assay Procedure ---- 153
3.6.1.2 Calibration Curves ---- 153
3.6.1.3 Assay Validation ---- 157
3.6.1.4 Fluoxetine and Norfluoxetine Levels ---- 157
3.6.1.5 Fluvoxamine Levels ---- 161
3.6.2 Despramine Analysis ---- 161
3.6.2.1 Assay Procedure ---- 161
3.6.2.2 Calibration Curves ---- 161
3.6.2.3 Assay Validation ---- 166
3.6.2.4 Desipramine Levels ---- 166
3.7 Discussion ---- 166
3.7.1 Fluoxetine, Norfluoxetine and Fluvoxamine Analysis ---- 166
3.7.2 Desipramine Analysis ---- 170
3.7.3 Effect of Metoprolol on the Metabolism of Fluoxetine, Fluvoxamine and Desipramine ---- 171
3.7.3.1 Fluoxetine and Norfloxetine ---- 171
3.7.3.2 Fluvoxamine ---- 171
3.7.3.3 Desipramine ---- 171
3.7.4 Antidepressant Levels and Their Effect on the Metabolism of Metoprolol ---- 172
3.8 References ---- 174
Chapter 4: Effect of the Antidepressants Paroxetine, Fluoxetine, Fluvoxamine and Desipramine on the Metabolism of Metoprolol by Human Liver Microsomes ---- 176
4.1 Introduction ---- 177

4.2 Experimental Procedures ---- 178

4.2.1 Instrumentation ---- 178

4.2.2 Assay Procedure ---- 178

4.2.2.1 Effect of Protein ---- 178

4.2.2.2 Calibration Curves ---- 179

4.2.2.3 Assay Validation ---- 179

4.2.3 Preliminary Studies ---- 180

4.2.3.1 Time Course ---- 180

4.2.3.2 Requirement of NADPH ---- 181

4.2.3.3 Enzyme Concentration ---- 181

4.2.4 Determination of Kinetic Constants (V_{max} and K_m) ---- 181

4.2.5 Inhibition Experiments ---- 182

4.2.6 Statistical Analysis ---- 185

4.2.6.1 K_m and V_{max} Determination ---- 185

4.2.6.2 IC_{50} and K_i Determination ---- 186

4.2.6.3 Power Equation ---- 187

4.3 Results ---- 188

4.3.1 Assay Procedure ---- 188

4.3.1.1 Effect of Protein ---- 188

4.3.1.2 Calibration Curves ---- 188

4.3.1.3 Assay Validation ---- 188

4.3.2 Preliminary Studies ---- 197

4.3.2.1 Time Course ---- 197

4.3.2.2 Requirement of NADPH ---- 197

4.3.2.3 Enzyme Concentration ---- 197

4.3.3 Kinetic Analysis ---- 197

4.3.4 IC_{50} and K_i Determination ---- 204

4.3.5 Power Equation ---- 212

4.4 Discussion ---- 212

4.4.1 Assay Procedure ---- 212

4.4.1.1 Effect of Protein ---- 212

4.4.1.2 Calibration Curves ---- 212

4.4.1.3 Assay Validation ---- 212

4.4.2 Preliminary Studies ---- 216

4.4.3 Kinetic Analysis ---- 217

4.4.4 IC_{50} and K_i Determination ---- 217

4.4.5 Power Equation ---- 219

4.5 References ---- 221

Chapter 5: Elucidation of the Enzymes Responsible for the Metabolism of Metoprolol ---- 223

5.1 Introduction ---- 224

5.2 Experimental Procedures ---- 225

5.2.1 Instrumentation ---- 225

5.2.2 Calibration Curves ---- 225

5.2.3 Preliminary Studies ---- 226

5.2.3.1 Metoprolol ---- 226

5.2.3.2 O-Desmethylmetoprolol ---- 226

5.2.3.2.1 Time Course ---- 226

5.2.3.2.2 Requirement of NADPH ---------- 227

5.2.3.2.3 Substrate Concentration Experiment ---------- 227

5.2.4 Experiments Using Human Liver Microsomes ---------- 228

5.2.5 Experiments Using Microsomes from Cells Expressing Individual CYP Enzymes ---------- 228

5.2.6 Statistical Analysis ---------- 229

5.3 Results ---------- 229

5.3.1 Calibration Curves ---------- 229

5.3.2 Preliminary Studies ---------- 230

5.3.2.1 Time Course ---------- 230

5.3.2.2 Requirement of NADPH ---------- 230

5.3.2.3 Substrate Concentration Experiment ---------- 230

5.3.3 The Metabolism of Metoprolol ---------- 230

5.3.3.1 Experiments Using Human Liver Microsomes ---------- 230

5.3.3.2 Experiments Using Microsomes from Cells Expressing Individual CYP Enzymes ---------- 235

5.3.4 The Metabolism of O-Desmethylmetoprolol ---------- 235

5.3.4.1 Experiments Using Human Liver Microsomes ---------- 235

5.3.4.2 Experiments Using Microsomes from Cells Expressing Individual CYP Enzymes ---------- 235

5.4 Discussion ---------- 235

5.4.1 Assay Conditions ---------- 235

5.4.2 Preliminary Studies ---------- 240

5.4.2.1 Time Course and Substrate Concentration Experiment ---------- 240

5.4.2.2 Requirement of NADPH ---- 240

5.4.3 The Metabolism of Metoprolol ---- 240

5.4.4 The Metabolism of O-Desmethylmetoprolol ---- 242

5.5 References ---- 248

Chapter 6: Conclusion ---- 250

6.1 Summary ---- 251

6.2 Limitations ---- 252

6.3 References ---- 255

LIST OF TABLES

Chapter 1

Table 1-1 The CYP families and their function ---------- 11

Table 1-2 Substrates, inhibitors and inducers of CYP2B6 ---------- 17

Table 1-3 Substrates, inhibitors and inducers of CYP2C19 ---------- 20

Table 1-4 Substrates, inhibitors and inducers of CYP2D6 ---------- 25

Table 1-5 Substrates, inhibitors and inducers of CYP2E1 ---------- 27

Table 1-6 Substrates, inhibitors and inducers of CYP3A4 ---------- 29

Table 1-7 Comparison of the pharmacokinetic parameters of several β-blockers ---------- 53

Table 1-8 Potency of antidepressants at blocking the reuptake of noradrenaline and serotonin ---------- 57

Table 1-9 Comparison of the relative abundance of the main urinary metabolites of the metabolism of MET in man, rat and dog ---------- 63

Table 1-10 Inhibitor constants (K_i values) for the inhibition of sparteine and desipramine metabolism ---------- 70

Table 1-11 Inhibition of CYP enzymes by FLU, NFLU, PAR, FVX and DMI ---------- 72

Table 1-12 Charaterization of Gentest human liver microsomes ---------- 89

Table 1-13 Characterization of CYP enzymes from cDNA-expressed cells --- 90

Chapter 2

Table 2-1 Chromatographic parameters for GC analysis of ODM and MET- 125

Table 2-2 MET and ODM levels (ng/g tissue, n=6) in rat heart, brain and liver ---------- 130

Chapter 3

Table 3-1 Cnhromatographic parameters for the GC analysis of FLU, NFLU and FVX ---------- 158

Table 3-2 FLU and NFLU levels (ng/g tissue, n=6) in rat heart, brain and liver ---------- 159

Table 3-3 FVX levels (ng/g tissue, n=6) in rat heart, brain and liver ---------- 162

Table 3-4 DMI levels (ng/g tissue, n=6) in rat heart, brain and liver ---------- 167

Chapter 4

Table 4-1 Chromatographic parameters for HPLC analysis---------- 196

Table 4-2 Within-run precision for the quantitation of AM, HM, ODM and NDM (n=5)---------- 198

Table 4-3 Between-run precision for the quantitation of AM, HM, ODM and NDM (n=10) ---------- 199

Table 4-4 K_m and V_{max} values for the formation of HM, ODM and NDM --- 203

Table 4-5 The IC_{50} and K_i values generated by PAR, FLU, FVX and DMI using 2000 μM of MET ---------- 208

Table 4-6 The IC_{50} and K_i values generated by PAR, FLU, FVX and DMI using 40 μM of MET ---------- 211

Table 4-7 Concentration of PAR, FLU, FVX and DMI that reduces ODM production to 50% of control using a MET concentration of 200 μM ---------- 214

Chapter 5

Table 5-1 A summary of the CYP enzymes implicated in the metabolism of MET ---- 239

LIST OF FIGURES

Chapter 1

Figure 1-1 Schematic of ferric protoporphyrin IX–the prosthetic group of CYP enzymes---------- 5

Figure 1-2 Active site of a CYP enzyme featuring the heme and apoprotein-- 6

Figure 1-3 The CYP enzyme catalytic cycle ---------- 8

Figure 1-4 CYP2D6 active site showing the correct orientation of amitriptyline for oxidation at the 10 position---------- 23

Figure 1-5 A Michaelis-Menten plot showing the parameters K_m and V_{max} --- 35

Figure 1-6 Determination of K_m and V_{max} values using a Hanes-Woolf plot and the difficulties of estimating K_m and V_{max} in the presence of two enzymes---------- 37

Figure 1-7 The effect of a competitive inhibitor as seen on a Michaelis-Menten plot ---------- 41

Figure 1-8 Sigmoid curves demonstrating the determination of IC_{50} values -- 44

Figure 1-9 Structures of some of the β-adrenergic receptor blockers---------- 51

Figure 1-10 Structures of some tricyclic antidepressants ---------- 55

Figure 1-11 Structures of the SSRIs---------- 56

Figure 1-12 Proposed metabolic pathways in the metabolism of MET ---------- 61

Figure 1-13 Frequency histograms of log metabolic ratios of MET/HM and MET/AM ---------- 65

Figure 1-14 Metabolism of MET in extensive and poor metabolizers of debrisoquine---------- 66

Figure 1-15 Schematic diagram of an HPLC ---------- 74

Figure 1-16 Schematic diagram of a GC---------- 79

Figure 1-17 Derivatizing reagents and their associated reactions---------- 84

Chapter 2

Figure 2-1 Flowchart for the analysis of MET and ODM in rat tissue homogenate---------- 116

Figure 2-2 Typical standard chromatograms from the analysis of MET and ODM in rat heart ---------- 120

Figure 2-3 Typical chromatograms from the analysis of MET and ODM in rat liver samples ---------- 121

Figure 2-4 Typical calibration curves for the quantitation of MET in rat brain---------- 122

Figure 2-5 Typical calibration curve for the quantitation of ODM in rat brain---------- 123

Figure 2-6 Mass spectrum analysis of the PFP derivatives of MET, ODM and IS ---------- 126

Figure 2-7 Proposed fragmentation pattern of the PFP derivative of MET ---- 127

Figure 2-8 Proposed fragmentation pattern of the PFP derivative of ODM --- 128

Figure 2-9 Proposed fragmentation pattern of the PFP derivative of IS-------- 129

Figure 2-10 MET levels (n = 6) in rat heart, brain and liver in the VEH-MET, FLU-MET, FVX-MET and DMI-MET treatment groups---------- 131

Figure 2-11 ODM levels (n = 6) in rat heart, brain and liver in the VEH-MET, FLU-MET, FVX-MET and DMI-MET treatment groups---------- 133

Chapter 3

Figure 3-1 Flowchart for the analysis of FLU, NFLU and FVX in rat heart, brain and liver ---------- 147

Figure 3-2 Flowchart for the analysis of DMI in rat heart, brain and liver----- 151

Figure 3-3 Typical chromatograms from the analysis of FLU, FVX and NFLU in rat heart ---------- 154

Figure 3-4 Typical calibration curves for the quantitation of FLU and NFLU in rat heart and liver respectively ---------- 155

Figure 3-5 Typical calibration curve for the quantitation of FVX in rat brain- 156

Figure 3-6 FLU and NFLU levels (n = 6) in rat heart, brain and liver in the FLU-VEH and FLU-MET treatment groups---------- 160

Figure 3-7 FVX levels (n = 6) in rat heart, brain and liver in the FVX-VEH and FVX-MET treatment groups---------- 163

Figure 3-8 Typical chromatograms from the analysis of DMI in rat brain----- 164

Figure 3-9 Typical calibration curve for the quantitation of DMI in rat brain- 165

Figure 3-10 DMI levels (n = 6) in rat heart, brain and liver in the DMI-VEH and DMI-MET treatment groups---------- 168

Chapter 4

Figure 4-1 Flowchart for conducting kinetic experiments---------- 183

Figure 4-2 Flowchart for conducting inhibition experiments ---------- 184

Figure 4-3 Calibration curves for AM and HM with and without the addition of protein---------- 189

Figure 4-4 Calibration curves for ODM and NDM with and without the addition of protein ---------- 190

Figure 4-5 Calibration curves for the quantitation of AM in human liver microsomes---------- 191

Figure 4-6 Calibration curves for the quantitation of HM in human liver microsomes---------- 192

Figure 4-7 Calibration curves for the quantitation of ODM in human liver microsomes---------- 193

Figure 4-8 Calibration curves for the quantitation of NDM in human liver microsomes---------- 194

Figure 4-9 Typical standard chromatographs resulting from HPLC analysis-- 195

Figure 4-10 Time course experiment for the production of HM, ODM and NDM ---------- 200

Figure 4-11 Production of HM, ODM and NDM with respect to protein concentration---------- 201

Figure 4-12 Michaelis-Menton graphs for the formation of HM, ODM and NDM ---------- 202

Figure 4-13 Typical HPLC chromatograms from the inhibition experiments using 2000 μM of MET ---------- 205

Figure 4-14 Typical HPLC chromatograms from the inhibition experiments using 40 μM of MET ---------- 206

Figure 4-15 Sigmoid curves demonstrating the inhibitory potential of PAR, FLU, FVX and DMI on the formation of ODM in the presence of 2000 μM of MET ---------- 207

Figure 4-16 Sigmoid curves demonstrating the inhibitory potential of PAR, FLU, FVX and DMI on the formation of ODM in the presence of 40 μM of MET ---------- 210

Figure 4-17 Inhibition of ODM production by PAR, FLU, FVX and DMI at a MET concentration of 200 μM ---------- 213

Chapter 5

Figure 5-1 The production of AM versus time in the presence and absence of NADPH ---------- 231

Figure 5-2 The production of AM as a function of ODM concentration ------- 232

Figure 5-3 Significant correlations resulting from the incubation of 100 μM of MET with human liver microsomes ---------- 233

Figure 5-4 Significant correlations resulting from the incubation of 3000 μM of MET with human liver microsomes ---------- 234

Figure 5-5 Chromatography from the incubations of MET with microsomes expressing CYP2D6, CYP3A4, CYP2E1 or CYP2C19 ---------- 236

Figure 5-6 Significant correlation resulting from the incubation of 30 μM of ODM with human liver microsomes ---------- 237

Figure 5-7 Chromatography from the incubations of ODM with microsomes expressing CYP2D6 or CYP3A4 ---------- 238

Figure 5-8 Proposed mechanism for the CYP-mediated oxidation of ethanol to ethanal ---------- 244

Figure 5-9 Proposed mechanism for the conversion of 11-oxo-Δ^8-tetrahydrocannabinol to Δ^8-tetrahydrocannabinol-11-oic acid ----- 245

Figure 5-10 Comparison of 3-phenylpropionaldehyde with the proposed aldehyde intermediate in the conversion of ODM to AM---------- 246

LIST OF ABBREVIATIONS

α----------selectivity factor

AA ----------acetic anhydride

ADH ----------alcohol dehydrogenase

ALDH ----------aldehyde dehydrogenase

ALP ----------alprenolol

AM----------acid metabolite of O-desmethylmetoprolol

amu/sec----------atomic mass units per second

AUC ----------area under the plasma concentration time curve

cDNA----------complementary deoxyribonucleic acid

CYP----------cytochrome P450

DMI----------desipramine

DQ ----------debrisoquine

ECD----------electron-capture detector

eV ----------electron volts

FAD----------flavin adenine dinucleotide

Fe^{2+}----------ferrous (oxidized) iron

Fe^{3+}----------ferric (reduced) iron

FLU ----------fluoxetine

FMO ----------flavin adenine dinucleotide containing monooxygenase

FVX----------fluvoxamine

GC----------gas chromatography

HI----------hydroxylation index

HM----------α-hydroxymetoprolol

HPLC ----------high performance liquid chromatography

I----------inhibitor

IC_{50}----------inhibitor concentration that produces 50% of maximum inhibition

ip ----------intraperitoneal

IS ----------propranolol internal standard

K'----------capacity factor

K_D ----------partition coefficient

K_i ----------inhibitor constant

$K_{m\ app}$ ----------apparent Michaelis constant

K_m ----------Michaelis constant

MAP ----------maprotiline

MET ----------metoprolol

MR ----------metabolic ratio

MS ----------mass spectrometer

N----------column efficiency

NAD^+ ----------β-nicotinamide adenine dinucleotide

$NADP^+$ ----------β-nicotinamide adenine dinucleotide phosphate

NADPH ----------reduced β-nicotinamide adenine dinucleotide phosphate

NDM----------N-dealkylmetoprolol

NFLU----------norfluoxetine

NPD----------nitrogen-phosphorus detector

ODM----------O-desmethylmetoprolol

PAR----------paroxetine

PFBC ----------pentafluorbenzoyl chloride

PFP----------pentafluoropropionate

PFPA----------pentafluoropropionic acid anhydride

PM ----------poor metabolizer

R----------resolution

R-MET ----------R enantiomer of metoprolol

S ----------substrate

SCOT ----------support-coated open tubular

SEM----------standard error of the mean

S-MET----------S enantiomer of metoprolol

SSRI ----------selective serotonin reuptake inhibitor

v ----------velocity

VEH----------vehicle

V_{max} ----------maximum velocity

WCOT----------wall-coated open tubular

Chapter 1: Introduction

1.1 GENERAL INTRODUCTION

The data presented in this thesis deal with the metabolism of metoprolol (MET) and drug-drug interactions of MET and the antidepressants desipramine (DMI), fluoxetine (FLU), fluvoxamine (FVX) and paroxetine (PAR). In that vein, the following discussion will deal with drug metabolism, enzyme kinetics and enzyme inhibition, both in general terms and specifically as it relates to these compounds. In addition, the predictive value of *in vitro* experiments in determining *in vivo* events will also be discussed.

1.2 DRUG METABOLISM

1.2.1 BASIC CONCEPTS

Xenobiotics are any organic compounds that are foreign to the body such as drugs, industrial chemicals, pesticides, pollutants, alkaloids and toxins produced by molds, plants and animals (Sherwin, 1984, Parkinson, 1996). Most pharmacologically active molecules are lipophilic and remain non-ionized or only partially ionized at physiological pH. This means that even after glomerular filtration in the kidney, these molecules can be reabsorbed in the body. Drug metabolism is a means of converting these molecules into substances that are more easily excreted. Biotransformation is the term used to describe the enzymatic transformation of molecules by functionalization (Phase I) reactions and/or conjugation (Phase II) reactions into metabolites that are polar and water-soluble (Meyer, 1996). In general, the more water-soluble products of Phase I reactions still require conjugation to be efficiently eliminated (Shen, 1997). The increased polarity reduces tubular reabsorption in the kidney, resulting in excretion of these compounds in the urine (Baker *et al.*, 1998). Some examples of Phase I reactions

are dehydrogenation/hydrogenation, oxidation, hydrolysis, reduction and mono-oxygenation. Phase II reactions consist of glucuronidation, sulphation, acetylation, methylation, glycine conjugation, glutamine conjugation and glutathione conjugation (Meyer, 1996).

In addition to increasing the water solubility of metabolites, another outcome of drug metabolism is to render these metabolites less active or even inactive in comparison to the parent. However, in some instances, metabolites may have enhanced lipophilicity, activity and/or toxicity (Baker *et al.*, 1998 and Meyer, 1996). The term active metabolite refers to a metabolite that possesses pharmacological activity and/or produces significant adverse effects (Baker *et al.*, 1998).

Although the liver is the major organ responsible for biotransformation of xenobiotics, almost every tissue has some ability to metabolize these compounds. The major enzymes are either cytosolic, as with acetyltransferases, sulfotransferases and xanthine oxidase, or are anchored in the membranes of the endoplasmic reticulum, as is seen with the P450-monooxygenases, epoxide hydrolase and glucuronyl-transferases (Meyer, 1996).

Although the drug metabolizing enzyme systems range in complexity, the cytochrome P450 (CYP) system seems to be most complex, with the discovery of 500 genes in all species tested, and will be discussed in more detail in the following section. The families of uridine diphosphate-glucuronyl-transferases and glutathione-transferases are also comprised of a considerable number of genes. The N-acetyltransferases appear less complex, and other systems such as the esterases and sulfotransferases have not been sufficiently studied to evaluate their complexity (Meyer, 1996).

1.2.2 CYTOCHROME P450 ENZYMES

1.2.2.1 GENERAL OVERVIEW

The CYP enzymes were believed to be similar to mitochondrial cytochromes and were distinguished based on their red pigment and maximal light absorption at 450 nm after adding a reducing agent, such as sodium dithionite, to the microsomes, followed by the bubbling of carbon monoxide gas into the solution (Spatzenegger and Jaeger, 1995). At first, there were believed to be only two relevant hepatic cytochromes - P450 and P448. That number has increased to 20. Although they are all grouped as P450s, there are some variations in the wavelength of light absorbed (Shen, 1997). These proteins are not actually cytochromes but the name persists due to historical usage. The term 'heme-thiolate protein' is considered to be more correct (Nelson *et al.*, 1996)

The CYP enzymes represent a class of enzymes that is one of the major enzyme systems that determines the body's ability to deal with drugs and chemicals. The CYP enzyme system is comprised of a hemoprotein and a flavoprotein. CYP itself is the hemoprotein and contains iron protoporphyrin IX as the prosthetic group (Figure 1-1), with the heme group non-covalently bound to the apoprotein (Figure 1-2). CYP is the substrate and oxygen binding site of the enzyme system in which the heme iron undergoes cyclic oxidation/reduction that is mandatory for its catalytic function and is the terminal oxidase component of the electron transfer system present in the endoplasmic reticulum.

The flavoprotein is called the NADPH-cytochrome P450 reductase. The prosthetic groups of this flavoprotein consist of one mole of flavin adenine dinucleotide and one mole of flavin mononucleotide per mole of apoprotein. This reductase, which is

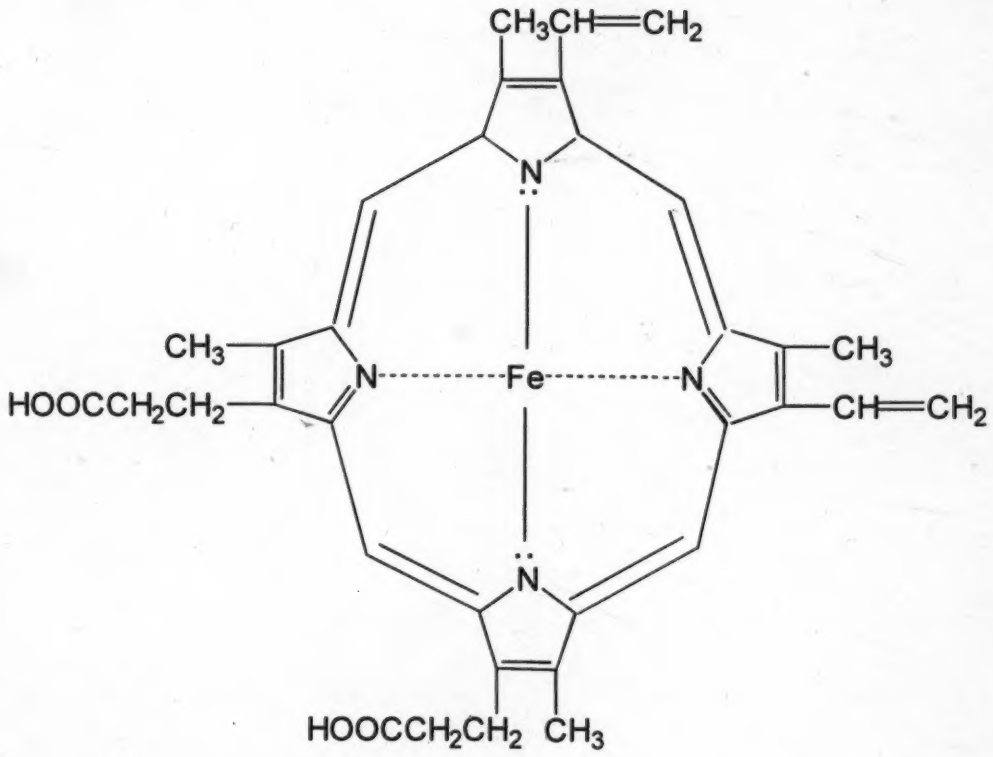

Figure 1-1: Schematic of ferric protoporphyrin IX – the prosthetic group of CYP enzymes (adapted from Gibson and Skett, 1994 and Coutts, personal communication).

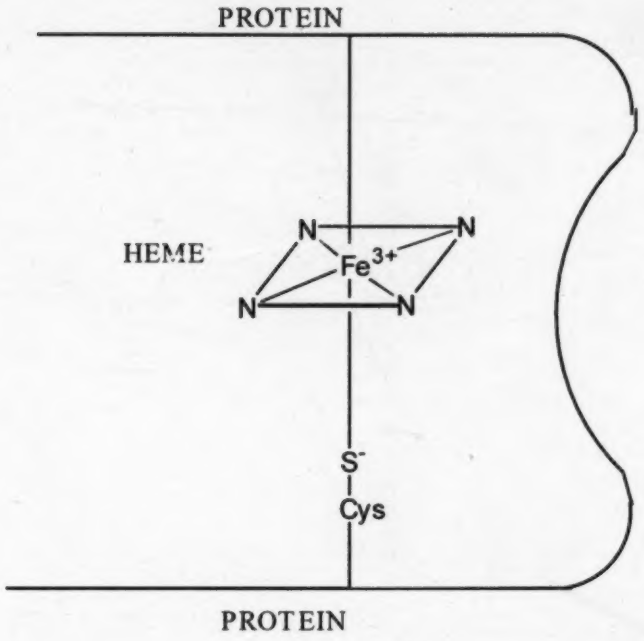

Figure 1-2: Active site of a CYP enzyme featuring the heme and apoprotein (adapted from Gibson and Skett, 1994).

sometimes referred to as NADPH-cytochrome c reductase, is the electron carrier, shuttling electrons from NADPH (reduced β-nicotinamide adenine dinucleotide phosphate) to the cytochrome P450 substrate complex (Meyer, 1996; Gibson and Skett, 1994).

In addition to CYP and the reductase, there seems to be a requirement for a heat-stable, lipid component for the enzyme system to be functional. Although the exact role of the lipid is unknown, it has been suggested that lipid may be required for substrate binding, facilitation of electron transfer or providing a template for the interaction of CYP and NADPH-cytochrome P450 reductase molecules (Gibson and Skett, 1994).

1.2.2.2 CATALYTIC CYCLE OF THE CYP ENZYME SYSTEM

Figure 1-3 illustrates the catalytic cycle of the CYP enzyme system as described by Gibson and Skett (1994). The first step involves drug binding to the oxidized (Fe^{3+}) form of cytochrome P450. There is an electron reduction of the substrate-bound ferric (Fe^{3+}) cytochrome P450 to the ferrous (Fe^{2+}) form of the hemoprotein. The reducing equivalent necesssary for this reduction is derived from NADPH + H^+ and is transferred by NADPH-cytochrome P450 reductase (Gibson and Skett, 1994). Oxygen binding to the ferrous (Fe^{2+}) CYP-substrate complex is rapid (Guengerich and MacDonald, 1990), although the exact mechanism of this reaction is poorly understood. The next steps seem to involve electron rearrangement, introduction of the second electron, oxygen insertion and product release. The oxidation states of the iron and oxygen during these steps is not known. The input into the system of the second electron may be derived from NADPH-cytochrome P450 reductase or cytochrome b_5, although the role of cytochrome b_5 remains controversial. The insertion of oxygen and the subsequent formation of product

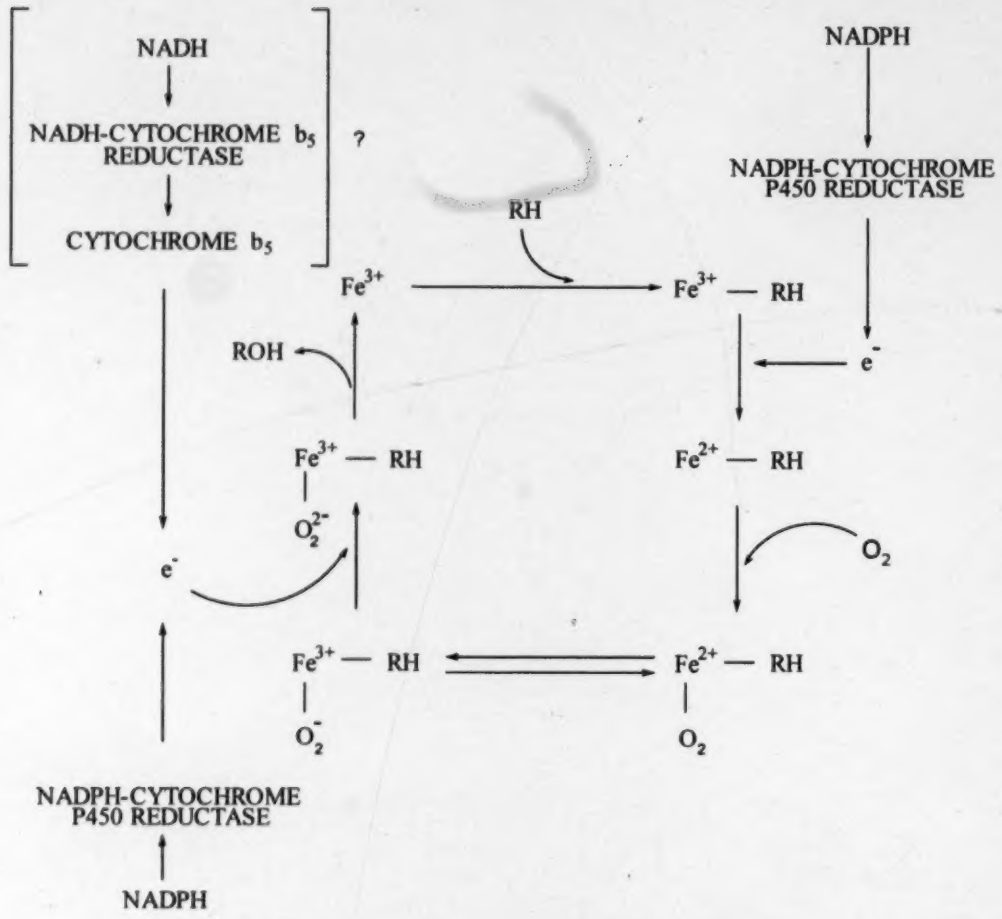

Figure 1-3: The CYP enzyme catalytic cycle (adapted from Gibson and Skett, 1994).

likely involve two steps which are the abstraction of hydrogen and oxygen rebound, represented as follows (Gibson and Skett, 1994):

$$(FeO)^{3+} + RH \longrightarrow (FeOH)^{3+}\ R^{\bullet} \longrightarrow Fe^{3+} + ROH$$

The overall stoichiometry of the CYP enzyme system is (Gibson and Skett, 1994):

$$NADPH + H^{+} + O_2 + RH \longrightarrow NADP^{+} + H_2O + ROH$$

Where: RH = drug substrate

ROH = hydroxylated metabolite

The rate-determining step in the overall catalytic sequence probably varies depending on the CYP enzyme and substrate under consideration. However, in general the overall sequence of oxygen activation is rate-limiting for the majority of CYP substrates (Guengerich and MacDonald, 1990). The different CYP enzymes have catalytic selectivity with regard to the substrates they oxidize. In addition, there is regioselectivity within a single substrate and stereoselectivity both with regard to which of two enantiomers is oxidized and the site of oxidation to yield enantiomorphic products (Guengerich, 1994). The key influence on selectivity of the various CYP enzymes was proposed to be the apoprotein (Smith and Jones, 1992). The protein structures were proposed to provide axial thiolate ligand to the heme, to control the juxtaposition of the substrate (and therefore the regio- and stereoselectivity of oxidation), to alter the effective oxidation potential of the $(FeO)^{3+}$ complex and possibly participate in specific acid-base catalysis in the oxidation of some substrates (Guengerich and MacDonald, 1990). However, theoretical studies on substrates suggest that the apoprotein alone does not provide an adequate explanation for the selectivity of an enzyme. The selectivity is likely a function of both binding characteristics of the enzyme and the ease with which various groups or functions within a molecule undergo oxidation (Smith and Jones, 1992).

1.2.2.3 THE DIVERSITY OF THE CYP ENZYMES

The CYP enzymes are important in the metabolism of diverse endogenous compounds such as steroids, bile acids, fatty acids, prostaglandins, leukotrienes, biogenic amines, retinoids, lipid hydroperoxides and phytoalexins. These enzymes also metabolize drugs, environmental chemicals and pollutants as well as natural plant products involved in flavour, odour, flower colour and the response to wounding (Nelson *et al.*, 1996).

Of the 74 gene families that have been described, at least 14 exist in all mammals. These 14 families consist of 26 mammalian subfamilies (clusters of genes), of which 20 have been mapped in the human genome (Nelson *et al.*, 1996). The 14 gene families are 1, 2, 3, 4, 5, 7, 8, 11, 17, 19, 21, 24, 27 and 51. CYP5, 7, 8, 24, 27 and 51 are involved in the metabolism and biosynthesis of eicosanoids, vitamins and bile acids. CYP11, 17, 19 and 21 are involved in the biosynthesis of steroid hormones from cholesterol. With respect to drug metabolism, families 1, 2, and 3 seem to play the greatest role (Table 1-1) (Baker *et al.*, 1998).

The enzymes that have garnered the most interest with respect to drug metabolism are CYP3A4, CYP2D6, CYP2C9, CYP2C19, CYP1A2 and CYP2E1 (Meyer, 1996; Bertz and Granneman, 1997). In addition, CYP2A6, CYP2B6 and CYP2C8 are also implicated in the metabolism of xenobiotics (Parkinson, 1996). Specific features of several of these CYP enzymes will be discussed in Section 1.2.2.6.

1.2.2.4 NOMENCLATURE ASSOCIATED WITH CYP ENZYMES

There is currently an attempt to standardize the nomenclature for the CYP enzymes. When naming a gene, the italicized root symbol *CYP* is used followed by an

Cytochrome P450 Family	Reactions
1	Xenobiotic metabolism
2	Xenobiotic and steroid metabolism
3	Xenobiotic and steroid metabolism
4	Fatty acid ω and ω-1 hydroxylase
5	Thromboxane synthase
7	Cholesterol 7 α-hydroxylase
8	Prostacyclin synthase
11	Steroid 11β-hydroxylase
17	Steroid 17α-hydroxylase
19	Aromatase
21	Steroid 21 hydroxylase
24	1-α-25-dihydroxyvitamin D3-24-hydroxylase
27	Cholesterol 27-hydroxylase
51	Lanosterol 14 α-demethylase

Table 1-1: The CYP families and their function (adapted from Gonzalez, 1992; Guengerich, 1996b; Eggertsen *et al.*, 1996; Miyamoto *et al.*, 1997; Rozman *et al.*, 1996).

Arabic number to designate the P450 family, a letter indicating the subfamily and an Arabic number representing the individual gene. The corresponding mRNA, cDNA and enzyme would have the same numbers and letters which would be non-italicized and all capital letters. For example *CYP1A2* would represent the gene and CYP1A2 would represent the enzyme. There are no spaces between any of the letters or numbers. The classification of families and subfamilies is based on shared sequence homology. The protein sequences within a gene family are usually >40% identical, while sequences within the same subfamily are always >55% identical (Nelson *et al.*, 1996).

1.2.2.5 VARIATIONS IN DRUG METABOLISM

Interindividual differences observed in the metabolism of drugs can be divided into four general categories (Wrighton *et al.*, 1996). The first category is the influence of genetics on the expression of the CYP enzymes. Genetic polymorphism is the occurrence of multiple alleles at a gene locus, when at least two alleles occur at frequencies of greater than 1%. A genetic locus is polymorphic when at least 2% of the population is heterozygous (Richelson, 1997). Genetic polymorphism results from gene mutations encoding either the CYP2D6 or CYP2C19 enzymes. Other CYP enzymes, including CYP1A2, CYP2A6, CYP2C9, CYP2E1 and CYP3A4 are sometimes claimed to be polymorphic, but genotypic evidence is lacking in most cases (Coutts and Urichuk, 1999). However, two structural variants of CYP2C9 have been characterized (Haining *et al.*, 1996). In addition, genetic variations could also be due to ethnic background, gender and, indeed, species variation (Wrighton *et al.*, 1996).

An extensive metabolizer refers to a person who metabolizes a probe drug at a rate similar to that of most of the population. A poor metabolizer is a person who

metabolizes a probe drug more slowly than does most of the population (Richelson, 1997). The therapeutic consequence of this phenotype can be lack of response due to the inability to convert a prodrug to its active form (i.e. codeine to morphine) (Coutts and Urichuk, 1999) or it may result in excessively high levels of the parent drug such that toxic side effects develop (Gibson and Skett, 1994).

An ultra-rapid metabolizer metabolizes drugs much more rapidly than most of the population due to the presence of multiple copies of the CYP2D6 gene (Coutts and Urichuk, 1999). Although CYP2D6 is the only CYP enzyme that has been shown to result in ultra-rapid metabolism, a recent report suggests that ultra-rapid metabolism of maprotiline was caused by enzymes other than CYP2D6 and suggested that CYP2C19 may be a candidate (Vormfelde *et al.*, 1997). Due to the increased metabolism of the parent drug, ultra rapid metabolizers fail to respond to conventional doses of drugs. These patients may be suspected of non-compliance when in fact they actually require very high doses of drugs to receive therapeutic effects (Coutts and Urichuk, 1999).

Poor, extensive and ultra-rapid metabolizers are recognized either through phenotyping or genotyping. In phenotyping for polymorphism of the CYP2D6 enzyme, the patient is administered either sparteine, debrisoquine (DQ) or dextromethorphan and the metabolic ratio (MR), which is the amount of parent drug/amount of metabolite, or logMR, is calculated. The MR of a poor metabolizer of CYP2D6 substrates would be >20 for sparteine, >12.6 for DQ and >0.3 for dextromethorphan (Brøsen and Gram, 1989). With respect to DQ, the logMR for poor metabolizers is greater than 1.1 whereas ultra-rapid metabolizers have a log MR of less than –1.0. In phenotyping for polymorphism of CYP2C19, racemic mephenytoin is used as the index drug. However, because mephenytoin is not excreted to any extent in the urine, a hydroxylation index

(HI) is determined. The HI is the dose of S-mephenytoin/amount of S-4'-OH-mephenytoin in the urine. Poor metabolizers of CYP2C19 substrates will have an HI of >5.6 (Coutts and Urichuk, 1999). With respect to genotyping, polymerase chain reaction is combined with restriction fragment length polymorphism. These molecular techniques provide complete structures of mutant alleles and the mutant enzymes expressed by them can be ascertained (Coutts and Urichuk, 1999).

The second source of interindividual variability is inhibition of CYP enzymes by drugs, endogenous agents or environmental compounds (Wrighton *et al.*, 1996). Impairment of any of the steps in the catalytic cycle of the CYP system can lead to inhibition of CYP activity. The inhibition may be reversible (competitive, noncompetitive, uncompetitive, mixed) or irreversible, depending on the interaction between the inhibitor and the enzyme and the step(s) in the cycle that are blocked. The clinical relevance of the inhibition in terms of drug-drug interactions in humans depends on the relative affinities of the two compounds for the enzyme, the concentrations achieved at the site after therapeutic doses, the role of the CYP enzyme in the overall elimination of the two compounds and the therapeutic index (Halpert, 1995). Enzyme inhibition will be discussed in more detail in section 1.4.

The third general source resulting in interindividual differences is enzyme induction by exposure of the CYP enzymes to particular classes of drugs, endogenous compounds or environmental agents (Wrighton *et al.*, 1996). These inducers can increase CYP enzyme expression by increasing synthesis, decreasing degradation, activating pre-existing components or a combination of these processes (Gibson and Skett, 1994). Induction actually lowers blood levels of the parent compound, which can compromise the therapeutic goal of a drug, but unlike enzyme inhibition, it does not cause an

exaggerated response to the drug. One exception to this generality is the enhanced activation of acetaminophen to its hepatotoxic metabolite, N-acetylbenzoquinoneimine, by the CYP2E1 inducers, ethanol and isoniazid, and possibly by CYP3A enzyme inducers. Other clinically important consequences of CYP enzyme induction include enhanced biotransformation of cyclosporin, warfarin, and contraceptive steroids by inducers of the CYP3A and CYP2C enzymes. Persistent induction of CYP enzymes leads to an increased demand for heme and can precipitate a disorder known as porphyria cutanea tarda which results from excessive accumulation of intermediates in the heme biosynthetic pathway (Parkinson, 1996). The major manifestations of this disorder are limited to the skin, which exhibits excessive mechanical fragility, changes in pigmentation, photosensitivity, diffuse thickening and blisters (Bauer, 1984).

The fourth source of interindividual variation involves host factors such as diet and disease states (Wrighton *et al.*, 1996). Both dietary and disease states may inhibit or induce CYP-mediated metabolism depending on the dietary items and disease processes in question (Gibson and Skett, 1994).

1.2.2.6 SPECIFIC FEATURES OF SEVERAL CYP ENZYMES, INCLUDING COMMENTS ON SPECIES VARIATION

1.2.2.6.1 CYP2B6

The CYP2B subfamily of enzymes seems to play a role in the activation of environmental mutagens as well as the oxidation of drugs and has been extensively studied in experimental animals. However, the hepatic CYP2B proteins are poorly expressed in experimental animals, usually accounting for less than 5% of total P450 contents (Mimura *et al.*, 1993). A gene encoding for CYP2B6 in humans has been identified, but the enzyme is poorly expressed in human livers. In one study, only about

50% of the samples tested had detectable levels of CYP2B6, and in those samples in which it was detected it amounted to only approximately 1% of total CYP (Wrighton *et al.*, 1996). In another study, only 24% of those livers tested had detectable levels of CYP2B6, and the highest level of CYP2B6 present in human livers was estimated to be less than 2% of total CYP. There are only a few studies dealing with the purification and characterization of human liver microsomal CYP2B enzymes, which probably reflects the lower levels of this enzyme in humans. It is not clear whether this low frequency is due to genetic polymorphism or environmental influences (Mimura *et al.*, 1993).

There is a 74% amino acid sequence homology between rat CYP2B1 and its human orthologue CYP2B6 (Souček and Gut, 1992). Analogous to CYP2B in rodents it is expected that CYP2B6 would be inducible by barbiturates and other drugs. However, the levels of CYP2B6 are extremely low even in individuals treated with phenobarbital (Parkinson, 1996).

Interestingly, livers with high levels of CYP2A6 also possess high levels of CYP2B6. The concordance of expression of these two genes and the fact that they are found close together on chromosome 19 suggest that they might be coordinately regulated. It is possible that the livers containing high mRNAs from these two genes may have been under the influence of inducers. In addition, cDNAs apparently corresponding to mutant CYP2B6 alleles have been isolated but it is unclear whether they are responsible for the large degree of interindividual variability in liver specimens (Gonzalez, 1992). A list of substrates, inhibitors and inducers of CYP2B6 is given in Table 1-2.

SUBSTRATES	INHIBITORS	INDUCERS
Cyclophosphamide Ifosphamide	Orphenadrine	Barbiturates

Table 1-2: Substrates, inhibitors and inducers of CYP2B6 in humans (adapted from Parkinson, 1996).

1.2.2.6.2 CYP2C19

The CYP2C subfamily accounts for 20% of total CYP based on hepatic protein mass (Bertz and Granneman, 1997), with CYP2C19 accounting for approximately 1% of total CYP2C (Coutts and Urichuk, 1999). Expression of CYP2C19 has not been detected in extrahepatic tissue (Gonzalez, 1992). Enzymes of the CYP2C subfamily are thought to account for metabolism of about 15% of all known drugs which undergo metabolism (Lewis *et al.*, 1997).

The gene encoding for CYP2C19 is inducible, found on chromosome 10 and is polymorphically expressed, being inherited as an autosomal recessive trait (Nelson *et al.*, 1996; Wrighton *et al.*, 1996). The most common defect originates from a point mutation that causes a splicing error and inactive product (Bertz and Granneman, 1997). Approximately 20% of Japanese are considered to be PMs of CYP2C19 substrates. Interestingly, Chinese in their native land demonstrate a high frequency of PMs (17%) whereas Chinese in Canada display a much lower frequency (5%), similar to that of Caucasians (2-7%) and Hispanics (5%). African Americans demonstrate a PM rate of 18% and East Indians have a rate of 21% (Smith and Lin, 1996). The activity of this enzyme has shown to vary by greater than 150-fold in a bank of human liver specimens (Wrighton *et al.*, 1996).

The principal characteristics of the human enzyme are an active site that accommodates molecules with areas of hydrophilicity and strong hydrogen bonding potential. The CYP enzymes of the 2C gene family have been isolated from rat, dog and man. The differences in metabolism and pharmacokinetics of known human CYP2C substrates in dog and rat indicate there may be marked differences in this enzyme across

species. Another species difference between rat and man is that some substrates for rat CYP2C enzymes are substrates for human CYP3A enzymes. For example in rat, nifedipine oxidation and lidocaine N-deethylation are catalyzed by CYP2C whereas in man, these reactions are catalyzed by CYP3A (Smith, 1991).

Sex differences in activities of enzymes of the 2C subfamily have been shown in rats, with preferential expression seen in the male rat (Smith, 1991). Gender differences have not been shown to definitively alter the expression of CYP enzymes in humans (Smith and Lin, 1996; George *et al.*, 1995). A list of substrates, inhibitors and inducers of CYP2C19 is given in Table 1-3.

1.2.2.6.3 CYP2D6

CYP2D6 is expressed in liver, intestine, kidney and brain (Gonzalez, 1992; Coutts, 1994). Based on hepatic protein mass, CYP2D6 accounts for 1-5% of total CYP (Bertz and Granneman, 1997). Approximately 30% of the drugs currently in clinical use are known to undergo metabolism by the CYP2D6 enzyme (Lewis *et al.*, 1997). The gene encoding for enzymes of the CYP2D family is located on chromosome 22. Nine identified mutant forms of CYP2D6 have been discovered to have decreased or absent enzyme activity (Richelson, 1997; Coutts and Urichuk, 1999). Incorrectly spliced CYP2D6 pre-mRNAs have been identified in the livers of PM subjects (reviewed in Coutts, 1994). The PM phenotype is inherited as an autosomal recessive trait. The frequency of PMs varies from less than 3% in Egyptians, Saudi Arabians, Chinese, Japanese, Malayans and Thai to 3-9% in Caucasians in Europe and North America and 5% in Hispanics. A wider range of frequencies is found in Black Africans, with 0-8% of Sub-Saharan Africans, 4% of Venda in South Africa, 2% of African Americans and 19%

SUBSTRATES		INHIBITORS	INDUCERS
Citalopram	S-Mephenytoin	Tranylcypromine	Rifampin
Diazepam	Mephobarbital		
Diphenylhydantoin	Omeprazole		
Hexobarbital	Pentamine		
Imipramine	Proquanil		
Lansoprazole	Propranolol		

Table 1-3: Substrates, inhibitors and inducers of CYP2C19 in humans (adapted from Parkinson, 1996).

of Sans Bushmen of South Africa being classified as PMs (Smith and Lin, 1996).

In addition to the poor metabolizer phenotype, recent studies have shown that a small fraction of the population are very rapid metabolizers, apparently as a result of gene amplification or duplication. Approximately 7% of Spaniards possess this phenotype (Coutts and Urichuk, 1999). The catalytic activity associated with CYP2D6 varies in human liver microsomes by 25-fold (Wrighton, 1996).

CYP enzymes of the 2D gene family have been isolated from rat and man. The presence of a similar enzyme in dog can be inferred from metabolism studies of CYP2D substrates (Smith, 1991). Mice have also been shown to contain CYP2D genes but they are not able to metabolize DQ and other CYP2D substrates (Gonzalez, 1992). Although these enzymes share similar substrate selectivity, differences in the active site between rat and man are demonstrated by the inhibitor specificity of the diastereomeric pair quinine and quinidine. Quinidine is the more potent inhibitor of the human enzyme (IC_{50} against DQ metabolism is 3.6 μM for quinidine and 223 μM for quinine) whereas quinine is the more potent inhibitor against rat enzyme (IC_{50} against DQ metabolism is 137 μM for quinidine and 2.4 μM for quinine) (Smith, 1991). This marked difference is possibly due to an amino acid change of serine to threonine at position 304 in the rat enzyme compared to the human enzyme (Lewis *et al.*, 1997). The *CYP2D6* gene is orthologous to the *CYP2D1* gene in rats, with a 71% amino acid sequence homology. Although there are generally conserved regions for the P450 reductase, the heme and signal peptide, it is important to note that a change in even a single amino acid can markedly alter CYP function, increase or decrease its activity, or even change its substrate specificity completely (Součèk and Gut, 1992).

Characteristics of this enzyme include an acidic binding site for the basic nitrogen of the substrate (Smith, 1991). Substrates for CYP2D6 possess common structural features and physical properties. The substrates tend to be lipophilic and are strong organic bases that become protonated at physiological pH. They possess a planar, usually aromatic ring system, which together with the positively charged nitrogen atom orient the drug correctly within the CYP2D6 protein active site where metabolic oxidation occurs. The drug molecule will adopt a conformation that orients the nitrogen atom towards an anionic location (a COO- group) on the protein while the aromatic ring aligns itself to a relatively planar region of the protein. The distance between the site of metabolic oxidation and the nitrogen atom is between 0.5-0.7 nm (reviewed in Coutts, 1994). A model for the active site of CYP2D6 with a correctly oriented substrate is shown in Figure 1-4. Given the structural limitations, it would seem that N-dealkylation and deamination reactions would not be favourable (Coutts, 1994). However, there are now several examples of N-dealkylation reactions involving CYP2D6 (Coutts and Urichuk, 1999). Indeed, the distance of 0.5-0.7 nm is not a critical one. More accurately, the fit to the site is governed by the position of the anionic binding site and its distance to the heme-oxygen complex (Smith and Jones, 1992).

The dependence on ion-pair formation as a major determinant of substrate enzyme binding, rather than simple hydrophobic forces, explains why DQ, a polar compound, is a substrate for CYP2D6 (Smith and Jones, 1992). Ion-pair binding between substrate and enzyme means the enzyme has a high affinity (low K_m) for its substrate and the enzyme is readily saturable. Ion pair binding also means polar

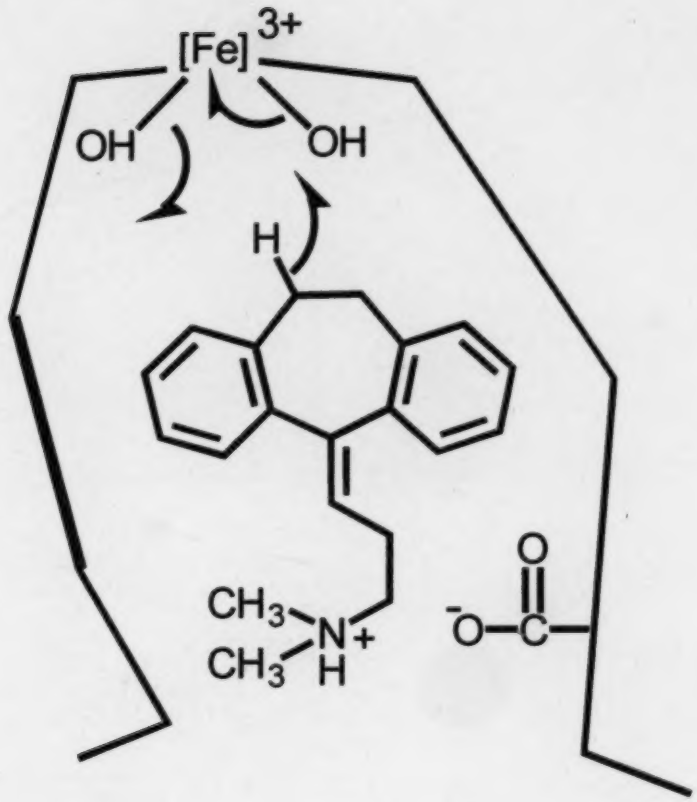

Figure 1-4: CYP2D6 active site showing the correct orientation of amitriptyline for oxidation at the 10 position (adapted from Coutts, 1994).

substrates may bind to the enzyme, and binding does not rely simply on hydrophobic interactions. The ionic binding results in the regioselective nature of the hydroxylations performed by this enzyme. There is evidence to suggest that the rat enzyme may have a more accommodating active site than other species, which may explain classical species differences. The high ionic binding energy of substrate and enzyme will apply to product and enzyme. Thus, products will not likely diffuse rapidly from the active site and any reactive metabolite formed should interact with this CYP enzyme and not other enzymes or proteins (Smith, 1991).

Inhibitors of CYP2D6 tend to have an extended hydrophobic region, a positively charged basic nitrogen and groups with negative potential and the ability to accept hydrogen bonds, positioned 0.5-0.7 nm from the nitrogen atom (Smith and Jones, 1992). No inducers of CYP2D6 have been identified (Parkinson, 1996). A list of substrates and inhibitors of CYP2D6 is given in Table 1-4.

1.2.2.6.4 CYP2E1

In addition to the CYP2C subfamily, genes located on chromosome 10 also encode the CYP2E subfamily (Nelson *et al.*, 1996). CYP2E1 accounts for 7% of total CYP based on hepatic protein mass (Bertz and Granneman, 1997) and is responsible for metabolizing approximately 1% of drugs (Lewis *et al.*, 1997). CYP2E1 has been studied in relationship to the formation of toxic metabolites and alcoholism (Bertz and Granneman, 1997). The levels of CYP2E1 vary by as much as 50-fold in human microsome samples. In addition, a mutated allele of the CYP2E1 gene has been identified that alters the expression of CYP2E1 (Wrighton *et al.*, 1996).

SUBSTRATES		INHIBITORS	INDUCERS
Amiflamine	Hydrocodone	Ajmalicine	None Known
Amitriptyline	Imipramine	Chimidin	
Aprindine	Indoramin	Corynanthine	
Brofaromine	Methoxyamphetamine	Fluoxetine	
Bufurolol	Metoprolol	Lobeline	
Captopril	Mexiletene	Propidin	
Cinnarizine	Miniaprine	Quinidine	
Citalopram	Nortriptyline	Trifluperidol	
Clomipramine	Ondansetron	Yohimbine	
Clozapine	Paroxetine		
Codeine	Perhexilene		
Debrisoquine	Perphenazine		
Deprenyl	Propafenone		
Desmethylcitalopram	Propranolol		
Desipramine	N-Propylajmaline		
Dextromethorphan	Remoxipride		
Encainide	Sparteine		
Flecainide	Thioridazine		
Fluoxetine	Timolol		
Flunarizine	Tomoxetine		
Fluphenazine	Trifluperidol		
Guanoxan	Tropisetron		
Haloperidol (reduced)			

Table 1-4: Substrates, inhibitors and inducers of CYP2D6 in humans (adapted from Parkinson, 1996).

CYP2E1 is expressed in liver, intestine and leukocytes and is the best-conserved CYP in the CYP2 family. A single *CYP2E* gene exists in humans, rats and mice and 2 similar genes are present in rabbits (Gonzalez, 1992). In fact, there is a 78% amino acid sequence homology between rat and human CYP2E1 (Souček and Gut, 1992). The catalytic activity of CYP2E1 across species is quite similar, suggesting it may play a role in the metabolism of some physiologically important compounds (Gonzalez, 1992). A list of substrates, inhibitors and inducers of CYP2E1 is given in Table 1-5.

1.2.2.6.5 CYP3A4

The CYP3 gene cluster is found on chromosome 7 (Nelson *et al.*, 1996). It is estimated that CYP3A is involved in the metabolism of more than 50% of the drugs used in humans, and it accounts for 30% of total CYP based on hepatic protein mass. CYP3A is inducible (Smith, 1991) and is expressed in liver, kidney, intestine, placenta, lung and brain (Bertz and Granneman, 1997). Although CYP3A3 and CYP3A4 are very similar, having only 11 amino acid substitutions and no known differences in catalytic activities, CYP3A4 appears to be the most abundant of the two forms in liver (Gonzalez, 1992). The levels of CYP3A3/4 are variably expressed across individuals, by as much as 60-fold (Wrighton, 1996). Although CYP3A4 is the most dominant member of the CYP3A subfamily, CYP3A5 and CYP3A7 seem to have some importance (Bertz and Granneman, 1997).

CYP enzymes of the *CYP3A* gene have been isolated from the rat, dog and man (Smith, 1991). Substrate specificity for CYP3A is broad, accommodating both large and small molecules that range in charge and lipophilicity (Bertz and Granneman, 1997).

SUBSTRATES		INHIBITORS	INDUCERS
Acetaminophen	Halogenated alkanes	3-Amino-1,2,4-triazole	Ethanol
Alcohols	Isoflurane	Diethyldithiocarbamate	Isoniazid
Aniline	Methylformamide	Dihydrocapsaicin	
Benzene	p-Nitrophenol	Dimethylsulfoxide	
Caffeine	Nitrosamines	Disulfiram	
Chlorzoxazone	Styrene	Phenethyl isothiocyanate	
Dapsone	Theophylline	4-Methylpyrazole	
Enflurane			

Table 1-5: Substrates, inhibitors and inducers of CYP2E1 in humans (adapted from Parkinson, 1996).

Evidence suggests that compounds bound to the active site of CYP3A are not constrained to the same defined substrate structure-activity relationship as with CYP2D6 (Smith and Jones, 1992). Although substrates can be very bulky, metabolism often occurs on small exposed substituents and many of the reactions involve electron abstraction from nitrogen (*i.e.* N-demethylations) (Smith, 1991). However, CYP3A is involved in a variety of biotransformations, including 6β-hydroxylation of steroids, N-dealkylation, aromatisation and aliphatic oxidation. It is not uncommon for the same substrate to be oxidized at different positions (Bertz and Granneman, 1997).

With respect to species differences, some substrates for rat CYP3A are actually substrates for CYP2C in humans. In rat CYP3A is a major enzyme for S-mephenytoin hydroxylation whereas in man CYP2C catalyzes that reaction (Smith, 1991). In spite of these differences, the amino acid sequence homology between rat CYP3A1 and human CYP3A3 and CYP3A4 is 78% and 73% respectively (Souček and Gut, 1992). Sex differences in expression of CYP3A are seen in the rat and depend on age (Smith, 1991). A list of substrates, inhibitors and inducers of CYP3A4 is given in Table 1-6.

1.2.3 ALCOHOL DEHYDROGENASE AND ALDEHYDE DEHYDROGENASE

Alcohol dehydrogenase (ADH) catalyzes the conversion of many alcohols to their corresponding aldehydes. ADH is localized in the soluble fraction of the liver, kidney and lungs and it uses NAD^+ as its co-factor. In non-induced situations, ADH is the major metabolizer of ethanol. Following induction by ethanol, CYP mediated metabolism of ethanol takes on greater importance and may account for 80% of ethanol clearance in certain cases (Gibson and Skett, 1994). Human ADH is a dimeric protein consisting of

SUBSTRATES		INHIBITORS	INDUCERS
Acetaminophen	Losartan	Clotrimazole	Carbamazepine
Aldrin	Lovastatin	Ethinylestradiol	Dexamethasone
Alfentanil	Midazolam	Gestodene	Phenobarbital
Amiodarone	Nifedipine	Itraconazole	Phenytoin
Astemizole	Omeprazole	Ketoconcazole	Rifampin
Benzphetamine	Quinidine	Miconazole	Sulfadimidine
Budsonide	Rapamycin	Naringenin	Sulfinpyrazone
Carbamazepine	Retinoic acid	Troleandomycin	Troleandomycin
Cyclophosphamide	Steroids (*e.g.* cortisol)	Activator: α-Naphthoflavone	
Cyclosporin	Tacrolimus		
Dapsone	Tamoxifen		
Digitoxin	Taxol		
Diltiazem	Teniposide		
Diazepam	Terfenadine		
Erythromycin	Tetrahydrocannabinol		
Ethinylestradiol	Theophylline		
Etoposide	Toremifene		
Flutamine	Triazolam		
Hydroxyarginine	Troleandomycin		
Ifosphamide	Verapamil		
Imipramine	Warfarin		
Lansoprazole	Zatosetron		
Lidocaine	Zonisamide		
Loratadine			

Table 1-6: Substrates, inhibitors and inducers of CYP3A4 in humans (adapted from Parkinson, 1996).

two subunits. The subunits (α, β, γ, π and χ) are encoded by 5 different gene loci: ADH_1 through ADH_5. Due to the three allelic variants of the β subunit and the two allelic variants of the γ subunit, the human ADH enzymes are composed of eight subunits which can combine as heterodimers or homodimers (Parkinson, 1996). Ethnic variations also exist for this enzyme. For example, the occurrence of the wildtype ADH_2^1 gene exceeds 90% in Caucasians but is only about 30% in Asians, whereas the atypical ADH_2^2 gene is found in 70% of Asians. Another atypical gene, ADH_2^3 is fairly common in blacks. Two common genes, the wild-type ADH_3^1 and the variant ADH_3^2 gene are common in Caucasians but the frequency of the variant is low in Asians. Some of these variants, especially the Asian type ADH_2^2 gene, are more efficient at converting alcohol to acetaldehyde (Smith and Lin, 1996).

The aldehyde dehydrogenase (ALDH) system transforms aldehydes to carboxylic acids and is mainly located in the mitochondria or cytosol. This oxidative reaction consists of two steps. The initial dehydrogenation of the aldehyde to form an acyl-enzyme complex is followed by hydrolysis of the complex (Watanabe *et al.*, 1990). As with ADH, ALDH uses NAD^+ as its cofactor (Gibson and Skett, 1994). Several ALDH enzymes have been identified. Both the cytosolic $ALDH_1$ and the mitochondrial $ALDH_2$ exhibit high activity for the oxidation of acetaldehyde and are considered to play a major role in acetaldehyde detoxification in the liver. $ALDH_1$ is activated only when acetaldehyde concentration reaches significantly high levels and is therefore not as efficient as $ALDH_2$ in the elimination of acetaldehyde. Approximately 50% of Asians lack $ALDH_2$ activity in their livers due to a mutation in the $ALDH_2$ locus. This trait

becomes more problematic when combined with increased efficiency of the ADH enzyme, resulting in higher accumulations of acetaldehyde (Smith and Lin, 1996).

A number of animal studies have suggested that alcohol metabolism differs between males and females. Similar research in humans has yielded inconsistent results. However, there is some evidence to suggest that ADH activity of stomach mucosa membranes is substantially higher in men than women, resulting in increased metabolism of alcohol in the stomachs of men. Due to the decreased activity of ADH in women, there is increased alcohol available for absorption. This fact, coupled with a decreased volume of distribution in women could potentially explain the higher peak blood alcohol level observed in women (Smith and Lin, 1996).

1.3 ENZYME KINETICS

Enzymes are by definition biological proteins with catalytic properties. They increase the rate of chemical reactions in cells and in *in vitro* systems that would otherwise proceed very slowly. Properties of enzymes include the fact that they are effective in very small amounts, they are unchanged by the reaction, they affect the speed of attaining equilibrium but do not change the final concentrations of the substrates and products of the equilibrium state and they demonstrate a great degree of specificity for the reactions they accelerate. An enzyme may have non-protein substances associated with it that are needed for optimal activity. These cofactors may be loosely or tightly bound to the protein part of the enzyme. Loosely bound cofactors which are organic in nature are called coenzymes whereas inorganic cofactors are referred to as activators. If a cofactor is so tightly bound to the enzyme that it is considered to be part of the enzyme, it is termed a prosthetic group. If the cofactor is a tightly bound metal ion, the enzyme is

referred to as a metalloenzyme. An enzyme without its associated cofactors is referred to as an apoenzyme and the complete enzyme-cofactor complex is a haloenzyme (Hohnadel, 1984).

Substrates for enzymes, including CYP enzymes, are often described in terms of kinetic parameters. Enzyme kinetics is the study of reaction rates and the factors that influence them. It does not deal with the chemical nature of the reactions taking place (Palmer, 1995). The interaction of enzyme and substrate is demonstrated by the following equation:

$$E + S \underset{k_{-1}}{\overset{k_1}{\rightleftharpoons}} ES \xrightarrow{k_p} E + P$$

Where: E = enzyme

S = substrate

ES = enzyme-substrate complex

P = product

The rates of the forward and back reactions for the interaction between E and S are given by the rate constants k_1 and k_{-1}, respectively, while the rate of product formation from ES is given by the rate constant k_p. In steady state kinetics, it is assumed that during a short initial period of equilibrium, the concentration of ES builds up to a constant steady state level. For most enzymes, ES decomposes to E + P extremely rapidly, and so the rate of product formation is directly proportional to [ES] (Holt, 1999). If the substrate concentration is sufficiently high, the enzyme becomes saturated such that each available enzyme molecule forms an ES complex. Since there is no free enzyme present, adding additional substrate will not result in the formation of any more ES. Thus, the reaction is independent of substrate concentration and is considered a zero-order reaction. At low substrate concentrations, the enzyme is far from saturated and the overall rate of reaction

is limited by the rate at which ES is formed. Thus, at constant enzyme concentrations, the reaction rate is proportional to the substrate concentration and is considered a first-order reaction. At intermediate concentrations of substrate, the enzyme population will be partially saturated and the reaction will be somewhere between first-order and zero-order (Palmer, 1995).

The relationship between substrate concentration and reaction velocity is hyperbolic in nature. Kinetic models proposed by Henri in 1903 and Michaelis and Menten in 1913 were used to explain the hyperbolic relationship between initial velocity and initial substrate concentration. However, due to the experimental work conducted by Michaelis and Menten to support their model, it is their name that is most familiar. In 1925, Briggs and Haldane modified the equation put forth by Michaelis and Menten to include the concept of steady-state. However, the form of the equation was the same as that put forth by Michaelis and Menten, and the name Michaelis-Menten Equation remained (Palmer, 1995). This equation is mathematically represented as follows:

$$v = \frac{V_{max}[S]}{[S] + K_m}$$

Where: v = initial reaction velocity at any given substrate concentration.

V_{max} = the maximum possible reaction velocity that occurs when all enzyme active sites are saturated with substrate.

$[S]$ = substrate concentration.

K_m = the concentration of substrate at which the enzyme is operating at half of the maximum possible velocity. This term is also referred to as the Michaelis constant.

The graphical presentation of the hyperbolic relationship between substrate concentration and velocity is referred to as a Michaelis-Menten plot, and the concepts of K_m and V_{max} can be easily presented (Figure 1-5) (Holt, 1999; Palmer, 1995). K_m provides an indication of the affinity between the enzyme and substrate. Thus, a low K_m indicates a high affinity for the substrate whereas a high K_m indicates a low affinity (Holt, 1999). Although K_m is independent of enzyme concentration, V_{max} will vary with the total amount of enzyme present in the system (Palmer, 1995). A compound that has a low K_m and a high V_{max} is considered a better substrate than one with a high K_m and a low V_{max} (Holt, 1999). A knowledge of V_{max} and K_m values is useful for the estimation of intracellular reaction rates, detection of metabolic control points, comparisons of isoenzymes from different tissues or organisms, determination of the molecular events of catalysis, determination of turnover numbers, quantitive comparison of alternative substrates and for definition of the potency of inhibitors or activators (Henderson, 1998).

Since the Michaelis-Menten plot is a hyperbola, it is easiest to determine K_m and V_{max} values by using a computer program. Alternately, the same data can be transformed and replotted in a variety of ways so that a straight line is obtained and the values for K_m and V_{max} can be ascertained from the slopes and intercepts of the straight line. Three examples of these linear plots are the Hanes-Woolf plot ([S]/v versus [S]), the Hofstee plot (v versus v/[S]) and the Lineweaver-Burk plot (1/v versus 1/[S]). The Hanes-Woolf plot is the preferred linear method by which K_m and V_{max} values are obtained since it causes the least distortion of experimental error and yields the most reproducible kinetic values. In addition, it yields the values closest to those obtained from computerized analysis of the hyperbola (Holt, 1999). However, Henderson (1998) suggests that these plots should not be used for anything other than display purposes. The one statistically

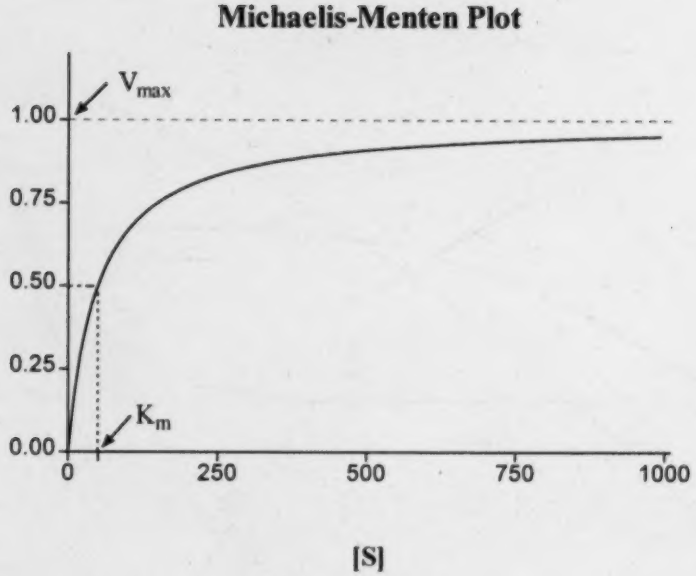

Figure 1-5: A Michaelis-Menten plot showing the parameters K_m and V_{max} (adapted from Holt, 1999).

sound method for the determination of the best fit K_m and V_{max} values is the direct linear plot (Henderson, 1998; Holt, 1999). Using the direct linear plot, values of [S] are plotted on a negative horizontal axis and experimentally determined values of *v* are plotted on the vertical axis. If this is done for two or more pairs of ([S], *v*) values, straight lines can be drawn through corresponding [S] and *v* points intersecting at $[S] = K_m$ and $v = V_{max}$ (Holt, 1999).

If a preparation contains two or more enzymes that catalyze the same reaction, the velocity at any substrate concentration is the sum of the velocities contributed by each enzyme. In these cases, a replotting of data on a linear plot will not give rise to a straight line and K_m and V_{max} values are not easily ascertained (Figure 1-6). The data would still need to be analyzed by computer to ascertain the K_m and V_{max} values of each enzyme involved in the reaction (Segal, 1975). Thus, it would seem more appropriate to determine the kinetic values of K_m and V_{max} by fitting data to a Michaelis-Menten Equation that is expanded to include terms for the separate enzymes and in which no transformation of data is required. The following equation would be the Michaelis-Menten equation if two enzymes were involved in a particular metabolic route:

$$v = \frac{V_{maxa}[S]}{[S] + K_{ma}} + \frac{V_{maxb}[S]}{[S] + K_{mb}}$$

The terms a and b refer to the two separate enzymes involved in one metabolic route (Segel, 1975).

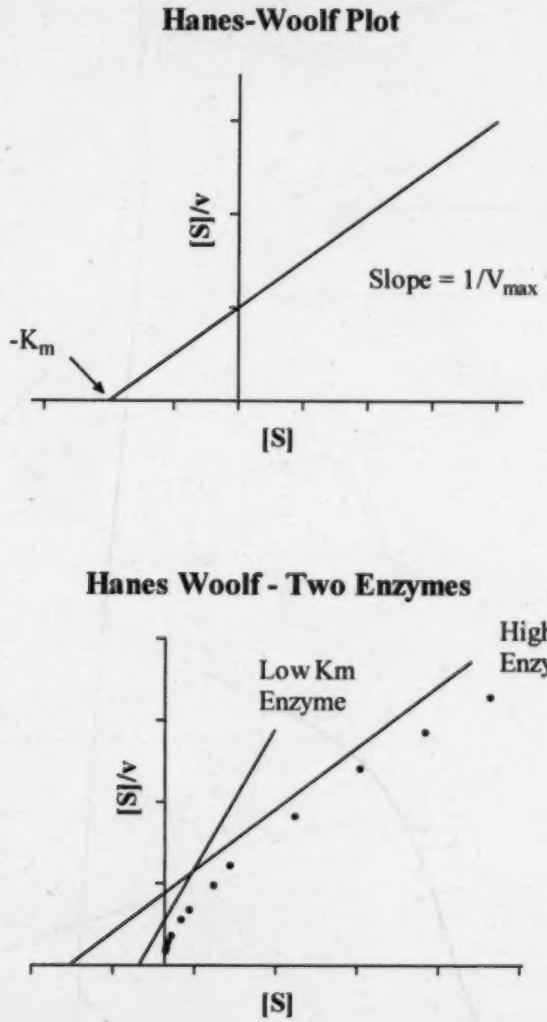

Figure 1-6: Determination of K_m and V_{max} values using a Hanes-Woolf plot and the difficulties of estimating K_m and V_{max} in the presence of two enzymes (adapted from Holt, 1999 and Segal, 1975).

1.4 INHIBITION OF DRUG METABOLISM

1.4.1 MECHANISM OF INHIBITION

Inhibitors are substances that decrease the rate of an enzyme-catalyzed reaction. Inhibitors may act on the substrate, cofactor or enzyme (Palmer, 1995). Although most enzyme inhibitors are reversible, some may be irreversible. Reversible inhibitors can be removed by dialysis, dilution or gel filtration, restoring enzyme activity (Holt, 1999). In addition, an equilibrium system is rapidly formed between the enzyme and the inhibitor, resulting in inhibition of the enzyme activity that will remain constant over time (Palmer, 1995). Irreversible inhibitors, on the other hand, covalently bind to the enzyme, and the enzyme activity cannot be restored by dialysis and related processes (Holt, 1999). In addition, the extent of the inhibition may increase over time. Irreversible inhibitors may act by preventing substrate binding or it may inactivate some part of the catalytic site (Palmer 1995).

Inhibitory drug interactions with the CYP enzymes usually fall into three categories. The simplest case involves competition for the enzyme's active site between two substrates that are metabolized by the same CYP enzyme (Murray, 1987; Parkinson, 1996). CYP enzymes are interesting in that they allow two binding modes, namely productive binding to the hydrophobic substrate binding site (substrate binding) and inhibitory binding to the heme iron (ligand binding) (Testa, 1990).

Besides competition between two substrates, ligand binding due to electrostatic interactions with the iron cation offers a second mechanism for CYP enzyme inhibition (Testa, 1990). This second inhibitory drug interaction is also competitive and reversible, but the inhibitor is not a substrate for the affected CYP enzyme (Parkinson, 1996;

Halpert, 1995). Examples of compounds that exert their inhibitor effect in this manner are nitrogen heterocycles such as the imidazoles (i.e. ketoconazole) and the quinolines (i.e. quinidine) (Murray, 1987; Halpert, 1995). Generally these compounds rely on hydrophobic interactions with the protein moiety of the CYP enzyme as well as specific interactions of the lone electron pair of the nitrogen and the heme iron. Because binding can occur to the oxidized (ferric) or reduced (ferrous) forms of the CYP enzyme as well as to both the protein and heme moieties, these nitrogen heterocycle compounds can interfere with substrate and oxygen binding (Halpert, 1995). The kinetics associated with competitive inhibitors will be discussed in section 1.4.2.

The third type of inhibition involves drugs that undergo metabolic activation by the CYP system, forming inhibitory products. The metabolic products may form relatively stable complexes with the CYP enzyme so that it is sequestered in a functionally inactive state, and this inactivation may be reversible. In another scenario, the metabolite may inactivate the enzyme by heme or apoprotein modification which is irreversible; this effect is referred to as suicide processing or autocatalytic inactivation. An example of a drug class that forms metabolite complexes with the CYP enzyme is the macrolide antibiotics (*e.g.* erythromycin) (Murray, 1987); it has been proposed that once metabolized, a nitroso derivative traps the CYP enzyme in its Fe^{2+} oxidation state (Murray, 1987) and prevents oxygen binding (Halpert, 1995). Irreversible heme modification involves such drugs as fluroxene (a general anesthetic agent); alkylation of the heme group by reactive intermediates results in the subsequent loss of the heme iron from the CYP which renders the enzyme catalytically inactive (Murray, 1987). Irreversible apoprotein modification is an example of inhibition caused by the oxamyl chloride metabolite of the antibiotic chloramphenicol. This drug apparently modifies one

or more lysine residues in the protein moiety of CYP2B1, preventing electron transfer from NADPH-cytochrome P450 reductase (Halpert, 1995).

1.4.2 COMPETITIVE INHIBITION

Competitive inhibitors often resemble the substrates whose metabolism they inhibit (Palmer 1995). The inhibitor can bind at the enzyme active site, preventing binding of the substrate or it can bind at an allosteric site, causing a conformational change at the enzyme active site, preventing substrate binding (Holt, 1999). Once the inhibitor has bound to the enzyme, a dead end complex is formed since the enzyme-catalyzed reaction cannot take place. The inhibitor must dissociate from the enzyme and be replaced by a molecule of substrate before a reaction can take place (Palmer, 1995).

The effect of the competitive inhibitor will depend on the inhibitor concentration, the substrate concentration and the relative affinities of the substrate and inhibitor for the enzyme. Thus at a particular inhibitor and enzyme concentration, if the substrate concentration is low, the inhibitor is free of competition and can bind to the enzyme, resulting in a high degree of inhibition. Conversely, at very high concentrations of substrate, the inhibitor is less successful in binding to the enzyme and the effect of the inhibitor is negligible. Thus, in the presence of a competitive inhibitor the V_{max} of the reaction remains unchanged and the K_m is increased (Palmer, 1995). In the presence of inhibitor, the K_m is now apparently increased and is termed $K_{m\ app}$ (Holt, 1999). The action of the competitive inhibition can be graphically presented on a Michaelis-Menten plot (Figure 1-7) (Palmer, 1995).

The interaction of enzyme with inhibitor and substrate can be represented by the following equation (Palmer, 1995):

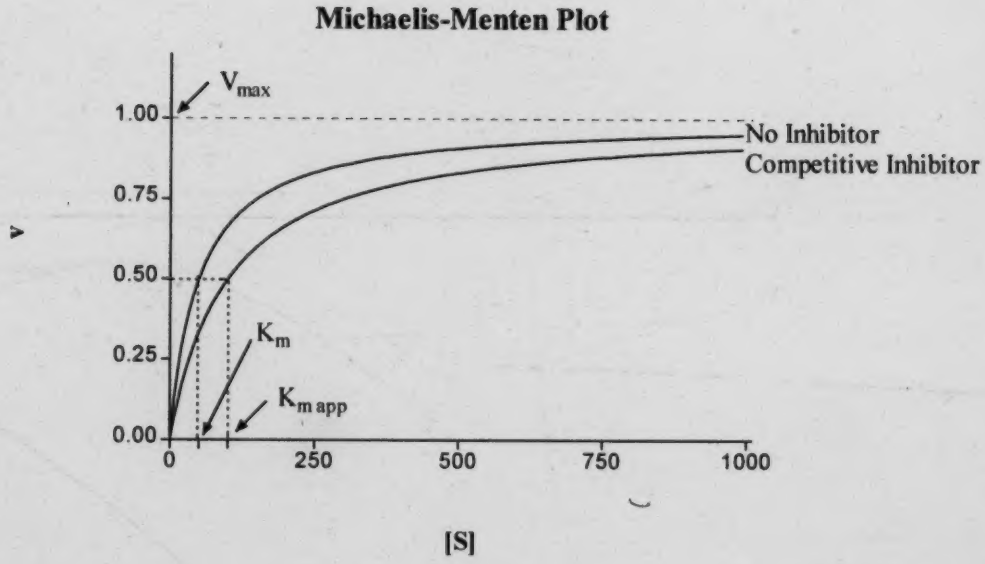

Figure 1-7: The effect of a competitive inhibitor as seen on a Michaelis-Menten plot (adapted from Palmer, 1995).

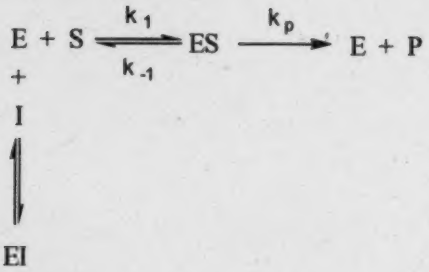

Where: E = enzyme

S = substrate

ES = enzyme-substrate complex

P = product

I = inhibitor

EI = enzyme-inhibitor complex

Reversible inhibitors can associate and dissociate from the enzyme and thus equilibrium will exist between bound and unbound enzyme. The potency of the inhibitor can be quantitated by determining the equilibrium (or dissociation) constant. The equilibrium constant for an enzyme-inhibitor interaction is more commonly referred to as the inhibitor constant and is in fact a measure of the affinity of the inhibitor for the enzyme. The inhibitor constant is given the symbol K_i. The K_i value is numerically equal to the concentration of inhibitor required to occupy 50% of the enzyme active sites at equilibrium. The higher the affinity of the inhibitor for the enzyme, the lower the K_i value (Holt, 1999).

1.4.3 DETERMINING INHIBITION CONSTANTS

A K_i value for an inhibitor can be ascertained in a variety of ways. Commonly, it involves a secondary plot of slopes (corresponding to the value $K_{m\ app}/V_{max}$) obtained

from Lineweaver-Burk plots at several inhibitor concentrations. The slope of each line is plotted against the inhibitor concentration and the intercept with the x-axis is equal to $-K_i$. Due the inherent problems associated with Lineweaver-Burk plots, it may be more appropriate to determine values for $K_{m\ app}/V_{max}$ from Hanes-Woolf plots and plot those against inhibitor concentrations (Holt 1995). Dixon plots can also be used to determine K_i. According to Dixon, plotting 1/v versus inhibitor concentration when substrate concentration is kept constant will produce a straight line. If this experiment is conducted at two different substrate concentrations the lines will intersect at a point of $-K_i$ (Dixon, 1953).

In inhibition studies using human liver microsomes, more than one CYP enzyme may catalyze the same reaction. Thus, it is necessary to obtain an inhibitor constant for each of the enzymes in question. This would be complicated using secondary plots of Lineweaver-Burk and Hanes-Woolf plots, simply because the primary plots will not easily generate the different K_m and V_{max} values necessary to construct the secondary plot. Even in the case of Dixon plots, the inhibition will represent the effect of the inhibitor on all the enzymes contributing to a metabolic pathway.

Due to the limitations of these approaches, an alternate approach may prove useful. In this approach, an IC_{50} value is generated. An IC_{50} value is the concentration of inhibitor that produces 50% of maximum inhibition. The IC_{50} value is determined from a sigmoid plot of velocity expressed as a percent of control versus inhibitor concentration expressed as $\log_{10}$ values (Holt, 1999). If two enzymes are contributing to the same metabolic pathway, the IC_{50} can be calculated for each enzyme (Holt, personal communication) (Figure 1-8).

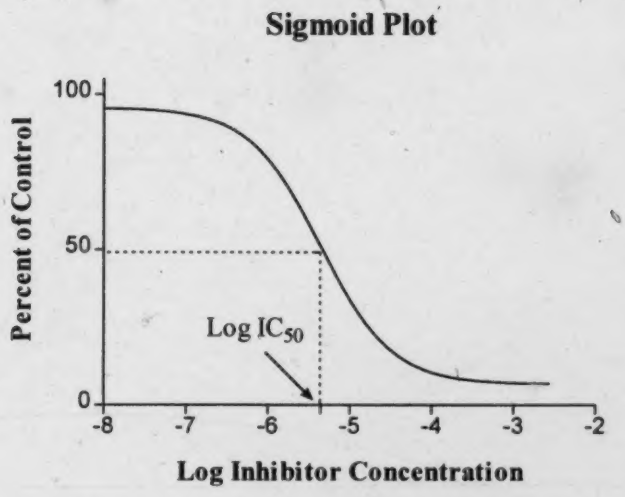

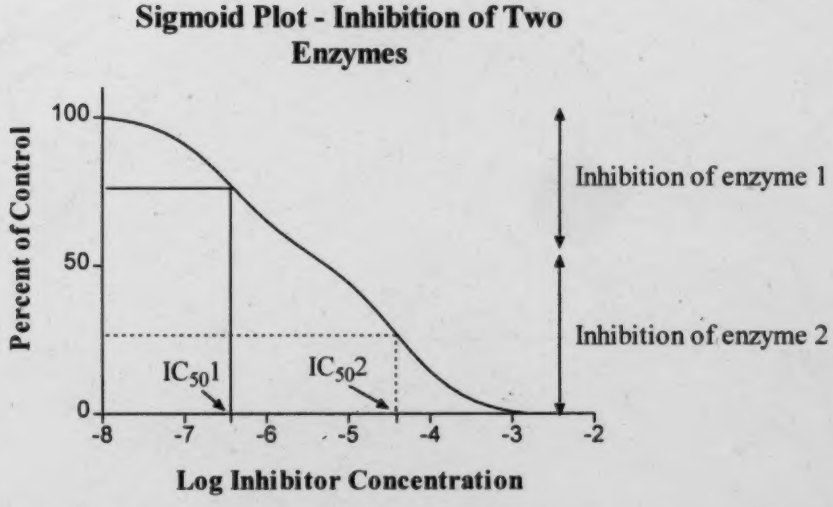

Figure 1-8: Sigmoid curves demonstrating the determination of IC_{50} values (adapted from Holt, personal communication).

The IC_{50} is related to K_i by the Cheng-Prusoff equation as follows:

$$K_i = \frac{IC_{50}}{1 + \frac{[S]}{K_m}}$$

Where: K_i = inhibitor constant

IC_{50} = concentration of inhibitor that produces half of its maximum inhibition

S = substrate concentration

K_m = concentration of substrate that produces half maximum velocity

Since both K_i and K_m are constants, the IC_{50} value will depend on the value of [S]. Since the IC_{50} value will depend on assay conditions, inhibitor potency is more easily compared by comparing K_i values (Holt, 1999; Cheng and Prushoff, 1973).

1.5 COMPARISON OF IN VITRO AND IN VIVO DATA

The relevance of drug metabolism data obtained *in vitro* to the clinical situation *in vivo* is always an area of concern. Numerous approaches have been developed to identify human CYP enzymes involved in the metabolism of xenobiotics *in vitro*. These approaches include correlation between activities of enzyme-selective substrates with use of a bank of human liver samples; analysis of the competitive inhibition of enzyme-selective substrates with the use of human liver microsomes; study of the effects of enzyme-selective inhibitory probes; determination of drug metabolism by transgenic human cells expressing drug metabolizing enzymes; and characterization of drug metabolism in the presence of specific inhibitory antibodies (Bourrié *et al.*, 1996). A

combination of these approaches provides a higher degree of certainty in the identification of enzymes involved in the metabolism of a xenobiotic (Bourrié *et al.*, 1996; Guengerich, 1996a).

Because kinetic experiments are conducted *in vitro*, it cannot be assumed that the values for K_m and V_{max} are the same for the enzyme *in vivo* (Holt, 1997). The rates of metabolism for *in vitro* systems are dependent on a number of factors, including pH and protein and phospholipid content. Typically, no plasma proteins are present, pH is adjusted to non-physiological values to enhance the metabolic rate and the role of phospholipids is ignored (Bertz and Granneman, 1997). Additional considerations should include evaluation of drug metabolism and particularly drug-drug interactions at relevant therapeutic concentrations and the possibility of metabolic switching between oxidative, reductive and conjugative pathways. Consideration of absorption and bioavailability, extrahepatic metabolism, the contribution of protein and tissue binding, drug transport, and other pathways of elimination (renal and biliary) to the overall disposition of drugs is also necessary (Remmel and Burchell, 1993).

Iwatsubo *et al.* (1997) demonstrated that *in vitro* intrinsic clearance data could successfully predict *in vivo* intrinsic clearance data for some compounds. Intrinsic clearance is the maximum ability of the liver to extract drug in the absence of blood flow restrictions (Gibson and Skett, 1994). With respect to MET, the *in vitro* and *in vivo* intrinsic clearances were considered to be comparable. The *in vitro* intrinsic clearance calculated using microsome preparations was 0.179 and 0.955 for the α-hydroxylation and O-desmethylation pathways, respectively whereas the *in vivo* intrinsic clearance was 0.1 and 0.586, respectively (Iwatsubo *et al.*, 1997). However, for some metabolic reactions the intrinsic clearance values were not comparable. The differences were

possibly due to metabolism in tissues other than liver; incorrect assumption of rapid equilibrium of drugs between blood and hepatocytes; presence of active transport through the sinusoidal membrane; and interindividual variability (Iwatsubo *et al.*, 1997).

However, determining drug concentrations to use in *in vitro* microsome experiments poses several problems. Although plasma concentrations of the drugs being used are probably readily known, there is often little information regarding the hepatic concentrations of those drugs. In an attempt to determine the extent to which plasma drug concentrations correspond to those in hepatic tissues, von Molke *et al.*, (1994a) measured liver:water partition ratios. Simply, mouse liver homogenate was spiked with 5 μg of the drug being studied and centrifuged at 400 g for 10 min. The amount of drug in the pellet was then compared to the drug in the supernatant. This ratio would be multiplied by the plasma concentration to ascertain a liver concentration. This *in vitro* partitioning method assumes distribution by passive diffusion (von Molke *et al.*, 1994b). Since partitioning of lipophilic drugs between plasma and hepatic tissue depends on a variety of factors such as time after dosage, size of dose, route of administration, the extent of presystemic extraction, plasma protein binding and plasma:red cell distribution, this *in vitro* partitioning method is likely to present an oversimplification of the process (von Molke *et al.*, 1994b) which may or may not be valid (Popli *et al.*, 1995). Determining liver:plasma ratios could also be determined using animal and human postmortem samples. These approaches are not without their disadvantages but they do, however, demonstrate that liver concentrations of lipophilic compounds exceed total plasma concentrations (von Molke *et al.*, 1998). Another limitation is that hepatic concentrations are not constant, with the highest concentration occurring during first pass metabolism (Tucker, 1982).

Even if hepatic concentrations are known, it is sometimes difficult to use therapeutic concentrations in *in vitro* experiments due to the limit of quantitation of the analytical method. In the event that microsome experiments adequately reflect *in vivo* events such as intrinsic clearance, the drug concentration used in *in vitro* experiments is still of importance. If, for example, a low and a high affinity enzyme is responsible for the metabolism of a substrate, using a high concentration of drug in the *in vitro* experiment could seriously underestimate the intrinsic metabolic activity responsible for the high affinity metabolic pathway (Iwatsubo *et al.*, 1997).

Although there are limitations to *in vitro* experiments, there have been attempts to ascertain the clinical relevance of drug interactions. One approach is to compare K_i values estimated *in vitro* with hepatic concentrations of the inhibitor *in vivo*. If the K_i is less than or similar to the hepatic concentration, than the inhibition would be considered clinically relevant (Harvey and Preskorn, 1995). Another approach involves predicting the percent inhibition of the substrate's clearance in the presence of inhibitor by using the concentration of inhibitor in the plasma and the estimated *in vitro* values for K_m and K_i according to the following equation:

$$\% \text{ Inhibition} = \frac{I}{I + K_i\,(1 + ([S]/K_m))} \times 100$$

Where: I = inhibitor concentration *in vivo*

K_i = inhibitor constant determined *in vitro*

K_m = Michaelis-Menten constant determined *in vitro*

[S] = substrate concentration *in vivo*

If the substrate concentration is much less than the estimated K_m, the equation reduces to:

$$\% \text{ Inhibition} = \frac{I}{I + K_i} \times 100$$

Using hepatic concentrations of I and S would likely increase the predictive value of this model (von Molke *et al.*, 1994a, 1994b, 1998). However, based on the previous discussion, determining hepatic concentrations is not without its own limitations. One suggestion is that *in vitro* work offers an early warning system for rational selection of drugs for *in vivo* studies (Tucker, 1992).

1.6 CLINICAL IMPLICATIONS OF THE PROJECT DESCRIBED IN THIS THESIS

1.6.1 HYPERTENSION

Hypertension is one of the most common chronic medical conditions, with a lifetime prevalence rate of 17.9% (Wells *et al.*, 1989). Hypertension is defined as a persistent elevation of blood pressure, even in a resting state, with the majority of cases having an etiology of unknown origin (Bremner, 1984). One of the major advances in cardiovascular therapeutics was the introduction, in the 1960s, of drugs which block β-adrenergic receptors (Östhholm, 1975). β-blockers continue to be important components of the treatment approach to hypertension (Asperheim, 1996). In addition to their use in hypertension, β-blockers are also used to treat essential tremor, migraine and the physical symptoms associated with anxiety. These drugs have also been shown to be effective in reducing the frequency of reinfarction and death after myocardial infarction (Emilien and Maloteaux, 1998).

β-Blockers function to prevent the persistent stimulatory input of β-adrenergic receptor sites of muscle cells (Bremner, 1984). β-Blockers are ethanolamine or

propanolamine derivatives that are weak bases (Lennard, 1989). The structures of some of these drugs are shown in Figure 1-9. The β-blockers show marked differences not only in their pharmacodynamic properties but also in their pharmacokinetic characteristics. The pharmacodynamic properties deal with their selectivity for β-adrenergic receptors found in the heart (β_1) and bronchi and peripheral vessels (β_2). Ideally, the β-blockers would show good therapeutic efficacy and have sufficient cardioselectivity so as to have reduced risks of provoking bronchial asthma and other possible drawbacks of β-receptor blockade (Östhholm, 1975).

The pharmacokinetic differences deal with variation in absorption in the gastrointestinal tract, liver metabolism, plasma protein binding, volume of distribution and renal or biliary elimination of the drugs (Borchard, 1990). The broad range of lipophilicity of the β-blockers determines to a large extent how they are metabolized. Some compounds, such as atenolol, nadolol and sotalol, are hydrophilic and are excreted predominantly unchanged in the urine and feces (Lennard, 1989). Other compounds, such as pindolol, acebutalol and to a lesser extent timolol, are considered to have a better-balanced renal and hepatic clearance. The lipophilic drugs such as MET, propranolol and oxprenolol are eliminated almost exclusively by the hepatic route (Meier, 1982). The lipophilic drugs can also cross the blood-brain barrier and may cause a number of central nervous system side-effects such as confusion and blurring of vision. However, adverse reactions to β-blockers are uncommon (Prichard *et al.*, 1981). There have also been claims that β-blockers cause depression but the evidence for such an association is not

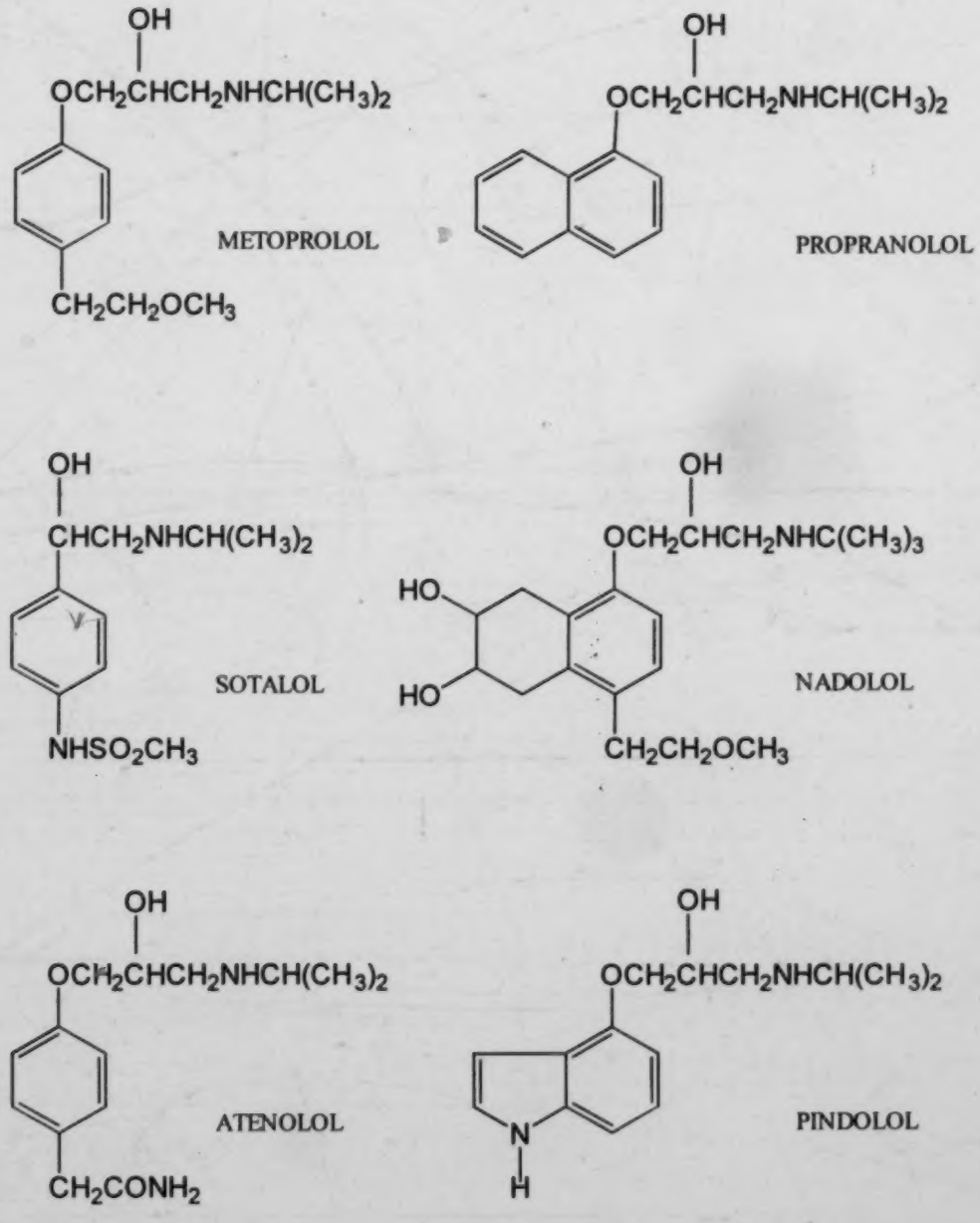

Figure 1-9: Structures of some of the β-adrenergic receptor blockers (adapted from Meier, 1982).

scientifically persuasive (Ried *et al.*, 1998). Table 1-7 lists the pharmacological properties of several β-blockers. Although these tables are not exhaustive, they do demonstrate the variability in this drug class.

According to the list published by *Pharmacy Practice* in December, 1998, MET is the most commonly prescribed β-blocker (Anonymous, 1998) even after being in the marketplace for nearly 30 years (Östhholm, 1975). It is a frequently prescribed compound in general, ranking as number 59 on this list of the top 200 prescription products in Canada (Anonymous, 1998). MET is a relatively selective antagonist for β_1-adrenergic receptors that is devoid of agonist activity. It is this relative β_1 selectivity that is probably the basis for its potential therapeutic advantage over less selective agents (Weiner, 1980). However, this selectivity is lost with higher doses or plasma concentrations of MET (Lennard *et al.*, 1982).

1.6.2 DEPRESSION

Affective disorders are diseases of mood regulation and are accompanied by altered rates of cognition and by physical signs and symptoms (Garver, 1984). Affective disorders include major depression, mania and dysthymia. The lifetime prevalence rate of major depression is about 15% (Kaplan and Sadock, 1998), with some studies reporting prevalence rates of as high as 27.4% (Lespérance *et al.*, 1996). In addition, depression is twice as prevalent in the female population (Kaplan and Sadock, 1998). Major depression is diagnosed based on the presentation of at least five different symptoms, one of which must be depressed mood or loss of interest which persist for at least 2 weeks. The other symptoms include significant weight loss or weight gain (*e.g.* a change of more than 5% of body weight in a month); insomnia or hypersomnia;

β-Adrenergic Selectvity	Drug	Bio-availability (%)	First-pass Efect	Active Metabolite	Renal Elimination (%)		$t_{1/2}$ (hour)
					Unchanged	Total	
β_1	Atenolol	50	-	-	95	95	6-9
β_1/β_2	Nadolol	30	-	-	95	95	14-24
β_1/β_2	Sotalol	75-90	-	-	95	95	15
β_1/β_2	Pindolol	100	-	-	40	95	3-4
β_1	Metoprolol	50	+	-	3	95	3-4
β_1/β_2	Propranolol	30	+	+	1	95	3-4

Table 1-7: Comparison of the pharmacokinetic parameters of several β-blockers [- denotes negligible activity or effect] (adapted from Borchard, 1990 and Weiner, 1980).

psychomotor agitation or retardation; fatigue; feelings of worthlessness or excessive or inappropriate guilt; diminished ability to think or concentrate, or indecisiveness; recurrent thoughts of death, recurrent suicidal ideation without a specific plan, or a suicide attempt or a specific plan for committing suicide (Kaplan and Sadock, 1998).

There are numerous drugs used in the treatment of depression. They can be classified according to structure or presumed mechanism of action (Preskorn, 1994). Two of these classes are the tricyclic antidepressants [a class based on structure (Figure 1-10)] and the selective serotonin reuptake inhibitors (SSRIs) [a class based on common pharmacological activity (Figure 1-11)]. The tricyclic antidepressants block both noradrenaline and serotonin reuptake to varying degrees. In addition, the tricyclics interact to varying degrees with H_1 histaminergic, α_1 adrenergic and muscarinic cholinergic receptors. The SSRIs are considered selective inhibitors of the reuptake of serotonin (Frazer, 1997). Table 1-8 lists the relative potency of several of the tricyclics and SSRIs in blocking serotonin and noradrenaline reuptake.

1.6.3 COMORBIDITY

The prevalence rates of both hypertension and depression lead to questions regarding the comorbidity of these two disorders. The prevalence of lifetime affective disorder in persons with lifetime hypertension is 16.4% (Wells *et al.*, 1989). More specifically, in a study of depressed patients receiving ongoing care (not necessarily for depression) the prevalence of hypertension in those patients with a lifetime depressive disorder was 43.1% or 24.4%, depending if the treating clinician was a general medical provider or a mental health specialist, respectively (Wells *et al.*,1991). The prevalence of comorbid disorders is of clinical interest for several reasons, including difficulty in

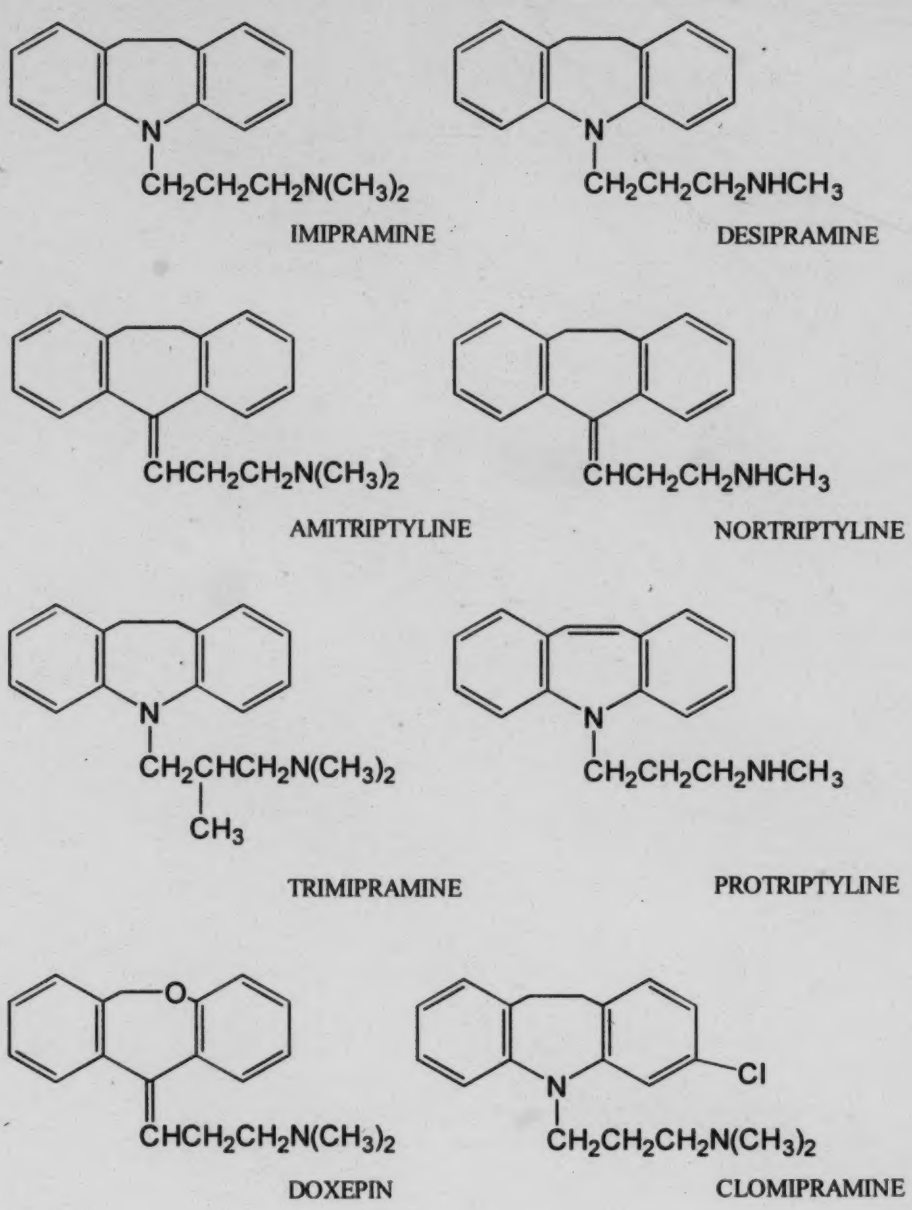

Figure 1-10: Structures of some tricyclic antidepressants (adapted from Potter *et al.*, 1998).

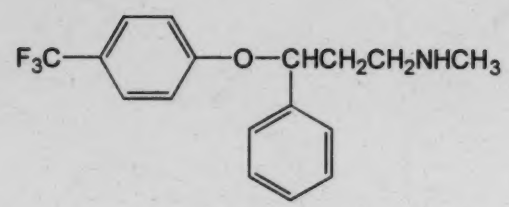

FLUOXETINE

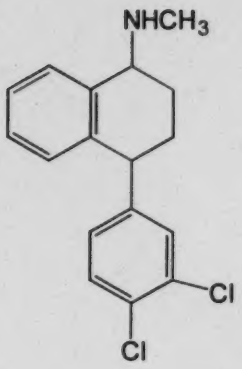

SERTRALINE

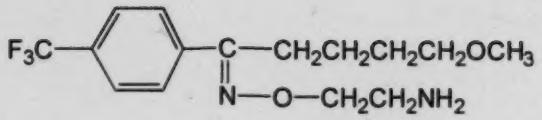

FLUVOXAMINE

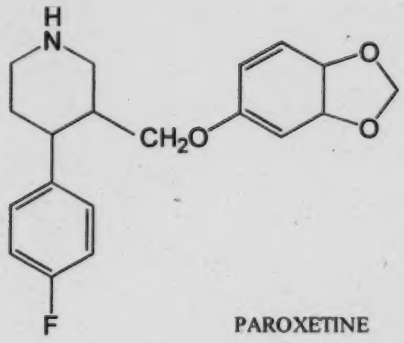

PAROXETINE

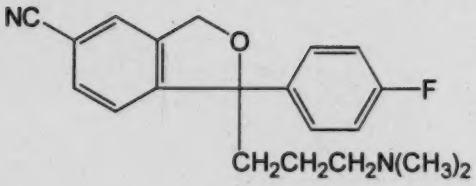

CITALOPRAM

Figure 1-11: Structures of the SSRIs (adapted from Tollefson and Rosenbaum, 1998).

Classification	Drug	K_i Values (nM)	
		Noradrenaline Reuptake	Serotonin Reuptake
Tricyclic Antidepressants	Amitriptyline	24	66
	Clomipramine	28	5.4
	Desipramine	0.9	340
	Doxepin	19	280
	Imipramine	13	42
	Nortriptyline	4	260
	Protriptyline	0.97	280
	Trimipramine	510	2500
Selective Serotonin Reuptake Inhibitors	Citalopram	4000	1.3
	Fluoxetine	280	12
	Fluvoxamine	500	7
	Paroxetine	33	0.73
	Sertraline	220	3.4

Table 1-8: Potency of antidepressants at blocking the reuptake of noradrenaline and serotonin (data obtained from Richelson and Pfenning, 1984 and Bolden-Watson and Richelson, 1993).

adequately detecting and assessing the individual conditions. In addition, the drug treatments for the two types of disorders may interact (Wells *et al.*, 1988).

1.6.4 DRUG-DRUG INTERACTIONS

Drug-drug interactions may be of a pharmacokinetic or pharmacodynamic nature. Pharmacokinetic drug interactions occur when one drug potentiates or diminishes the actions of another by affecting its absorption from the site of administration, its disposition within the body, its metabolism or excretion. Pharmacodynamic interactions occur when one drug potentiates or diminishes an effect of another drug while not affecting its metabolism or disposition (Preskorn, 1995). With respect to MET, there have been several reports in the literature involving drug-drug interactions. One report deals with a drug-drug interaction between MET and FLU in which the patient experienced profound lethargy and bradycardia (Walley *et al.*, 1993). Another report deals with the interaction of MET and PAR in which the patient experienced bradycardia (Konig *et al.*, 1996). Other reports involve coadministration of MET and verapamil in which patients experienced symptoms such as hypotension, bradycardia and congestive cardiac failure (Wayne *et al.*, 1982). In other reports, the addition of verapamil to MET resulted in an increase in the plasma concentrations of MET (McLean *et al.*, 1985; Keech *et al.*, 1986).

From the above examples it is obvious that drug-drug interactions with coadministered medications may occur with MET. Given the prevalence of comorbidity of hypertension and depression, possible drug-drug interactions between MET and selected antidepressants are a concern. Interestingly, comorbidity may become more of an issue with increasing age in women, in contrast to men, who have a higher risk of

hypertension in early adulthood, women have a higher risk of hypertension in later life (He *et al.*, 1998). This increased risk of hypertension, coupled with the fact that women are more prone than men to depression (Kaplan and Sadock, 1998), will undoubtedly increase the risk of being administered both a β-blocker and an antidepressant in aging women. In addition, it has been shown that depression following myocardial infarct is a significant predictor of mortality (Lespérance *et al.*, 1996; Frasure-Smith *et al.*,1993). Thus, treatment of both the myocardial infarct and the depression may lead to another scenario where drug-drug interactions between MET and antidepressants occur.

1.7 METOPROLOL

1.7.1 PHARMACOKINETICS OF METOPROLOL

MET is administered as a racemate, although the β-blocking activity is believed to reside in the S-enantiomer (Lennard, 1989). MET is a weak base having a pKa of 9.7. An oral dose of MET is rapidly and completely absorbed from the gastrointestinal tract (Regårdh *et al.*, 1974), resulting in a rapid onset of action (Johnsson *et al.*, 1975). Approximately 60% of the oral dose is metabolized during the initial transfer from the intestinal lumen to the systemic circulation, presumably due to hepatic removal of the drug, the so-called first–pass effect of the liver. Thus, MET is mainly eliminated from the body first by biotransformation which essentially takes place in the liver followed by excretion of the metabolites as well as the remaining fraction of the parent drug by the kidney (Regårdh *et al.*, 1974). The renal elimination of an oral dose of MET accounts for approximately 95% of the dose in man, and only 3% of that is unchanged MET (Borg *et al.*,1975; Borchard, 1990). MET has a half-life of approximately 3.1 hours after oral

administration (Regårdh *et al.*, 1974) and is about 12% bound to human serum proteins (Åblad *et al.*, 1975).

The original studies on metabolism using tritium labelled MET demonstrated there were three major routes of metabolism, as demonstrated in Figure 1-12. MET underwent O-demethylation, α-hydroxylation and N-dealkylation. These three routes accounted for approximately 85% of the dose in man, 63% of the dose in dogs and 88% of the dose in rats (Borg *et al.*, 1975). O-Desmethylmetoprolol (ODM) is further metabolized to an acid metabolite (AM) (Arfwidsson *et al.*, 1976). However, ODM was not detected in the urine of man but was found in the urine of rats (Borg *et al.*, 1975). ODM has been detected in *in vitro* studies using either rat or human liver microsomes (Arfwidsson *et al.*, 1976; Otton *et al.*, 1988). AM has been detected in human,dog and rat urine and in *in vitro* studies using rat liver microsomes (Arfwidsson *et al.*, 1976, Borg *et al.*, 1975). N-Dealkylmetoprolol (NDM) is also further metabolized to an acid metabolite which is found in the urine of man, dog and rat (Borg *et al.*, 1975). The acid metabolite of NDM has also been detected in rat liver microsomes. This acid metabolite may in fact result from two different pathways, with each pathway having a common aldehyde intermediate. (Arfwidsson *et al.*, 1976). The metabolite resulting from the α-hydroxylation of MET has been detected in rat and human urine, and in *in vitro* studies using rat and human liver microsomes (Arfwidsson *et al.*, 1976, Borg *et al.*, 1975, Otton *et al.*, 1988). The metabolites labelled 6, 7 and 8 have only been detected in rat urine (Arfwidsson *et al.*, 1976). The compound labelled as metabolite 9 has only been detected *in vitro* using rat liver microsomes (Arfwidsson *et al.*, 1976).

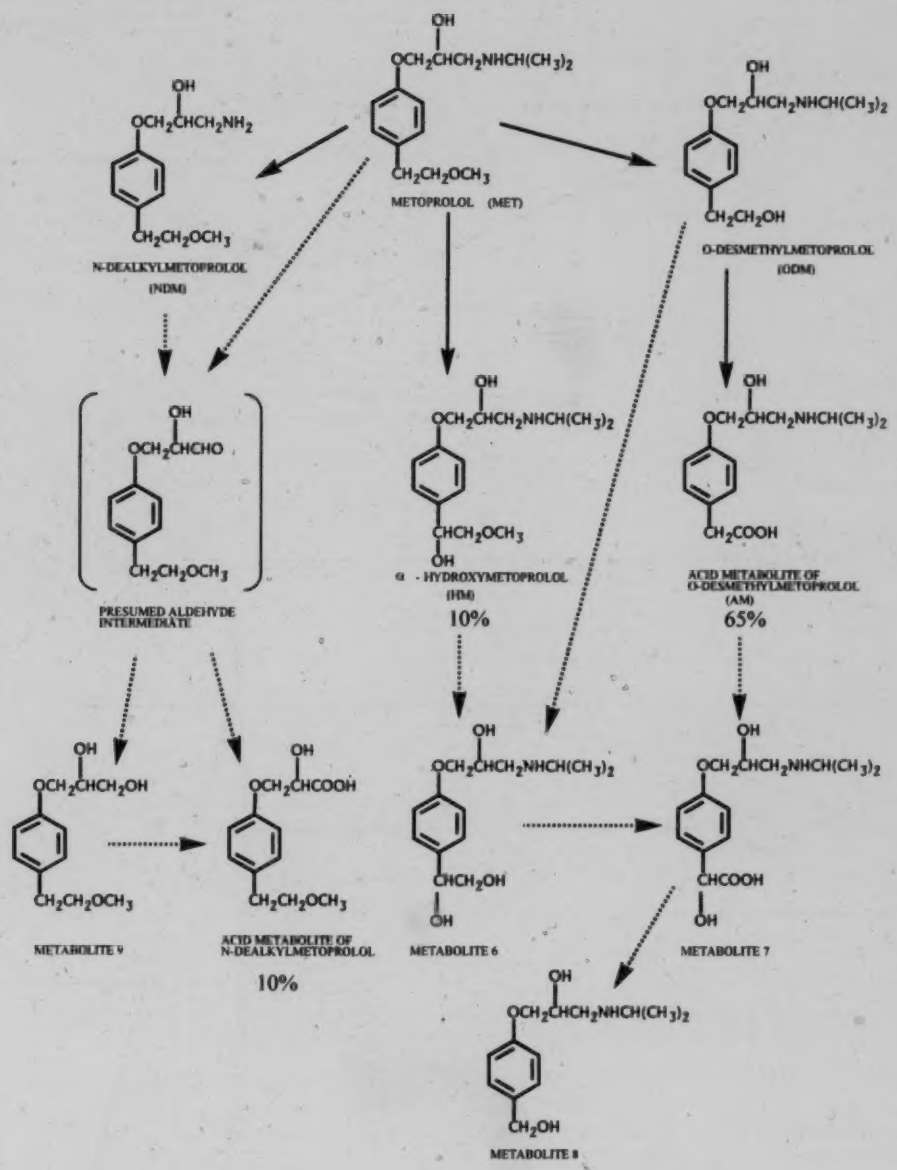

Figure 1-12: Proposed metabolic pathways in the metabolism of MET. The bold arrows indicate pathways studied in this thesis (adapted from Arfwidsson *et al.*, 1976; Walle and Gaffney, 1972).

The metabolites are not conjugated to any large extent before excretion. There are also differences in the abundances of the metabolites in each of these species, but in all three species, the O-demethylation route predominates. In man, the O-demethylation route accounts for 65% of the dose whereas the N-dealkylation and α-hydroxylation routes account for 10% each. In the rat, the O-demethylation route accounts for 62% of the dose whereas the N-dealkylation and the α-hydroxylation routes account for 1% and 25% of the dose respectively. In the dog, the O-demethylation route accounts for only 33% of the dose whereas the N-dealkylation route accounts for 21% of the dose; the α-hydroxylation route accounted for 9% of the dose (Table 1-9) (Borg *et al.*, 1975).

Both ODM and α-hydroxymetoprolol (HM) are considered to have β-blocking activity with the same effect pattern as MET, but their potency is considerably lower. There is no evidence to suggest that these metabolites make an important contribution to the pharmacological effect of MET (Borg *et al.*, 1975). In fact, even when the concentration of HM is 20 times higher than that of MET, the metabolite makes an insignificant contribution to the β-blocking effect of MET in man (Regårdh *et al.*, 1979).

1.7.2 RELEVANT CYP ENZYMES

The first evidence that MET was oxidized by CYP enzymes was provided by studies linking the metabolism of MET to the polymorphic CYP enzyme of the DQ type, now referred to as CYP2D6 (Kim *et al.*, 1993). It was shown that poor hydroxylators of DQ had six-fold higher areas under the plasma concentration-time curve (AUC) and a three-fold prolongation of the elimination half life of MET, compared to extensive hydroxylators of DQ. In addition, the urinary MET:HM ratios were widely divergent between the poor and extensive metabolizers of DQ, with the differences similar to those

Species	Dose	Relative abundance of each metabolite expressed as a percentage of amount excreted		
		Acid metabolite of ODM	Acid metabolite of NDM	HM
Man	50 mg *p.o.*	65	10	10
	5 mg *p.o.*	60	13	10
	5 mg *i.v.*	62	10	10
Dog	10 mg/kg	33	21	9
Rat	100 mg/kg	62	1	25

Table 1-9: Comparison of the relative abundance of the main urinary metabolites of MET in man, rat and dog (adapted from Borg *et al.*, 1975).

obtained with the DQ:4-hydroxyDQ ratio. However, given that the α-hydroxylation of MET is only a minor pathway in the metabolism of MET, it was put forward that another pathway in the metabolism of MET must also be under genetic control to account for the large increase in the AUC of poor metabolizers (Lennard *et al.*, 1982). However, there was no clear separation of the MET:AM ratio into two distinct phenotypes even though poor metabolizers had values at the upper end of the range for the population (Figure 1-13). The fact that there was a significant correlation between the MET/AM ratio, the DQ/4-hydroxyDQ ratio and the MET/HM ratio, suggested that the pathways were linked (McGourty *et al.*, 1985). However, Jack *et al.* (1983) believed the evidence was lacking for a claim of polymorphism in MET metabolism. Indeed, further studies have shown that even the correlation between DQ and MET hydroxylation phenotypes have been moderate to poor (Koytchev *et al.*, 1998). However, this does not negate the involvement of CYP2D6. It may be difficult to separate individuals into distinct populations due to heterozygous expression of CYP2D6. Interestingly, the administration of MET to volunteers homozygous (*CYP2D6*1/ CYP2D6*1*) and heterozygous (*CYP2D6*1/ CYP2D6*4*) for the wildtype allele showed that there could be up to a two-fold difference in the effective dose of MET (Koytchev *et al.*, 1998).

Additional studies demonstrated that the elimination of MET was stereoselective, with extensive metabolizers eliminating R-MET faster than S-MET, resulting in a 35% higher AUC of the S-enantiomer. In poor metabolizers, the clearance of R-MET was equal to or less than that for S-MET, but any differences seen were not as great as seen in extensive metabolizers (Figure 1-14). In addition, in poor, but not extensive metabolizers, β-adrenoceptor blockade is well maintained for 24 hours (Lennard *et al.*, 1983).

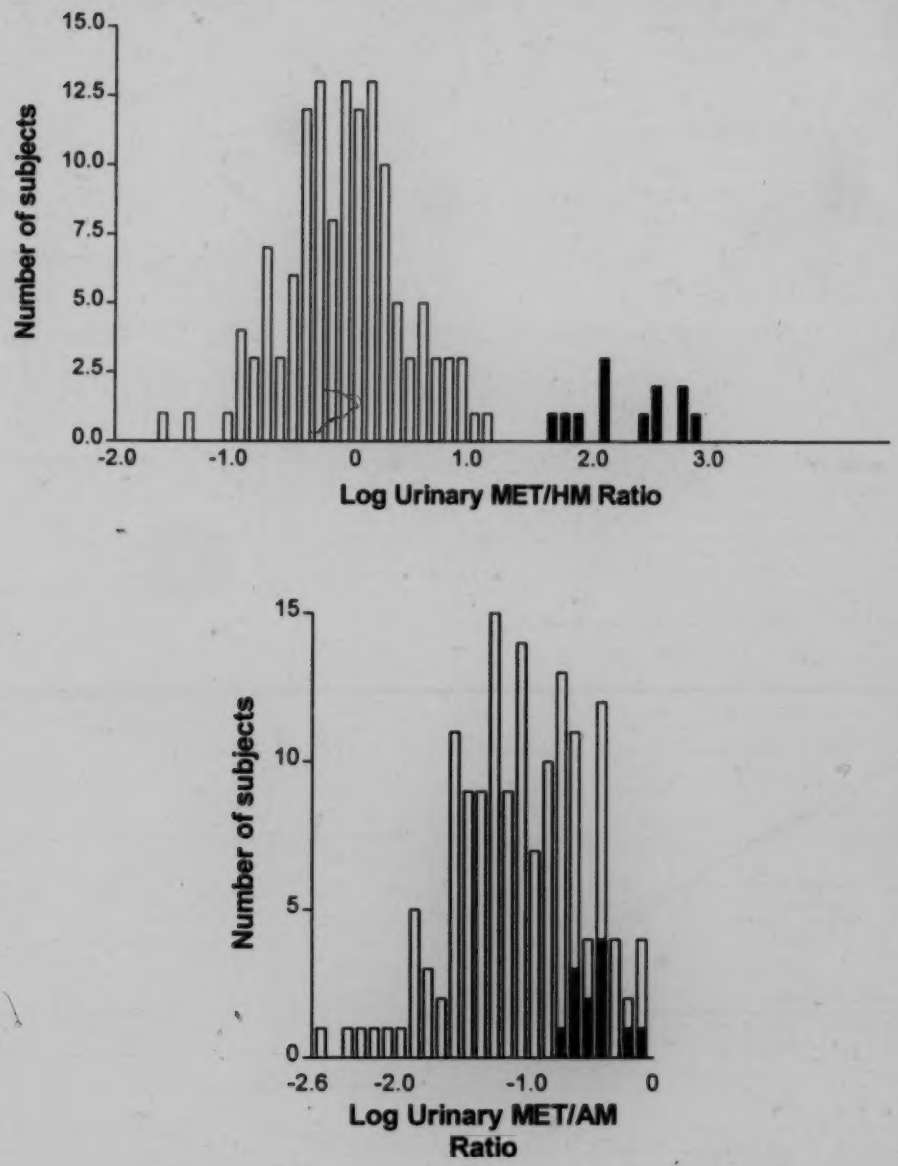

Figure 1-13: Frequency histograms of log metabolic ratios of MET/HM and MET/AM. Bolded bars indicate poor metabolizers of debrisoquine (adapted from McGourty *et al.*, 1986).

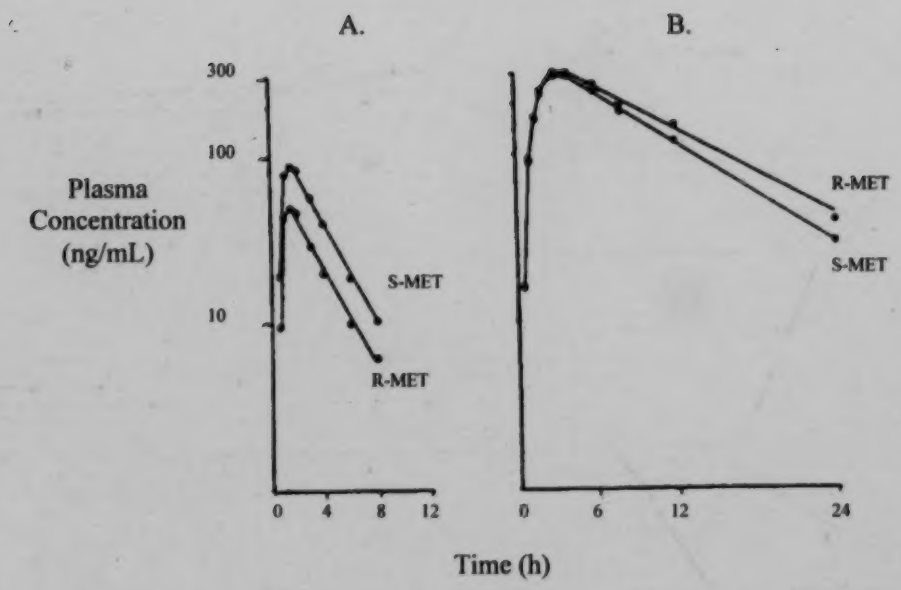

Figure 1-14: Metabolism of MET in an extensive (A) and a poor (B) metabolizer of debrisoquine (adapted from Lennard, 1983).

It has been demonstrated that the α-hydroxylation reaction is either not enantioselective in human liver microsomes (Otton *et al.*, 1988) or only slightly so, with a mean R/S ratio of approximately 0.9 in rat liver microsomes, human liver microsomes and human urine (Murthy *et al.*, 1990; Kim *et al.*, 1993). In addition, the α-hydroxylation of MET results in the formation of a new chiral centre, resulting in four products (R′R; R′S; S′R; S′S), with the formation of the new R′ enantiomer predominating regardless of the stereochemistry of the original compound (Murthy *et al.*, 1990).

The O-demethylation of the R-enantiomer seems to predominate slightly over the S-enantiomer in both human and rat liver microsomes, with R/S ratios of 1.09 and 1.18 respectively (Murthy *et al.*, 1990), although the difference was not significant in another study using human liver microsomes (Otton, *et al.*, 1988). The R/S ratio decreases with increasing concentrations of pseudoracemic MET, such that at concentrations greater than 400 μM the metabolism of the S-enantiomer predominates (Kim *et al.*, 1993). In human urine the R/S ratio of AM was 1.15 (Murthy *et al.*, 1990).

Both the O-demethylation and α-hydroxylation reactions appear to be biphasic, although the data did not always definitively support the involvement of two enzymes in the formation of HM (Otton *et al.*, 1988; Kim *et al.*, 1993). Observed enantioselectivity would therefore be a composite of the enantioselectivity of each of the different enzymes contributing to a metabolic pathway (Murthy *et al.*, 1990).

The O-demethylation process in human liver microsomes predominated over α-hydroxylation by 7-12 fold (Murthy *et al.*, 1990), consistent with the original studies in urine by Borg *et al.* (1975). Interestingly, in rat liver microsomes the α-hydroxylation reaction proceeded faster than the O-demethylation reaction (Murthy *et al.*, 1990;

Lennard *et al.*, 1986), which would seem contrary to the original studies by Borg *et al.* (1975). This contradiction may result from the inability to detect the acid metabolite in the microsome studies and thus underestimating the O-demethylation pathway. In fact, the study by Arfwidsson *et al.* (1976) has shown that the amount of AM in rat liver microsomes exceeds ODM. However, the combination of ODM plus AM will exceed HM production.

Both quinidine and quinine inhibited HM and ODM formation, with the quinine inhibition curves shifted to the right of those for quinidine, demonstrating that quinine is a less potent inhibitor of MET metabolism than quinidine. Although HM formation was totally inhibited by both quinine and quinidine in that study, part of the O-demethylation activity was resistant to inhibition by quinidine and quinine, supporting the hypothesis that the α-hydroxylation reaction was catalyzed by CYP2D6 but this enzyme was only partly responsible for the O-demethylation reaction. In addition, at low concentrations of MET where the high affinity enzyme makes its greatest contribution, O-demethylation of the R-(+)-enantiomer will predominate, which is consistent with the faster *in vivo* clearance of this enantiomer in extensive metabolizer subjects. Microsomes from a putative poor metabolizer demonstrated that no detectable levels of HM were formed and there was a preference for O-demethylating the S-(-)-enantiomer. This finding was consistent with the *in vivo* observation that poor metabolizer subjects clear S-MET more rapidly than R-MET (Otton *et al.*, 1988). Kim *et al.* (1993) also demonstrated inhibition by verapamil, a known inhibitor of CYP3A (Pichard *et al.*, 1990), of both the low and high affinity enzymes associated with ODM formation. With respect to HM formation, verapamil inhibited the high affinity component and verapamil was a more potent inhibitor of α-hydroxylation than O-demethylation. In addition, verapamil inhibited both

the low and high affinity components for O-demethylation enantioselectively, with R-MET inhibited to a greater degree than S-MET. However, this enantioselectivity decreased when higher concentrations of MET and verapamil were used (Kim *et al.*, 1993). This set of experiments demonstrated that the concentrations of substrates and inhibitors used in *in vitro* experiments may affect observed enantioselectivity. In addition, based on the *in vitro* experiments Kim *et al.* (1993) suggest that other factors, besides inhibition of hepatic clearance, may be responsible for the inbition of the metabolism of MET *in vivo* when coadministered with verapamil.

Although MET has been shown to competitively inhibit the metabolism of other CYP2D6 substrates, it does not seem to do so with much potency. The inhibitor constants for the competitive inhibition of sparteine metabolism to 2-dehydrosparteine (Otton *et al.*, 1984, Crewe *et al.*, 1992) and of desipramine 2-hydroxylation (von Bahr *et al.*, 1985) by MET are given in Table 1-10. For comparative purposes, the inhibitor constants of DMI, FLU, norfluoxetine (NFLU), FVX and PAR are also given. In addition MET was not shown to significantly change the DQ/4-hydroxyDQ MR in patients treated with MET (Kallio *et al.*, 1990).

1.8 PUTATIVE INHIBITORS OF THE METABOLISM OF METOPROLOL

The antidepressants FLU, FVX, PAR and DMI were investigated in this thesis to determine the extent to which these inhibitors decreased the metabolism of MET. DMI is metabolized to 2- hydroxydesipramine by CYP2D6 and should thus competitively inhibit other substrates of CYP2D6, as shown by its inhibition of 2-dehydrosparteine metabolism (Otton *et al.*,1983; Crewe *et al.*, 1992). CYP2D6 is also responsible for the metabolism of PAR. FLU is metabolized by CYP2C9 and to some extent by CYP3A and CYP2D6

Substrate	Inhibition of 2-dehydrosparteine formation			Inhibition of 2-hydroxydesipramine formation
	Crewe *et al.* (1992)	Otton *et al.*, (1984)	Otton *et al.*, (1983)	von Bahr *et al.* (1985)
Quinidine	0.03	0.06	nd	0.27
Quinine	-	15	nd	12
Metoprolol	37	18	nd	570
Paroxetine	0.15	nd	nd	nd
Fluoxetine	0.6	nd	nd	nd
Fluvoxamine	8.2	nd	nd	nd
Desipramine	2.3	nd	6	nd

Table 1-10: Inhibitor constants (K_i values) for the inhibition of sparteine and desipramine metabolism (nd = not determined).

and forms an active metabolite, NFLU. FVX is metabolized by CYP1A2 and CYP2D6 (Greenblatt *et al.*, 1998). Thus, there is a potential for competitive inhibition with other substrates of these enzymes (Reisenman, 1995).

Even prior to the elucidation of the CYP enzymes responsible for the biotransformation of these SSRIs, a great deal of attention was paid to the enzymes that these SSRIs inhibited. FLU and NFLU substantially inhibit CYP2D6 and moderately inhibit CYP2C19 and CYP2C9. NFLU also inhibits CYP3A4. PAR is a potent inhibitor of CYP2D6. Fluvoxamine substantially inhibits CYP2C19 and CYP1A2 and moderately inhibits CYP3A4 and CYP2C9 (Greenblatt, 1998; Preskorn, 1996). Table 1-11 summarizes the inhibitory effects of PAR, FLU, FVX and DMI on several of the CYP enzymes.

1.9 ANALYTICAL PROCEDURES

1.9.1 GENERAL PRINCIPLES OF CHROMATOGRAPHY

Modern chromatography began in 1906 with a separation of chlorophylls using a column of calcium carbonate (Tabor, 1984). Chromatography is a collective term applied to a wide variety of separation techniques based upon the sample partitioning between a moving phase which can be gas or liquid, and a stationary phase that can be either a liquid or a solid (Johnson and Stevenson, 1978). The two broad classes of chromatographic methods are gas chromatography and liquid chromatography classified according to the nature of their mobile phase. The discussion which follows will focus on two subdivisions of these methodologies: high performance liquid chromatography (HPLC) and capillary column gas chromatography (GC) (Tabor, 1984).

Antidepressant	Cytochrome P450 Enzymes					
	CYP1A2	CYP2C9	CYP2C19	CYP2D6	CYP2E1	CYP3A
Fluoxetine	+	++	+ → ++	+++	NA	+
Norfloxetine	+	++	+ → ++	+++	NA	++
Paroxetine	+	+	+	+++	NA	+
Fluvoxamine	+++	++	+++	+	NA	++
Desipramine	NA	NA	NA	++	NA	NA

Key:
+ = Mild inhibition
++ = Moderate inhibition
+++ = Strong inhibition
NA = No data available

Table 1-11: Inhibition of CYP enzymes by FLU, NFLU, PAR, FVX and DMI (adapted from Greenblatt *et al.*,1998 and Crewe *et al.*, 1992).

1.9.2 HIGH PERFORMANCE LIQUID CHROMATOGRAPHY

1.9.2.1 THEORY (Partition Chromatography with UV Detection)

A schematic diagram of an HPLC is shown in Figure 1-15. Briefly, the liquid mobile phase is taken from its reservoir and moved through the attached column by the use of a pump (Bowers, 1984). The pump can operate in either a gradient mode or isocratic mode. In the isocratic mode, the mobile phase composition remains constant throughout the chromatographic run. In the gradient mode, the mobile phase composition is either changed in a stepwise or continuous fashion throughout the run (Burtis *et al.*, 1987). The sample is introduced into the mobile phase before that phase reaches the column. Differential equilibrium of the analytes between the mobile phase and the stationary phase of the column results in their separation. The column effluent can be collected for further analysis or analyzed by a variety of detection systems (Bowers, 1984).

The theory surrounding separation of compounds in partition chromatography is actually a competition, in terms of solubility, between the mobile and stationary phases for the analyte (Bowers, 1984). A partition system in which the stationary phase is more polar than the mobile phase is classified as normal phase (Johnson and Stevens, 1978). In this system, non-polar analytes would elute first followed by more polar compounds (Bowers, 1984). A system in which the mobile phase is more polar than the stationary phase is classified as reverse phase (Johnson and Stevens, 1978). In this system, polar analytes would elute first. Reverse phase has become more popular than normal phase in biological applications due to the polar nature of many biological compounds (Bowers, 1984). To prevent dissolution of the stationary phase by the mobile phase, bonded

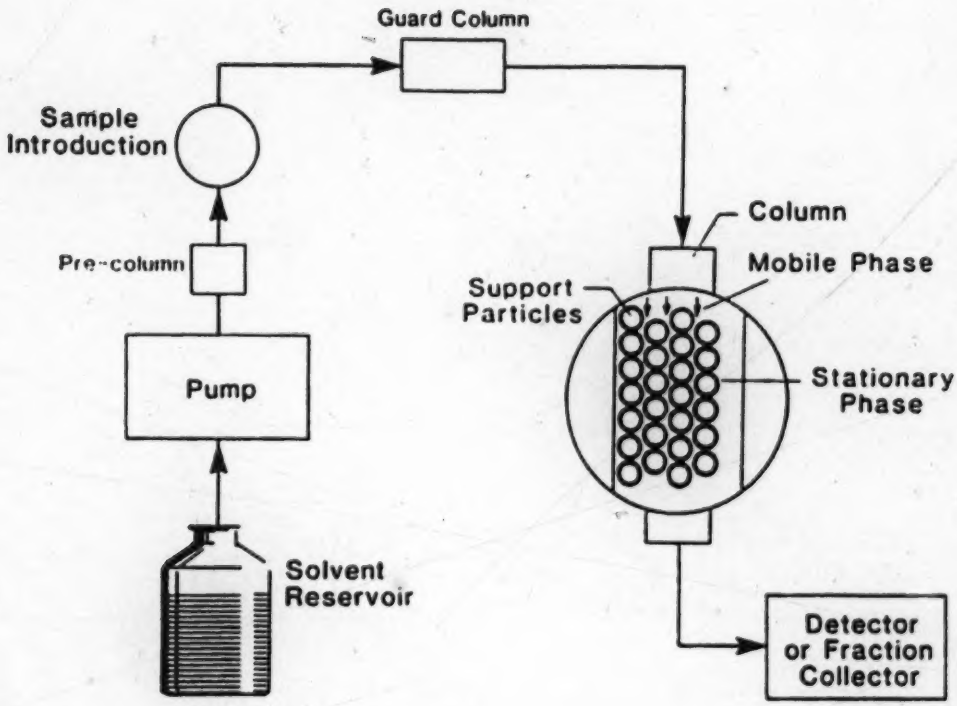

Figure 1-15: Schematic diagram of an HPLC (adapted from Bowers, 1984).

stationary phases were developed by covalently binding an organic moiety onto the surface of the support particle, which is usually silica. Nonpolar organic groups include octadecylsilane (ODS or C-18) or octylsilane (C-8). Polar groups include cyanopropyl (CN), aminopropyl (NH_2) and glycidoxypropyl (diol) silanes (Bowers, 1984).

In the studies presented in this thesis, a photometer was used to detect compounds has they eluted from the column. In photometry, a wavelength in the ultraviolet or visible spectrum is chosen that corresponds to the maximum absorption of the compound of interest. The light will pass through the flowcell and be absorbed by the analyte as it is eluted from the column. The absorption is reflected as a peak on the integrator and the peak area or peak height is measured and is proportional to the concentration of analyte present (Bowers, 1984).

1.9.2.2 METHOD DEVELOPMENT

Optimizing the process of chromatography involves balancing the maximization of separation while minimizing band broadening (Syed, 1998). For effective separation, individual solutes must elute from the column at different times and the peaks must be narrow enough to minimize overlap (Burtis *et al.*, 1987). Resolution is defined mathematically as follows (Tabor, 1984):

$$R = \frac{d_2 - d_1}{1/2\,(w_2 + w_1)}$$

Where: R = resolution

d = distance from injection to apex of eluting peak.

w = peak width

Resolution is therefore controlled by factors that affect peak width (i.e. efficiency) and peak retention (i.e. capacity factor and selectivity) (Bowers, 1984). The most cost- and time-effective approach to improvement of resolution is to first adjust the capacity factor, then the selectivity factor and then the efficiency factor (Burtis *et al.*, 1987).

The capacity factor (K′) is the ratio of the number of solute molecules on the column packing to the number of those in the mobile phase (Burtis *et al.*, 1987). It is calculated from a chromatogram according to the following equation (Tabor, 1984):

$$K' = \frac{t_R - t_o}{t_o}$$

Where: t_R = retention time of retained solute

t_o = time taken for unretarded solvent front to elute from the column.

Thus, K′ is a measure of the degree of retention (Syed, 1998). A K′ value of 2-6 is considered optimal, although in practice values between 1 and 10 are used. If K′ is large there is a greater number of solute molecules associated with the column packing and the solute band migrates slowly. Although this situation may improve separation of analytes there is increased broadening of solute bands (Burtis *et al.*, 1987). Retention time is easily adjusted by changing the amount of organic solvent. One rule of thumb is that a 10% change in the fraction of organic solvent in water will cause a two- or threefold change in K′ (Bowers, 1984).

Once a reasonable retention time has been achieved, it is then necessary to separate the analytes from each other by increasing the selectivity factor (α), which is the most important in terms of resolution (Syed, 1998). Selectivity is a measure of the relative separation between solute peak centers (Burtis *et al.*, 1987) and can also be

referred to as the separation factor (Syed, 1998). Thus, selectivity is the ratio of the capacity factors for two substances measured under identical conditions and is calculated according to the following equation (Tabor, 1984):

$$\alpha = \frac{K'_2}{K'_1}$$

Because selectivity is a function of the column packing, the mobile phase and the solute chemistry it can be manipulated by changing: 1) the composition of the mobile phase (i.e. organic solvent, buffer and pH); 2) the stationary phase; 3) the sample chemistry through derivatization; and 4) the separation temperature. To increase the likelihood of having acceptable resolution, the α value should be greater than 1.1 (Burtis *et al.*, 1987).

The efficiency of a column (N) is obtained by calculating the number of theoretical plates for a column. A theoretical plate is a microscopic segment of a column where a perfect equilibrium is assumed to exist between the solute in the mobile and stationary phases (Tabor, 1984). Efficiency can be calculated according to a variety of equations depending on where peak width measurement is made (Anonymous, 1995). One such equation is as follows:

$$N = 16\left(\frac{t_R}{W}\right)^2$$

Where: t_R = retention time of solute

W = base width of the chromatographic peak

A large number of theoretical plates (i.e. N is large) indicates relatively narrow peaks and, thus, an efficient column. To maximize column efficiency, band broadening must be decreased. This is accomplished by using a well-packed column that contains a stationary phase packing that is small and uniform with respect to the size distribution of particles (Tabor, 1984). In addition to column packing characteristics, column length and mobile phase flow rate are some other factors which influence column efficiency.

Increasing column length will increase efficiency. Increasing mobile phase flow rate will also increase column efficiency but only to a certain point. After that, increases in flow rate will decrease column efficiency (Burtis *et al.*, 1987).

By manipulating factors that control efficiency, selectivity and capacity, adequate resolution can be obtained. A resolution value of 1.25 or greater is considered necessary for good chromatographic analyses (Tabor, 1984).

1.9.3 GAS CHROMATOGRAPHY

1.9.3.1 THEORY (Capillary Chromatography)

A schematic representation of a gas chromatographic system is shown in Figure 1-16. Gas chromatographic separation is achieved by injecting a sample into a heated block that causes its vaporization. A stream of carrier gas, the mobile phase, sweeps the sample vapour to the column. The components of the sample are adsorbed onto the stationary phase at the head of the column. These components are gradually desorbed by fresh carrier gas (Poklis, 1984). The components separate from each other according to their partition coefficients between the carrier gas and the stationary phase (Baker *et al.*, 1982). As the components are eluted, they enter a detector where their presence is converted to an electric signal that is recorded (Baker *et al.*, 1982; Poklis, 1984).

The partition coefficient (K_D) can be expressed by the following equation:

$$K_D = \frac{\text{Time sample is in stationary phase}}{\text{Time sample is in mobile phase}}$$

The more time a compound spends adsorbed to the stationary phase, the higher its K_D. Since retention of a solute depends on its affinity for the stationary phase, polar solutes

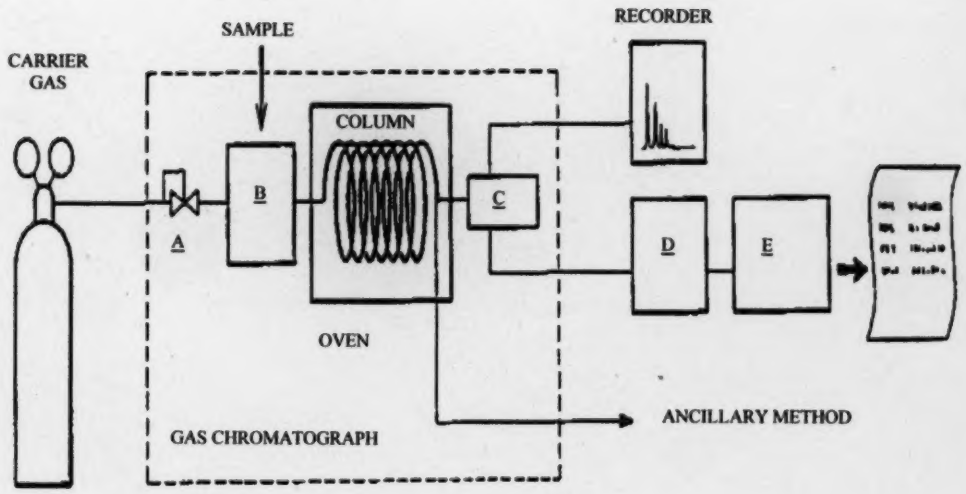

WHERE: A = FLOW CONTROL

B = SAMPLE INTRODUCTION SYSTEM

C = DETECTOR

D = INTERFACE

E = INTEGRATOR

Figure 1-16: Schematic diagram of a GC (adapted from Poklis, 1984).

will have greater K_D values and longer retention times on hydrophilic (polar) phases than hydrophobic (nonpolar) phases. In the same manner, hydrophobic solutes exhibit greater K_D values and longer retention times on nonpolar rather than polar stationary phases (Poklis, 1984).

The previous discussion of capacity factor (K′), selectivity (α) and efficiency (N) is as applicable to GC as it is to HPLC and values are calculated in the same manner. Acceptable resolution is achieved by manipulating those factors affecting K′, α and N. However, in GC the flowing gas has little interaction with the solutes and separation is achieved with the stationary phase only (Johnson and Stevenson, 1978). In addition, temperature is the single most important parameter in a gas chromatographic separation. The higher the column temperature, the lower the K_D, resulting in decreased retention times (Poklis, 1984). Chromatographic separations can be performed isothermally, in which the column temperature is kept constant, or by temperature programming, in which the column temperature is altered at preset rates (Baker *et al.*, 1982).

Capillary columns used in GC are classified as wall-coated open tubular (WCOT) columns or support-coated open tubular (SCOT) columns. In WCOT columns a thin liquid phase is coated directly onto the inside of the surface of the capillary. In SCOT columns, the inside surface of the capillary is coated with a thin layer of support material which is coated with the liquid phase (Baker *et al.*, 1982). The liquid supports vary in terms of their polarity and the maximum temperature they can withstand (Burtis *et al.*, 1987). The amount of stationary phase coated onto the column affects the sample capacity and efficiency of the column (Poklis, 1984).

The column effluent, containing the individual separated components, enters the detector, producing an electrical signal proportional to the amount of substance present in

the carrier gas stream. There are several detectors that can be used, the choice of which depends on the nature of the compounds being separated and the required sensitivity (Poklis, 1984). The three detectors used in the work presented in this thesis are discussed below.

1.9.3.2 DETECTORS

1.9.3.2.1 NITROGEN-PHOSPHORUS DETECTOR

In a nitrogen-phosphorus detector (NPD), ions of an alkali metal such as rubidium are introduced into a hydrogen flame (Poklis, 1984). When a compound containing nitrogen or phosphorus is burned in the flame, the rate of release of alkali metal is increased, possibly by increasing the volatility of the alkali metal salt (Poklis, 1984 and Burtis *et al*, 1987). The alkali metal vapour ionizes in the flame and increases the current flow. The selective interaction of alkali metal ions with nitrogen and phosphorus is complex and poorly understood. In addition to nitrogen and phosphorus, it is considered that halogens, sulfur, arsenic, tin, silicon or lead will also increase the volatility of the alkali metal salt (Burtis *et al.*, 1987).

1.9.3.2.2 ELECTRON-CAPTURE DETECTOR

The electron-capture detector (ECD) is very selective in the compounds it can detect. Essentially only those compounds that have an affinity for and can capture electrons are detectable. The use of an electron-capture detector is suited to compounds which contain halogen atoms, ketone or nitro groups or other electrophoric groups (Baker *et al.*, 1982). In an electron-capture detector, a radioactive isotope releases beta particles that collide with the carrier gas molecules, producing many low-energy electrons. These electrons are collected on electrodes and produce a small measurable standing current

(Baker *et al.*, 1982; Poklis, 1984). As sample components that have the ability to capture the low-energy electrons elute from the column, the standing current decreases (Baker *et al.*, 1982). Thus, the current is inversely proportional to the concentration of the sample components (Burtis *et al*, 1987).

1.9.3.2.3 MASS SPECTROMETRY IN THE ELECTRON IMPACT MODE

The mass spectrometer (MS) is often considered a separate instrument rather than a component of a gas chromatograph because samples may be directly inserted into the MS or it may be coupled to an HPLC. In order to combine GC with MS the sample must elute from the gas chromatograph that operates at a positive pressure to the MS, which operates under high vacuum. This is accomplished through the use of vacuum pumps that maintain a vacuum despite the large gas flow from the gas chromatograph (Poklis, 1984). The column effluent will pass through a separator which removes most of the carrier gas and is then directed into the ionization chamber of the MS where it is bombarded with high-energy electrons (70 eV) (Poklis, 1984; Baker *et al.*,1982). After the initial ionization the compound undergoes fragmentation, forming positive, negative and neutral compounds. The charged fragments are separated and converted into an electric current which is amplified and recorded and is proportional to the amount of compound entering the mass spectrometer (Baker *et al.*, 1982). The mass spectrum is a display of the different masses of the charged fragments and their relative abundance (Poklis, 1982). Mass spectrometry may be conducted in one of several modes. In selective ion monitoring, the MS is adjusted so that only a few selected ions are monitored. The sensitivity is increased since only a part of the spectrum is detected, and thus, the time spent on each ion is increased. Alternatively, all ions of a spectra can be

recorded. In this mode, sensitivity is decreased since the time spent on each ion is short (Durden and Boulton, 1982).

1.9.4 DERIVATIZATION

Derivatization is a process by which the compound is chemically modified to make it more suitable for detection by GC or HPLC (Poklis, 1984). Most derivatives are formed by replacing the active hydrogen atom of polar groups (*i.e.* NH, OH, SH) by chemical procedures (Baker *et al.*, 1982) such that the new product has properties preferable to the original sample molecule (Poklis, 1984). This modification can increase volatility of the sample molecule, increase sensitivity, and/or selectivity for a given separation, decrease retention time, produce sharper peaks, reduce peak tailing and provide stability to thermally labile compounds (Baker *et al.*, 1982; Poklis, 1984).

The derivatizing agents used in the work presented in this thesis were pentafluoropropionic acid anhydride (PFPA), pentafluorobenzoyl chloride (PFBC) and acetic anhydride (AA) (Figure 1-17). PFPA was used to acylate the amine group and esterify alcohol group(s) of MET and ODM, to increase compound sensitivity to the electron-capture detector. PFBC was used to acylate amine groups of FLU, NFLU and FVX to also increase compound sensitivity to the electron-capture detector. AA was used to acylate the amine group of DMI with the purpose of improving peak shape (Baker, personal communication).

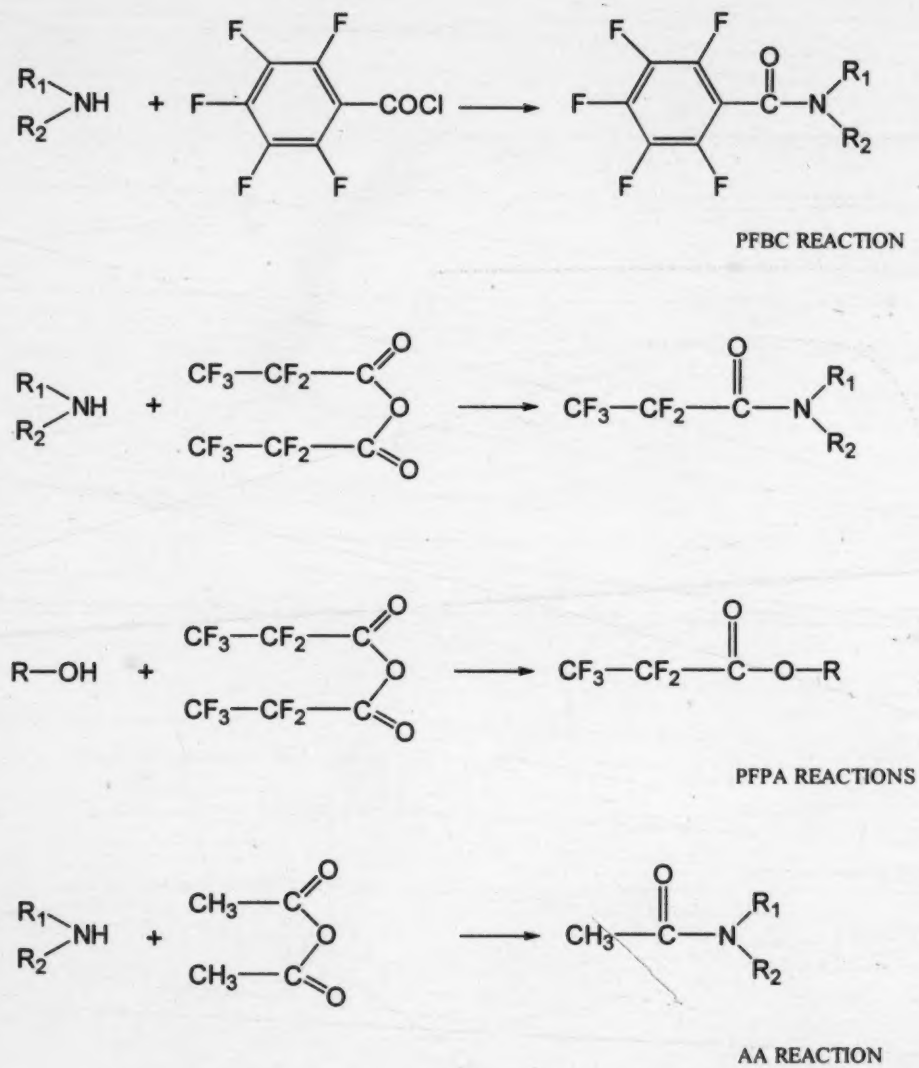

Figure 1-17: Derivatizing reagents and their associated reactions (adapted from Baker *et al.*, 1982 and Baker, personal communication).

1.10 THESIS OBJECTIVES

The objectives of the work described in this thesis were as follows:

1. Develop a novel assay for the quantitation of MET and ODM in rat tissue.
2. Investigate potential drug-drug interactions involving MET and the antidepressants FLU, FVX and DMI in rat tissue.
3. Develop a novel assay for the quantitation of ODM, NDM, AM and HM in microsomal preparations.
4. Investigate the kinetics of the major pathways of the metabolism of MET using human liver microsomes.
5. Investigate potential drug-drug interactions involving MET and the antidepressants PAR, FLU, FVX and DMI in human liver microsomes.
6. Elucidate the enzymes involved in the major pathways in the metabolism of MET using both human liver microsomes and microsomes from cDNA expressed cells.

1.11 MATERIALS

1.11.1 INSTRUMENTATION

1.11.1.1 HIGH PERFORMANCE LIQUID CHROMATOGRAPH

The HPLC system consisted of a Waters Model 510 pump, a Waters WISP 710 B autosampler, a Waters 2487 Duel λ Absorbance Detector (Waters Associates, Milford, MA), coupled to a μBondapak CN guard column (Waters Associates, Milford, MA) and a Hypersil 5 CN column (4.6 x 25 cm) (Phenomenex, Torrance, CA). Data processing was carried out using a Pegasus Pentium 2, 400 MHz computer (Pegasus Computer Company, Edmonton, AB) with Waters Millennium^{32} software-Version 3.05 (Waters Associates, Milford, MA).

1.11.1.2 GAS CHROMATOGRAPHS

1.11.1.2.1 NITROGEN-PHOSPHORUS DETECTOR

All samples were analysed using a Hewlett-Packard (HP) model 5890A gas chromatograph equipped with a nitrogen phosphorus detector and linked to a HP 6890 Series Injector and a HP 3396 Series II Integrator (Hewlett Packard, Palo Alto, CA). A fused DB5 silica capillary column (15 m x 0.25 mm) coated with 0.25 μm film thickness of 5% phenylmethylpolysiloxane was employed (Chromatographic Specialties, Brockville, ON). The carrier and make-up gases were pure helium (Praxair Canada Inc, Edmonton, AB). The detector was purged with pure hydrogen and dry air (Praxair Canada Inc, Edmonton, AB).

1.11.1.2.2 ELECTRON-CAPTURE DETECTOR

Two different GC-ECD instruments were used. Samples were analysed using either a HP model 5880 gas chromatograph equipped with a ^{63}Ni electron-capture detector and linked to a HP 5880A integrator or an HP model 5890A gas chromatograph equipped with a ^{63}Ni electron-capture detector and linked to a HP 7673A automatic sampler and a HP 3392A integrator (Hewlett Packard, Palo Alto, CA). A fused HP5 silica capillary column (25 m x 0.32 mm) coated with 1.05 μm film thickness of 5% phenylmethylsilicone was employed in both systems (Hewlett Packard, Palo Alto, CA) The carrier gas was pure helium and the make-up gas was argon-methane (95:5) (Praxair Canada Inc, Edmonton, AB).

1.11.1.2.3 MASS SPECTROMETRY DETECTOR

The GC-MS system consisted of an HP5890 gas chromatograph coupled to an HP5970 mass selective detector in the electron impact mode. A fused HP5 silica

capillary column (12.5 m x 0.21 mm) coated with 0.5 μm film thickness of 5% phenylmethylsilicone was employed (Hewlett Packard, Palo Alto, CA).

1.11.2 MICROSOMAL PRODUCTS

1.11.2.1 HUMAN LIVER MICROSOMES

The human liver microsomes used in all experiments, with the exception of the correlation experiments, were from lot number HHM-0205 and were purchased from the International Institute for the Advancement of Medicine and Science (IIAMS) (Exton, PA, USA). These microsomes were characterized by the manufacturer for protein content and CYP enzyme activity. This lot number of microsome had 23 mg/mL of protein as determined by the Pierce protein assay. The activity of seven CYP enzymes were determined based on their ability to metabolize a specific substrate. CYP1A2 activity was 347 pmol/mg/min based on the rate of phenacetin O-deethylation. CYP2A6 activity was 0.67 nmol/mg/min based on the rate of coumarin 7-hydroxylation. CYP2C19 activity was 152 pmol/mg/min based on the rate of mephenytoin 4-hydroxylation. CYP2D6 activity was 180 pmol/mg/min based on the rate of dextromethorphan O-demethylation. CYP2E activity was 811 pmol/mg/min based on the rate of chlorzoxazone 6-hydroxylation. CYP3A4 activity was 3.6 nmol/mg/min based on the fractional production of [^{14}C]6β-hydroxytestosterone. CYP4A activity was 1.4 nmol/mg/min based on the fractional production of [^{14}C]omega-hydroxylauric acid. These microsomes were received frozen and were stored at -80°C until needed

Human liver microsomes used in the correlation experiments were purchased from Gentest Corporation (Woburn, MA). These microsomes were prepared from 12 different human livers and were characterized by the manufacturer for protein content,

the activity of 10 CYP enzymes and microsomal FAD-containing monooxygenase (FMO) activity. The microsomes were prepared to contain 20 mg/mL of protein. A comprehensive detailing of the characterization of the CYP enzymes and FMO is given in Table 1-12. When received, these microsomes were thawed, aliquoted and then stored at -80°C until needed.

1.11.2.2 MICROSOMES FROM cDNA–EXPRESSED CELLS

Microsomes prepared from cells expressing cDNA for human CYP1A2, CYP2A6, CYP2B6, CYP2C8, $CYP2C9_{arg}$, CYP2C19, CYP2D6, CYP2E1, CYP3A4, CYP3A5 or CYP4A11 were purchased from Gentest Corporation (Woburn, MA). All enzymes were coexpressed with P450 reductase except CYP1A2 and CYP4A11 which have reductase activity endogenous to the cell line. $CYP2C9_{arg}$, CYP3A4 and CYP2E1 were coexpressed with cytochrome b_5. These microsome products were prepared from either metabolically competent derivatives of the AHH-1 TK+/- human lymphoblastoid cell line or baculovirus (*Autographa californica*)-infected insect cells (BTI-TN-5B1-4). Table 1-13 lists the characteristics of these microsomes. Interestingly, the parent AHH-1 TK+/- cell line contains a low level of native human CYP activity which is inducible by polycyclic aromatic hydrocarbons. The insect host cell line does not seem to have detectable CYP activity.

1.11.3 EQUIPMENT

1.11.3.1 BALANCE

A Mettler AE 160 electronic balance (Mettler Instrument Corporation, Highstown, NJ) was used to accurately weigh chemicals and tissue samples.

Assay	Enzyme Tested	Specimen Designation												
		3	6	23	30	42	43	56	66	70	89	93	112	
Phenacetin O-deethylase	CYP1A2	112	798	658	2102	561	356	2009	264	496	1197	501	244	ENZYME ACTIVITY
Coumarin 7-hydroxylase	CYP2A6	2358	502	642	1207	1807	471	1333	1571	2047	514	329	426	
(S)-Mephenytoin N-demethylase	CYP 2B6	15.2	12.7	9.5	32.6	85.5	7.4	15.2	20.3	20.9	31.9	15.0	59.1	
Paclitaxel 6α-hydroxylase	CYP 2C8	188	142	86.9	335	308	55.6	169	142	307	140	140	157	
Diclofenac 4′-hydroxylase	CYP 2C9	2290	3175	3335	7367	1708	1314	3801	2063	4249	2576	2462	5042	
(S)-Mephenytoin 4′-hydroxylase	CYP2C19	12.8	9.8	60.6	139	10.0	212	169	7.4	67.4	84.7	36.9	260	
Bufuralol 1′-hydroxylase	CYP 2D6	124	ND	222	ND	109	10.6	140	170	32	5	63	23	
Chlorzoxazone 6-hydroxylase	CYP 2E1	2509	2089	2233	1789	2165	1109	2692	2116	2170	2214	2383	2598	
Testosterone 6β-hydroxylase	CYP 3A4	5854	2677	3564	9664	13151	3408	5028	5802	8960	11732	2090	17519	
Lauric acid 12-hydroxylase	CYP 4A	1878	1030	2122	2132	1665	1785	2380	1125	1415	2008	1555	1177	
Methyl ρ-tolyl sulfide oxidase	FMO	3471	1832	1770	3326	3168	1356	2464	1879	3104	3291	1580	2630	

Table 1-12: Characterization of Gentest human liver microsomes. Activities are expressed as pmol/mg/min. Information supplied by Gentest corporation. (ND = None Detected)

CYP Enzyme Expressed	Assay	Activity (pmol/mg x min)	Protein Content (mg/mL)	Expression System
1A2	7-Ethoxyresorufin deethylase	101	10	Human lymphoblastoid cell line
2A6	Coumarin 7-hydroxylase	1500	10	Human lymphoblastoid cell line
2B6	7-Ethoxy-4-trifluoromethyl-coumarin deethylase	920	10	Human lymphoblastoid cell line
2C8	Paclitaxel 6α-hydroxylase	1353	3.4	Baculovirus infected insect cells
$2C9_{ARG}$	Diclofenac 4′-hydroxylase	13810	2.1	Baculovirus infected insect cells
2C19	(S)-Mephenytoin 4′-hydroxylase	3143	2.1	Baculovirus infected insect cells
2D6	(±) Bufuralol 1′-hydroxylase	1895	11.4	Human lymphoblastoid cell line
2E1	p-Nitrophenol hydroxylase	4082	4.9	Baculovirus infected insect cells
3A4	Testosterone 6β-hydroxylase	12389	11.3	Baculovirus infected insect cells
3A5	Testosterone 6β-hydroxylase	3944	3.6	Baculovirus infected insect cells
4A11	Lauric acid ω-hydroxylase	570	10	Human lymphoblastoid cell line
Control	7-Ethoxyresorufin deethylase	0.3	10.0	Human lymphoblastoid cell line
Control			5.0	Baculovirus infected insect cells

Table 1-13: Characterization of CYP enzymes from cDNA-expressed cells (adapted from Gentest Batch Data Sheets).

1.11.3.2 CENTRIFUGES

A Sorvall GLC-2B General Laboratory Centrifuge (Dupont Instruments, Wilmington, DE) was used for processing samples that required low g values (i.e. 1000 g), small volume (up to 10 mL) centrifugations. Centrifugation of samples requiring a higher g value (ie. 10,000 – 13,000 g) was carried out using a Beckman Microfuge B (Palo Alto, CA) or a Micro-Centaur Centrifuge (MSE Scientific Instruments, Sussex, England). The maximum sample volume for these micro-centrifuges is 1.5 mL.

1.11.3.3 FILTER APPARATUS FOR MOBILE PHASE PREPARATION

Mobile phase was filtered and degassed using a Millipore filtering system (Millipore Corporation, Bedford, MA) in which the mobile phase was forced under vacuum through a 0.2 μM, 47 mm Nylon Filter Membrane (Phenomenex, Torrance, CA).

1.11.3.4 GLASSWARE CLEANING

All test tubes were manually scrubbed using Sparkleen® Manual Washing Soap (Fisher Scientific, Nepean, ON) followed by sonication in an Ultra-Sonic Cleaner (Mettler Electronics, Highstown, NJ) and rinsed in a G7704 Lavador dishwasher (Miele Laboratory Technology, Unionville, ON). All other glassware was rinsed with tap water and then washed with Sparkleen® Dishwasher Soap in the dishwasher. The water utilized by the dishwasher was from a central deionized water source. A mechanical convection oven (Model 28, Precision Scientific Group, Chicago,IL) was used to dry all glassware upon removal from the dishwasher.

1.11.3.5 pH METER

The pH value of solutions were adjusted using an Accumet® pH Meter 915 equipped with an Accumet® probe (Fisher Scientific,Nepean, ON).

1.11.3.6 TISSUE HOMOGENIZER

Brain and liver samples were homogenized using a TRI-R STIR-R Model S63C Variable Speed Laboratory Motor (TRI-R Instruments, Rockville Center, NY) equipped with a Teflon® pestle and a glass grinding tube. Heart samples were homogenized using an IKA®-Labortechnik Ultra-Turrex T25 (Janke and Kunkel, Staufen, Germany).

1.11.3.7 VACUUM EVAPORATOR

A Savant Speed Vac SS1 (Savant Instruments, Inc., Farmington, NY) was used to remove solvent, concentrate and dry samples using a combination of vacuum and centrifugal force. This system consisted of a concentrator (a rotor chamber with heater), a chemical trap with disposable cartridges, a refrigerated condensation trap and a vacuum pump.

1.11.3.8 VORTEX MIXER

A thermolyne Maxi Mix (Sybron/Thermolyne Instruments, Dubuque, IO) was used for mixing samples.

1.11.3.9 VORTEX SHAKER

The vortex shaker used for extraction and/or derivatizing of sample homogenates was an IKA Vibrax-VXR with a Typ VX2 attachment (Janke and Kunkel, Staufen, Germany).

1.11.3.10 WATERBATH

Microsomal incubations were carried out in a Fisher Isotemp® Waterbath (Fisher Scientific, Nepean, ON) that was set at 37°C.

1.11.3.11 WATER STILL

Double distilled water was prepared using a Mega-Pure® Three Liter Automatic

Water Still (Corning® Waterware, Corning,NY) that utilized a central deionized water source. This double distilled water was further purified for HPLC purposes using a Mixed Bed Organic Removal Cartridge (Fisher Scientific, Palo Alto, CA).

1.11.4 CHEMICALS AND REAGENTS

The following is a list of chemicals and reagents along with their suppliers used in the analyses discussed in this thesis.

Acetic Anhydride .....Fisher Scientific (Nepean, ON)

Acetonitrile (HPLC grade).....Fisher Scientific (Nepean, ON)

Acid metabolite HCl .....Astra Hässle (Mississauga, ON)
(Acid metabolite of O-desmethylmetoprolol)

(-)-Alprenolol d-tartrate .....Sigma Chemical Company (St. Louis, MO)

L-Ascorbic acid.....Fisher Scientific (Nepean, ON)

Carbon dioxide (solid) .....Liquid Carbonic (Edmonton, AB)

N-Dealkylmetoprolol .....Astra Hässle (Mississauga, ON)

Desipramine HCl .....Sigma Chemical Company (St. Louis, MO)

O-Desmethylmetoprolol maleate .....Ciba-Geigy (Calgary, AB)

EDTA.....Fisher Scientific (Nepean, ON)
(Disodium Ethylenediamine-tetraacetate)

Ethyl acetate.....Fisher Scientific (Nepean, ON)

Fluoxetine HCl.....Lilly Research Laboratories (Indianapolis, IN)

Fluvoxamine Maleate.....Solvay Duphar (Hanover, Germany)

Glacial acetic acid .....Fisher Scientific (Nepean, ON)

Glucose-6-phosphate dehydrogenase.....Sigma Chemical Company (St. Louis, MO)

Glucose-6-phosphate (monosodium salt) ...Sigma Chemical Company (St. Louis, MO)

Hydrochloric acid (concentrated) .....Fisher Scientific (Nepean, ON)

α-Hydroxymetoprolol benzoic acid salt .....Ciba-Geigy (Calgary, AB

Isopentane .....Fisher Scientific (Nepean, ON)

Magnesium chloride.....Fisher Scientific (Nepean, ON)

Maprotiline.....Sigma Chemical Company ((St. Louis, MO)

Methanol (HPLC grade) .....Fisher Scientific (Nepean, ON)

(±)-Metoprolol(+)-tartrate.....Sigma Chemical Company (St. Louis, MO)

β-Nicotine adenine dinucleotide phosphate.Sigma Chemical Company (St. Louis, MO)

Norfluoxetine .....Lilly Research Laboratories (Indianapolis, IN)

Paroxetine HCl.....Smithkline Beecham (Oakville, ON)

Pentafluorobenzoyl chloride .....Aldrich Chemical Company (Milwaukee, WI)

Pentafluoropropionic anhydride.....Aldrich Chemical Company (Milwaukee, WI)

Perchloric acid (60%) .....Fisher Scientific (Nepean, ON)

Potassium carbonate.....Fisher Scientific (Nepean, ON)

Potassium phosphate dibasic.....J T Baker (Phillipsburg, NJ)

Potassium phosphate monobasic.....Fisher Scientific (Nepean, ON)

Propranolol HCl.....Wyeth-Ayerst (St. Laurent, Qué)

Sodium acetate.....Fisher Scientific (Nepean, ON)

Sodium bicarbonate .....Fisher Scientific (Nepean, ON)

Sodium borate .....Fisher Scientific (Nepean, ON)

Sulfuric acid.....Fisher Scientific (Nepean, ON)

Toluene (HPLC grade).....Fisher Scientific (Nepean, ON)

Triethylamine (HPLC grade) .....Fisher Scientific (Nepean, ON)

Tris .....Fisher Scientific (Nepean, ON)

1.12 SOLUTION PREPARATION

1.12.1 0.1 M POTASSIUM PHOSPHATE BUFFER (pH = 7.4)

The 0.1 M potassium phosphate buffer was prepared by acidifying a solution of dibasic potassium phosphate with a 0.1 M solution of monobasic potassium phosphate. The monobasic solution was prepared by dissolving 1.3609 g of monobasic potassium phosphate in 100 mL of double distilled water. Then, 1.7418 g of dibasic potassium phosphate was dissolved in 60 mL of double distilled water and was acidified to a pH value of 7.4 with the monobasic solution. This acidified solution was transferred to a 100 mL volumetric flask and brought to volume with double-distilled water.

1.12.2 0.1 M TRIS BUFFER (pH = 7.5)

The Tris buffer was prepared by dissolving 1.2114 g of Tris in 50 mL of double distilled water and acidifying to a pH value of 7.5 with 1.0 N hydrochloric acid. The solution was transferred to a 100 mL volumetric flask and brought to volume with double-distilled water.

1.12.3 NADPH-GENERATING SYSTEM

The NADPH-generating system was prepared fresh with each experimental run. It contained 4 mg/mL of β-nicotine adenine dinucleotide phosphate ($NADP^+$), 4 mg/mL of glucose-6-phosphate, 3.2 units/mL of glucose-6-phosphate dehydrogenase and 2.64 mg/mL of $MgCl_2 \bullet H_2O$, in a 0.1 M potassium phosphate buffer (pH = 7.4) or a 0.1 M Tris buffer (pH=7.5).

1.12.4 1N PERCHLORIC ACID

The perchloric acid solution used in the microsome experiments was prepared by adding 10.88 mL of 60% perchloric acid, 8.8 mg of ascorbic acid and 100 mg of EDTA

to 60 mL of double-distilled water. The solution was mixed until all components had dissolved, transferred to a 100 mL volumetric flask and brought to volume with double-distilled water.

1.13 REFERENCES

Åblad B, Borg KO, Carlsson E, Ek L, Johnsson G, Malmfors T and Regårdh CG (1975) A survey of the pharmacological properties of metoprolol in animals and man. *Acta Pharmacol Toxicol* 36 (Suppl V): 7-23.

Anonymous (1995) *Waters Chromatography-Developing HPLC Separations (Revision 3).* Printing Services, McMaster University.

Anonymous (1998) The top 200 drugs of 1998. *Pharmacy Practice* 14: 53-64.

Arfwidsson A, Borg KO, Hoffman K-J and Skanberg I (1976) Metabolism of metoprolol in the rat *in vitro* and *in vivo*. *Xenobiotica* 6: 691-711.

Asperheim MK (1996) In *Pharmacology: An Introductory Text (Edition 8)* WB Saunders Company, Toronto, ON.

Baker GB, Coutts RT and Legatt, DF (1982) Gas chromatographic analysis of amines in biological systems. In Baker GB and Coutts RT (Eds) *Analysis of Biogenic Amines (Part A)* Elsevier Scientific Publishing Company, New York, NY.

Baker GB, Urichuk LJ and Coutts RT (1998) Drug metabolism and metabolic drug-drug interactions in psychiatry. *Child Adol Psychopharmacol News* Supplement 1-8.

Bauer JD (1984) Hemoglobin, porphyrin, and iron metabolism. In Kaplan LA and Pesce AJ (Eds) *Clinical Chemistry: Theory, Analysis and Correlation* (pp. 611–655). St. Louis, Missouri, CV Mosby Company.

Bertz RJ and Granneman GR (1997) Use of *in vitro* and *in vivo* data to estimate the likelihood of metabolic pharmacokinetic interactions. *Clin Pharmacokinet* 32: 210-258.

Bolden-Watson C and Richelson E (1993) Blockade by newly-developed antidepressants of biogenic amine uptake into rat brain synaptosomes. *Life Sci* 52: 1023-1029.

Borchard U (1990) Pharmacokinetics of beta-adrenoceptor blocking agents: clinical significance of hepatic and/or renal clearance. *Clin Physiol Biochem* 8 (Suppl 2): 28-34.

Borg KO, Carlsson E, Hoffmann K-J, Jönsson T-E, Thorin H and Wallin B (1975) Metabolism of metoprolol-(^{3}H) in man, the dog and the rat. *Acta Pharmacol Toxicol* 36(Suppl V): 125-135.

Bowers LD (1984) Liquid chromatography. In Kaplan LA and Pesce AJ (Eds) *Clinical Chemistry: Theory, Analysis and Correlation* (pp. 100 – 116). St. Louis, Missouri, CV Mosby Company.

Bourrié M, Meunier V, Berger Y and Fabre G (1996) Cytochrome P450 isoform inhibitors as a tool for the investigation of metabolic reactions catalyzed by human liver microsomes. *J Pharmacol Exp Ther* 277: 321-332.

Bremner WF (1984) Cardiac disease and hypertension. In Kaplan LA and Pesce AJ (Eds) *Clinical Chemistry: Theory, Analysis and Correlation* (pp. 488 – 508). St. Louis, Missouri, CV Mosby Company.

Brøsen K and Gram LF (1989) Clinical significance of the sparteine/debrisoquine oxidation polymorphism. *Eur J Clin Pharmacol* 36: 537-547.

Burtis CA, Bowers LD, Chattoraj SC and Ullman MD (1987) Chromatography. In Tietz NW (Ed) *Fundamentals of Clinical Chemistry (3rd Edition)*. WB Saunders Company, Philadelphia, PA.

Cheng YC and Prusoff WH (1973) Relationship between the inhibitor constant (K_I) and the concentration of inhibitor which causes 50 percent inhibition (I_{50}) of an enzymatic reaction. *Biochem Pharmacol* 22: 3099-3108.

Coutts RT (1994) Polymorphism in the metabolism of drugs, including antidepressant drugs: comments on phenotyping. *J Psychiatr Neurosci* 19: 30-44.

Coutts RT and Urichuk LJ (1999) Polymorphic cytochromes P450 and drugs used in psychiatry. *Cell Mol Neurobiol* 19: 325-354.

Crewe HK, Lennard MS, Tucker GT, Woods FR and Haddock RE (1992) The effect of selective serotonin re-uptake inhibitors on cytochrome P4502D6 (CYP2D6) activity in human liver microsomes. *Br J Clin Pharmacol* 34: 262-265.

Dixon M (1953) The determination of enzyme inhibitor constants. *Biochem J* 55: 170-171.

Durden DA and Boulton AA (1982) Mass spectrometric analysis of some neurotransmitters and their precursors and metabolites. In Lajtha A (Ed) *Handbook of Neurochemistry (Second Edition): Volume 2 Experimental Neurochemistry* (pp. 397-428), New York, NY, Plenum Press.

Eggertsen G, Olin M, Anderssen U, Ishida H, Kuboto S, Hellman U, Okuda KI and Bjorkhem I (1996) Molecular cloning and expression of rabbit sterol 12-alpha-hydroxylase. *J Biol Chem* 271: 32269-32275.

Emilien G and Maloteaux J-M (1998) Current therapeutic uses and potential of β-adrenergic agonists and antagonists. *Eur J Clin Pharmacol* 53: 389-404.

Fraser A (1997) Pharmacology of antidepressants. *J Clin Psychopharmacol* 17(Suppl 1): 2S-18S.

Frasure-Smith N, Lespérance F and Talajic M (1993) Depression following myocardial infarct-impact on 6-month survival. *JAMA* 270: 1819-1825.

Garver DL (1984) Psychiatric disorders. In Kaplan LA and Pesce AJ (Eds) *Clinical Chemistry: Theory, Analysis and Correlation* (pp. 864 – 881), St. Louis, Missouri, CV Mosby Company.

George J, Byth K and Farrell GC (1995) Age but not gender selectively affects expression of individual cytochrome P450 proteins in human liver. *Biochem Pharmacol* 50: 727-730.

Gibson GG and Skett P (1994) in *Introduction to Drug Metabolism, Second Edition*, Blackie Academic and Professional, Glasgow, UK.

Gonzalez FJ (1992) Human cytochromes P450: problems and prospects. *TIPS* 13: 346-352.

Greenblatt DJ, von Molke L, Harmatz JS and Shader RI (1998) Drug interactions with newer antidepressants: role of human cytochromes P450. *J Clin Psychiatry* 59 (Suppl 15): 19-27.

Guengerich FP (1994) Catalytic selectivity of human cytochrome P450 enzymes: relevance to drug metabolism and toxicity. *Toxicol Letters* 70: 133-138.

Guengerich FP (1996a) *In vitro* techniques for studying drug metabolism. *J Pharmacokinet Biopharmaceutics* 24: 521-533.

Guengerich FP (1996b) Human cytochrome P450 enzymes. In Ortiz de Montellano PR (Ed) *Cytochrome P450-Structure, Mechanism and Biochemistry (Second Edition)* (pp. 473-535), New York, New York, Plenum Press.

Guengerich FP and MacDonald TL (1990) Mechanisms of cytochrome P-450 catalysis. *FASEB J* 4: 2453-2459.

Haining RL, Hunter AP, Veronese ME, Trager WF and Rettie AE (1996) Allelic variants of human cytochrome P450 2C9: Baculovirus-mediated expression, purification, structural characterization, substrate stereoselectivity, and prochiral selectivity of the wild-type and I359L mutant forms. *Arch Biochem Biophys* 333: 447-458.

Halpert JR (1995) Structural basis of selective cytochrome P450 inhibition. *Ann Rev Pharmacol Toxicol* 35: 29-53.

Harvey AT and Preskorn SH (1995) Interactions of serotonin reuptake inhibitors with tricyclic antidepressants. *Arch Gen Psychiatry* 52: 783-784.

He J, Klag MJ, Appel LJ, Charleston J and Whelton PK (1998) Seven-year incidence of hypertension in a cohort of middle-aged african americans and whites. *Hypertension* 31: 1130-1135.

Henderson PJF (1998) Statistical analysis of enzyme kinetic data. In Eisenthal R and Danson MJ (Eds) *Enzyme Assays: A Practical Approach* (pp 277-316). New York, NY, Oxford University Press.

Hohnadel DC (1984) Enzymes. In Kaplan LA and Pesce AJ (Eds) *Clinical Chemistry: Theory, Analysis and Correlation* (pp. 927 – 952). St. Louis, Missouri, CV Mosby Company.

Holt A (1999) On the measurement of enzymes and their inhibitors. In Boulton AA, Baker GB and Bateson AN (Eds) *Neuromethods 33: Cell Neurobiology Techniques* (pp.131-194) Humana Press Inc., Totowa, NJ.

Iwatsubo T, Hirota N, Ooie T, Susuki H, Shimada N, Chiba K, Ishizaki T, Green CE, Tyson CA and Sugiyama Y (1997) Prediction of *in vivo* drug metabolism in the human liver from *in vitro* metabolism data. *Pharmacol Ther* 73: 147-171.

Jack DB, Wilkins M and Quarterman CP (1983) Lack of evidence for polymorphism in metoprolol metabolism. *Br J Clin Pharmacol* 16: 188-190.

Johnson EL and Stevenson R (1978) *Basic Liquid Chromatography* Varian Associates, Palo Alto, CA.

Johnsson G, Regårdh CG and Sölvell L (1975) Combined pharmacokinetic and pharmacodynamic studies in man of the adrenergic β_1-receptor antagonist metoprolol. *Acta Pharmacol Toxicol* 36(Suppl V): 31-44.

Kaplan HI and Sadock BJ (1998) *Kaplan and Sadock's Synopsis of Psychiatry*, Williams and Wilkins, Baltimore, Maryland.

Kallio J, Huupponen R, Seppälä M, Säkö E and Iisalo E (1990) The effects of β-adrenoceptor antagonists and levomepromazine on the metabolic ratio of debrisoquine. *Br J Clin Pharmacol* 30: 638-643.

Keetch AC, Harper RW, Harrison PM, Pitt A and McLean AJ (1986) Pharmacokinetic interaction between oral metoprolol and verapamil for angina pectoris. *Am J Cardiol* 58: 551-552.

Kim M, Shen DD, Eddy AC and Nelson WL (1993) Inhibition of the enantioselective oxidative metabolism of metoprolol by verapamil in human liver microsomes. *Drug Metab Dispos* 21: 309-317.

Konig F, Hafele M, Hauger B, Lobie M, Wossner S and Wolfersdorf M (1996) Bradykardie nach therapiegeginn mit metoprolol and paroxetine. *Psychiatr Prax* 23: 244-245.

Koytchev R, Alken R-G, Vlahov V, Kirkov V, Kaneva R, Thyroff-Friesinger U and Rehak E (1998) Influence of the cytochrome *P4502D6*4* allele on the

pharmacokinetics of controlled-release metoprolol. *Eur J Clin Pharmacol* 54: 469-474.

Lennard MS (1989) The polymorphic oxidation of beta-adrenoceptor antagonists. *Pharmac Ther* 41:461-477.

Lennard MS, Silas JH, Freestone S, Ramsay LE, Tucker GT and Woods HF (1982) Oxidation phenotype-a major determinant of metoprolol metabolism response. *New Eng J Med* 307: 1558-1560.

Lennard MS, Tucker GT, Silas JH, Freestone S, Ramsay LE and Woods HF (1983) Differential stereoselective metabolism of metoprolol in extensive and poor debrisoquin metabolizers. *Clin Pharmacol Ther* 34: 732-737.

Lennard MS, Crewe HK, Tucker GT and Woods HF (1986) Metoprolol oxidation by rat liver microsomes. *Biochem Pharmacol* 35: 2757-2761.

Lespérance F, Frasure-Smith N and Talajic M (1996) Major depression before and after myocardial infarction: its nature and consequences. *Psychosom Med* 58: 99-110.

Lewis DFV, Eddershaw PJ, Goldfarb PS and Tarbit MH (1997) Molecular modelling of cytochrome P4502D6 (CYP2D6) based on an alignment with CYP102: structural studies on specific CYP2D6 substrate metabolism. *Xenobiotica* 27: 319-340.

McGourty JC, Silas JH, Lennard MS, Tucker GT and Woods HF (1985) Metoprolol metabolism and debrisoquine oxidation polymorphism-population and family studies. *Br J Clin Pharmacol* 20: 555-566.

McLean AJ, Knight R, Harrison PM and Harper RW (1985) Clearance–based oral drug interaction between verapamil and metoprolol and comparison with atenolol. *Am J Cardiol* 55:1628-1629.

Meier J (1982) Pharmacokinetic comparison of pindolol with other beta-adrenoceptor-blocking agents. *Am Heart J* 104: 364-373.

Meyer UA (1996) Overview of enzymes of drug metabolism. *J Pharmacol Biopharm* 24: 449-459.

Mimura M, Baba T, Yamazaki H, Ohmori S, Inui Y, Gonzalez F, Guengerich P and Shimada T (1993) Characterization of cytochrome P450 2B6 in human liver microsomes. *Drug Metab Dispos* 21: 1048-1056.

Miyamoto Y, Shinki T, Yamamoto K, Ohyama Y, Iwasaki H, Hosotani R, Kasama T, Takayama H, Yamada S and Suda T (1997) 1-Alpha, 25-dihydroxyvitamin D3-24-hydroxylase (CYP24) hydroxylates the carbon at the end of the side chain (C-26) of the C-24-fluorinated analog of 1-alpha, 25-dihydroxyvitamin D3. *J Biol Chem* 272: 14115-14119.

Murray M (1987) Mechanisms of the inhibition of cytochrome P-450-mediated drug oxidaion by therapeutic agents. *Drug Metab Rev* 18: 55-81.

Murthy SS, Shetty HU, Nelson WL, Jackson PR and Lennard MS (1990) Enantioselective and diastereoselective aspects of the oxidative metabolism of metoprolol. *Biochem Pharmacol* 40: 1637-1644.

Nelson DR, Koymans L, Kamataki T, Stegeman JJ, Feyereisen R, Waxman DJ, Waterman MR, Gotoh O, Coon MJ, Estabook RW, Gunsalus IC and Nebert DW (1996) P450 superfamily: update on new sequences, gene mapping, accession numbers and nomenclature. *Pharmacogenetics* 6: 1-42.

Östholm I (1975) Introduction. *Acta Pharmacol Toxicol* (suppl V): 125-135.

Otton SV, Crewe HK, Lennard MS, Tucker GT and Woods HF (1988) Use of quinidine to define the role of the sparteine/debrisoquine cytochrome P450 in metoprolol oxidation by human liver microsomses. *J Pharmacol Exp Ther* 247: 242-247.

Otton SV, Inaba T and Kalow W (1983) Inhibition of sparteine oxidation in human liver by tricyclic antidepressants and other drugs. *Life Sci* 32: 795-800.

Otton SV, Inaba T and Kalow W (1984) Competitive inhibition of sparteine oxidation in human liver by β-adrenoceptor antagonists and other cardiovascular drugs. *Life Sci* 34: 73-80.

Palmer T (1995) *Understanding Enzymes, Fourth Edition*. Prentice Hall/Ellis Horwood, Hemel Hempstead, Hertfordshire.

Parkinson A (1996) Biotransformation of xenobiotics. In CD Klassen (Ed) *Casarett and Doull's Toxicology. The Basic Science of Poisons, Fifth Edition* (pp. 113-186) New York: Mcgraw-Hill.

Poklis A (1984) Gas Chromatography. In Kaplan LA and Pesce AJ (Eds) *Clinical Chemistry: Theory, Analysis and Correlation* (pp. 117 – 135). St. Louis, Missouri, CV Mosby Company.

Popli A, Baldessarini RJ and Cole JO (1995) Interactions of serotonin reuptake inhibitors with tricyclic antidepressants. Letter-Reply. *Arch Gen Psychitry* 52: 784-785.

Potter WZ, Manji HK and Rudorfer MV (1998) Tricyclics and tetracyclics. In Schatzberg AF and Nemeroff CB (Eds) *American Psychiatric Press Textbook of Psychopharmacology* (pp 199-218). American Psychiatric Press, Washington, DC

Preskorn SH (1994) Antidepressant drug selection: criteria and options. *J Clin Psychiatry* 55 (Suppl A): 6-22.

Preskorn SH (1995) Update on clinical aspects of cytochrome P450 mixed function oxidases. *Currents in Affective Illness* 14: 5-20.

Preskorn SH (1996) *Clinical Pharmacology of Selective Serotonin Reuptake Inhibitors*. Professional Communications, Caddo, OK.

Prichard BNC, Owens CWI and Tuckman J (1981) Clinical features of adrenergic agonists and antagonists. In Szekeres L (Ed) *Adrenergic Activators and Inhibitors Part II* (559-697). Springer-Verlag, New York, NY.

Regårdh CG, Borg KO, Johansson R, Johnsson G and Palmer L (1974) Pharmacokinetic studies on the selective β_1-receptor antagonist metoprolol in man. *J Pharmacokinet Biopharm* 2: 347-364.

Regårdh CG, Ek L and Hoffmann KJ (1979) Plasma levels and β-blocking effect of α-hydroxymetoprolol-metabolite of metoprolol-in the dog. *J Pharmacokinet Biopharm* 7: 471-479.

Ried LD, McFarland BH, Johnson RE and Brody KK (1998) β-Blockers and depression: the more the murkier. *Ann Pharmacother* 32: 699-708.

Remmel RP and Burchell B (1993) Validation and use of cloned, expressed human drug-metabolizing enzymes in heterologous cells for analysis of drug metabolism and drug-drug interactions. *Biochem Pharmacol* 46: 559-566.

Richelson E (1997) Pharmacokinetic drug interactions of new antidepressants: a review of the effects on the metabolism of other drugs. *Mayo Clin Proc* 72: 835-847.

Richelson E and Pfenning M (1984) Blockade by antidepressants and related compounds of biogenic amine uptake into rat brain synaptosomes: most antidepressants selectively block norepinephrine uptake. *Eur J Pharmacol* 104: 277-286.

Riesenman C (1995) Antidepressant drug interactions and the cytochrome P450 system: A critical appraisal. *Pharmacotherapy* 15: 84S-99S.

Rozman D, Stromstedt M and Waterman MR (1996) The three human cytochrome P450 lanosterol 14 alpha-demethylase (CYP51) genes reside on chromosomes 3, 7 and 13: structure of the two retrotransposed pseudogenes, association with a line-1 element, and evolution of the human CYP51 family. *Arch Biochem Biophys* 333: 466-474.

Segal IH (1975) *Enzyme Kinetics. Behavior and Analysis of Rapid Equilibrium and Steady-State Enzyme Systems*. Wiley Interscience, New York NY.

Shen WW (1997) The metabolism of psychoactive drugs: A review of enzymatic biotransformation and inhibition. *Biol Psychiatry* 41: 814-826.

Sherwin JE (1984) Liver function. In Kaplan LA and Pesce AJ (Eds) *Clinical Chemistry: Theory, Analysis and Correlation* (pp. 420 – 438). St. Louis, Missouri, CV Mosby Company.

Smith DA (1991) Species differences in metabolism and pharmacokinetics: are we close to an understanding? *Drug Metab Rev* 23: 355-373.

Smith DA and Jones BC (1992) Speculations on the substrate structure-activity relationship (SSAR) of cytochrome P450 enzymes. *Biochem Pharmacol* 44: 2089-2098.

Smith M and Lin K-H (1996) Gender and ethnic differences in the pharmacogenetics of psychotropics. In Jensvold MF, Halbreich U and Hamilton, JA (Eds) *Psychopharmacology and Women: Sex, Gender and Hormones*. (pp. 121-136) American Psychiatric Press, Washington, DC.

Souček P and Gut I (1992) Cytochromes P-450 in rats: structures, functions, properties and relevant human forms. *Xenobiotica* 22: 83-103.

Swatzenegger M and Jaeger W (1995) Clinical importance of hepatic cytochrome P450 in drug metabolism. *Drug Metab Rev* 27: 397-415.

Syed SEH (1998) High performance liquid chromatographic assays. In Eisenthal R and Danson MJ (Eds) *Enzyme Assays: A Practical Approach* (pp 123-133).

Tabor MW (1984) Chromatography: theory and practice. In Kaplan LA and Pesce AJ (Eds) *Clinical Chemistry: Theory, Analysis and Correlation* (pp. 74 – 99). St. Louis, Missouri, CV Mosby Company.

Testa B (1990) Mechanisms of inhibition of xenobiotic-metabolizing enzymes. *Xenobiotica* 20: 1129-1137.

Tollefson GD and Rosenbaum JF (1998) Selective serotonin reuptake inhibitors. In Schatzberg AF and Nemeroff CB (Eds) *American Psychiatric Press Textbook of Psychopharmacology* (pp 219-237). American Psychiatric Press, Washington, DC.

Tucker GT (1992) The rationale selection of drug intreaction studies: implications of recent advances in drug metabolism. *Int J Clin Pharmacol Ther Toxicol* 30: 550-553.

von Bahr C, Spina E, Birgersson C, Ericsson Ö, Göransson M, Henthorn T and Sjöqvist F (1985) Inhibition of desmethylimipramine 2-hydroxylation by drugs in human liver microsomes. *Biochem Pharmacol* 34: 2501-2505.

von Molke LL, Greenblatt DJ, Coteau-Bibbo MM, Harmatz JS and Shader RI (1994a) Inhibitors of alprazolam metabolism *in vitro*: effect of serotonin-reuptake

inhibitor antidepressants, ketoconazole and quinidine. *Br J Clin Pharmacol* 38: 23-31.

von Molke LL, Greenblatt DJ, Coteau-Bibbo MM, Duan SX, Harmatz JS and Shader RI (1994b) Inhibition of desipramine hydroxylation *in vitro* by serotonin-reuptake inhibitor antidepressants, and by quinidine and ketoconazole: a model system to predict drug interactions *in vivo*. *J Pharmacol Exp Ther* 268: 1278-1283.

von Molke LL, Greenblatt DJ, Schmider J, Wright CE, Harmatz JS and Shader RI (1998) *In vitro* approaches to predicting drug interactions *in vivo*. *Biochem Pharmacol* 55: 113-122.

Vormfelde SV, Bitsch A, Meineke I, Gundert-Remy UM and Gleiter CH (1997) Non-response to maprotiline caused by ultra-rapid metabolism that is different from CYP2D6? *Eur J Clin Pharmacol* 52: 387-390.

Walle T and Gaffney TE (1972) Propranolol metabolism in man and dog: Mass spectrometric identification of six neew metabolites. *J Pharmacol Exp Ther* 182: 83-92.

Walley T, Pirmohamed M, Proudlove C and Maxwell D (1993) Interaction of metoprolol and fluoxetine. *Lancet* 341: 967-968.

Watanabe K, Narimatsu S, Yamamoto I and Yoshimura H (1990) Hepatic microsomal oxygenation of aldehydes to carboxylic acids. *Biochem Biophys Res Commun* 166: 1308-1312.

Wayne VS, Harper RW, Laufer E, Federman J, Anderson ST and Pitt A (1982) Adverse interaction between beta-adrenergic blocking drugs and verapamil - report of three cases. *Aust NZ J Med* 12: 285-289.

Weiner N (1980) Drugs that inhibit adrenergic nerves and block adrenergic receptors. In Goodman Gilman A, Goodman LS and Gilman A (Eds) *Goodman and Gilman's: The Pharmacological Basis of Therapeutics, Sixth Edition* (pp 176-210). Collier MacMillan Canada Ltd, Toronto, ON.

Wells KB, Golding JM and Burnam MA (1988) Psychiatric disorder in a sample of the general population with and without chronic medical conditions. *Am J Psychiatry* 145: 976-981.

Wells KB, Golding JM and Burnam MA (1989) Affective, substance use, and anxiety disorders in persons with arthritis, diabetes, heart disease, high blood pressure, or chronic lung conditions. *Gen Hosp Psychiatry* 11: 320-327.

Wells KB, Rogers W, Burnam MA, Greenfield S and Ware JE (1991) How the medical comorbidity of depressed patients differs across health care settings: results from the medical outcomes study. *Am J Psychiatry* 148: 1688-1696.

Wrighton SA, VandenBranden M and Ring BJ (1996) The human drug metabolizing cytochromes P450. *J Pharmacokinet Biopharm* 24: 461-473.

Chapter 2: The Effect of the Antidepressants Desipramine, Fluoxetine and Fluvoxamine on the Metabolism of Metoprolol in Rat Tissue

2.1 INTRODUCTION

Metoprolol (MET), a frequently prescribed cardiac β-blocker, undergoes extensive hepatic metabolism. The major metabolic pathways are α-hydroxylation, O-demethylation and N-dealkylation. These three major routes of metabolism account for 85% of the dose in man (Lennard, 1989). The α-hydroxylation of MET occurs predominantly via cytochrome P450 (CYP) 2D6 whereas O-demethylation is catalyzed by CYP2D6 and as yet other unidentified enzymes (Otton *et al.*, 1988). Due to the involvement of the CYP isoenzymes in the metabolism of MET, drug-drug interactions with other cytochrome substrates and inhibitors become a concern. An interaction between MET and the antidepressant fluoxetine (FLU) has been documented, in which the patient experienced profound lethargy and bradycardia (Walley *et al.*, 1993). An interaction between paroxetine (PAR) and MET has been documented, in which the patient experienced bradycardia (Konig *et al.*, 1996). Interactions between MET and verapamil have also been documented in which patients experienced cardiac failure, hypotension and bradycardia (Wayne *et al.*, 1982). FLU inhibits CYP2D6, CYP2C19, CYP2C9 and CYP3A3/4 to varying degrees, PAR inhibits CYP2D6 (Preskorn, 1997; Riesenman, 1995; Greenblatt *et al.*, 1998) and verapamil is known to inhibit CYP3A (Pichard *et al.*, 1990).

In order to study more extensively possible metabolic drug-drug interactions occurring with MET, a sensitive electron-capture gas chromatographic procedure was developed for the simultaneous analysis of MET and O-desmethylmetoprolol (ODM) in tissue samples. Other methodologies have been reported for the quantitation of MET in urine and/or plasma samples utilizing a variety of techniques, including HPLC (Lennard

and Silas, 1983; Chiu *et al.*, 1997; Pautler *et al.*, 1982; Godbillon and Duval, 1984; Horai *et al.*, 1988; Sioufi *et al.*, 1983; Toon *et al.*, 1988; Musch *et al.*, 1989 and Xie *et al.*, 1995) and gas chromatography combined with flame ionization detection (GC-FID) (Gyllenhaal *et al.*, 1984), mass spectrometry (GC-MS) (Ervik *et al.*, 1981), or electron-capture detection (GC-ECD) (Ervik *et al.*, 1986 and Kinney, 1981). The simultaneous quantitation of MET and ODM in urine was described in a report by Lennard (1985) in which HPLC was used. Quarterman *et al.*, (1980) describes the simultaneous quantitation of MET and ODM in plasma and urine using GC-ECD and a packed column. One report by Winkler *et al.* (1982) described an HPLC method for the quantitation of metoprolol in both plasma and tissue samples. No methods were found which described the simultaneous quantitation of MET and ODM in tissue samples.

The method described in this chapter represents a relatively simple extraction procedure, followed by derivatization and injection on a gas chromatograph equipped with a capillary column and an electron capture detector. Using this assay, MET and ODM concentrations were determined in brain, heart and liver tissue of rats with or without pretreatment with desipramine (DMI), FLU or fluvoxamine (FVX). DMI is a known substrate (Spatzenegger and Jaeger, 1995) and inhibitor (Crewe *et al.*, 1992) of CYP2D6. FLU has strong inhibitory effects on CYP2D6, with moderate inhibition of CYP2C19 and CYP2C9 and weak inhibition of CYP3A3/4 (Preskorn 1997; Riesenman, 1995, Greenblatt *et al.*, 1998). FVX is a potent inhibitor of CYP1A2 and CYP2C19, with moderate inhibition of CYP3A3/4 and CYP2C9. It is considered to have a low to minimal CYP2D6 inhibitory potential (Riesenman, 1995; Greenblatt *et al.*, 1998).

2.2 ANIMAL EXPERIMENT

Male Sprague-Dawley rats weighing 200-250 g were injected intraperitoneally (*ip*) with either DMI (10 mg/kg), or FLU (5 mg/kg), or FVX (20 mg/kg) or with distilled water vehicle (VEH). After 1 hour the rats were injected with either MET (20 mg/kg) or VEH, resulting in eight treatment groups: VEH-VEH, VEH-MET, DMI-VEH, DMI-MET, FLU-VEH, FLU-MET, FVX-VEH and FVX-MET (n=6 per group). The animals were sacrificed by decapitation 2.0 hours after the second injection. Whole brains were removed and submerged in isopentane on solid carbon dioxide for rapid freezing. Hearts and livers were also removed and placed on solid carbon dioxide. All samples were stored at -60°C until analysis. All procedures involving animals were conducted according to the Canadian Council on Animal Care guidelines and were approved by the University of Alberta Health Sciences Animal Welfare Committee.

2.3 ANALYSIS OF METOPROLOL AND O-DESMETHYLMETOPROLOL

2.3.1 ASSAY PROCEDURE

Rat brain, heart or liver was homogenized in 5 volumes of ice-cold double-distilled water. Aliquots (500 μL) were added to screw-cap culture tubes, and to each of these was added 1000 ng of propranolol as internal standard (IS). Samples were diluted by the addition of 1.5 mL of deionized water and basified with 1.0 g of solid potassium carbonate, after which all tubes were vortex mixed. To each tube, 4 mL of glass-distilled toluene was added. The tubes were capped, shaken vigorously for 5 min using a vortex-shaker and then centrifuged at 1000 g for 5 min. The toluene layers were removed to a second set of screw-cap culture tubes and extracted with 3.0 mL portions of 0.05 M H_2SO_4. The tubes were capped, shaken vigorously for 5 minutes and centrifuged at 1000 g for 5 minutes. The toluene layers were aspirated to waste and the remaining acid

layers basified with 1.6 g of solid potassium carbonate. To each tube, 4.0 mL of toluene was added. The tubes were capped, shaken vigorously for 5 minutes and centrifuged at 1000 g for 5 minutes. The toluene layers were transferred to screw-cap tubes and taken to dryness under a stream of nitrogen.

The samples were then derivatized by adding 25 µL of ethyl acetate followed by 75 µL of pentafluoropropionic anhydride (PFPA) and leaving them to sit at room temperature for 30 min. Each reaction mixture was then partitioned between 300 µL of toluene and 3 mL of saturated sodium borate. The mixture was vortexed briefly and centrifuged at 1000 g for 1 min. The toluene layer was retained and a 2 µL aliquot was used for gas chromatographic analysis (Figure 2-1).

2.3.2 CALIBRATION CURVES

Calibration curves (0-1000 ng of MET and 0-200 ng of ODM) were run in parallel with each assay run and were prepared using naïve rat brain, heart or liver tissue homogenate. To each standard was added the appropriate dilution of MET and ODM stock solution and 1000 ng of IS. The standards were then processed in the same manner as the samples, as described in Section 2.3.1.

2.3.3 ASSAY VALIDATION

Determining the limit of detection, between-run and within-run coefficients of variation and recoveries validated the method.

Within-run precision was calculated by preparing and analyzing in one analytical run 5 standards that were spiked with 200 ng of MET and 50 ng ODM. To determine the between-run coefficient of variation, an "in-house control" was prepared and run with each analytical run. This control was prepared by spiking naïve homogenate with a

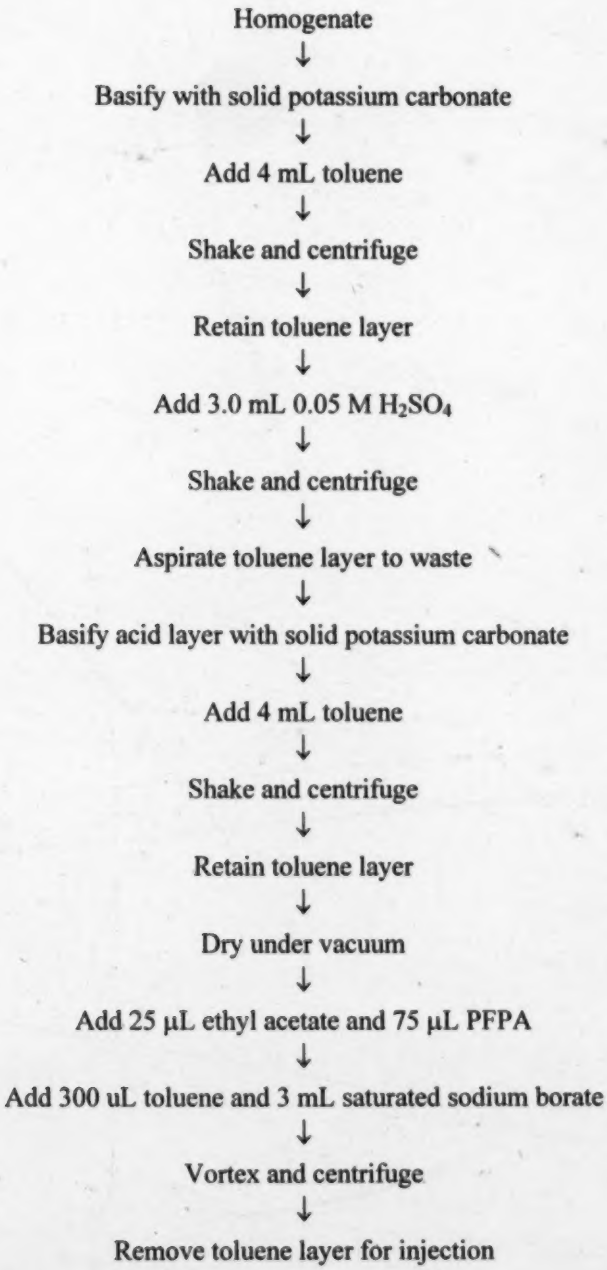
Homogenate
Basify with solid potassium carbonate
Add 4 mL toluene
Shake and centrifuge
Retain toluene layer
Add 3.0 mL 0.05 M H_2SO_4
Shake and centrifuge
Aspirate toluene layer to waste
Basify acid layer with solid potassium carbonate
Add 4 mL toluene
Shake and centrifuge
Retain toluene layer
Dry under vacuum
Add 25 µL ethyl acetate and 75 µL PFPA
Add 300 uL toluene and 3 mL saturated sodium borate
Vortex and centrifuge
Remove toluene layer for injection

Figure 2-1: Flowchart for the analysis of MET and ODM in rat tissue homogenate.

known amount of MET and ODM. The spiked homogenate was aliquoted into 500 µL portions and frozen, with each aliquot containing 100 ng of MET and 20 ng of ODM. Each time an analytical run was performed, one of these controls was thawed and run as a sample.

To ascertain the efficiency of the extraction process, recoveries for MET, ODM and IS were determined. The recovery procedure consisted of comparing samples of spiked naïve brain homogenate which were carried through the assay procedure to tubes which contained only the equivalent amounts of MET, ODM and IS and reacted directly with PFPA.

To further determine the efficiency of the chromatographic system, a 100 ng standard was used to calculate capacity (K′), selectivity (α) and resolution (R) according to the equations described in Section 1.9.2.2.

2.3.4 INSTRUMENTATION

2.3.4.1 Gas Chromatography with Electron-Capture Detection

All samples were analysed using a HP model 5880 gas chromatograph equipped with a ^{63}Ni electron-capture detector and linked to a HP 5880A integrator. A fused HP5 silica capillary column (25 m x 0.32 mm) coated with 1.05 µm film thickness of 5% phenylmethylsilicone was employed. The carrier gas was pure helium at a flow rate of 4 mL/min. The make-up gas was argon-methane (95:5) at a flow rate of 30 mL/min.

For brain tissue, the oven temperature was set at an initial temperature of 105°C for 0.5 min. The temperature was increased by 5° per minute to 225°C, and held for 4.0 min. The oven temperature was then increased by 20° per minute to a final temperature of 295°C which was maintained for 2.0 min.

When injecting the heart and liver samples, the oven temperature programming was altered slightly. The oven temperature was again set at an initial temperature of 105°C for 0.5 min. The temperature was increased by 5° per minute to 230°C, and held for 5.0 min. The oven temperature was then increased by 20° per minute to a final temperature of 295°C that was maintained for 2.0 min.

Injection port and detector temperatures were 250°C and 325°C, respectively. All injections were carried out using the splitless mode of injection with a purge off time of 0.5 min.

2.3.4.2 Gas Chromatography with Mass Spectrometry Detection

Mass spectrometric analysis was performed in the electron impact mode with the operating conditions as follows: ion source temperature, 200°C; interface temperature, 275 °C; column pressure, 34.5 kPa; accelerating voltage, 2200 eV; ionization voltage, 70 eV; scan speed, 200 amu/sec; and dwell time, 200 msec.

2.3.5 STATISTICAL ANALYSIS

Main treatment effects were determined by a two-way analysis of variance (ANOVA) of square root transformed data using SPSS® software. Where significant ($p<0.05$) main effects were reached, *post hoc* multiple comparisons with Dunnet's test were employed to identify individual group differences.

2.4 RESULTS

2.4.1 ASSAY PROCEDURE

This assay for the simultaneous quantitation of MET and ODM produces derivatives with good chromatographic properties and no interfering peaks. Typical

chromatograms from the analysis of the standards and test samples are shown in Figures 2-2 and 2-3 respectively.

2.4.2 CALIBRATION CURVES

Calibration curves for MET were generated by plotting the peak height ratio of derivatized MET to a fixed amount of derivatized IS on the y-axis versus the concentration of MET on the x-axis. Calibration curves for ODM were generated in the same manner, in which the peak height ratio of derivatized ODM to a fixed amount of derivatized IS was plotted on the y-axis versus the concentration of ODM on the x-axis. Calibration curves, which were run in parallel with the experimental tissue in every assay, were linear, with r^2 values >0.99 obtained consistently.

Typical calibration curves for MET and ODM are shown in Figures 2-4 and 2-5 respectively. Due to the necessity of quantitating a wide range of concentrations for MET, two calibration curves were generated. The first curve was constructed using 0, 10, 20, 50 and 100 ng standards. The second curve used 0, 100, 200, 500 and 1000 ng standards. The calibration curves for ODM were constructed using standard concentrations of 0, 5, 10, 20, 50, 100 and 200 ng.

2.4.3 ASSAY VALIDATION

The limit of detection for MET was 50 pg "on column". ODM had a detection limit of 20 pg "on column". The mean between-run coefficients of variation of the "in-house control" were determined to be 5.5% for MET and 7.1% for ODM (n=3). The within-run coefficients of variation were 2.6% and 1.5% for MET and ODM respectively (n=5). The mean recoveries of MET, ODM and IS were determined to be 88%, 74% and

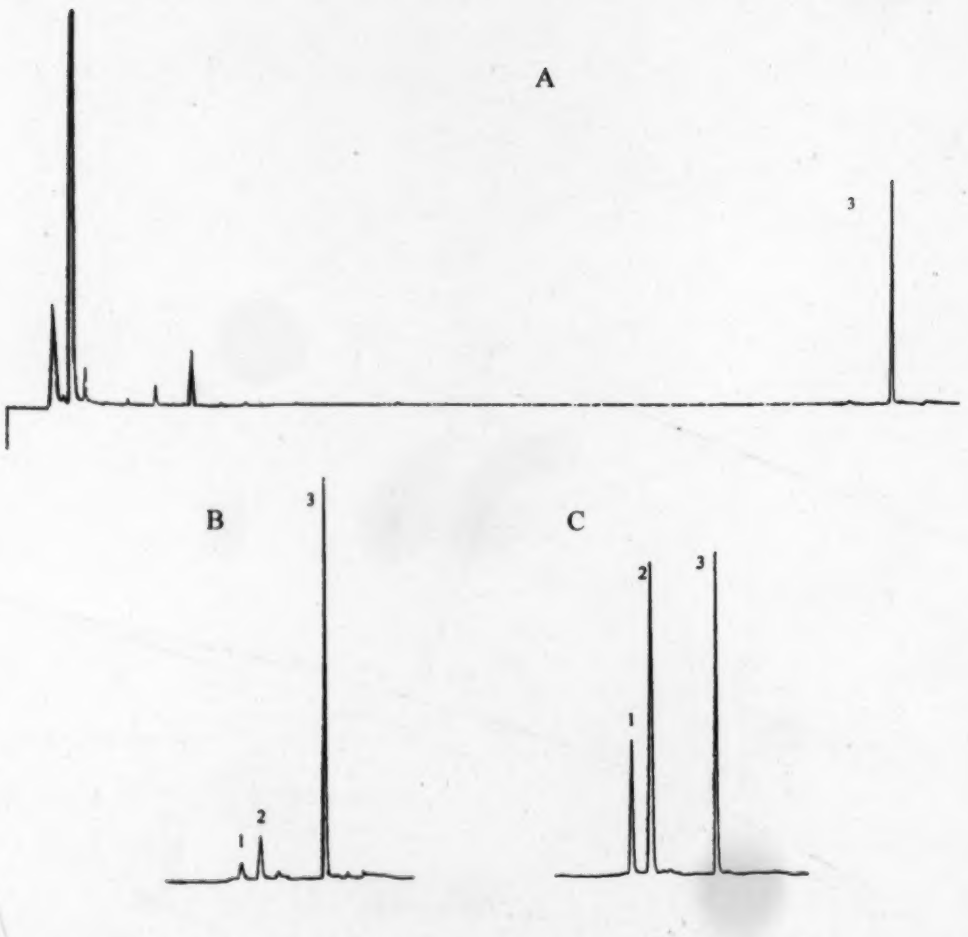

Figure 2-2: Typical standard chromatograms from the analysis of ODM and MET in rat heart. A) A standard that has only IS. B) A standard that has 20 ng of ODM and 100 ng of MET. C) A standard that has 200 ng of ODM and 1000 ng of MET. Peak 1 is ODM with a retention time of 29.96 min, Peak 2 is MET with a retention time of 30.60 min, and Peak 3 is IS with a retention time of 32.76 min.

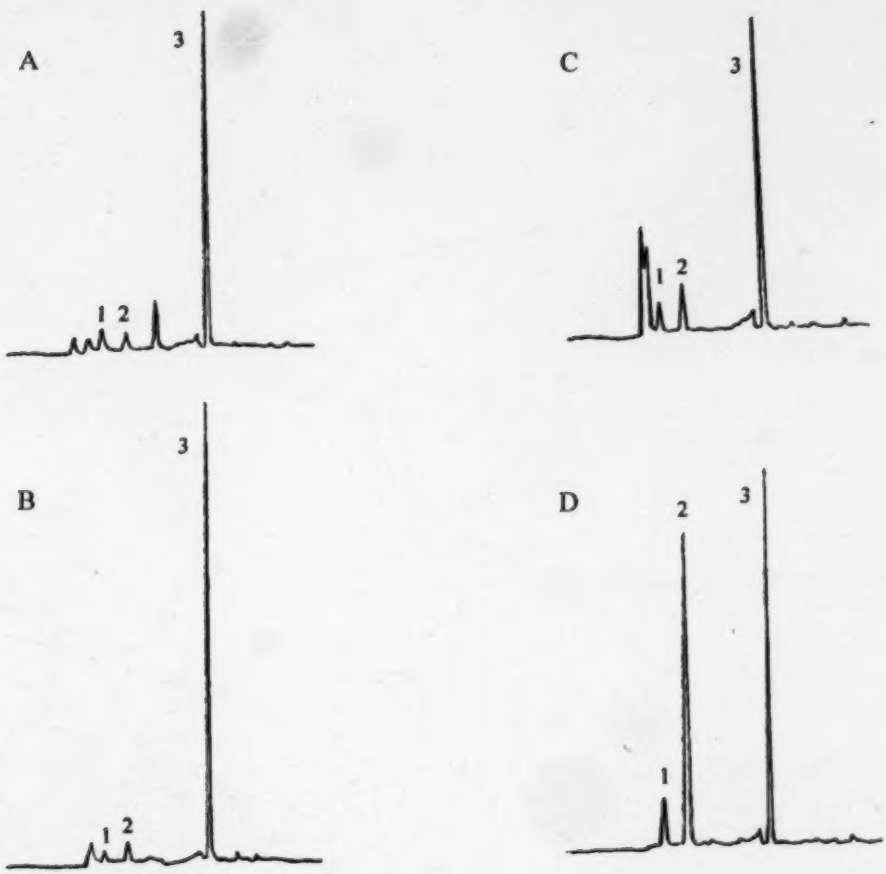

Figure 2-3: Typical chromatograms from the analysis of ODM and MET in rat liver samples. A) A sample from the VEH-MET treatment group. B) A sample from the FLU-MET treatment group. C) A sample from the FVX-MET treatment group. D) A sample from the DMI-MET treatment group. Peak 1 is ODM with a retention time of 29.96 min, Peak 2 is MET with a retention time of 30.60 min, and Peak 3 is IS with a retention time of 32.76 min.

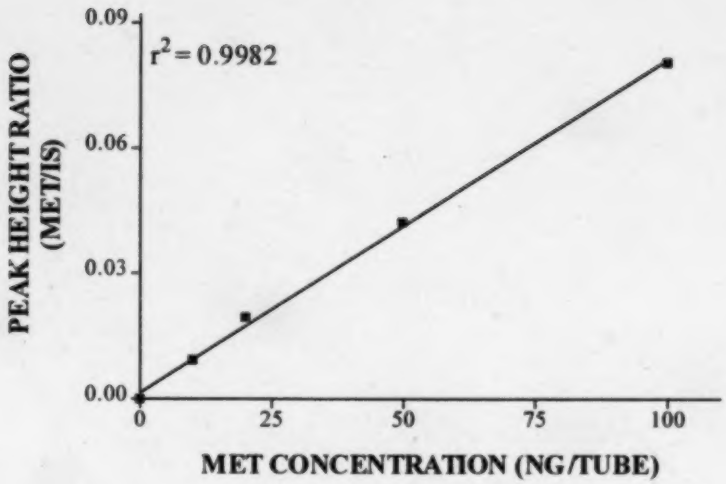

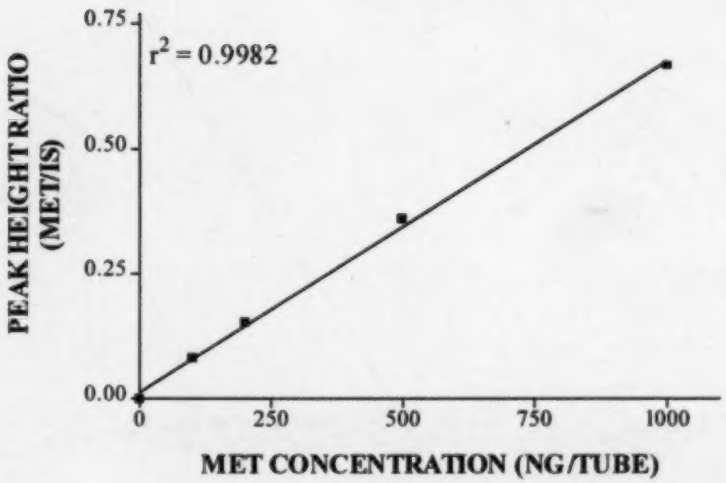

Figure 2-4: Typical calibration curves for the quantitation of MET in rat brain.

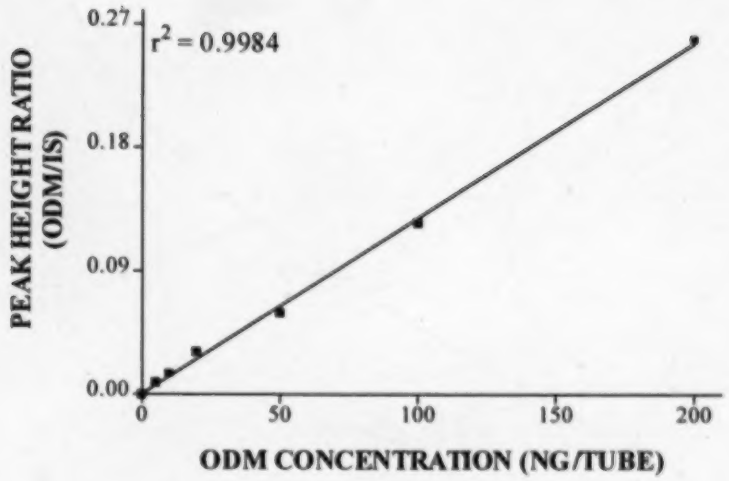

Figure 2-5: Typical calibration curve for the quantitation of ODM in rat brain.

88% respectively (n=5). The chromatographic parameters of K′, α and R are given in Table 2-1.

2.4.4 CONFIRMATION OF STRUCTURES OF DERIVATIVES

The structures of the derivatives of MET, ODM and IS were confirmed using combined gas chromatography-mass spectrometry in the electron impact mode. The mass spectra of the pentafluoropropionate (PFP) derivatives of ODM, MET and IS are shown in Figure 2-6. The proposed fragmentation patterns for the derivatives of MET ODM, and IS are shown in Figures 2-7, Figure 2-8 and Figure 2-9 respectively.

2.4.5 METOPROLOL LEVELS

The levels of MET in brain, heart and liver are presented in Table 2-2; these data are presented graphically in Figure 2-10. The levels (mean ± standard error of the mean [SEM]) in heart, brain and liver of the VEH-MET treatment group (n=6) were 244 ± 78 ng/g, 339 ± 84 ng/g and 379 ± 119 ng/g of tissue, respectively. These values increased markedly in the DMI-MET treatment group (n=6) to 5113 ± 462 in heart, 7003 ± 693 ng/g in brain and 8659 ± 817 ng/g in liver. These values showed a significant increase in MET levels compared to the MET-VEH treatment group. In the FVX-MET treatment group (n=6) the values in heart, brain and liver were 846 ± 148 ng/g, 1199 ± 260 ng/g and 1255 ± 224 ng/g of tissue, respectively. These levels also represented a significant increase over the MET-VEH group. The MET levels in the FLU-MET treatment group (n=6) were not significantly different from those in the MET-VEH treatment group. The values obtained were 393 ± 96 ng/g in heart, 517 ± 139 ng/g in brain and 570 ± 148 ng/g in liver. No metoprolol was detected in the VEH-VEH, DMI-VEH, FVX-VEH or the

Standard	Temperature Program					
	Brain			Heart/Liver		
	K′	α	R	K′	α	R
ODM	23.4	1.01	2.2	16.5	1.02	2.8
MET	23.7	1.08	14.2	16.9	1.07	11.3
IS	25.7			18.1		

Table 2-1: Chromatographic parameters for GC analysis of ODM and MET (n = 3) calculated using the equations described in Section 1.9.2.2.

A

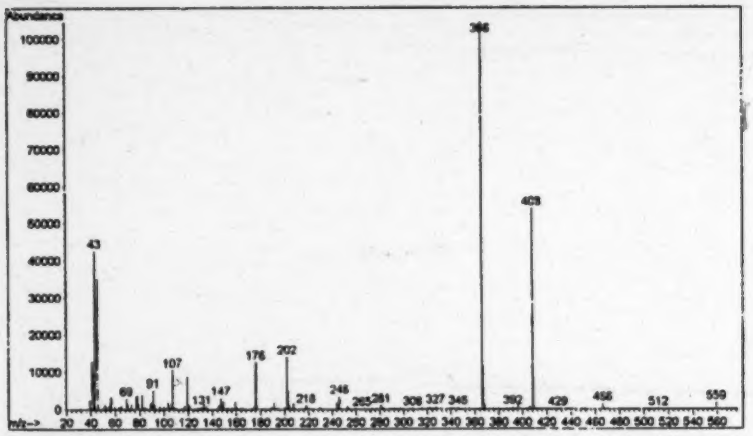

B

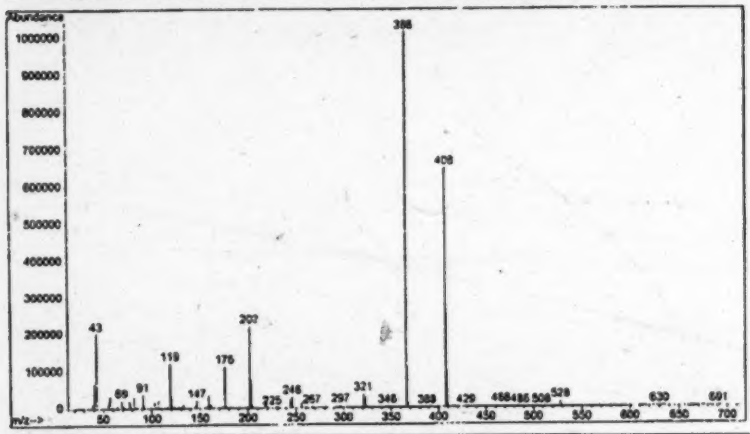

C

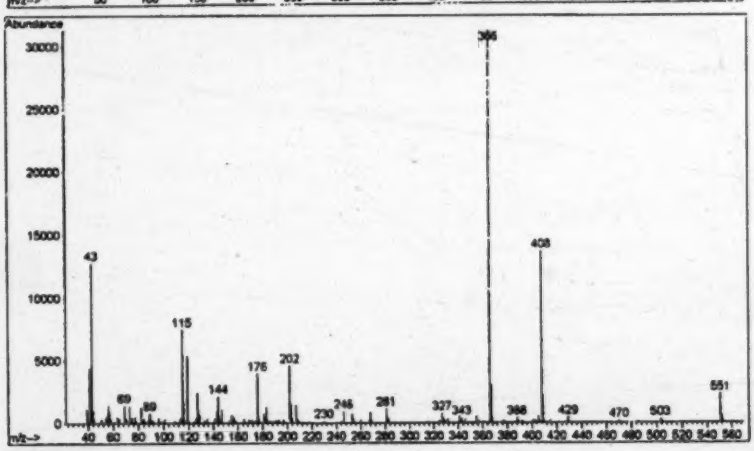

Figure 2-6: Mass spectrum analysis of the PFP derivatives of A) MET, B) ODM and C) IS.

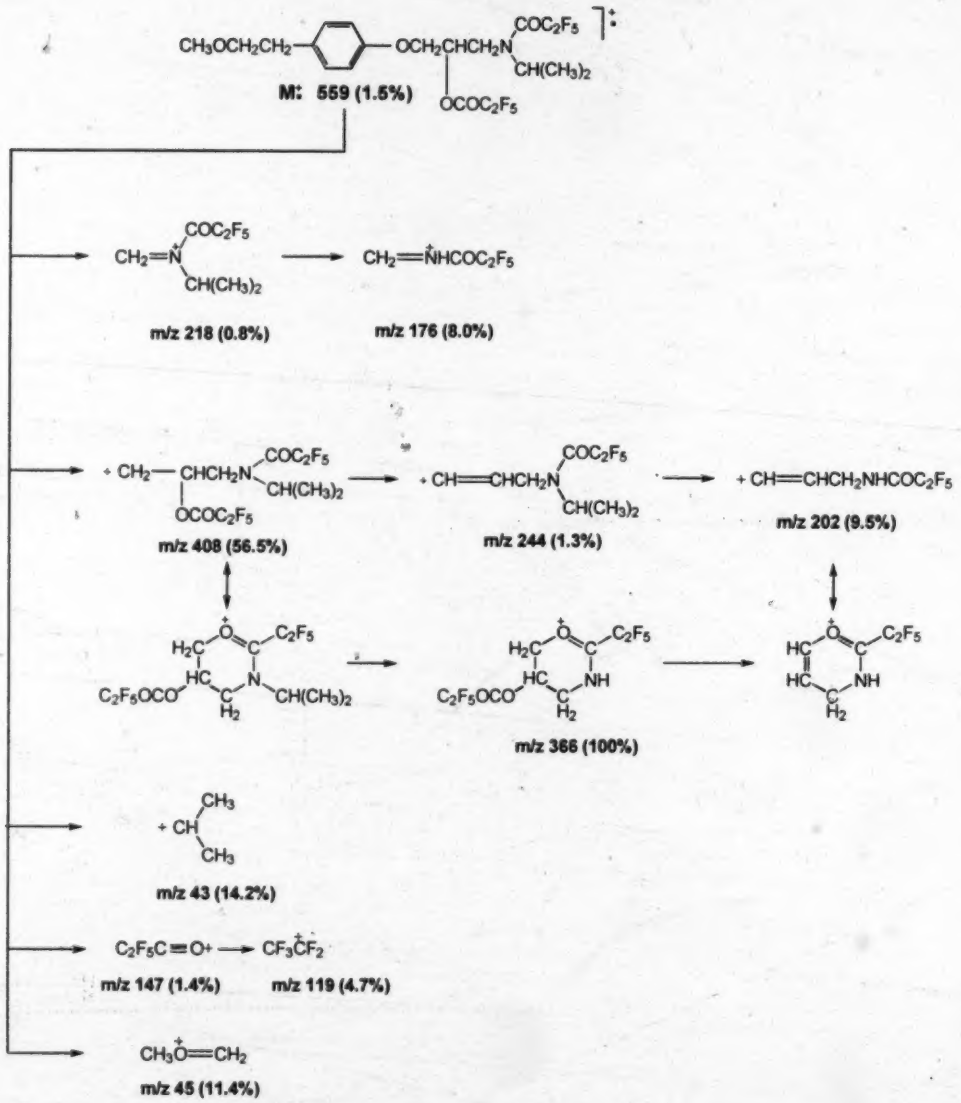

Figure 2-7: Proposed fragmentation pattern of the PFP derivative of MET.

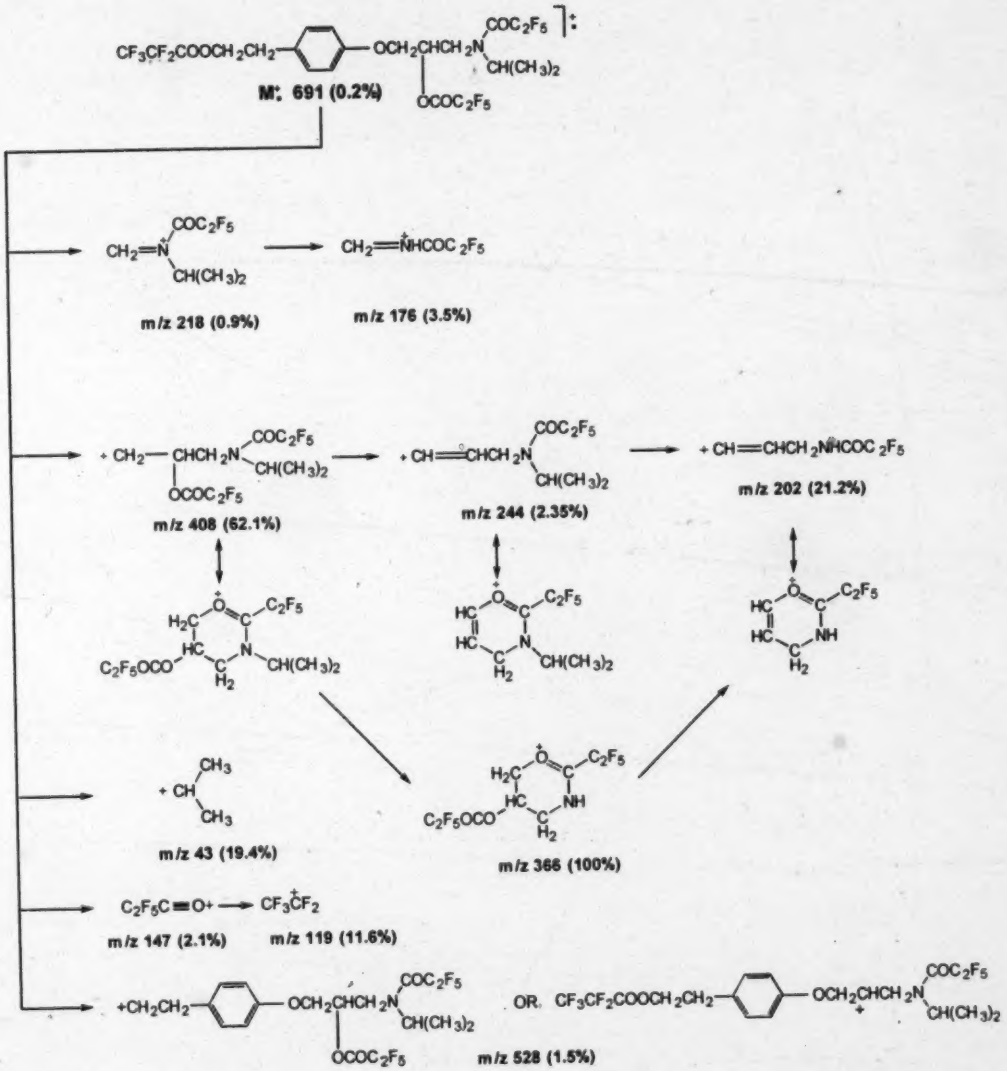

Figure 2-8: Proposed fragmentation pattern of the PFP derivative of ODM.

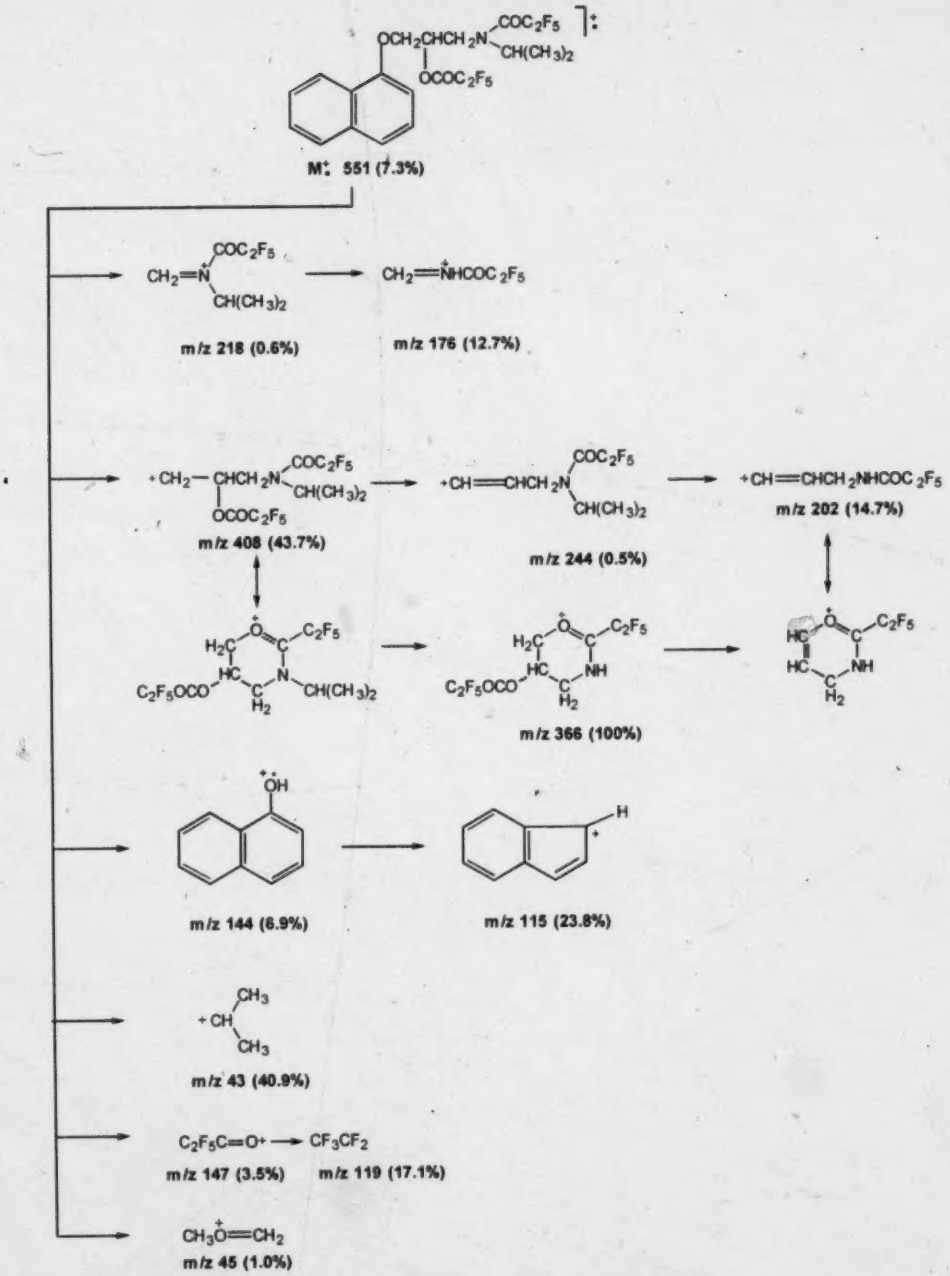

Figure 2-9: Proposed fragmentation pattern of the PFP derivative of IS.

TISSUE	TREATMENT GROUP	MET		ODM	
		Mean	SEM	Mean	SEM
HEART	VEH-MET	244	78	152	33
	FLU-MET	393	96	241	33
	FVX-MET	846*	148	338*	41
	DMI-MET	5113*	462	697*	82
BRAIN	VEH-MET	339	84	128	22
	FLU-MET	517	139	101	14
	FVX-MET	1199*	260	138	17
	DMI-MET	7003*	693	295*	20
LIVER	VEH-MET	379	119	158	33
	FLU-MET	570	148	234	42
	FVX-MET	1255*	224	440*	54
	DMI-MET	8659*	817	973*	131

Table 2-2: MET and ODM levels (ng/g tissue, n = 6) in rat heart, brain and liver.

* denotes a significant difference of <0.05 compared to the VEH-MET treatment group.

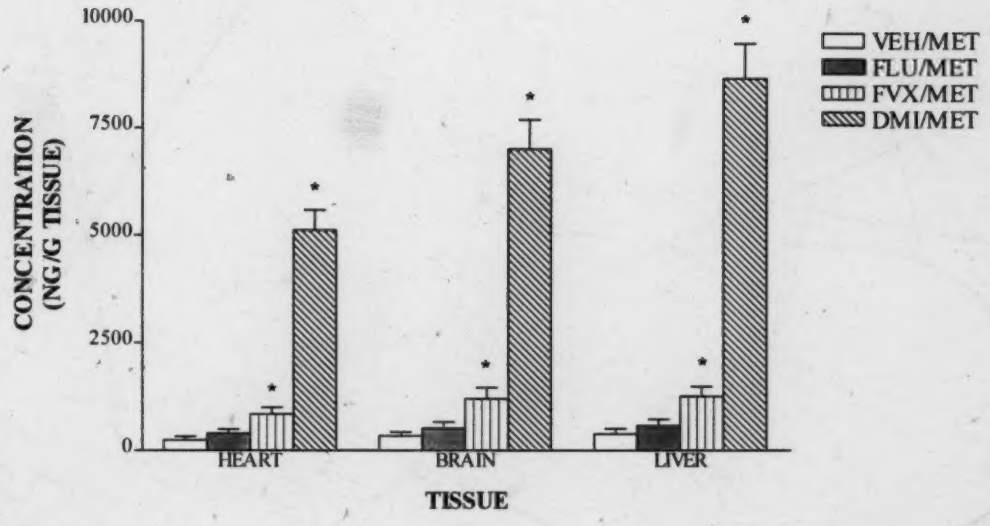

Figure 2-10: MET levels (n = 6) in rat heart, brain and liver in the VEH-MET, FLU-MET, FVX-MET and DMI-MET treatment groups. Values are presented as means ± SEM. * denotes a significant difference of <0.05 compared to the VEH-MET treatment group.

FLU-VEH treatment groups, effectively demonstrating that neither DMI, FVX, FLU nor any of their metabolites interfere with the quantitation of MET.

2.4.6 O-DESMETHYLMETOPROLOL LEVELS

Levels of ODM in brain, heart and liver are also presented in Table 2-2; these data are presented graphically in Figure 2-11. The levels in heart, brain and liver of the VEH-MET treatment group (n=6) were 152 ± 33 ng/g, 128 ± 22 ng/g and 158 ± 33 ng/g of tissue, respectively. These values increased significantly in the DMI-MET treatment group (n=6) to 697 ± 82 in heart, 295 ± 20 ng/g in brain and 973 ± 131 ng/g in liver. In the FVX-MET treatment group (n=6) the values in heart, brain and liver were 338 ± 41 ng/g, 138 ± 17 ng/g and 440 ± 54 ng/g of tissue, respectively. With respect to FVX, the heart and liver levels, but not brain levels, showed a significant increase over those of the MET-VEH group. The ODM levels in the FLU-MET treatment group (n=6) were not significantly different from the MET-VEH treatment group. The values obtained were 241 ± 33 ng/g of heart tissue, 101 ± 14 ng/g of brain tissue and 234 ± 42 ng/g of liver tissue. Neither MET nor ODM was detected in the VEH-VEH, DMI-VEH, FVX-VEH or the FLU-VEH treatment groups.

2.5 DISCUSSION

2.5.1 ASSAY PROCEDURE

This novel analytical procedure for analyzing both MET and ODM in tissue samples is simple and reproducible, producing a derivative with good chromatographic properties. The relatively long retention time of the assay was necessary to ensure that the quantitations of ODM and MET were not compromised by interfering peaks. When comparing the chromatograms of the standards (Figure 2-2) and test samples

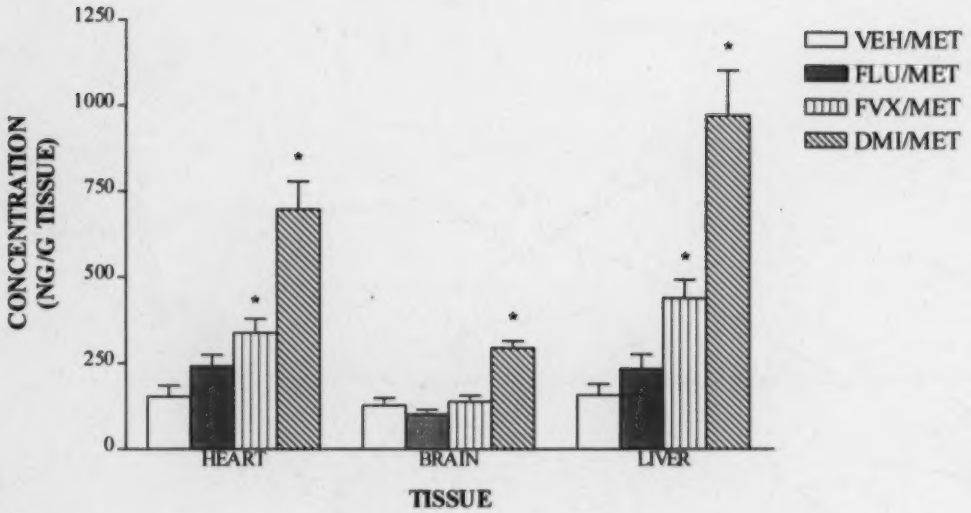

Figure 2-11: ODM levels (n = 6) in rat heart, brain and liver in the VEH-MET, DMI-MET, FLU-MET and FVX-MET treatment groups. Values are presented as means ± SEM. * denotes a significant difference of <0.05 compared to the VEH-MET treatment group.

(Figure 2-3), it is obvious that the FLU and FVX samples have extraneous peaks that would cause difficulty unless complete separation of the peaks from ODM and MET was achieved. The oven temperature programming allowed for this separation. Indeed, if DMI had been the only coadministered antidepressant used in the study, the run time would have been less than 20 min.

2.5.2 CALIBRATION CURVES

The decision to generate two curves for MET was necessary to ensure accuracy in determination of both low and high concentrations of MET.

2.5.3 ASSAY VALIDATION

The sensitivity of this assay for MET is comparable to those of other reported GC-ECD assays (Ervik, 1975; Ervik *et al.*, 1986; Kinney, 1981; Sioufi *et al.*, 1983). The paper by Winkler *et al.* (1982), which reports the quantitation of MET in rat tissue samples, has a similar limit of detection but a lower recovery of MET (ranging from 57.5-64.1%, depending on tissue type).

The decision to use toluene as the extraction solvent was made based on the decreased extraction of interfering substances and an increased recovery for MET and IS. The recoveries of MET and IS using ethyl acetate were 76% and 73% respectively. Unfortunately, the recovery of ODM was much greater using ethyl acetate compared to toluene, with the recovery in ethyl acetate being 100%. However, due to the interfering peaks present in the ethyl acetate extracted samples, toluene was a better choice. Also, solid K_2CO_3 was more effective in increasing the recovery of ODM, MET and IS from the sample homogenates compared to a solution K_2CO_3, tribasic sodium phosphate or

sodium hydroxide. In addition, recovery was improved by using 0.05 M H_2SO_4 as opposed to 1.0 M hydrochloric acid.

Although the K′ values are greater and the α-values are less than what is considered ideal, the resolution was quite acceptable, having values greater than 1.25 (Tabor, 1984).

2.5.4 CONFIRMATION OF STRUCTURES OF DERIVATIVES

The MS fragmentation patterns for MET, ODM and IS confirm the theoretical structures of the pentafluoroproprionate derivatives.

2.5.5 METOPROLOL LEVELS

The data shown here suggest that DMI, a known inhibitor of CYP2D6 in man (Crewe *et al.*, 1992), inhibits metoprolol metabolism to a significant degree. The magnitude of the effect (an approximately 20-fold increase in brain, heart and liver levels of MET), was remarkable. The results generated from the DMI-MET treatment group would suggest that other inhibitors of CYP2D6 would have a similar effect. However, the results from the FLU-MET treatment group do not support this finding. In studies using human liver microsomes to investigate sparteine metabolism, the rank order of potency of CYP2D6 inhibition is FLU>DMI>FVX (Crewe *et al.*, 1992).

There are several reasons why the discrepancy between the human liver microsome study and the rat study may exist. It is possible the discrepancy is due to major differences in the characteristics of the CYP enzymes in rats and humans. Borg *et al.*, (1975) has demonstrated that the O-demethylation pathway accounts for 65% and 62% of a given dose in both man and rat, respectively. Thus, the difference is not attributable to differences in the major pathway of MET metabolism. Also, the CYP2D6

enzyme is thought to be analogous to the CYP2D1 enzyme in rats. In fact there is more than 70% sequence homology between the two enzymes (Souček and Gut, 1992). However, even with this high sequence homology, there are important differences between the rat and human CYP2D enzymes. Perhaps most applicable to this discussion is the difference in inhibitor specificity of quinidine and quinine. Quinidine is the more potent inhibitor of the human enzyme whereas quinine is the more potent against the rat enzyme (Smith, 1991). Obviously, there are significant differences in the active site of the CYP2D1 enzyme in rats and the CYP2D6 enzyme in humans.

Another reason for the discrepancy between human liver microsome studies and the rat study described here may be due to the substrate used. In competitive inhibition, the potency of an inhibitor for a particular enzyme will depend on the substrate it is competing with. Thus, although FLU and norfluoxetine (NFLU) are potent inhibitors of CYP2D6 when determining their effect on sparteine metabolism in human liver microsomes, their effect may not be as potent when determining their effect on MET.

One more possible reason for the discrepancy between the results is that the levels of FLU and NFLU obtained in the rats *in vivo* may not have been sufficient to cause inhibition of the CYP2D1 enzyme.

These different possibilities were investigated by determining the levels of the antidepressants obtained in the rat tissues (Chapter 3) and by conducting an in-depth analysis of the inhibitory potential of DMI, FLU and FVX in human liver microsomes using MET as the substrate (Chapter 4).

2.5.6 O-DESMETHYLMETOPROLOL LEVELS

The first instinct when looking at metabolite levels is to assume that as the parent drug is being metabolized, the metabolite levels should increase. As is apparent from the ODM levels, the situation is not that simple. There are several reasons why this simple assumption may be invalid. The first reason is that the production of ODM is going to be based on the level of MET. In the case of DMI, there are much greater levels of MET in the system, allowing for an increased production of metabolite. Secondly, as ODM is being produced it will also be metabolized to AM and excreted. If the conversion of ODM to AM is inhibited in the same manner as the metabolism of MET to ODM, then once ODM is formed it cannot be as readily metabolized and excreted. In addition, the antidepressant maybe inhibiting only one of the enzymes involved in the formation of ODM, allowing the other enzyme to metabolize MET to ODM. Given these scenarios, it then seems logical that the levels of ODM are increased in the same manner as the levels of MET, with greater levels of ODM found in the DMI-MET treatment group, followed by the FVX-MET treatment group and the lowest levels found in the FLU-MET treatment group.

2.6 RFERENCES

Borg KO, Carlsson E, Hoffmann K-J, Jönsson T-E, Thorin H and Wallin B (1975) Metabolism of metoprolol-(^{3}H) in man, the dog and the rat. *Acta Pharmacol Toxicol* 36(Suppl V): 125-135.

Chiu FCK, Damani LA, Li RC and Tomlinson B (1997) Efficient high-performance liquid chromatographic assay for the simultaneous determination of metoprolol and two main metabolites in human urine by solid phase extraction and fluorescence detection. *J Chromatogr B* 696: 69-74.

Crewe HK, Lennard MS, Tucker GT, Woods FR and Haddock RE (1992) The effect of selective serotonin re-uptake inhibitors on cytochrome P4502D6 (CYP2D6) activity in human liver microsomes. *Br J Clin Pharmac* 34: 262-265.

Ervik M (1975) Quantitative determination of metoprolol in plasma and urine by gas chromatography. *Acta Pharmacol Toxicol* 36 (suppl V): 136-144.

Ervik M, Hoffman KJ and Kylberg-Hanssen K (1981) Selected ion monitoring of metoprolol and two metabolites in plasma and urine using deuterated internal standards. *Biomed Mass Spectrom* 8: 322-326.

Ervik M, Kylberg-Hanssen K and Johansson L (1986) Determination of metoprolol in plasma and urine using high resolution gas chromatography and electron- capture detection. *J Chromatogr* 381: 168-174.

Godbillon J and Duval M (1984) Determination of two metoprolol metabolites in human urine by high performance liquid chromatography. *J Chromatogr* 309: 198-202.

Greenblatt DJ, von Molke LL, Harmatz JS and Shader RI (1998) Drug interactions with newer antidepressants: role of human cytochromes P450. *J Clin Psychiatry* 59 (Suppl 15): 19-27.

Gyllenhaal O and Hoffman K-J (1984) Simultaneous determination of metoprolol and metabolites in urine by capillary column gas chromatography as oxazolidineone and trimethylsilyl derivatives. *J Chromatogr* 309: 317-328.

Horai Y, Ishizaki T, Kusaka M, Tsujimoto G and Hashimoto K (1988) Simultaneous determination of metoprolol and α-hydroxymetoprolol in human plasma and urine by liquid chromatography with a preliminary observation on metoprolol oxidation in Japanese subjects. *Ther Drug Monit* 10: 428-433.

Kim M, Shen DD, Eddy AC and Nelson WL (1993) Inhibition of the enantioselective oxidative metabolism of metoprolol by verapamil in human liver microsomes. *Drug Metab Dispos* 21: 309-317.

Kinney CD (1981) Determination of metoprolol in plasma and urine by gas-liquid chromatography with electron-capture detection. *J Chromatogr* 225: 213-218.

Konig F, Hafele M, Hauger B, Lobie M, Wossner S and Wolfersdorf M (1996) Bradykardie nach therapiegeginn mit metoprolol and paroxetine. *Psychiatr Prax* 23: 244-245.

Lennard MS (1985) Quantitative analysis of metoprolol and three of its metabolites in urine and liver microsomes by high performance liquid chromatography. *J Chromatogr* 342: 199-205.

Lennard MS (1989) The polymorphic oxidation of beta-adrenoceptor antagonists. *Pharmac Ther* 41:461-477.

Lennard MS and Silas JH (1983) Rapid determination of metoprolol and α-hydroxymetoprolol in human plasma and urine by high-performance liquid chromatography. *J Chromatogr* 272: 205-209.

Murthy SS, Shetty HU, Nelson WL, Jackson PR and Lennard MS (1990) Enantioselective and diastereoselective aspects of the oxidative metabolism of metoprolol. *Biochem Pharmacol* 40: 1637-1644.

Musch G, Buelens Y and Massart DL (1989) A strategy for the determination of beta blockers in plasma using solid-phase extraction in combination with high performance liquid chromatography. *J Pharmaceut Biomed Analysis* 7: 483-497.

Otton SV, Crewe HK, Lennard MS, Tucker GT and Woods HF (1988) Use of quinidine to define the role of the sparteine/debrisoquine cytochrome P450 in metoprolol oxidation by human liver microsomses. *J Pharmacol Exp Ther* 247: 242-247.

Pautler DB and Jusko WJ (1982) Determination of metoprolol and α-hydroxymetoprolol in plasma by high-performance liquid chromatography. *J Chromatogr* 228: 215-222.

Pichard L, Fabre I, Fabre G, Domergue J, Saint Aubert B, Mourad G and Maurel P (1990) Cyclosporin A drug interactions: Screening for inducers and inhibitors of cytochrome P450 (cyclosporin A oxidase) in primary cultures of human hepatocytes and in liver microsomes. *Drug Metab Dispos* 18: 595-605.

Preskorn SH (1997) Clinically relevant pharmacology of selective serotonin reuptake inhibitors: An overview with emphasis on pharmacokinetics and effects on oxidative drug metabolism. *Clin Pharmacokinet* 32 (suppl 1): 1-21.

Quarterman CP, Kendall MJ and Jack DB (1980) Determination of metoprolol metabolites in plasma and urine by electron-capture gas-liquid chromatography. *J Chromatogr* 183: 92-98.

Riesenman C (1995) Antidepressant drug interactions and the cytochrome P450 system: A critical appraisal. *Pharmacotherapy* 15: 84S-99S.

Sioufi A, Leroux F and Sandrenan N (1983) Gas chromatographic determination of metoprolol in human plasma. *J Chromatogr* 272: 103-110.

Smith DA (1991) Species differences in metabolism and pharmacokinetics: are we close to an understanding? *Drug Metab Rev* 23: 355-373.

Souček P and Gut I (1992) Cytochromes P-450 in rats: structures, functions, properties and relevant human forms. *Xenobiotica* 22: 83-103.

Tabor MW (1984) Chromatography: theory and practice. In Kaplan LA and Pesce AJ (Eds) *Clinical Chemistry: Theory, Analysis and Correlation* (pp. 74 – 99). St. Louis, Missouri, CV Mosby Company.

Toon S, Davidson EM, Garstang FM, Bartra H, Bowes RJ and Rowland M (1988) The racemic metoprolol H_2-antagonist interaction. *Clin Pharmacol Ther* 43: 283-289.

Walley T, Pirmohamed M, Proudlove C and Maxwell D (1993) Interaction of metoprolol and fluoxetine. *Lancet* 341: 967-968.

Wayne VS, Harper RW, Laufer E, Federman J, Anderson ST and Pitt A (1982) Adverse interaction between beta-adrenergic blocking drugs and verapamil - report of three cases. *Aust NZ J Med* 12: 285-289.

Winkler H, Ried W and Lemmer B (1982) High-performance liquid chromatographic method for the quantitative analysis of the aryloxypropanolamines propranolol, metoprolol and atenolol in plasma and tissue. *J Chromatogr* 228: 223-234.

Xie HG and Zhou HH (1995) Assay of metoprolol and alpha-hydroxymetoprolol in human urine by reversed-phase liquid chromatography with direct-injection. *Acta Pharmacologica Sinica* 16: 32-35.

Chapter 3: The Levels of the Antidepressants Desipramine, Fluoxetine and Fluvoxamine in Rat Tissue and the Effect of Metoprolol.

3.1 INTRODUCTION

The metabolism of DMI to its 2-hydroxy- and 10 hydroxy- metabolites has been established to be a result of CYP2D6 activity (von Bahr *et al.*, 1985, Shen, 1997). In addition, CYP2D6 is also inhibited by DMI, as determined by studies using human liver microsomes in which sparteine was used as a substrate and the inhibition of the formation of 2-dehydrosparteine was ascertained (Otton *et al.*, 1983 and Crewe *et al.*, 1992). In a study involving rat liver microsomes it was noted that the inhibition of CYP enzymes may result from a metabolite intermediate complexation which is a metabolic route distinct from those routes responsible for the formation of 2-hydroxydesipramine, 10-hydroxydesipramine and N,N-didesmethylimipramine. However, the inhibitory effect was only ascertained on CYP2C11-, CYP2A1- and CYP3A2-mediated metabolism. Whether or not DMI produces a metabolite intermediate complexation with enzymes of the CYP2D family was not determined. It was also noted that the formation of the metabolite intermediate complexation was not the only mechanism by which DMI inhibits the CYP enzymes. However, the mechanistic nature of other possible inhibitions was not addressed (McNeil and Murray, 1996).

Evidence suggests that CYP2C9, with a minor contribution from CYP2D6 and CYP3A3/4, is responsible for the metabolism of FLU (Greenblatt *et al.*, 1998). It has also been established that FLU inhibits CYP2D6, CYP2C19, CYP2C9 and CYP3A3/4 (Preskorn 1997; Riesenman, 1995, Greenblatt *et al.*, 1998). In addition, NFLU has an inhibitory potential similar to that of FLU except that it has an inhibitory potential greater than FLU with respect to inhibition of CYP3A3/4 (Preskorn 1997; Greenblatt *et al.*, 1998).

The enzymes responsible for the metabolism of FVX appear to be CYP1A2 and CYP2D6 (Greenblatt *et al.*, 1998). FVX is a potent inhibitor of CYP1A2 and CYP2C19, with moderate inhibition of CYP3A3/4 and CYP2C9. It is considered to have a low to minimal CYP2D6 inhibitory potential (Riesenman, 1995; Greenblatt *et al.*, 1998).

In this chapter, the adaptation of previously reported methods is described for the simultaneous quantitation of FVX, FLU and NFLU. The adaptation of a previously reported method for the quantitation of DMI is also described. These assays were used to determine the levels of the antidepressants in the presence and absence of MET to determine the effect of MET on the metabolism of the antidepressants. Also, given the unexpected results of the effect of these antidepressants on the metabolism of MET in rats, as described in Chapter 2, it was useful to determine the tissue levels of DMI, FVX, FLU and NFLU.

3.2 ANIMAL EXPERIMENT

The tissue samples used in the experiments described in this chapter are from the same animal experiment as described in Section 2.2. Male Sprague-Dawley rats weighing 200-250 g were injected (*ip*) with DMI (10 mg/kg), or FLU (5 mg/kg), or FVX (20 mg/kg) or with distilled water vehicle (VEH). After 1 hour the rats were injected with either MET (20 mg/kg) or VEH, resulting in eight treatment groups: VEH-VEH, VEH-MET, DMI-VEH, DMI-MET, FLU-VEH, FLU-MET, FVX-VEH and FVX-MET (n=6 per group). The animals were sacrificed by decapitation 2.0 hours after the second injection. Whole brains were removed and submerged in isopentane on solid carbon dioxide for rapid freezing. Hearts and livers were also removed and placed on solid carbon dioxide. All samples were stored at -60°C until analysis. All procedures

involving animals were conducted according to the Canadian Council on Animal Care guidelines and were approved by the University of Alberta Health Sciences Animal Welfare Committee.

3.3 ANALYSIS OF FLUOXETINE, NORFLUOXETINE AND FLUVOXAMINE

3.3.1 ASSAY PROCEDURE

Samples were analyzed using a slight modification of the procedures described by Aspeslet (1994) and Rotzinger *et al.* (1995). Rat brain, heart or liver was homogenized in 5 volumes of ice-cold double-distilled water. Aliquots (1000 μL) were added to screw-cap culture tubes, and to each of these were added 2500 ng of the internal standard alprenolol (ALP). Samples were basified with 500 μL of a 25% solution of potassium carbonate, after which all tubes were vortex mixed. To each tube, 4 mL of a toluene: pentafluorobenzoyl chloride (PFBC) (10 mL:10 μL) solution was added to simultaneously derivatize and extract the compounds of interest. The tubes were capped, shaken vigorously for 15 min using a vortex-shaker and then centrifuged at 1000 g for 5 min. The toluene/PFBC layers were transferred to screw cap tubes and taken to dryness using a vacuum evaporator. The residue was reconstituted in 300 μL of toluene and a 1 μL aliquot was used for gas chromatographic analysis (Figure 3-1).

3.3.2 CALIBRATION CURVES

Calibration curves (0-1000 ng of FLU and 0-2000 ng of FVX and NFLU) were run in parallel with each assay run and were prepared using naïve rat brain, heart or liver tissue homogenate. To each standard was added the appropriate dilution of FLU, FVX

Homogenate

↓

Basify with 25% potassium carbonate

↓

Add 4 mL toluene:PFBC solution

↓

Shake and centrifuge

↓

Retain toluene:PFBC layer

↓

Dry under vacuum

↓

Reconstitute in 300 μL toluene

Figure 3-1: Flowchart for the analysis of FLU, NFLU and FVX in rat heart, brain and liver.

and NFLU stock solutions and 2500 ng of ALP. The standards were then processed in the same manner as the samples described in Section 3.3.1.

3.3.3 ASSAY VALIDATION

The assay procedure was validated by determining between-run and within-run coefficients of variation. Within-run precision was calculated by preparing and analyzing in one analytical run 4 standards that were spiked with 200 ng of FLU, NFLU and FVX. Between-run precision was calculated by preparing and analyzing with each run an "in-house" control. This control was prepared by spiking naïve homogenate with a previously prepared standard. This control contained 100 ng of FLU, NFLU and FVX. The control was processed as a sample and read against the calibration curve prepared for that run.

To further determine the efficiency of the chromatographic system, a 200 ng standard was used to calculate capacity (K'), selectivity (α) and resolution (R) according to the equations described in Section 1.9.2.2.

3.3.4 INSTRUMENTATION

All samples were analysed using a Hewlett-Packard (HP) model 5890A gas chromatograph equipped with a ^{63}Ni electron-capture detector and linked to a HP 7673A automatic sampler and a HP 3392A integrator. A fused HP5 silica capillary column (25 m x 0.32 mm) coated with 1.05 μm film thickness of 5% phenylmethylsilicone was employed. The carrier gas was pure helium (Praxair Canada Inc.) at a flow rate of 4 mL/min. The make-up gas was argon-methane (95:5) (Praxair Canada Inc.) at a flow rate of 30 mL/min.

The oven temperature was set at an initial temperature of 105°C for 0.5 min. The temperature was increased by 10° per minute to 260°C, and held for 10.0 min. The oven temperature was then increased by 30° per minute to a final temperature of 295°C which was maintained for 30 min.

Injection port and detector temperatures were 270°C and 325°C, respectively. All injections were carried out using the splitless mode of injection with a purge off time of 0.5 min.

3.4 ANALYSIS OF DESIPRAMINE

3.4.1 ASSAY PROCEDURE

DMI analysis was carried out using a modification of the procedure described by Goodnough *et al.* (1995). Rat brain, heart or liver was homogenized in 5 volumes of ice-cold double-distilled water. Aliquots (1000 µL) were added to screw cap culture tubes, and to each of these were added 500 ng of maprotiline (MAP) as internal standard. Samples were basified by adding 400 µL of a 25% solution of potassium carbonate. After vortex mixing, 4 mL of glass-distilled ethyl acetate was added to all tubes. The tubes were capped, shaken vigorously for 5 min using a vortex-shaker and then centrifuged at 1000 g for 5 min. The ethyl acetate layers were removed to a second set of screw-cap culture tubes which were placed in a hot water bath. The solvent was taken to dryness under a stream of N_2. The resulting residue was reconstituted using 2 ml of deionized water. Excess sodium bicarbonate was added to each tube followed by 300 µL of acetic anhydride. The tubes were agitated until the bubbling ceased, signalling the completion of the derivatization reaction. The mixture was decanted into clean screw cap culture tubes and 4 mL of ethyl acetate were added to each tube. The tubes were then

shaken vigorously for 5 minutes and centrifuged at 1000 g for 5 minutes. The ethyl acetate layers were transferred to screw cap culture tubes and taken to dryness under vacuum. The residue was reconstituted in 150 μL of toluene and a 2 μL aliquot was used for gas chromatographic analysis (Figure 3-2).

3.4.2 CALIBRATION CURVES

Calibration curves (0-1000 ng of DMI) were run in parallel with each assay run and were prepared using naïve rat brain, heart or liver tissue homogenate. To each standard was added the appropriate dilution of DMI and 500 ng of MAP. The standards were then processed in the same manner as the samples as described in Section 3.4.1.

3.4.3 ASSAY VALIDATION

The assay procedure was first validated by determining between-run and within-run coefficients of variation. Within-run precision was calculated by preparing and analyzing in one analytical run 5 standards that were spiked with 200 ng of DMI. To determine between-run precision, an "in-house" control was prepared and run with each analytical run. This control was prepared by spiking naïve homogenate with a known amount of DMI. The spiked homogenate was aliquoted into 1000 μL portions and frozen with each aliquot containing 200 ng of DMI. Each time an analytical run was performed, one of these controls was thawed and run as a sample.

To further determine the efficiency of the extraction process, recoveries for DMI and MAP were determined by comparing samples of spiked naive liver homogenate which were carried through the assay procedure to tubes which contained the equivalent amounts of DMI and MAP in deionized water. These tubes were not carried through the

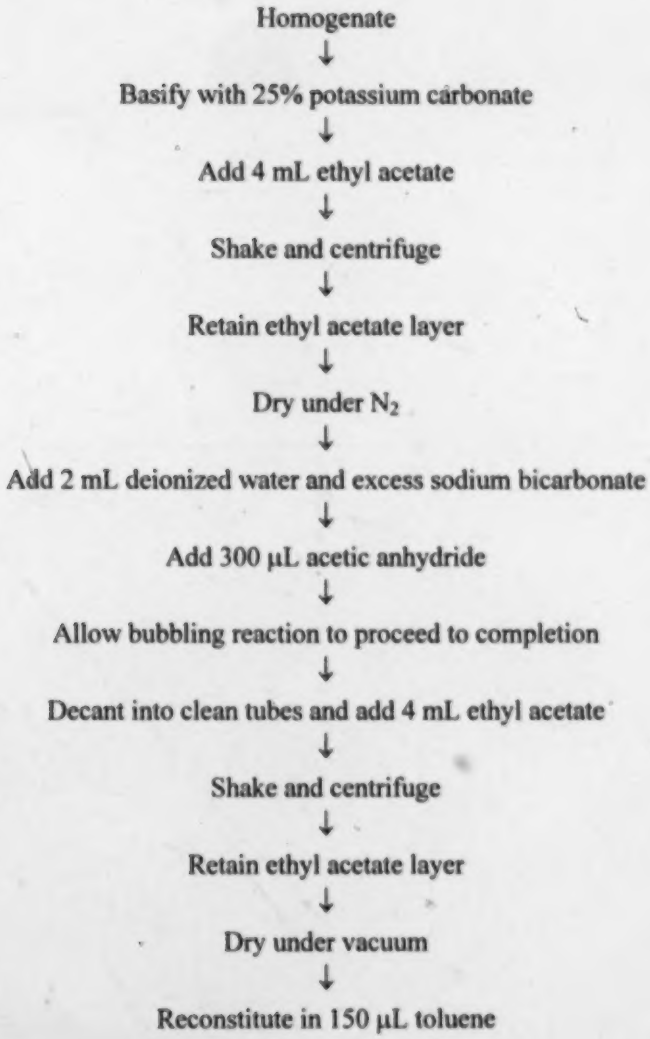
Homogenate
Basify with 25% potassium carbonate
Add 4 mL ethyl acetate
Shake and centrifuge
Retain ethyl acetate layer
Dry under N_2
Add 2 mL deionized water and excess sodium bicarbonate
Add 300 µL acetic anhydride
Allow bubbling reaction to proceed to completion
Decant into clean tubes and add 4 mL ethyl acetate
Shake and centrifuge
Retain ethyl acetate layer
Dry under vacuum
Reconstitute in 150 µL toluene

Figure 3-2: Flowchart for the analysis of DMI in rat heart, brain and liver.

initial extraction step. The processing of these samples was initiated at the derivitization step.

In addition, the efficiency of the chromatographic system was determined by using a 200 ng standard to calculate resolution (R) according to the equation described in Section 1.9.2.2. Capacity (K′) and selectivity (α) were not calculated since the time for an unretarded solvent front to elute from the colmun could not be ascertained from the chromatography.

3.4.4 INSTRUMENTATION

All samples were analysed using an HP5890A gas chromatograph equipped with a nitrogen phosphorus detector and linked to a HP6890 Series Injector and a HP3396 Series II Integrator. A fused DB5 silica capillary column (15 m x 0.251 mm) coated with 0.25 μm film thickness of pentadecane was employed. The carrier gas was pure helium at a flow rate of 3 mL/min. The make-up gas was also helium at a flow rate of 30 mL/min. The detector was purged with pure hydrogen at 3.5 mL/min and dry air at 80 mL/min.

The oven temperature was set at an initial temperature of 105°C for 0.5 min. The temperature was increased by 10° per minute to 250°C. The oven temperature was then increased by 20° per minute to a final temperature of 295°C, which was maintained for 3 min.

Injection port and detector temperatures were 270°C and 325°C, respectively. All injections were carried out using the splitless mode of injection with a purge off time of 0.5 min.

3.5 STATISTICAL ANALYSIS

Main treatment effects were determined by a two-way analysis of variance (ANOVA) of square root transformed data using SPSS® software. Where significant ($p<0.05$) main effects were reached, *post hoc* multiple comparisons with Dunnet's test were employed to identify individual group differences.

3.6 RESULTS

3.6.1 FLUOXETINE, NORFLUOXETINE AND FLUVOXAMINE ANALYSIS

3.6.1.1 ASSAY PROCEDURE

This assay for the simultaneous quantitation of FLU, NFLU and FVX produces derivatives with good chromatographic properties and no interfering peaks. Typical chromatograms from the analysis of the standards and test samples are shown in Figure 3-3.

3.6.1.2 CALIBRATION CURVES

Calibration curves for FLU, NFLU and FVX were generated by plotting the peak height ratio of FLU, NFLU or FVX to a fixed amount of derivatized ALP on the y-axis versus the concentration of each compound on the x-axis. Calibration curves, which were run in parallel with the experimental tissue in every assay, were linear, with r^2 values >0.99 obtained consistently.

Typical calibration curves for FLU and NFLU are shown in Figure 3-4. A typical calibration curve for FVX is shown in Figure 3-5. Due to the high concentrations of NFLU encountered in the tissue samples, it was necessary to reanalyze some samples after dilution to obtain accurate quantitative values.

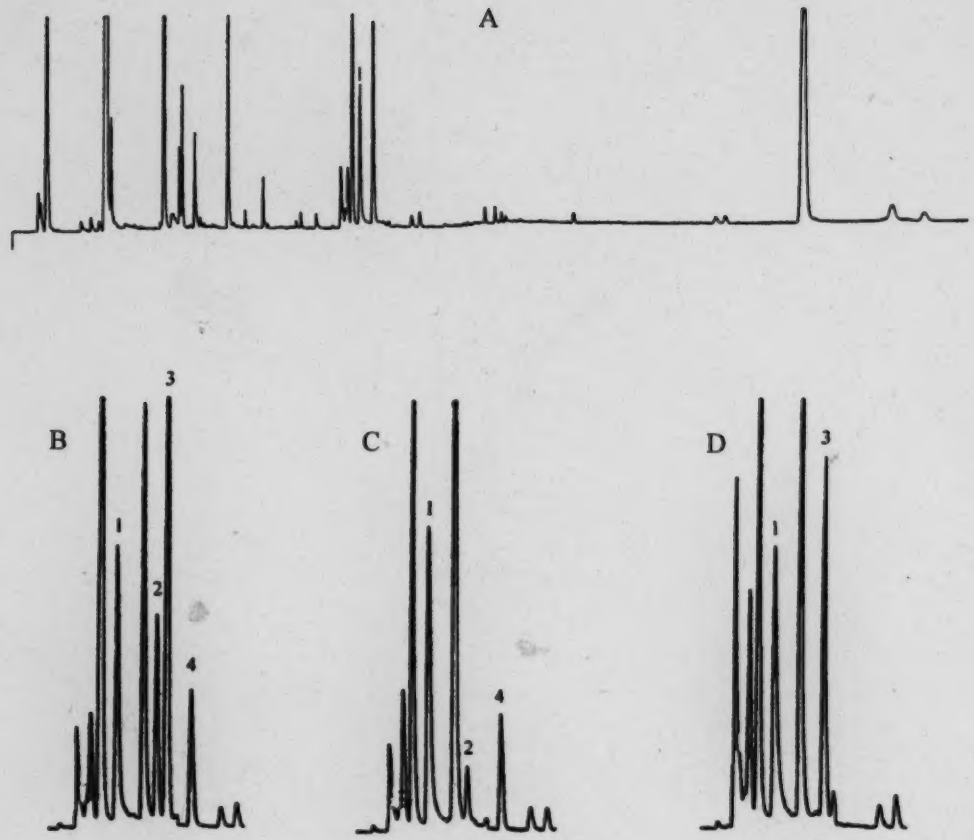

Figure 3-3: Typical chromatograms from the analysis of FLU, FVX and NFLU in rat heart. A) A standard that has only ALP. B) A standard that has 500 ng of FLU, FVX and NFLU. C) A sample from the FLU-MET treatment group. D) A sample from the FVX-MET treatment group. Peak 1 is ALP with a retention time of 20.67 min, Peak 2 is FLU with a retention time of 21.86 min, Peak 3 is FVX with a retention time of 22.15 min and Peak 4 is NFLU with a retention time of 22.90 min.

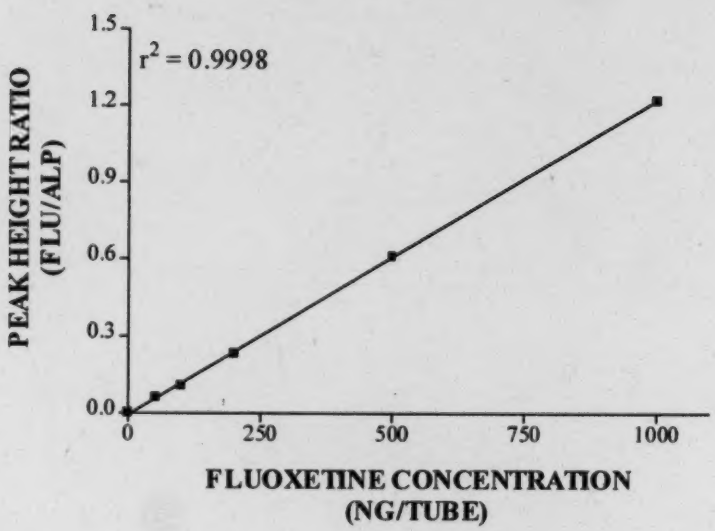

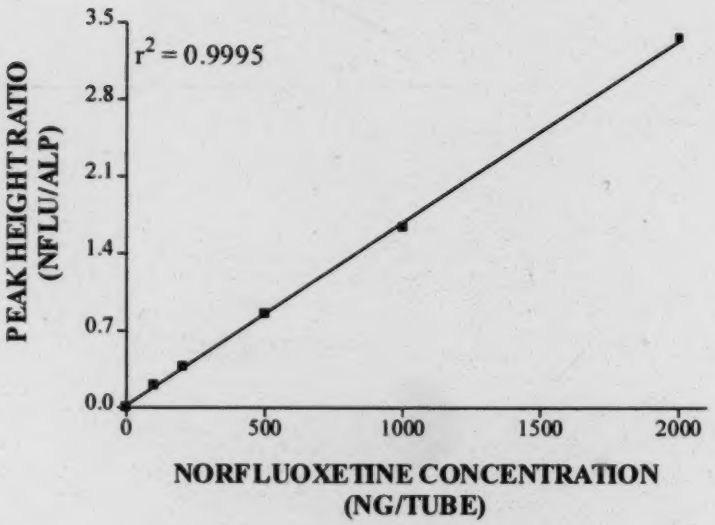

Figure 3-4: Typical calibration curves for the quantitation of FLU and NFLU in rat heart and liver respectively.

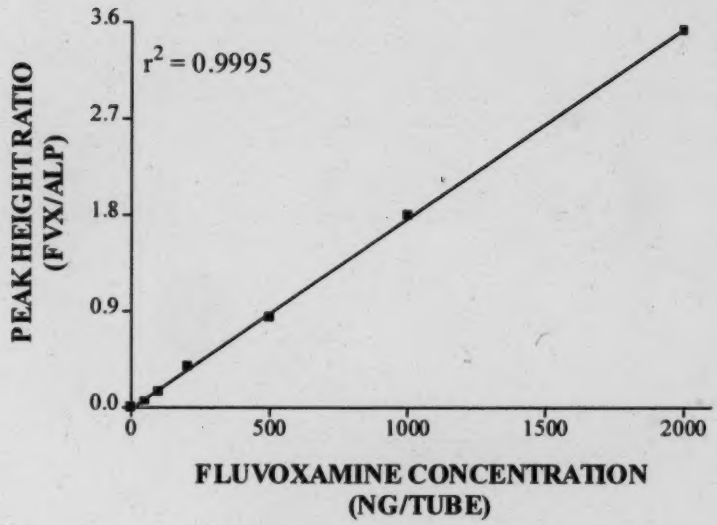

Figure 3-5: Typical calibration curve for the quantitation of FVX in rat brain.

3.6.1.3 ASSAY VALIDATION

The limit of detection for FLU and FVX was 167 pg "on column". NFLU had a detection limit of 333 pg "on column". Mean between-run coefficients of variation of the "in-house" control containing 100 ng of FLU, NFLU and FVX were determined to be 4.6%, 1.5% and 5.6% respectively (n=4). The within-run coefficients of variation of samples containing 200 ng of FLU, NFLU and FVX were 7.0%, 7.5% and 6.8% respectively. The chromatographic parameters of K′, α and R are given in Table 3-1.

3.6.1.4 FLUOXETINE AND NORFLUOXETINE LEVELS

The levels of FLU and NFLU in heart, brain and liver are presented in Table 3-2; these data are presented graphically in Figure 3-6. The FLU levels in heart, brain and liver of the FLU-VEH treatment group (n=6) were 732 ± 167 ng/g, 1770 ± 439 ng/g and 1096 ± 239 ng/g of tissue, respectively. The values were not significantly different in the FLU-MET treatment group (n=6), with FLU levels of 898 ± 218 in heart, 2155 ± 684 ng/g in brain and 1482 ± 520 ng/g in liver. The NFLU levels in heart, brain and liver of the FLU-VEH treatment group (n=6) were 3641 ± 418 ng/g, 4795 ± 854 ng/g and 9120 ± 1085 ng/g of tissue, respectively. Again, the values were not significantly different in the FLU-MET treatment group, with NFLU levels of 3359 ± 506 ng/g of heart, 4699 ± 1169 ng/g of brain and 8015 ± 1256 ng/g of liver.

Peak	Chromatographic Parameter		
	K′	α	R
U1	12.16	1.03	2.65
ALP	12.50	1.04	3.51
U2	13.05	1.02	1.83
FLU	13.33	1.02	1.63
FVX	13.54	1.02	3.35
NFLU	14.06		

Table 3-1: Chromatographic parameters for the GC analysis of FLU, NFLU and FVX (n = 3) calculated using the equations described in Section 1.9.2.2. U1 and U2 are unknown peaks that precede the peaks for ALP and FLU respectively.

TISSUE	TREATMENT GROUP	FLU		NFLU	
		Mean	SEM	Mean	SEM
HEART	FLU-VEH	732	167	3641	418
	FLU-MET	898	218	3359	506
BRAIN	FLU-VEH	1770	439	4795	854
	FLU-MET	2155	684	4699	1169
LIVER	FLU-VEH	1096	239	9120	1085
	FLU-MET	1482	520	8015	1256

Table 3-2: FLU and NFLU levels (ng/ g tissue, n = 6) in rat heart, brain and liver.

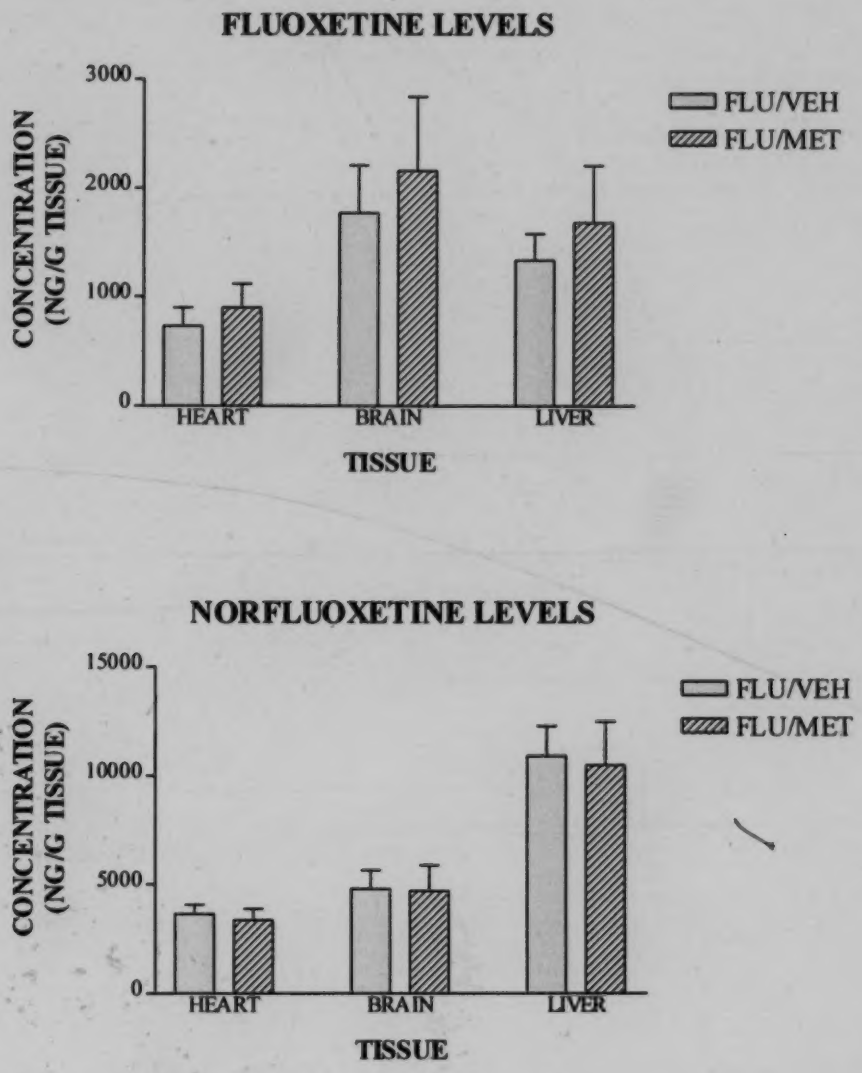

Figure 3-6: FLU and NFLU levels (n = 6) in rat heart, brain and liver in the FLU-VEH and FLU-MET treatment groups. Values are presented as means ± SEM.

3.6.1.5 FLUVOXAMINE LEVELS

The heart, brain and liver levels of FVX are presented in Table 3-3. These data are presented graphically in Figure 3-7. The levels in heart, brain and liver of the FVX-VEH treatment group (n=6) were 1261 ± 359 ng/g, 2151 ± 541 ng/g and 2833 ± 372 ng/g of tissue, respectively. These values were not significantly different in the brain and heart of the FVX-MET treatment group (n=6), with FVX levels of 1396 ± 390 ng/g in heart and 2340 ± 742 ng/g in brain. The FVX level in the liver of the FVX-MET treatment group (n=6) was 4821 ± 600 ng/g of tissue. This result was significantly higher than the result obtained in the liver of the FVX-VEH treatment group.

3.6.2 DESIPRAMINE ANALYSIS

3.6.2.1 ASSAY PROCEDURE

This assay for the quantitation of DMI produces a derivative with good chromatographic properties and no interfering peaks. Typical chromatograms from the analysis of the standards and test samples are shown in Figure 3-8.

3.6.2.2 CALIBRATION CURVES

Plotting the peak height ratio of derivatized DMI to a fixed amount of derivatized MAP on the y-axis versus the concentration of DMI on the x-axis generated calibration curves for DMI. Calibration curves, which were run in parallel with the experimental tissue in every assay, were linear, with r^2 values >0.99 consistently obtained. A typical calibration curve for DMI is shown in Figure 3-9.

TISSUE	TREATMENT GROUP	FVX	
		Mean	SEM
HEART	FVX-VEH	1261	359
	FVX-MET	1396	390
BRAIN	FVX-VEH	2151	541
	FVX-MET	2340	742
LIVER	FVX-VEH	2833	372
	FVX-MET	4821*	600

Table 3-3: FVX levels (ng/g tissue, n = 6) in rat heart, brain and liver. * denotes a significant difference of <0.05 compared to the FVX-VEH treatment group.

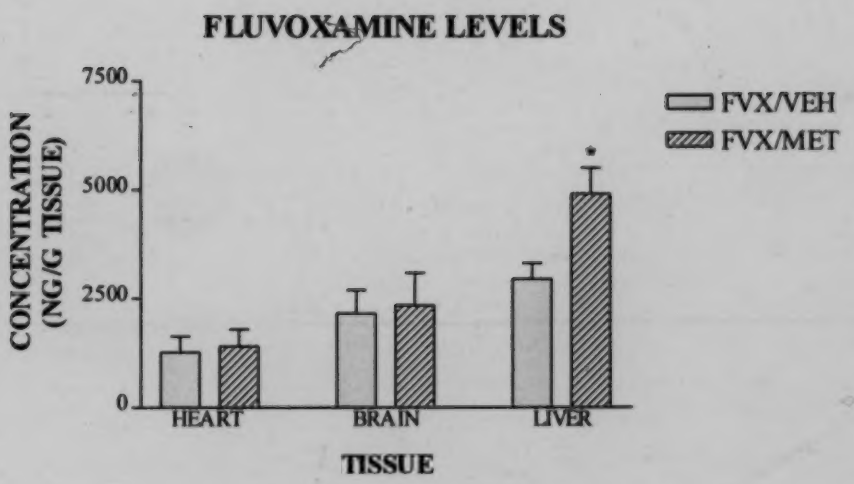

Figure 3-7: FVX levels (n = 6) in rat heart, brain and liver in the FVX-VEH and FVX-MET treatment groups. Values are presented as means ± SEM. * denotes a significant difference of <0.05 compared to the FVX-VEH treatment group.

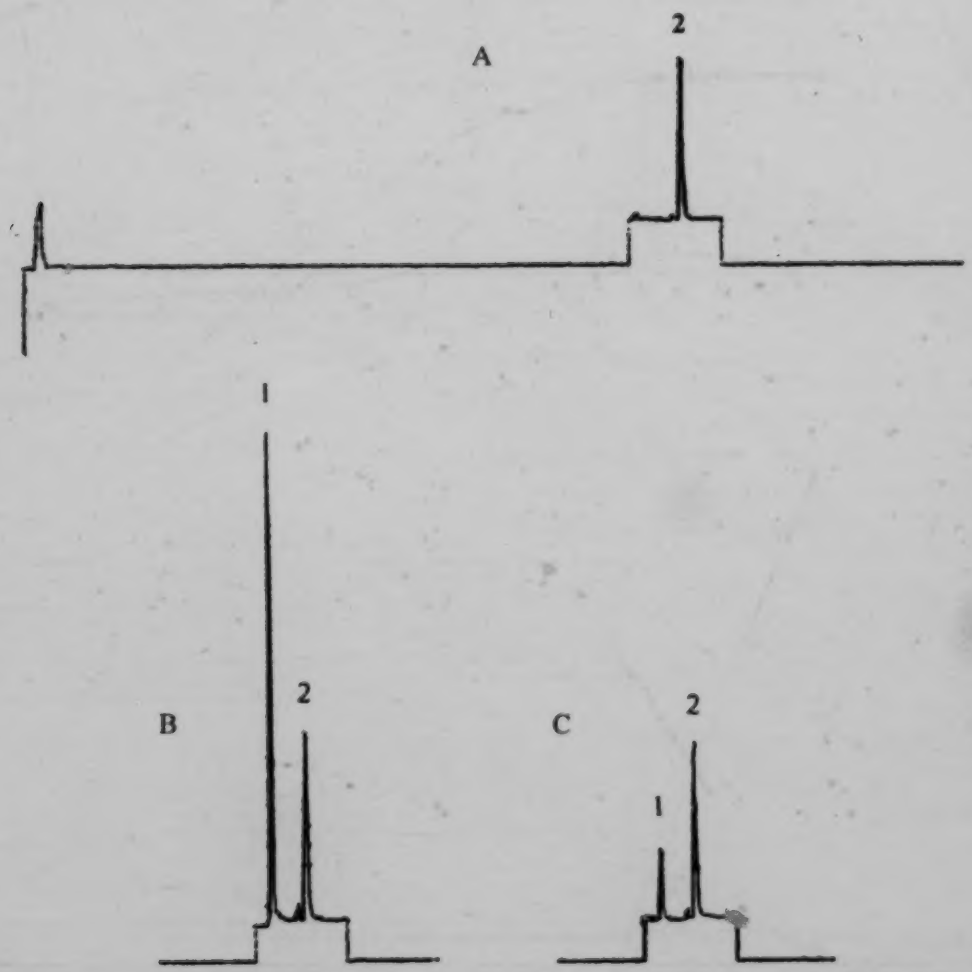

Figure 3-8: Typical chromatograms from the analysis of DMI in rat brain. A) A standard that has only MAP. B) A standard that has 500 ng of DMI. C) A sample from the DMI-MET treatment group. Peak 1 is DMI with a retention time of 12.92 min and Peak 2 is MAP with a retention time of 13.64 min.

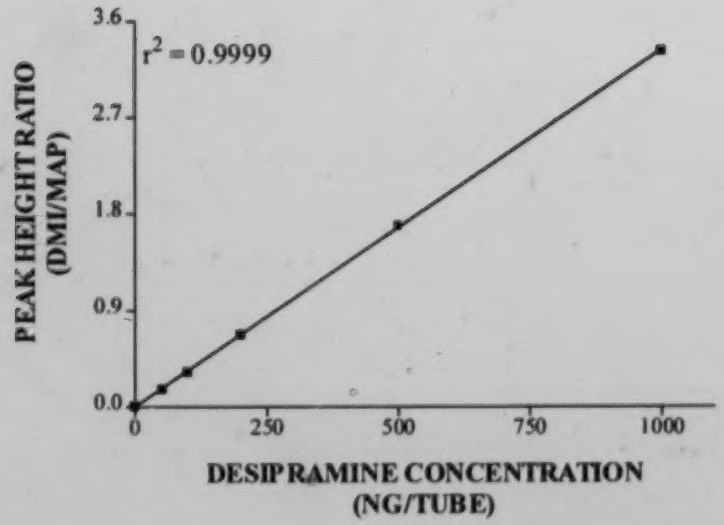

Figure 3-9: Typical calibration curve for the quantitation of DMI in rat liver.

3.6.2.3 ASSAY VALIDATION

The limit of detection for DMI was 133 pg "on column". The mean between-run coefficient of variation of the "in-house" control containing 200 ng of DMI was determined to be 11.8% (n=4). The within-run coefficient of variation of samples containing 200 ng of DMI was 1.4% (n=5). The mean recoveries of DMI and MAP were determined to be 65% and 63% respectively (n=5). The R value for the separation of DMI and MAP was 6.59.

3.6.2.4 DESIPRAMINE LEVELS

The heart, brain and liver levels of DMI are presented in Table 3-4; these data are presented graphically in Figure 3-10. The levels in heart, brain and liver of the DMI-VEH treatment group (n=6) were 1079 ± 250 ng/g, 1571 ± 433 ng/g and 3524 ± 525 ng/g of tissue, respectively. DMI levels in the DMI-MET treatment group (n=6) were 963 ± 384 ng/g in heart, 1177 ± 532 ng/g in brain and 2667 ± 576 ng/g in liver. These values were not signficantly different from those values obtained in the DMI-VEH treatment group.

3.7 DISCUSSION

3.7.1 FLUOXETINE, NORFLUOXETINE AND FLUVOXAMINE ANALYSIS

The assay described herein for the quantitation of FLU, NFLU and FVX is simple and produces derivatives with good chromatographic properties and no interfering peaks. Although the K′ values are greater and the α-values are less than what is considered ideal, the resolution was quite acceptable having values greater than 1.25 (Tabor, 1984). In addition, the calibration curves were consistently linear. However, this assay does have a relatively high limit of detection especially when compared to the assay

TISSUE	TREATMENT GROUP	DMI	
		Mean	SEM
HEART	DMI-VEH	1079	250
	DMI-MET	963	384
BRAIN	DMI-VEH	1571	433
	DMI-MET	1177	532
LIVER	DMI-VEH	3524	525
	DMI-MET	2667	576

Table 3-4: DMI levels (ng/g tissue, n = 6) in rat heart, brain and liver.

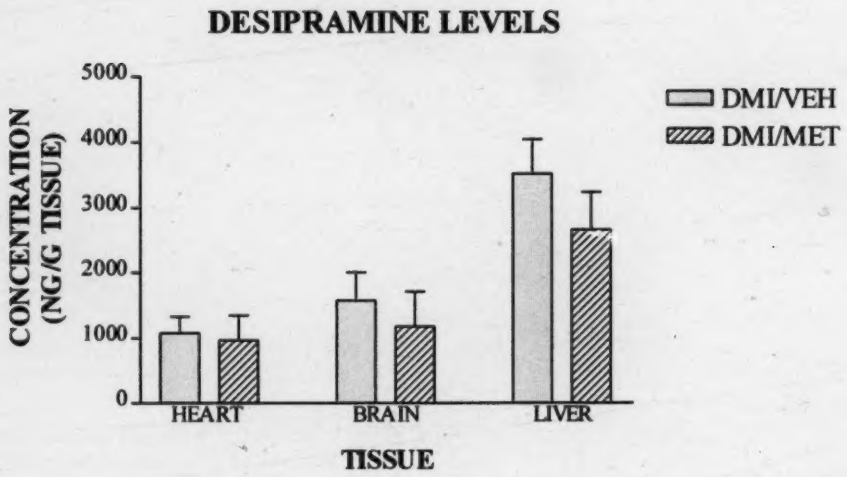

Figure 3-10: DMI levels (n = 6) in rat heart, brain and liver in the DMI-VEH and DMI-MET treatment groups.

for MET and ODM as described in Chapter 2. The issue is not necessarily the inability to detect these compounds at lower levels but the inability to distinguish the peaks of interest from underlying interferences, especially when the samples used are tissue samples. Given another sample matrix, the limit of detection would no doubt be improved. The assay described herein is simple with relatively few steps. It is the simplicity that is in fact the weakness of this assay due to the absence of any cleanup steps. However, given the relatively high levels of the drugs in this study, this assay was sufficient for the current purpose.

The method described by Goodnough *et al.* (1995) for the simultaneous quantitation of DMI, FLU and NFLU using aqueous acetylation followed by GC-NPD, was attempted to simultaneously quantitate DMI, FLU, NFLU and FVX. However, this method did not prove to be useful for the studies described herein due to a coelution of the FLU and FVX peaks. In addition, the simultaneous quantitation of DMI, FLU and NFLU was not even successful due to an interference with the FLU peak. There was also an attempt to quantitate FLU, NFLU and FVX simultaneously with MET and ODM. Although these compounds could be derivatized with pentafluoropropionic anhyride (PFPA), the extraction efficiency of the assay was insufficient. The decision to quantitate FVX with FLU and NFLU simultaneously was simply a time-saving measure. Using this approach, only one set of calibration curves was needed and the appropriate vehicle samples did not need to be analyzed twice.

Toluene was used as an extraction solvent instead of ethyl acetate simply because the toluene extractions produced cleaner chromatography with fewer interfering peaks. The sensitivity of this assay is comparable to the assays described by Aspeslet (1994) for

the quantitation of FLU and NFLU and by Rotzinger *et al.* (1995) for the quantitation of FVX.

The confirmation of the structures of the PFB derivatives of FLU and NFLU by mass spectrometry was previously determined by Aspeslet (1994). The structure of the PFB derivative of FVX was also previously confirmed by Rotzinger *et al.* (1995).

3.7.2 DESIPRAMINE ANALYSIS

The assay for DMI quantitation was relatively simple, producing a derivative with good chromatographic properties and no interfering peaks. Resolution of MAP and DMI was quite acceptable having a value greater than 1.25 (Tabor, 1984).

Because a nitrogen phosphorus detector was used in this assay, an obvious question is why bother derivatizing? An acetylated derivative would not be expected to increase the sensitivity of a compound to this particular type of detector. The answer lies in the structure of DMI itself. Since DMI is a secondary amine, it has a tendency to have a tailing edge when chromatographed. The derivatization converts the secondary amine into an amide and prevents the tailing from occurring, resulting in a peak more Gaussian in shape.

The sensitivity of the assay described in this Chapter seems to be slightly better than that described by Goodnough *et al.* (1995). However, the recovery of DMI was higher in that assay.

The confirmation of the structures of the acetylated derivatives of DMI and MAP by mass spectrometry was previously determined by Goodnough *et al.* (1995) and Drebit *et al.* (1988), respectively.

3.7.3 EFFECT OF METOPROLOL ON THE METABOLISM OF FLUOXETINE, FLUVOXAMINE AND DESIPRAMINE

3.7.3.1 FLUOXETINE AND NORFLUOXETINE

The data shown here suggest that MET does not inhibit the metabolism of FLU to a significant degree. It would seem, at least in rats, that MET does not inhibit to any significant degree those enzymes responsible for the majority of the metabolism of FLU which seems to be CYP2C9 (Greenblatt *et al.*,1998). The fact that NFLU levels are not significantly different between the FLU-VEH and FLU-MET treatment groups further supports this finding.

3.7.3.2 FLUVOXAMINE

The data shown here suggest that MET does have some capacity to inhibit the metabolism of FVX. However, this effect was seen only in the liver samples. It would seem, at least in rats, that MET does have some ability to inhibit either CYP2D6 or CYP1A2 (or their equivalents in rats) or both. A likely scenario is that since both MET and FVX are metabolized by CYP2D6 in humans (Greenblatt *et al.*, 1998; Kim *et al.*, 1993) there is a competitive inhibition between MET and FVX.

3.7.3.3 DESIPRAMINE

As with the metabolism of FLU, the metabolism of DMI does not seem to be influenced by MET. There was no significant difference between the DMI-VEH and the DMI-MET treatment groups. Given the fact that both DMI and MET are metabolized by CYP2D6 (von Bahr *et al.*, 1985; Shen, 1997; Kim *et al.*, 1993) it would not have been surprising that MET would have competitively inhibited the metabolism of DMI. However, considering the influence of DMI on the metabolism of MET (Section 2.4.4), it is possible that MET has minimal interaction with the CYP2D1 enzyme and is therefore

unable to exert any competitive influence on the metabolism of DMI. In fact, a study by von Bahr et al (1985) demonstrated that in human liver microsomes the Ki of MET for the inhibition of the 2-hydroxylation of DMI was 570 (Ki of quinidine was 0.27 and that of quinine was 12). Thus, even in human liver microsomes MET is a weak inhibitor of DMI metabolism.

3.7.4 ANTIDEPRESSANT LEVELS AND THEIR EFFECT ON THE METABOLISM OF METOPROLOL

As discussed in Chapter 2, it was surprising that while DMI and FVX inhibited the metabolism of MET, FLU did not. To aid in the understanding of those results it was necessary to quantitate the levels of the co-administered antidepressants to determine if there was an obvious correlation between their levels and the inhibition of the metabolism of MET. Simply, if the tissue level of DMI was much greater than that of FLU and NFLU or FVX and the level of FVX greater than the level of FLU and NFLU, the results could possibly be explained in terms of the drug levels achieved *in vivo*. However this was not the case. In fact, the levels of DMI were lower than the levels of both FVX and NFLU. The levels of DMI were not greater than FLU in all tissue samples due to the fact that FLU had been metabolized to NFLU. However, the ability of both FLU and NFLU to inhibit CYP2D6 in human liver microsomes is considered to be greater than that of DMI (Crewe *et al.*, 1992). Therefore, although the levels of FLU were lower than those of DMI in some cases, the high levels of NFLU should have been compensatory. Therefore, the increased ability of DMI to inhibit the metabolism of MET involves more than the actual quantity of DMI in tissue samples. A likely scenario is that as DMI is being metabolized, it is competitively inhibiting the metabolism of MET. It is possible that compared to MET, the affinity of DMI for CYP2D1 in rats is so much

greater that it virtually prevents the interaction of MET with the enzyme's active site, preventing the metabolism of MET.

It is obvious from the results generated in this study that FLU is being readily metabolized to NFLU in all tissues, with mean NFLU levels approximately 2-5 times greater than mean FLU levels. This leads to the possibility that the affinity of FLU for enzyme(s) responsible for its own metabolism is greater than its affinity for the enzymes responsible for the metabolism of MET. Thus, even though both FLU and NFLU are potent inhibitors of CYP2D6 (Greenblatt *et al.*, 1998), they seem to have little influence on the metabolism of MET in the rat.

Since FVX is capable of inhibiting the metabolism of MET in rats, it would seem that FVX has the ability to inhibit enzymes responsible for the metabolism of MET. In rats, the major metabolic pathways with respect to the metabolism of MET are the O-demethylation pathway which accounts for approximately 62% and the α-hydroxylation pathway which accounts for 25% of the dose. In comparison, the N-dealkylation pathway acounts for only 1% (Borg *et al.*, 1975). It would seem that FVX has the ability to inhibit those enzymes responsible for the formation of one or both of ODM and HM. An inhibition of enzymes responsible for the N-dealkylation pathway would probably have very little effect on the overall metabolism of MET. It may be that FVX has very little effect on any one enzyme, but its effect on several enzymes may be enough to inhibit the metabolism of MET to a significant degree.

3.8 RFERENCES

Aspeslet L (1994) Chirality and Metabolism: Studies on the Antidepressants *rac*-Tranylcypromine and *rac*-Fluoxetine. PhD Thesis, University of Alberta, Edmonton, Alberta.

Borg KO, Carlsson E, Hoffmann K-J, Jönsson T-E, Thorin H and Wallin B (1975) Metabolism of metoprolol-(^{3}H) in man, the dog and the rat. *Acta Pharmacol Toxicol* 36(Suppl V): 125-135.

Crewe HK, Lennard MS, Tucker GT, Woods FR and Haddock RE (1992) The effect of selective serotonin re-uptake inhibitors on cytochrome P4502D6 (CYP2D6) activity in human liver microsomes. *Br J Clin Pharmacol* 34: 262-265.

Drebit R, Baker G and Dewhurst WG (1988) Determination of maprotiline and desmethylmaprotiline in plasma and urine by gas chromatography with nitrogen-phosphorus detection. *J Chromatogr Biomed Appl* 432: 334-339.

Goodnough DB, Baker GB and Coutts RT (1995) Simultaneous quantification of fluoxetine, norfluoxetine and desipramine using gas chromatography with nitrogen-phosphorus detection. *J Pharmacol Toxicol Methods* 34: 143-147.

Greenblatt DJ, von Molke LL, Harmatz JS and Shader RI (1998) Drug interactions with newer antidepressants: role of human cytochromes P450. *J Clin Psychiatry* 59 (Suppl 15): 19-27.

Kim M, Shen DD, Eddy AC and Nelson WL (1993) Inhibition of the enantioselective oxidative metabolism of metoprolol by verapamil in human liver microsomes. *Drug Metab Dispos* 21: 309-317.

McNeil CM and Murray M (1996) Inhibition of microsomal cytochromes P450 in rat liver by the tricycleC antidepressant drug desipramine and its primary oxidized metabolites. *Biochem Pharmacol* 51: 15-20.

Otton SV, Inaba T and Kalow W (1983) Inhibition of sparteine oxidation in human liver by tricyclic antidepressants and other drugs. *Life Sci* 32: 795-800.

Preskorn SH (1997) Clinically relevant pharmacology of selective serotonin reuptake inhibitors: An overview with emphasis on pharmacokinetics and effects on oxidative drug metabolism. *Clin Pharmacokinet* 32 (suppl 1): 1-21.

Riesenman C (1995) Antidepressant drug interactions and the cytochrome P450 system: A critical appraisal. *Pharmacotherapy* 15: 84S-99S.

Rotzinger S, Todd KG, Bourin M, Coutts RT, Baker GB (1995) A rapid electron-capture gas chromatographic method for the quantification of fluvoxamine in brain tissue. *J Pharmacol Toxicol Methods* 37: 129-133.

Tabor MW (1984) Chromatography: theory and practice. In Kaplan LA and Pesce AJ (Eds) *Clinical Chemistry: Theory, Analysis and Correlation* (pp. 74 – 99). St. Louis, Missouri, CV Mosby Company.

Shen WW (1997) The metabolism of psychoactive drugs: A review of enzymatic biotransformation and inhibition. *Biol Psychiatry* 41: 814-826.

von Bahr C, Spina E, Birgersson C, Ericsson Ö, Göransson M, Henthorn T and Sjöqvist F (1985) Inhibition of desmethylimipramine 2-hydroxylation by drugs in human liver microsomes. *Biochem Pharmacol* 34: 2501-2505.

Chapter 4: Effect of the Antidepressants Paroxetine, Fluoxetine, Fluvoxamine and Desipramine on the Metabolism of Metoprolol Using Human Liver Microsomes.

4.1 INTRODUCTION

As previously discussed, MET undergoes extensive hepatic metabolism, with the major metabolic pathways being α-hydroxylation, O-demethylation and N-dealkylation. Both the O-demethylated and the N-dealkylated metabolites are further oxidized to acid metabolites. The O-demethylation pathway accounts for 65% of the dose in man, whereas the α-hydroxylation and the N-dealkylation pathways account for 10% each (Borg *et al.*, 1975). The α-hydroxylation of MET has been reported to occur predominantly *via* cytochrome P450 (CYP) 2D6 whereas O-demethylation is catalyzed by CYP2D6 and as yet other unidentified enzymes (Otton *et al.*, 1988). There are no known reports elucidating the enzymes involved in either the N-dealkylation reaction or the oxidation of O-desmethylmetoprolol (ODM) to its acid metabolite (AM).

Previous reports on the metabolism of MET have shown that the oxidation of MET to ODM is biphasic, with a low affinity/high capacity enzyme and a high affinity/low capacity enzyme contributing to the formation of ODM. The formation of α-hydroxymetoprolol (HM) also appears to be biphasic (Kim *et al.*, 1993; Belpaire *et al.*, 1998). However, the kinetic data did not always definitively support the involvement of two enzymes since the data did not necessarily fit a two-enzyme model much better than it fit a one-site model (Otton *et al.*, 1988). Based on studies with quinidine and quinine, the high affinity enzyme responsible for the formation of ODM has been elucidated to be CYP2D6. Quinidine caused approximately 80% inhibition of ODM formation, which was supportive of the involvement of two enzymes, one of which was not susceptible to inhibition by quinidine. Quinidine also was shown to inhibit completely the formation of HM in that particular study (Otton *et al.*, 1988).

This chapter highlights the development of a novel assay for the quantitation of the major metabolites of MET, including AM and N-dealkylmetoprolol (NDM) in human liver microsomes. In addition, the kinetics of the metabolism of MET to its major metabolites are described. Using the values obtained for K_m and V_{max}, the inhibitory potentials of FLU, fluvoxamine (FVX), desipramine (DMI) and paroxetine (PAR) were investigated with respect to both the low and the high affinity components of the oxidation of MET to ODM.

4.2 EXPERIMENTAL PROCEDURES

4.2.1 INSTRUMENTATION

All samples were analysed by HPLC using a Waters Model 510 pump, a Waters WISP 710 B autosampler, a Waters 2487 Duel λ Absorbance Detector set at 222 nm and a sensitivity setting of 0.1 absorbance units full scale (AUFS), and a Phenomenex CN5 column (4.6 x 25 cm). Data processing was carried out using a Pegasus Pentium II, 400 mhz computer with Waters Millennium[32] software (Version 3.05). The mobile phase consisted of sodium acetate (2.8 mM)-acetonitrile-methanol-triethylamine in a ratio of (80:10:10:0.01). A final pH value of 4.5 was attained using glacial acetic acid. The mobile phase was pumped at a flow rate of 1.5 mL/min, giving an operating pressure of approximately 1800 psi. All metabolite peaks had retention times of less than 20 min. A run time of 35 min was used to allow sufficient time for the MET peak to be chromatographed. All analyses were carried out isocratically at room temperature.

4.2.2 ASSAY PROCEDURE

4.2.2.1 Effect of Protein

Initially two sets of calibration curves, consisting of 0 – 50 μM of AM, HM,

ODM and NDM, were set up to determine if protein concentration affected the quantitation of the metabolites of MET. In this initial experiment, one set of standards was prepared by diluting the appropriate amount of each metabolite in 0.1 M potassium phosphate buffer to which was added 25 μL of the NADPH-generating system, giving a final volume of 100 μL. The second set of standards was prepared by diluting the appropriate amount of each metabolite in 0.1 M potassium phosphate buffer to which was added 10 μL of control protein, giving a final volume of 100 μL with a final protein concentration of 0.5 mg/mL (50 μg/100 μL). To both sets of standards, 20 μL of 1 N perchloric acid were added. After sitting on ice for 10 min, the standards were centrifuged for 1 min and the supernatants transferred to autosampler vials for injection.

4.2.2.2 Calibration Curves

After the initial experiment, calibration curves consisting of 0 - 50 μM of AM, HM, ODM and NDM were prepared by diluting the appropriate amount of each metabolite in 0.1 M potassium phosphate buffer to which was added 25 μL of the NADPH-generating system, giving a final volume of 100 μL. To this solution, 20 μL of 1 N perchloric acid were added. The standards sat on ice for a minimum of 10 min at which time they were centrifuged for 1 min. The resulting supernatants were then transferred to autosampler vials and a 20 μL aliquot was used for analysis.

4.2.2.3 Assay Validation

The assay procedure was validated by determining between-run and within-run coefficients of variation. The within-run precision was calculated by preparing and analyzing, in one analytical run, 5 sets of standards with concentrations of 0.15, 0.25, 2.5, 10.0 and 50.0 μM. Standards from 10 analytical runs were collated to calculate the

between-run precision of the assay. Precision was calculated according to the following equation (Campbell and Campbell, 1984):

$$\%CV = \frac{s}{\bar{X}} \times 100$$

Where: CV = coefficient of variation

s = standard deviation

$\bar{X}$ = mean

To further determine the efficiency of the chromatographic system, a 2.5 μM standard was used to calculate capacity (K′), selectivity (α) and resolution (R) according to the equations as described in Section 1.9.2.2.

4.2.3 PRELIMINARY STUDIES

4.2.3.1 Time Course

An experiment was conducted to determine the correct incubation time for the microsome studies. In this experiment, MET in phosphate buffer was incubated with 25 μL of the NADPH-generating system and 10 μL of the microsome solution. The total incubation volume was 100 μL, giving a final concentration of MET of 100 μM and a final protein concentration of 2.3 mg/mL (230 μg/100 μL). The reactions were carried out in a 37 °C waterbath for time periods of 5, 10, 30, 45 or 60 min. After the elapsed time, the samples were placed on ice and 20 μL of 1 N perchloric acid were added to terminate the reaction and to precipitate the protein. After sitting on ice for a minimum of 10 min, the samples were centrifuged for 1 min and the resulting supernatants were transferred to autosampler vials.

4.2.3.2 Requirement of NADPH

MET, in a final concentration of 50 μM, was incubated with 10 μL of microsomal protein, with and without $NADP^+$. All other components of the NADPH-generating system were present. The samples were incubated for 30 min, at which time they were placed on ice and a 20 μL aliquot of 1N perchloric acid was added to each sample. The samples remained on ice for a minimum of 10 min at which time they were centrifuged for 1 min and the supernatants transferred to autosampler vials.

4.2.3.3 Enzyme Concentration

To determine the concentration of enzyme to be used in the microsome experiments, MET in a final concentration of 100 μM was incubated with 25 μL of the NADPH-generating system and decreasing concentrations of microsomal protein. The concentrations of protein used were 230, 115, 57.5, 38.3 and 28.75 and 23.0 μg/100 μL. The samples were incubated for 30 min in a 37 °C waterbath, at which time they were placed on ice and 20 μL of 1 N perchloric acid was added. The samples remained on ice for 10 min and were than centrifuged for 1 min. The supernatants were transferred to autosampler vials.

4.2.4 DETERMINATION OF KINETIC CONSTANTS (V_{max} and K_m)

The microsomal incubation medium consisted of 25 μL of an NADPH-generating system, 50 μL of MET substrate solution (in a final concentration of 0 – 5000 μM prepared in 0.1 M phosphate buffer), 10 μL of microsomal solution and 15 μL of buffer. The total volume was 100 μL, resulting in a final protein concentration of 2.3 mg/mL (230 μg/100 μL). The metabolic reaction was allowed to proceed for 30 min in a 37°C waterbath. When the incubation time was complete, the samples were placed on ice and

20 μL of 1 N perchloric acid were added to precipitate the protein and effectively stop the reaction from continuing. The samples sat on ice for a minimum of 10 min at which time they were centrifuged for 1 min. The supernatants were then transferred to autosampler vials and a 20 μL aliquot was used for analysis (Figure 4-1). This experiment was performed in triplicate over 3 experimental days.

4.2.5 INHIBITION EXPERIMENTS

The microsomal incubation medium consisted of 25 μL of an NADPH-generating system, 50 μL of the putative inhibitor (in a final concentration of 0 – 3000 μM), 10 μL of microsomal solution, 5 μL of buffer and 10 μL of the substrate solution (final concentration of 40 or 2000 μM MET prepared in 0.1 M phosphate buffer). The total volume was 100 μL, resulting in a final protein concentration of 2.3 mg/mL (230 μg/100 μL). The experiment was conducted by incubating the NADPH-generating system with the appropriate inhibitor in the presence of microsomes for 15 minutes at 37°C. At this time, MET was added and the sample incubated again at 37°C for an additional 30 min. When the incubation time was complete, the samples were placed on ice and 20 μL of 1 N perchloric acid were added to precipitate the protein. The samples sat on ice for a minimum of 10 min, at which time they were centrifuged for 1 min. The supernatants were then transferred to autosampler vials and a 20 μL aliquot was used for analysis (Figure 4-2). Each experiment was performed at least in triplicate over different experimental days.

The above experiment was repeated using 200 μM of MET and 0, 25, 50, 100 and 200 μM concentrations of PAR, FLU, FVX and DMI. Again, this set of experiments was also performed at least in triplicate over different experimental days.

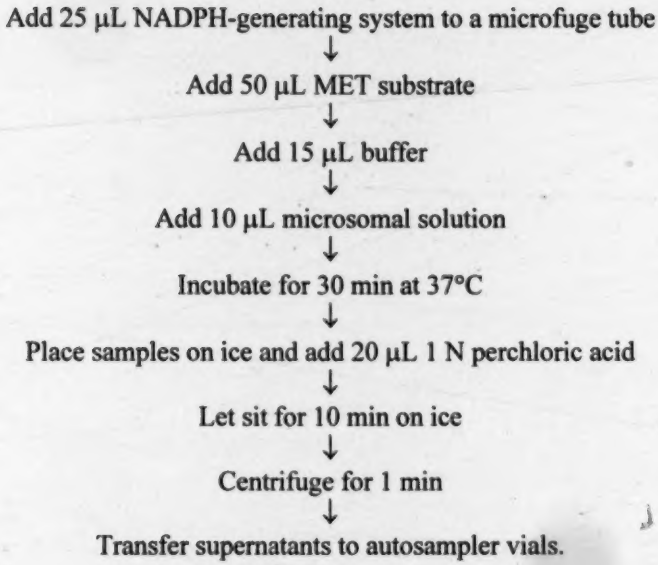
Add 25 µL NADPH-generating system to a microfuge tube
Add 50 µL MET substrate
Add 15 µL buffer
Add 10 µL microsomal solution
Incubate for 30 min at 37°C
Place samples on ice and add 20 µL 1 N perchloric acid
Let sit for 10 min on ice
Centrifuge for 1 min
Transfer supernatants to autosampler vials.

Figure 4-1: Flow chart for conducting kinetic experiments.

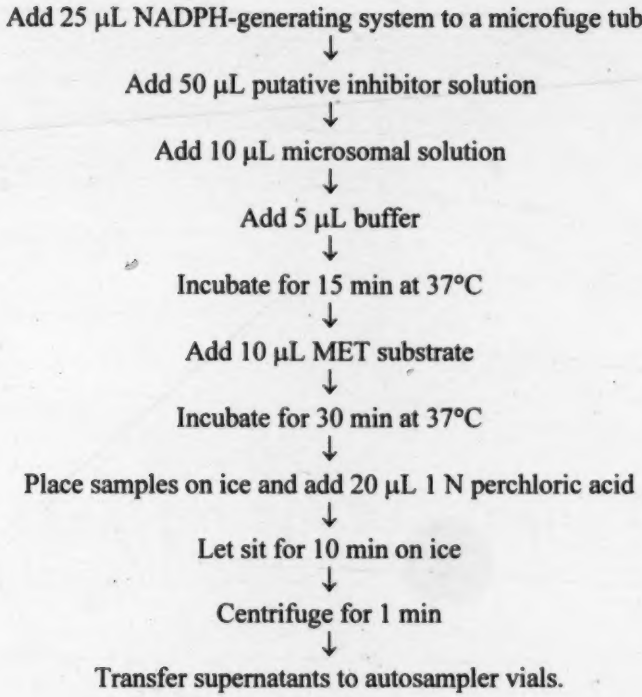
Add 25 µL NADPH-generating system to a microfuge tube
Add 50 µL putative inhibitor solution
Add 10 µL microsomal solution
Add 5 µL buffer
Incubate for 15 min at 37°C
Add 10 µL MET substrate
Incubate for 30 min at 37°C
Place samples on ice and add 20 µL 1 N perchloric acid
Let sit for 10 min on ice
Centrifuge for 1 min
Transfer supernatants to autosampler vials.

Figure 4-2: Flow chart for conducting inhibition experiments.

4.2.6 STATISTICAL ANALYSIS

4.2.6.1 K_m and V_{max} Determination

A least squares best fit analysis (GraphPad Prism Software, San Diego, CA, USA) was carried out using a one, two and three enzyme model by plotting the velocity of metabolite production against the substrate concentration according to the following equations:

One Enzyme: $v = (V_{max})[S]/[S]+K_m$

Two Enzyme: $v = [(V_{maxa})[S]/[S]+K_{ma}] + [(V_{maxb})[S]/[S]+K_{mb}]$

Three Enzyme:

$v=[(V_{maxa})[S]/[S]+K_{ma}]+[(V_{maxb})[S]/[S]+K_{mb}]+[(V_{maxc})[S]/[S]+K_{mc}]$

Where: v = velocity

V_{max} = maximal velocity

K_m = concentration of substrate that produces half the maximum velocity

[S] = substrate concentration

a, b, c = refers to the different enzymes

4.2.6.2 IC_{50} and K_i Determination

Using GraphPad Prism software, IC_{50} values were generated for each inhibitor at both 2000 and 40 μM concentrations of MET using a one and two site competition model.

One site: $$Y = \text{Bottom} + \frac{(\text{Top} - \text{Bottom})}{1 + 10^{X - \text{LogIC}_{50}}}$$

Two site: $$Y = \text{Bottom} + (\text{Top-Bottom}) \left[\frac{\text{Fraction1}}{1 + 10^{X - \text{LogIC}_{50}1}} - \frac{\text{1-Fraction1}}{1 + 10^{X - \text{LogIC}_{50}2}} \right]$$

Where: Bottom = Y value at the bottom plateau

Top = Y value at the top plateau

IC_{50} = concentration of inhibitor that gives a response halfway between Bottom and Top.

Fraction 1 = the fraction of enzyme that has an affinity described by $LogIC_{50}1$.

Fraction 2 = the fraction of enzyme that has an affinity described by $LogIC_{50}2$.

The IC_{50} value generated for the low affinity enzyme at 2000 μM was used to calculate the Ki of that inhibitor using the Cheng-Prushoff equation:

$$K_i = \frac{IC_{50}}{1 + \frac{[S]}{K_m}}$$

Where: K_i = enzyme dissociation constant

IC_{50} = concentration of inhibitor that produces half of its maximum inhibition

[S] = substrate concentration

K_m = concentration of substrate that produces half maximum velocity

Since the K_i for the enzyme is constant, a theoretical IC_{50} of the low affinity enzyme could then be calculated at 40 μM MET by using a simple rearrangement of the Cheng-Prushoff equation:

$$IC_{50} = K_i\left(1 + \frac{[S]}{K_m}\right)$$

This calculation was necessary to discriminate the IC_{50} of the low affinity enzyme from that of the high affinity enzyme at 40 μM MET.

4.2.6.3 Power Equation

The following power equation was used to generate curves for the inhibition experiments using 200 μM of MET:

$$Y = (100)(C)[(X+(1/C)^{1/D})^{D}]$$

Where: Y = percent inhibition

X = concentration of inhibitor

A rearrangement of this equation than allows for the determination of the inhibitor concentration at which inhibition of the formation of ODM is 50% of control.

$$X = (0.5/C)^{1/D}-(1/C)^{1/D}$$

This experiment only demonstrates the importance of choosing appropriate experimental substrate concentrations.

4.3 RESULTS

4.3.1 ASSAY PROCEDURE

4.3.1.1 Effect of Protein

Initially, two sets of calibration curves were analyzed to determine if protein concentration affected the quantitation of the metabolites. Superimposing the two calibration curves demonstrated that protein, at the concentration tested, did not have any effect on the calibration of the metabolites of MET (Figure 4-3 and Figure 4-4).

4.3.1.2 Calibration Curves

Calibration curves were generated by plotting the peak height of the metabolite on the y-axis versus the concentration of that metabolite on the x-axis. Calibration curves, which were run in parallel with the experimental samples in every assay, were linear, with r^2 values >0.99 consistently obtained. Typical calibration curves for each of the metabolites are shown in Figures 4-5, 4-6, 4-7 and 4-8. Due to the necessity of quantitating a wide range of concentrations for each metabolite, two calibration curves were generated for each metabolite. The first curve was constructed using 0, 0.15, 0.25, 0.5, 1.0 and 2.5 μM standards. The second curve used 0, 2.5, 5.0, 10.0, 20.0 and 50.0 μM standards.

4.3.1.3 Assay Validation

The metabolite peaks chromatographed well and all four metabolites had retention times of less than 20 min (Figure 4-9). The chromatographic parameters of K′, α and R are given in Table 4-1. The limit of detection for all metabolites was 0.15 μM (or 4.0, 4.3, 3.8 and 3.4 ng/100 μL incubation volume for AM, HM, ODM and NDM respectively). Within-run precision (n = 5) was less than 10% for all metabolites

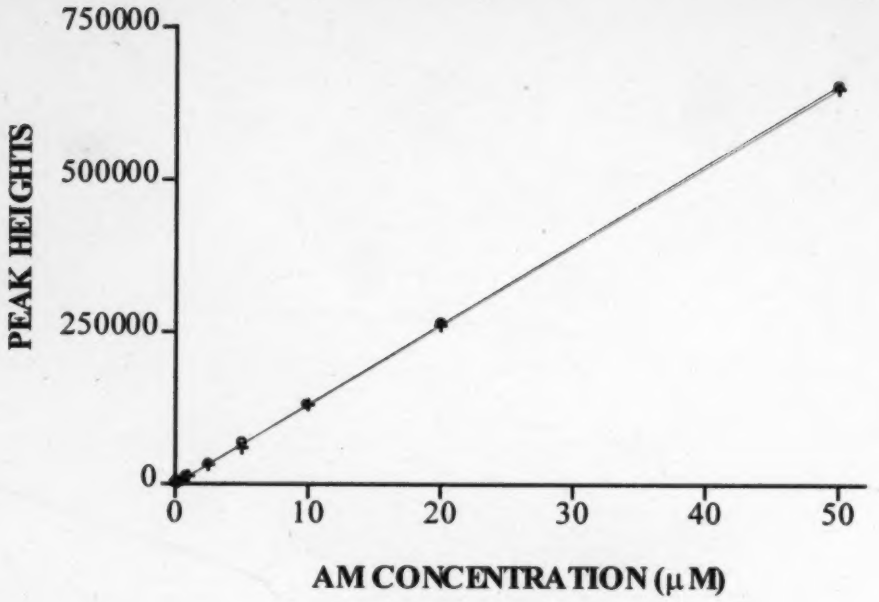

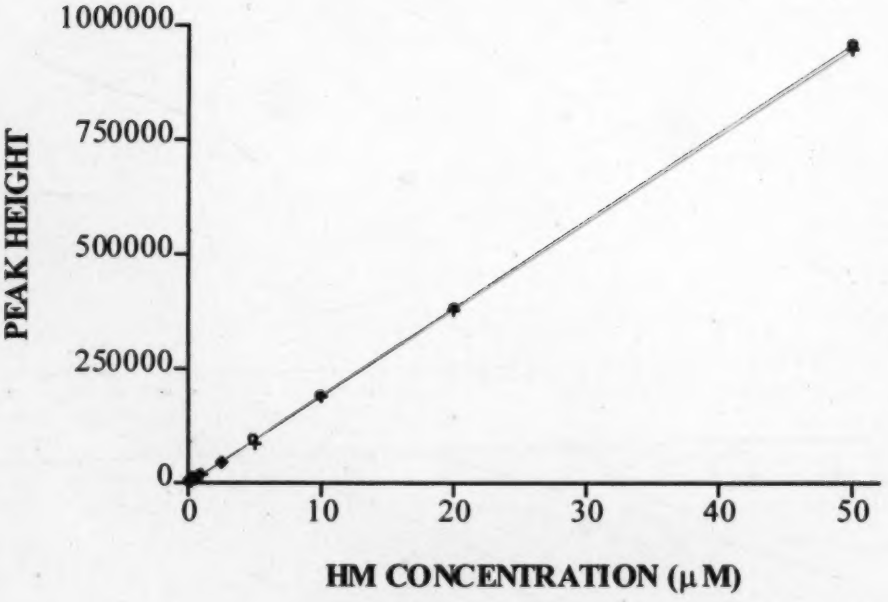

Figure 4-3: Calibration curves for AM and HM with (o) and without (+) the addition of protein.

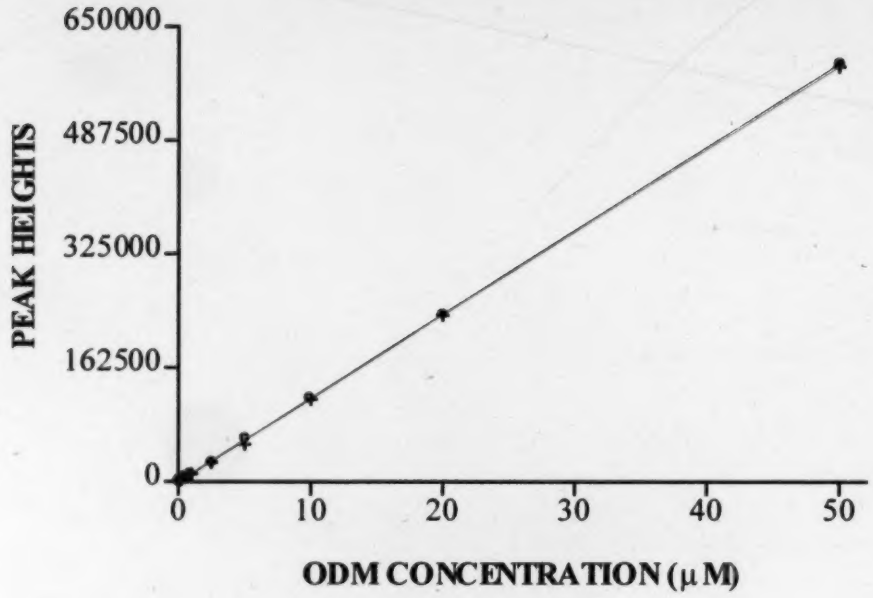

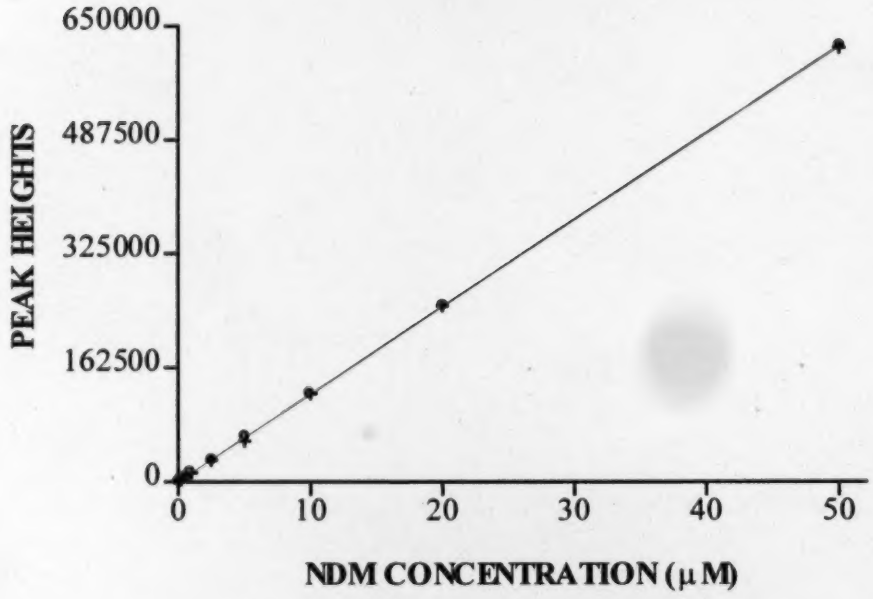

Figure 4-4: Calibration curves for ODM and NDM with (o) and without (+) the addition of protein.

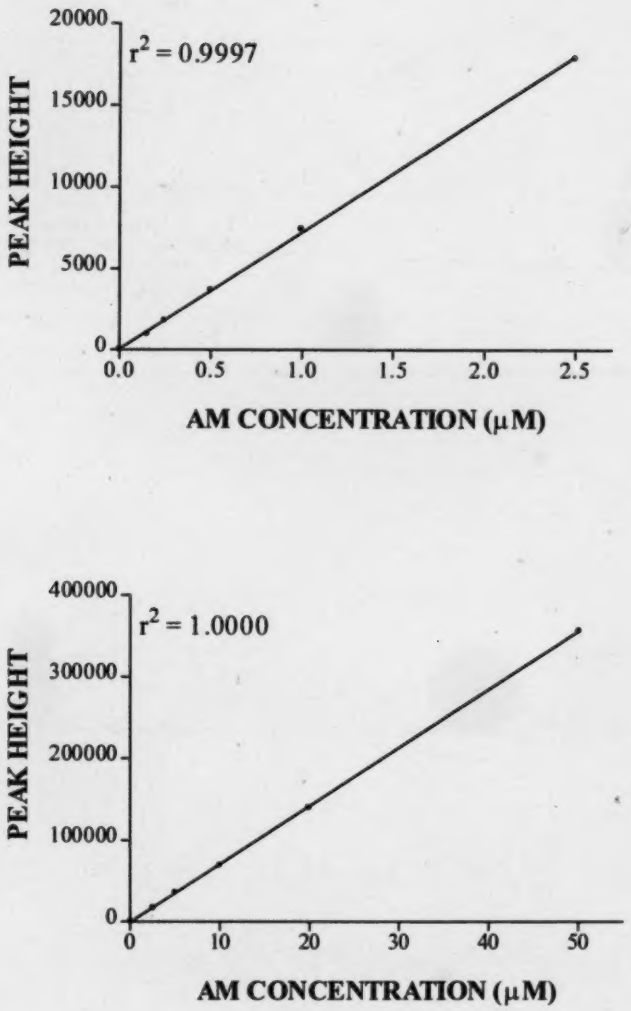

Figure 4-5: Calibration curves for the quantitation of AM in human liver microsomes.

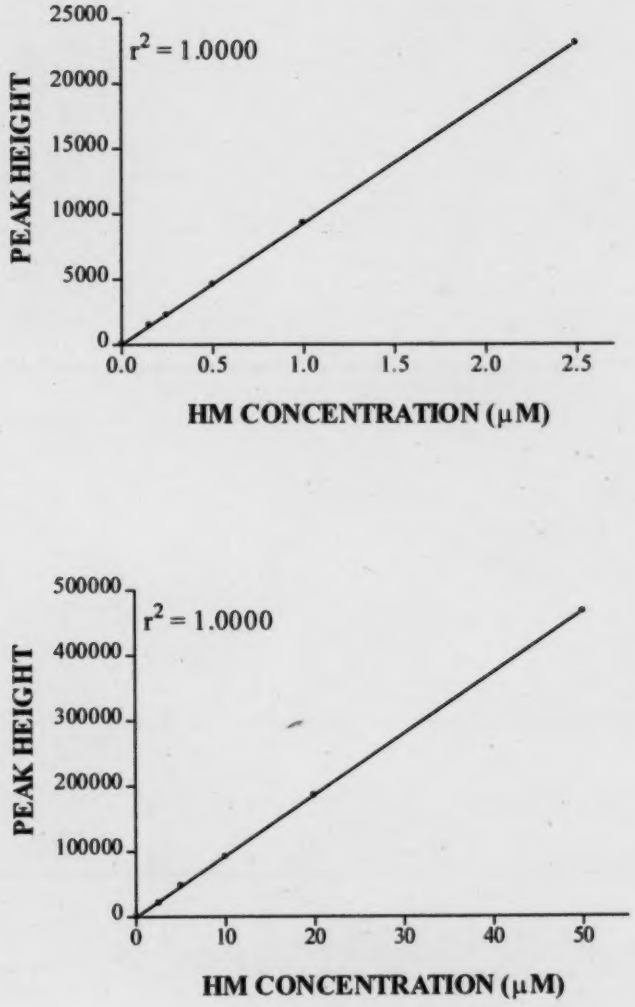

Figure 4-6: Calibration curves for the quantitation of HM in human liver microsomes.

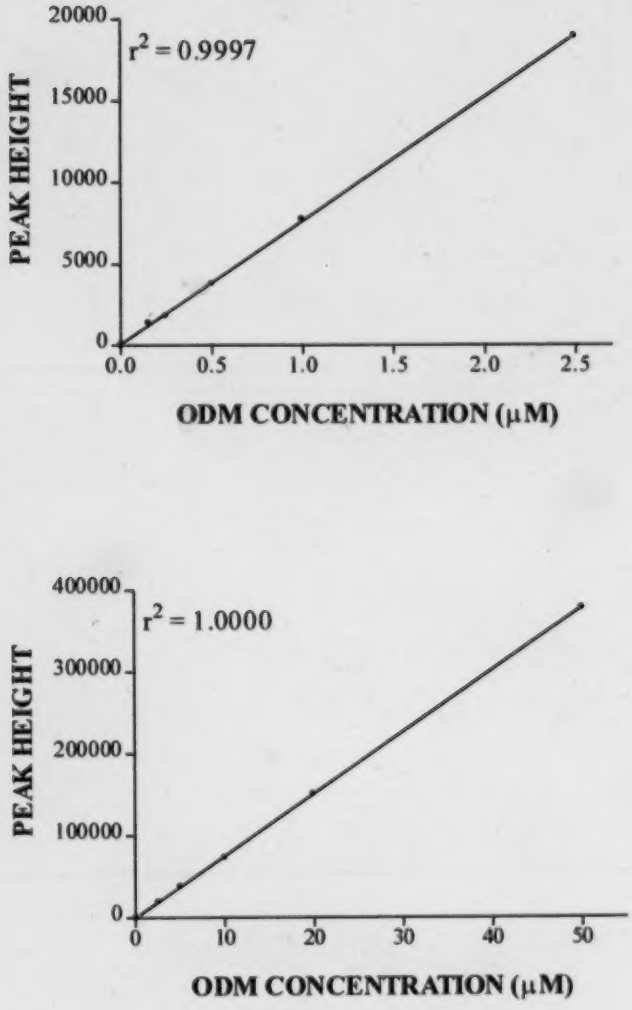

Figure 4-7: Calibration curves for the quantitation of ODM in human liver microsomes.

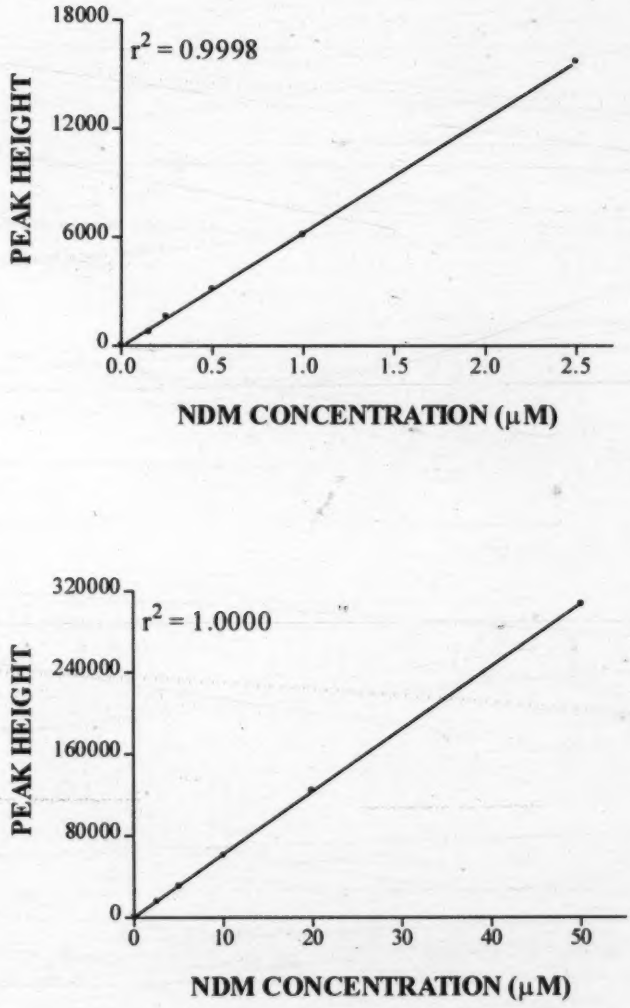

Figure 4-8: Calibration curves for the quantitation of NDM in human liver microsomes.

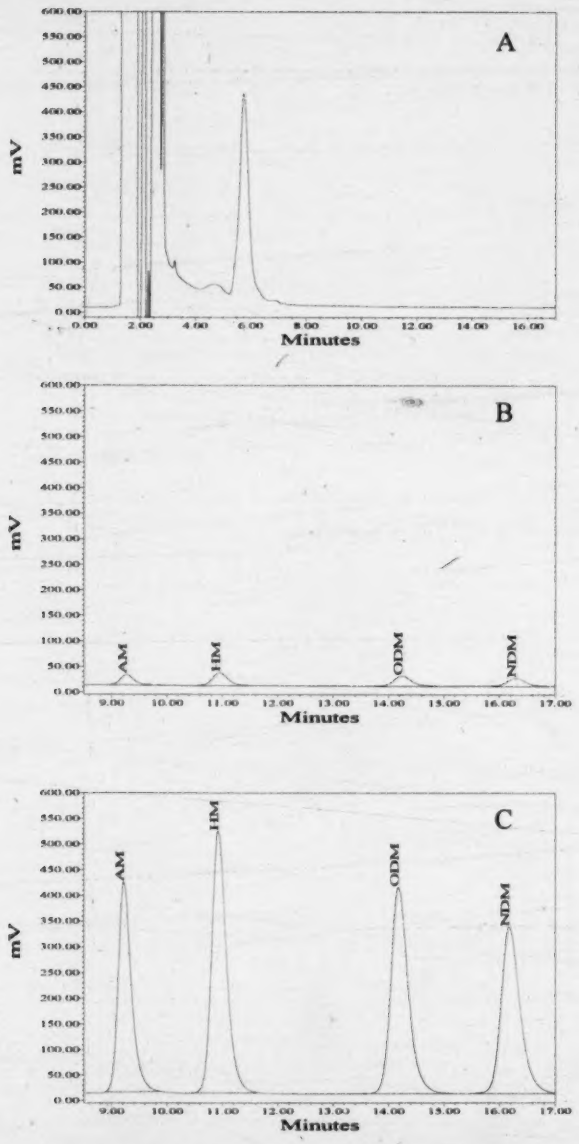

Figure 4-9: Typical standard chromatographs resulting from HPLC analysis. A) A blank standard. B) A standard containing 2.5 μM of AM, HM, ODM and NDM. C) A standard containing 50 μM of AM, HM, ODM and NDM.

METABOLITE	CHROMATOGRAPHIC PARAMETERS		
	K′	α	R
AM	4.83	] 1.20	] 2.28
HM	5.82	] 1.35	] 4.23
ODM	7.86	] 1.16	] 2.19
NDM	9.04		

Table 4-1: Chromatographic parameters for HPLC analysis (n =4) calculated using the equations described in Section 1.9.2.2.

measured at 0.15, 0.25, 1.0, 2.5, 10 and 50 μM concentrations (Table 4-2). The between-run precision (n = 10) was less than 15% for all metabolites at all standard concentrations (Table 4-3).

4.3.2 PRELIMINARY STUDIES

4.3.2.1 Time Course

Quantitating the production of ODM, NDM and HM after incubation times of 5, 10, 30, 45 and 60 min demonstrated that metabolite production was linear for at least 30 min (Figure 4-10). In subsequent experiments, 30 min was used as the incubation time.

4.3.2.2 Requirement of NADPH

Incubating MET with and without $NADP^+$ demonstrated a requirement for NADPH with respect to the production of ODM, HM and NDM.

4.3.2.3 Enzyme Concentration

The production of ODM, HM and NDM at the different protein concentrations demonstrated that metabolite production was relatively linear with respect to enzyme concentrations (Figure 4-11). A protein concentration of 2.3 mg/mL was chosen for subsequent experiments.

4.3.3 KINETIC ANALYSIS

HM, ODM and NDM were fitted to one-, two- and three-enzyme models. The data best fitted a two-enzyme model for HM and ODM. Interestingly, the data for NDM fitted best to a three-enzyme model (Figure 4-12). K_m and V_{max} values are given in Table 4-4. The values for both the two-enzyme and three-enzyme models are given for NDM. In addition, the regression coefficient (r^2) is given to show the goodness of fit of the data to the model used.

Standard Concentration of Each Metabolite (μM)	Within-run Precision for Each Metabolite			
	AM	HM	ODM	NDM
0.15	5.2 %	8.8 %	4.5 %	8.7 %
0.25	3.5 %	4.4 %	6.2 %	9.2 %
1.0	1.4 %	1.5 %	1.9 %	2.6 %
2.5	1.9 %	1.4 %	1.3 %	1.4 %
10	2.4 %	2.5 %	2.5 %	2.4 %
50	1.0 %	1.0 %	1.0 %	0.9 %

Table 4-2: Within-run precision for the quantitation of AM, HM, ODM and NDM (n=5) calculated using the equation described in Section 4.2.2.3.

Standard Concentration of Each Metabolite (μM)	Between-run Precision for Each Metabolite			
	AM	HM	ODM	NDM
0.15	15.0 %	13.2 %	13.3 %	11.8 %
0.25	5.5 %	8.0 %	12.0 %	9.2 %
0.5	11.0 %	9.8 %	7.9 %	7.0 %
1.0	11.2 %	11.2 %	6.7 %	6.9 %
2.5	9.5 %	9.4 %	7.4 %	5.0 %
5.0	5.4 %	6.1 %	5.2 %	5.2 %
10	7.3 %	7.7 %	4.9 %	4.1 %
20	6.4 %	7.4 %	5.0 %	4.5 %
50	7.3 %	6.0 %	3.6 %	4.3 %

Table 4-3: Between-run precision for the quantitation of AM, HM, ODM and NDM (n=10) calculated using the equation described in Section 4.2.2.3.

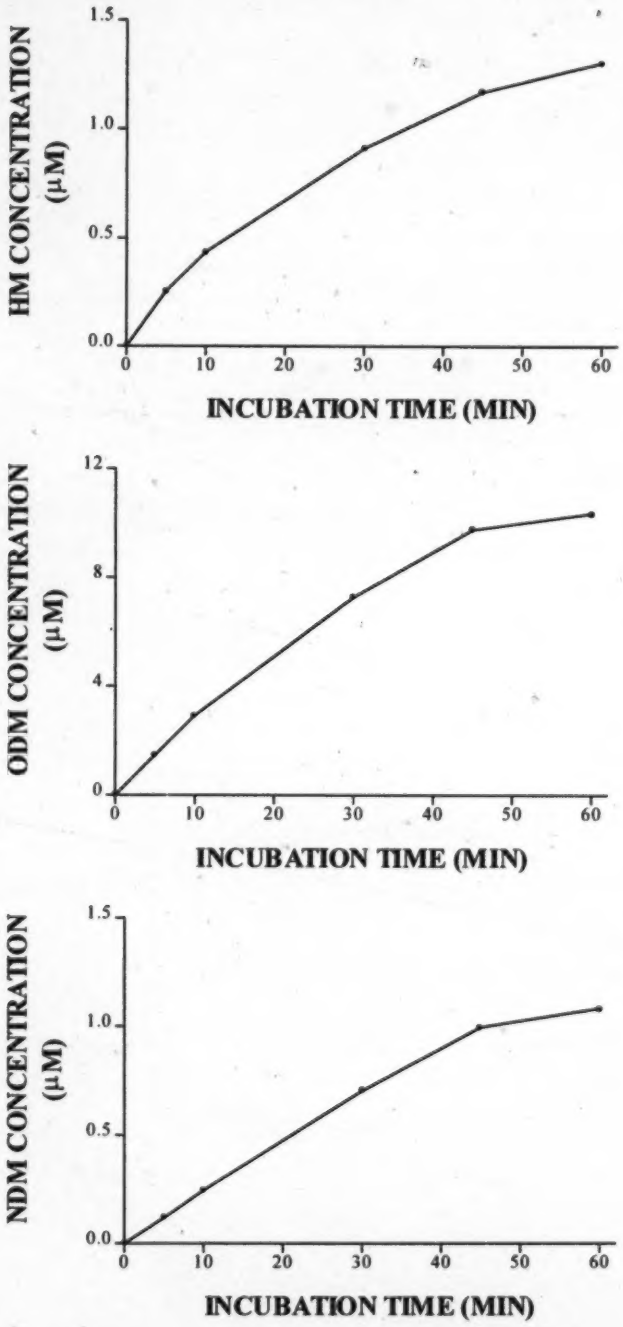

Figure 4-10: Time course experiment for the production of HM, ODM and NDM.

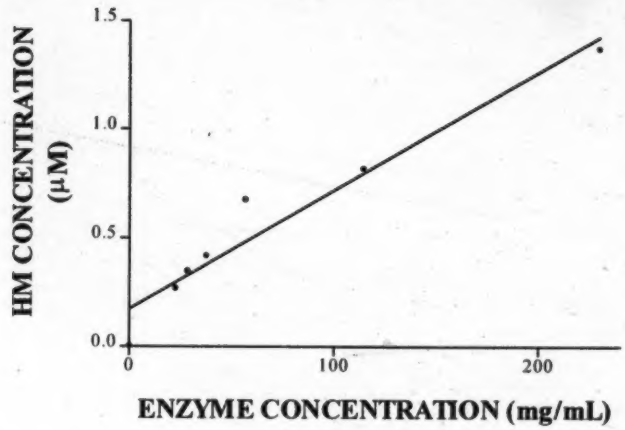

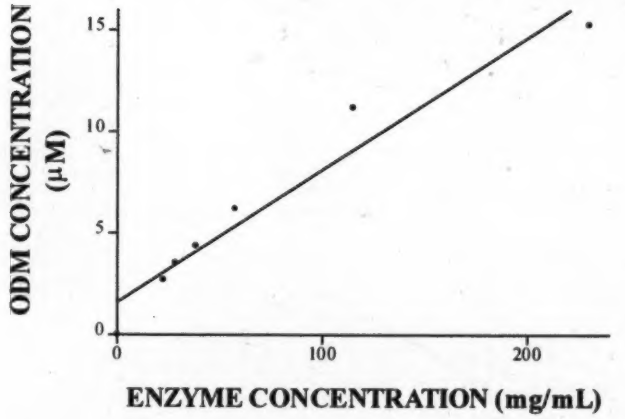

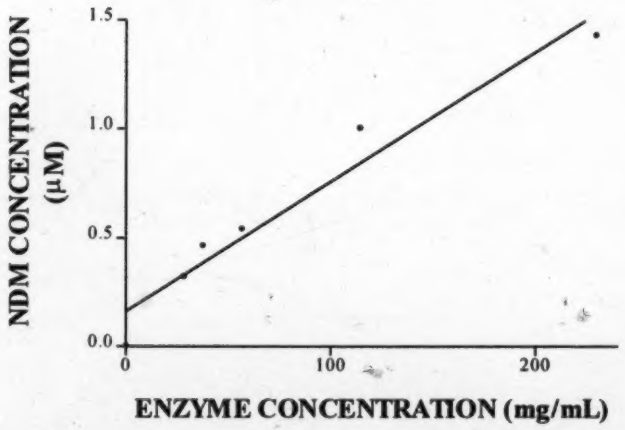

Figure 4-11: Production of HM, ODM and NDM with respect to protein concentration.

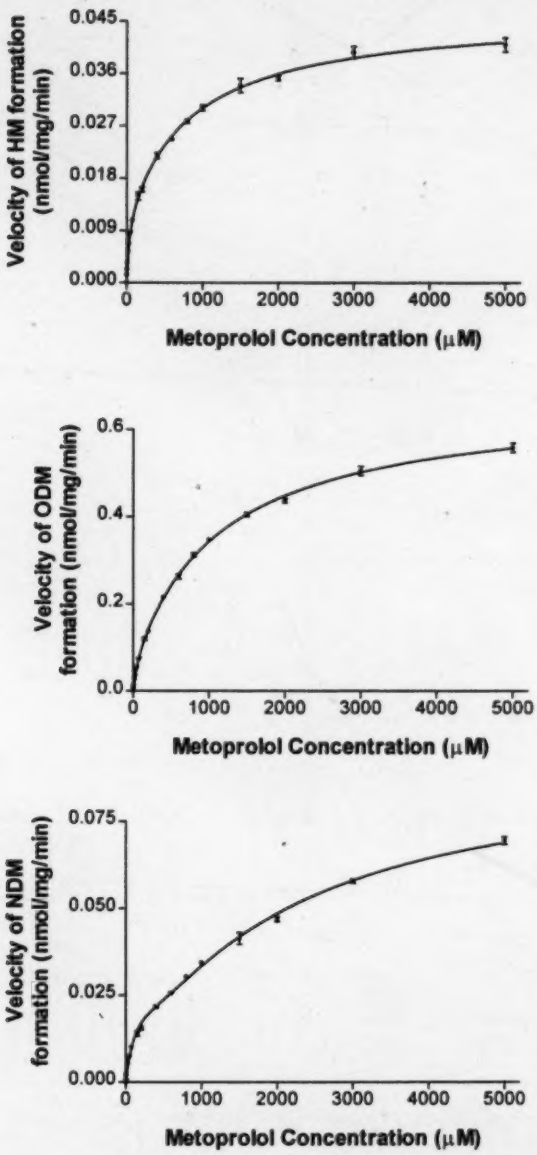

Figure 4-12: Michaelis-Menten graphs for the formation of HM, ODM and NDM. The graphs for HM and ODM represent data fitted to a 2 enzyme model whereas the graph for NDM is of data fitted to a 3 enzyme model. Each point is the mean ± SEM of three experiments conducted on different experimental days.

Enzyme Model	Michaelis-Menten Constants	Metabolite		
		HM	ODM	NDM
Two Enzyme Model	K_{ma} (μM)	26.02	54.77	500.0
	V_{maxa} (nmol/mg/min)	0.01052	0.06530	0.2040
	K_{mb} (μM)	818.0	1157	1750
	V_{maxb} (nmol/mg/min)	0.03590	0.6060	0.06301
	r^2	0.9962	0.9986	0.9785
Three Enzyme Model	K_{ma} (μM)			72.15
	V_{maxa} (nmol/mg/min)			0.01816
	K_{mb} (μM)			1169
	V_{maxb} (nmol/mg/min)			-0.1601
	K_{mc} (μM)			1667
	V_{maxc} (nmol/mg/min)			0.2413
	r^2			0.9979

Table 4-4: K_m and V_{max} values for the formation of HM, ODM and NDM.

4.3.4 IC_{50} and K_i DETERMINATION

Incubation of PAR, FLU, FVX and DMI with MET did not show any chromatographic interferences. Typical chromatograms are shown in Figure 4-13 and Figure 4-14. IC_{50} values of DMI, FVX, FLU and PAR with respect to the formation of ODM were first obtained using a MET concentration of 2000 μM (Figure 4-15). The use of such a high concentration of MET effectively selects the low affinity (high K_m) enzyme. This selectivity is easily demonstrated by using the Michaelis-Menten equation and inserting the appropriate V_{max} and K_m values generated for the formation of ODM (Table 4-4). By conducting this calculation, it is simple to see that at 2000 μM of MET, 86% of the resulting metabolism is due to the low affinity enzyme.

$$v = ((V_{maxa}[S])/(K_{ma} + [S])) + ((V_{maxb}[S])/(K_{mb} + [S]))$$

$$v = (((0.06530)(2000))/(54.77 + 2000)) + (((0.6060)(2000))/(1157 + 2000))$$

$$v = 0.06356 + 0.3839 = 0.4475$$

Thus: $0.06356/0.4475 = 0.14$ (14% of the resulting velocity is due to the high affinity enzyme)

$0.3839/0.4475 = 0.86$ (86% of the resulting velocity is due to the low affinity enzyme)

The IC_{50} values that are generated using 2000 μM of MET are then converted into K_i values. It is these K_i values which are then used to determine the theoretical IC_{50} of the low affinity enzyme when using 40 μM of MET (Table 4-5).

By using the same equation as above but substituting 40 for 2000, it is clear that at a concentration of MET of 40 μM, 42% of the metabolism is due to the low affinity

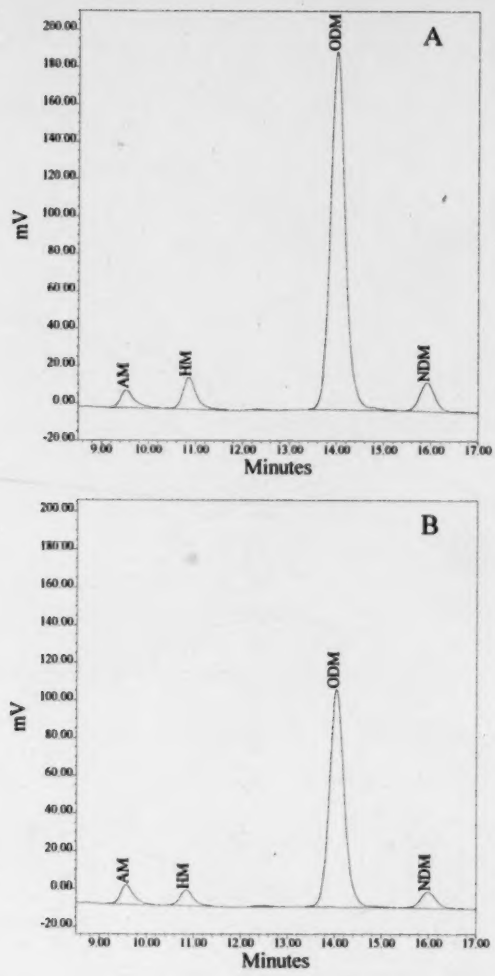

Figure 4-13: Typical HPLC chromatograms from the inhibition experiments using 2000 μM of MET. A) A sample to which was added 200 nmol of MET (final concentration is 2000 μM). B) A sample to which was added 200 nmol of MET (final concentration is 2000 μM) and 3 nmol of PAR (final concentration is 30 μM).

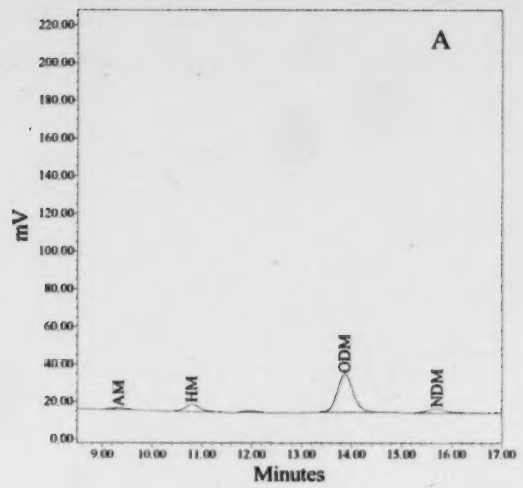

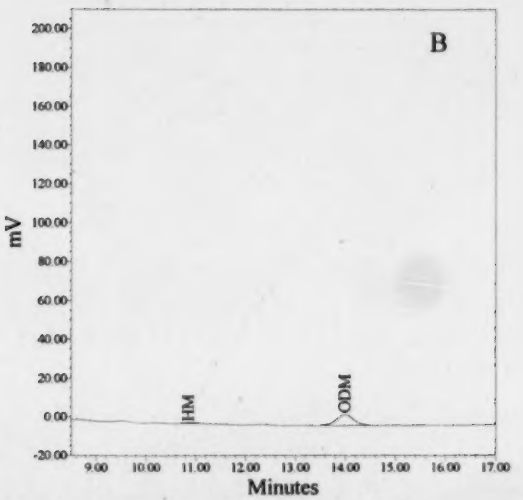

Figure 4-14: Typical HPLC chromatograms from the inhibition experiments using 40 μM of MET. A) A sample to which was added 4 nmol of MET (final concentration is 40 μM). B) A sample to which was added 4 nmol of MET (final concentration is 40 μM) and 3 nmol of PAR (final concentration is 30 μM).

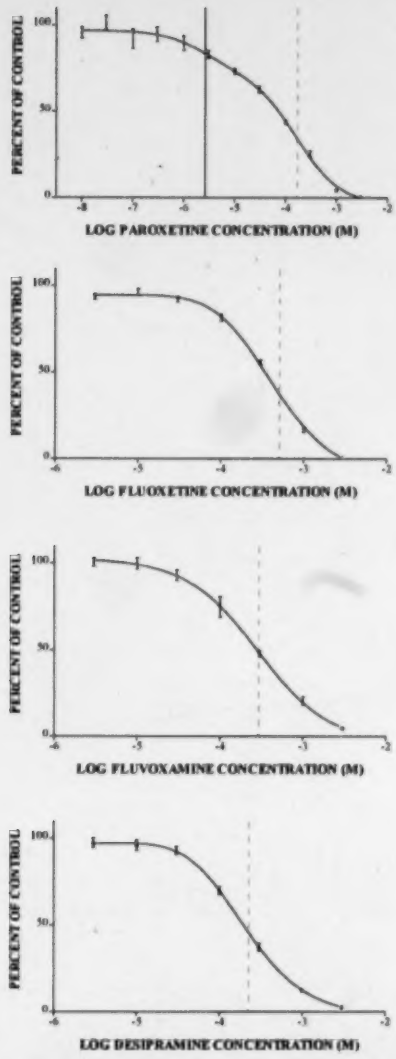

Figure 4-15: Sigmoid curves demonstrating the inhibitory potential of PAR, FLU, FVX and DMI on the formation of ODM in the presence of 2000 μM of MET. The IC_{50} values of the low affinity enzyme are shown by the dotted (---) lines. The IC_{50} value of the high affinity enzyme is shown by the solid (—) line. Each point represents the mean ± SEM of three separate experiments conducted on different experimental days.

Inhibitor	Enzyme Component					
	High Affinity Enzyme			Low Affinity Enzyme		
	IC_{50} (μM)	K_i (μM)	Theoretical IC_{50} (μM) at 40 μM MET	IC_{50} (μM)	K_i (μM)	Theoretical IC_{50} (μM) at 40 μM MET
PAR	2.66	0.07	0.07	167	61	63
FLU				508	186	192
FVX				292	107	111
DMI				222	81	84

Table 4-5: The IC_{50} and K_i values generated by PAR, FLU, FVX and DMI using 2000 μM of MET. The effect on both the low and high affinity enzymes responsible for ODM formation is shown.

enzyme and 58% of the metabolism is due to the high affinity enzyme (low K_m enzyme). Therefore, at 40 μM of MET, IC_{50} values must be calculated using a two-site model in order to separate the effect of each antidepressant on both the low affinity and the high affinity enzymes (Figure 4-16). When the two IC_{50} values are generated, it is then necessary to determine which value belongs to which enzyme. Due to the experiment conducted at 2000 μM of MET, a theoretical IC_{50} value for the low affinity enzyme at 40 μM has been determined. Thus, by a process of elimination, the remaining IC_{50} value must belong to the high affinity enzyme. Subsequently, the K_i of each antidepressant for both the low and high affinity enzymes is ascertained (Table 4-6).

With respect to PAR, it was obvious from the IC_{50} curve generated using 2000 μM of MET that both the low affinity and high affinity enzymes were being inhibited. However, this did not prove to a major stumbling block. The IC_{50} value for the low affinity enzyme is ascertained by calculating the different possibilities of IC_{50} values, K_i values and theoretical IC_{50} values at 40 μM of MET and matching the theoretical values with the values actually obtained at 40 μM of MET.

The rank order of inhibitor potency of the high affinity enzyme associated with the formation of ODM is PAR>FLU>FVX>DMI. The rank order of inhibitor potency of the low affinity enzyme associated with the formation of ODM is PAR>DMI>FVX>FLU. The sigmoid curves that were generated for each of the antidepressants also demonstrate that each antidepressant is capable of inhibiting both the high and the low affinity enzymes with respect to the formation of ODM. In the experiments using 40 μM of MET, if the antidepressant inhibited only one of the

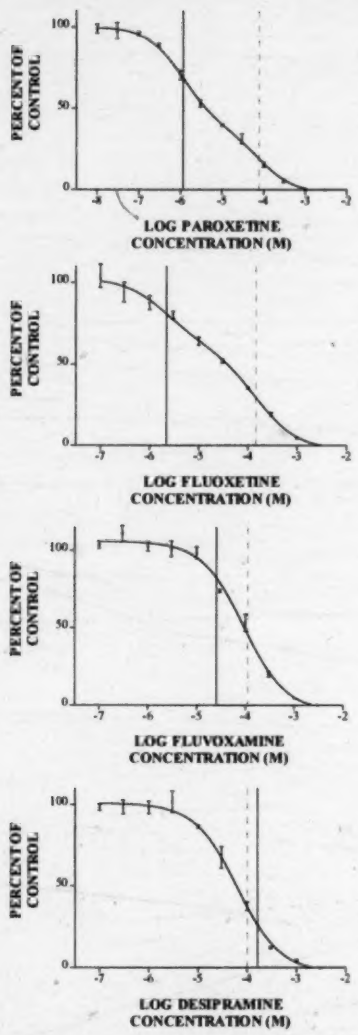

Figure 4-16: Sigmoid curves demonstrating the inhibitory potential of PAR, FLU, FVX and DMI on the formtion of ODM in the presence of 40 μM of MET. The IC_{50} values of the low affinity enzyme are shown by the dotted (---) line. The IC_{50} values of the high affinity enzyme are shown by the solid (—) line. Each point represents the mean ± SEM of three separate experiments conducted on different experimental days.

Inhibitor	Enzyme Component			
	High Affinity Enzyme		Low Affinity Enzyme	
	IC_{50} (μM)	K_i (μM)	IC_{50} (μM)	K_i (μM)
PAR	1.16	0.67	78	75
FLU	2.21	1.28	144	139
FVX	26	15	112	108
DMI	163	94	100	96

Table 4-6: The IC_{50} and K_i values generated by PAR, FLU, FVX and DMI using 40 μM of MET. The effect on both the low and high affinity enzymes responsible for ODM formation is shown.

enzymes, there would have been approximately 40% or 60% of enzyme activity remaining.

4.3.5 POWER EQUATION

The experiment conducted using 200 μM of MET shows the inhibitory effect of PAR, FLU, FVX and DMI (Figure 4-17). The rank order of inhibitor potency is PAR>DMI>FVX>FLU (Table 4-7). This rank order is in agreement with the results generated using 2000 μM MET. It must be noted that the values generated using this experiment are not IC_{50} values. They are simply the concentration of inhibitor that inhibits metabolite production to 50% of control.

4.4 DISCUSSION

4.4.1 ASSAY PROCEDURE

4.4.1.1 Effect of Protein

The purpose of conducting this experiment was to demonstrate that protein would have a neglible effect in the processing of the standards and thus the inclusion of protein in the standards was not necessary. This experiment was done primarily to prevent unnecessary use of control microsomes.

4.4.1.2 Calibration Curves

The calibration curves were always linear, with acceptable y-intercepts. The decision to generate two curves for each metabolite was made to ensure greatest accuracy at low metabolite concentrations.

4.4.1.3 Assay Validation

This novel analytical procedure for analyzing these four major metabolites of MET is simple and reproducible, with all metabolites being well resolved. A resolution

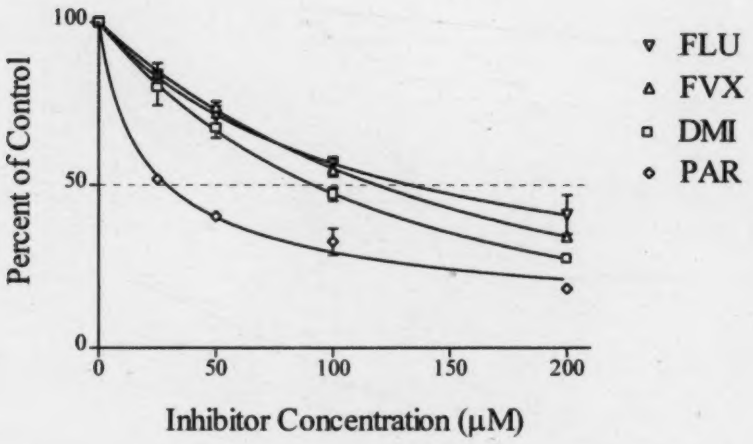

Figure 4-17: Inhibition of ODM production by PAR, FLU, FVX and DMI at a MET concentration of 200 μM. Each point represents the mean ± SEM of at least three separate experiments conducted on different experimental days.

Inhibitor	Concentration of Inhibitor (μM) that Inhibits to 50% of Control
PAR	29
FLU	133
FVX	119
DMI	92

Table 4-7: Concentration of PAR, FLU, FVX and DMI that reduces ODM production to 50% of control using a MET substrate concentration of 200 μM.

value of 1.25 or greater is considered necessary for good chromatographic analyses (Tabor, 1984). The resolution values generated by this assay were all greater than 2.1 and are thus quite acceptable.

No previous reports describing the quantitation of NDM could be found. There are also only a few papers that describe the quantitation of AM in urine samples. The first papers that were published describe the measurement of radioactively labelled metabolites (Borg, 1975) and a fairly involved phosgene derivatization, extraction and trimethylsilylation procedure (Gyllenhaal and Hoffmann, 1984). Other papers described the direct injection of dilute urine onto an HPLC (Godbillon and Duval, 1984; Lennard, 1985). However, the limits of detection of those assays were 500 ng/100 μL and 50 ng/100 μL respectively, which were not sufficient for the studies described herein. Lennard (1985) also briefly discussed the analysis of AM in microsome samples. However, the production of AM in both rat and human liver microsomes were considered to be negligible. Again, the limit of detection of the assay may not have been sufficient to measure the quantities of AM produced. Using a combination of radio-GC and GC-MS, Arfwidsson *et al.* (1976) demonstrated the levels of AM exceeded the levels of ODM in rat liver microsomes. A solid phase extraction procedure was described by Chiu *et al.* (1997). Although the limits of detection seem to have been quite acceptable for the microsome studies, the experimental procedure required the use of solid phase extraction cartridges.

One of the reasons for the lack of published methodologies for the quantitation of AM is its amphoteric structure which makes it difficult to quantitate AM when sample extraction is required. Indeed, it was AM that proved to be the greatest challenge in the development of the assay described herein. Due to the nature of the samples used in

these experiments, an extraction procedure was not necessary. Precipitating the protein at the end of the experiment was a sufficient cleanup step that allowed the samples to be injected directly onto the HPLC. However, it was necessay to use 1N perchloric acid. The use of higher or lower concentrations of perchloric acid, or the use of methanol or acetonitrile to precipitate the protein, resulted in a poor chromatographic peak for AM. It was also the AM peak that was most sensitive to changes in pH. If the pH value was too high, the peak would disappear into the solvent front. If all other conditions remained the same, but the pH was decreased, the AM will actually chromatograph after the peak for HM and start to co-elute with the ODM peak. Due to the limitations of pH, the buffers which could be used in the mobile phase were also limited.

Other problems encountered were an excessively tailing solvent front and an upward baseline drift, which started at approximately the same time NDM was being chromatographed. These problems were overcome using the mobile phase described herein. In fact, the main reason for using the triethylamine in the mobile phase was to prevent the baseline from drifting upward excessively. The triethylamine also had the effect of improving peak shape. A C18 column was also tried but did not prove useful. In actual fact, more than three dozen mobile phases were tested before one was found that proved satisfactory for all four metabolites.

MET could also be quantitated under the described conditions. However, the limit of detection for MET would be slightly higher due to its longer retention time.

4.4.2 PRELIMINARY STUDIES

The reason for conducting the time course and enzyme concentration experiments was to determine assay conditions that would result in the production of metabolite in

quantities that can easily be measured. These experiments give a starting point for conducting more in-depth analysis. The inability of MET to be metabolized to its major metabolites in the absence of $NADPH^+$ is supportive of the involvement of the CYP enzymes in the metabolism of MET.

4.4.3 KINETIC ANALYSIS

The determination of K_m and V_{max} values for the production of HM and ODM was in agreement with other papers in which the data best fit a two-enzyme model (Kim *et al.*, 1993; Belpaire *et al.*, 1998 and Otton *et al.*, 1988). The N-dealkylation reaction proved to be more elusive. The problem with fitting data to a three, or more, enzyme model is that the values generated for V_{max} are often not reasonable and much more work is needed to elucidate actual K_m and V_{max} values. A comparison of the r^2 values for the two- and three-enzyme models is strongly suggestive of more than two enzymes being involved in the metabolism of MET to NDM.

4.4.4 IC_{50} and K_i DETERMINATION

The inhibition constants were determined only for the inhibition of the formation of ODM, the major oxidative metabolite of MET metabolism. Fortuitously, the conversion of ODM to AM was relatively minor, with AM production amounting to approximately 10% of ODM production. Production of AM was therefore not a complicating factor. However, different livers will show varying amounts of AM formation and should not be ignored without proper investigation. If only ODM is quantitated and there is a major conversion of ODM to AM, then the rate of production of ODM will be underestimated.

At first, the determination of K_i values as described in this chapter may seem unnecessarily complicated. Indeed, the task would have been much simpler had there been only one enzyme involved in the production of each metabolite. It would also have been simpler if the low affinity enzyme had negligible activity at a low concentration of MET. Given a single enzyme, or one enzyme that could be effectively ignored, Dixon plots, secondary plots of Hanes-Woolf transformations, or IC_{50} sigmoids generated at only one concentration of MET could have been used. However, the nature of the activities of the low affinity and the high affinity enzymes make simpler approaches impossible. It does, in fact, underscore the importance of determining accurate K_m and V_{max} values for the enzyme-substrate combination that is being investigated. If, for example, a one site model was used to determine an IC_{50} value in the presence of 40 μM of MET, the value would represent an inhibitory effect that is a combination of two enzymes. If the experiment had been conducted at only 2000 μM of MET, the IC_{50} value generated would represent the inhibitory effect on the low affinity enzyme only.

These experiments show that the rank order of inhibition of the high affinity component of MET metabolism is PAR>FLU>FVX>DMI. At the time these experiments were being conducted, Belpaire *et al.* (1998) published a paper that was consistent with the findings for PAR, FLU and FVX discussed herein. DMI was not included in that study. With respect to the high affinity enzyme, PAR, FLU, and possibly FVX, may cause potentially dangerous drug-drug interactions if they are co-administered with MET. The rank order of inhibition of the low affinity component of the metabolism of MET to ODM is PAR>DMI>FVX>FLU. Belpaire *et al.* (1998) did not elucidate the effect of the antidepressants on the low affinity enzyme. Although all four antidepressants inhibit the low affinity enzyme, the K_i values are much greater than

would be considered to be of significance *in vivo*. Since the low affinity enzyme is relatively active, even at low concentrations of MET, it would seem that even in the presence of a potent inhibitor of the high affinity enzyme, MET would still be metabolized.

4.4.5 POWER EQUATION

This experiment underscores the need to understand the basics of enzyme kinetics and how a lack of understanding can lead to erroneous conclusions from experimental data. At first it seemed that inhibition experiments were a simple matter of incubating substrate with inhibitor, looking at a decrease in metabolite formation and determining when the inhibitor reduced metabolite formation to 50% of control. The only criterion would apparently be to choose experimental conditions in which metabolite formation was linear. The first problem in such reasoning is that there is a difference between an IC_{50} and 50% of control. An IC_{50} as defined in section 1.2.8.1 is the concentration of inhibitor that produces 50% of maximum inhibition; 50% of control is simply the concentration of inhibitor that produces 50% of metabolite when compared to control. The difference between these two terms is an important one. Using the power equation it is difficult to determine when the enzyme is actually maximally inhibited. That is one of the reasons why sigmoid curves are used to generate IC_{50} values. Due to the plateaus generated on a sigmoid, it becomes clearer when inhibition is at its minimum and maximum.

The second major factor which can lead to problems in such studies is a lack of understanding of the importance of the substrate concentration used in the experiments. A MET concentration of 200 μM is certainly in the linear portion of metabolite

production (Figure 4-11). However, the reason the results generated using 200 μM of MET correspond to those of the low affinity enzyme is simply due to the contribution of the low affinity and high affinity enzymes at this concentration. At 200 μM of MET, the low affinity enzyme and the high affinity enzyme contribute 64% and 36% respectively to the production of ODM. Conclusions based on the experiment using 200 μM of MET would be that the inhibitor potency was PAR>DMI>FVX>FLU. Without ascertaining accurate Km and Vmax values, and realizing the possible contribution of more than one enzyme, the insights generated by this experiment would have been flawed.

4.5 REFERENCES

Arfwidsson A, Borg KO, Hoffman K-J and Skanberg I (1976) Metabolism of metoprolol in the rat *in vitro* and *in vivo*. *Xenobiotica* 6: 691-711.

Belpaire FM, Winjnant P, Temmerman A, Rasmussen BB and Brøsen K (1998) The oxidative metabolism of metoprolol in human liver microsomes: inhibition by the selective serotonin reuptake inhibitors. *Eur J Clin Pharmacol* 54: 261-264.

Borg KO, Carlsson E, Hoffmann K-J, Jönsson T-E, Thorin H and Wallin B (1975) Metabolism of metoprolol-(^{3}H) in man, the dog and the rat. *Acta Pharmacol Toxicol* (suppl V): 125-135.

Campbell JM and Campbell JB (1984) in *Laboratory Mathematics: Medical and Biological Applications, Third Edition*, St. Louis, Missouri, CV Mosby Company.

Chiu FCK, Damani LA, Li RC and Tomlinson B (1997) Efficient high-performance liquid chromatographic assay for the simultaneous determination of metoprolol and two main metabolites in human urine by solid phase extraction and fluorescence detection. *J Chromatogr B* 696: 69-74.

Godbillon J and Duval M (1984) Determination of two metoprolol metabolites in human urine by high performance liquid chromatography. *J Chromatogr* 309: 198-202.

Gyllenhaal O and Hoffman K-J (1984) Simultaneous determination of metoprolol and metabolites in urine by capillary column gas chromatography as oxazolidineone and trimethylsilyl derivatives. *J Chromatogr* 309: 317-328.

Kim M, Shen DD, Eddy AC and Nelson WL (1993) Inhibition of the enantioselective oxidative metabolism of metoprolol by verapamil in human liver microsomes. *Drug Metab Dispos* 21: 309-317.

Lennard MS (1985) Quantitative analysis of metoprolol and three of its metabolites in urine and liver microsomes by high performance liquid chromatography. *J Chromatogr* 342: 199-205.

Otton SV, Crewe HK, Lennard MS, Tucker GT and Woods HF (1988) Use of quinidine to define the role of the sparteine/debrisoquine cytochrome P450 in metoprolol oxidation by human liver microsomses. *J Pharmacol Exp Ther* 247: 242-247.

Östholm I (1975) Introduction. *Acta Pharmacol et Toxicol* (suppl V): 125-135.

Tabor MW (1984) Chromatography: theory and practice. In Kaplan LA and Pesce AJ (Eds) *Clinical chemistry: Theory, Analysis and Correlation* (pp. 74 – 99). St. Louis, Missouri, CV Mosby Company.

Walley T, Pirmohamed M, Proudlove C and Maxwell D (1993) Interaction of metoprolol and fluoxetine. *Lancet* 341: 967-968.

Wayne VS, Harper RW, Laufer E, Federman J, Anderson ST and Pitt A (1982) Adverse interaction between beta-adrenergic blocking drugs and verapamil - report of three cases. *Aust NZ J Med* 12: 285-289.

Chapter 5: Elucidation of the Enzymes Responsible for the Metabolism of Metoprolol.

5.1 INTRODUCTION

As previously discussed, CYP2D6 has been implicated in both the O-demethylation and α-hydroxylation pathways in the metabolism of MET (Otton *et al.*, 1988). However, the kinetic data as presented in Chapter 4 indicate that these two oxidative pathways are biphasic, suggesting that enzymes in addition to CYP2D6 are involved in those pathways. This suggestion is supported by previous reports by Kim *et al.* (1993), Belpaire *et al.* (1998) and Otton *et al.* (1988). However, the biphasic nature of the α-hydroxylation pathway was not a definite conclusion of the work by Otton *et al.* (1988). No reports were found that elucidated the enzymes involved in either the N-dealkylation reaction or the oxidation of O-desmethylmetoprolol (ODM) to its acid metabolite (AM). Again, based on the kinetic data as discussed in Chapter 4, at least 3 enzymes seem to be implicated in the oxidation of MET through the N-dealkylation pathway.

This chapter highlights the approach taken to identify the enzymes involved in the major oxidative routes of MET metabolism. In addition, the metabolism of ODM to its acid metabolite was also studied to ascertain the enzymes involved in that reaction. Both human liver microsomes and microsomes from cells expressing individual CYP enzymes were employed to aid in the identification of those enzymes.The metabolism of the N-dealkylated product to its acid metabolite was not investigated due to lack of availability of this acid metabolite.

5.2 EXPERIMENTAL PROCEDURES

5.2.1 INSTRUMENTATION

Samples were analyzed, as discussed in Section 4.2.1, by HPLC using a Waters Model 510 pump, a Waters WISP 710 B autosampler, a Waters 2487 Duel λ Absorbance Detector set at 222 nm and a sensitivity setting of 0.1 absorbance units full scale (AUFS), and a Hyoersil 5 CN column (4.6 x 25 cm). Data processing was carried out using a Pegasus Pentium II, 400 MHz computer with Waters Millennium[32] software (Version 3.05). The mobile phase consisted of sodium acetate (2.8 mM)-acetonitrile-methanol-triethylamine in a ratio of 80:10:10:0.01. The mobile phase was pumped at a flow rate of 1.5 mL/min, giving an operating pressure of approximately 1800 psi. All metabolite peaks had retention times of less than 20 min. A run time of 35 min was used to allow sufficient time for the MET peak to be chromatographed. All analyses were carried out isocratically at room temperature.

In those experiments in which MET was the substrate, the mobile phase had a final pH value of 4.5. In those experiments in which ODM was used as the substrate the final pH value of the mobile phase was 4.57. These pH values were obtained using glacial acetic acid.

5.2.2 CALIBRATION CURVES

Calibration curves consisting of 0 - 50 μM of AM, HM, ODM and NDM were prepared as described in Section 5.2.2.2 and used in those experiments in which the substrate was MET.

Calibration curves used in the experiments in which ODM was used as the substrate were constructed by preparing standards consisting of 0-50 μM of AM only.

These standards were prepared by diluting the appropriate amount of AM in 0.1 M potassium phosphate buffer to which was added 25 μL of the NADPH generating system, giving a final volume of 100 μL. To this solution, 20 μL of 1 N perchloric acid were added. The standards sat on ice for a minimum of 10 min, at which time they were centrifuged for 1 min. The resulting supernatants were then transferred to autosampler vials and a 20 μL aliquot was used for analysis

5.2.3 PRELIMINARY STUDIES

5.2.3.1 Metoprolol

Preliminary studies had been conducted previously for MET as described in Sections 4.2.3.1, 4.2.3.2, 4.2.3.3. These studies demonstrated that metabolite production was linear for at least 30 min, there was a requirement for NADPH with respect to the formation of ODM, HM and NDM, and that metabolite production was relatively linear with respect to enzyme concentration.

5.2.3.2 O-Desmethylmetoprolol

5.2.3.2.1 Time Course

An experiment was conducted to determine the production of AM in relation to time. In this experiment, ODM in potassium phosphate buffer was incubated with 25 μL of the NADPH generating system and 10 μL of the microsome solution. The total incubation volume was 100 μL, giving a final concentration of ODM of 50 μM and a final protein concentration of 2.3 mg/mL (230 μg/100 μL). The reactions were carried out in a 37°C waterbath for time periods of 5, 10, 30, 45 or 60 min. After the elapsed time, the samples were placed on ice and 20 μL of 1 N perchloric acid were added to

terminate the reaction and to precipitate the protein. After sitting on ice for a minimum of 10 min, the samples were centrifuged for 1 min and the resulting supernatants were transferred to autosampler vials.

5.2.3.2.2 Requirement of NADPH

This experiment was conducted to determine if NADPH was required to oxidize ODM to AM. ODM, in a final concentration of 50 μM, was incubated with 10 μL of microsomal protein, without $NADP^+$. All other components of the NADPH generating system were present. The reactions were carried out in a 37°C waterbath for time periods of 5, 10, 30, 45 or 60 min, after which they were placed on ice and a 20 μL aliquot of 1N perchloric acid was added to each sample. The samples remained on ice for a minimum of 10 min, at which time they were centrifuged for 1 min and the supernatants transferred to autosampler vials.

5.2.3.2.3 Substrate Concentration Experiment

The microsomal incubation medium consisted of 25 μL of an NADPH generating system, 50 μL of ODM substrate solution (in a final concentration of 0 – 5000 uM prepared in 0.1 M potassium phosphate buffer), 10 μL of microsomal solution and 15 μL of buffer. The total volume was 100 μL resulting in a final protein concentration of 2.3 mg/mL (230 μg/100 μL). The metabolic reaction was allowed to proceed for 30 min in a 37°C waterbath. When the incubation time was complete the samples were placed on ice and 20 μL of 1 N perchloric acid were added to precipitate the protein and effectively terminate the reaction. The samples sat on ice for a minimum of 10 min, at which time they were centrifuged for 1 min. The supernatants were then transferred to autosampler vials and a 20 μL aliquot was used for analysis.

5.2.4 EXPERIMENTS USING HUMAN LIVER MICROSOMES

This experiment consisted of incubating MET or ODM with microsomes from a panel of 12 different human livers and performing a correlation of metabolite production versus enzyme activity. These 12 livers were characterized for the following CYP enzymes: 1A1, 2A6, 2B6, 2C8, 2C9, 2C19, 2D6, 2E1, 3A4 and 4A. They were also characterized for FMO activity. The microsomal incubation medium consisted of 25 μL of an NADPH generating system, 50 μL of substrate solution (at a final concentration of 100 μM of MET or 3000 μM of MET or 30 μM ODM prepared in 0.1 M potassium phosphate buffer), 10 μL of microsomal solution and 15 μL of buffer. The total volume was 100 μL, resulting in a final protein concentration of 2.0 mg/mL (200 μg/100 μL). The metabolic reaction was allowed to proceed for 30 min in a 37°C waterbath. When the incubation time was complete, the samples were placed on ice and 20 μL of 1 N perchloric acid were added to precipitate the protein and terminate the reaction. The samples sat on ice for a minimum of 10 min at which time they were centrifuged for 1 min. The supernatants were then transferred to autosampler vials and a 20 μL aliquot was used for analysis.

5.2.5 EXPERIMENTS USING MICROSOMES FROM CELLS EXPRESSING INDIVIDUAL CYP ENZYMES

These experiments consisted of incubating MET or ODM with microsomes from cDNA expressed cells to determine the individual enzymes that are capable of metabolizing MET to any of its major metabolites or ODM to AM. The individual CYP enzymes expressed were 1A1, 1A2, 2A6, 2B6, 2C8, $2C9_{arg}$, 2C19, 2D6, 2E1, 3A4, 3A5 and 4A11. The enzymes that were co-expressed with cytochrome b_5 were $2C9_{arg}$, 3A4 and 2E1. The microsomal incubation medium consisted of 25 μL of an NADPH

generating system, 50 μL of substrate solution (in a final concentration of 200 μM of MET or ODM prepared in 0.1 M potassium phosphate buffer), 10 μL of microsomal solution and 15 μL of buffer. The total volume was 100 μL, resulting in a final protein concentration of 0.21-1.14 mg/mL (21-114 μg/100 μL), depending on the microsome used. The metabolic reaction was allowed to proceed for 30 min in a 37°C waterbath. When the incubation time was complete, the samples were placed on ice and 20 μL of 1 N perchloric acid were added to precipitate the protein and terminate the reaction. The samples sat on ice for a minimum of 10 min, at which time they were centrifuged for 1 min. The supernatants were then transferred to autosampler vials and a 20 μL aliquot was used for analysis.

Potassium phosphate buffer was used in all incubations except those containing CYP2A6 or $CYP2C9_{arg}$, which are apparently susceptible to inhibition by phosphates (Gentest Corportion). In these instances Tris buffer was employed. Concurrent controls were also included in these experiments to ensure that metabolite production was due the specific enzyme being tested and not due to activity native to the cell line.

5.2.6 STATISTICAL ANALYSIS

Prism Graphpad® software was used to perform regression and correlation analysis of metabolite production versus enzyme activity.

5.3 RESULTS

5.3.1 CALIBRATION CURVES

Calibration curves were generated by plotting the peak height of the metabolite on the y-axis versus the concentration of that metabolite on the x-axis. Calibration curves,

which were run in parallel with the experimental samples in every assay, were linear, with r^2 values >0.99 obtained consistently.

5.3.2 PRELIMINARY STUDIES

5.3.2.1 Time Course

Quantitating the production of AM after incubation times of 5, 10, 30, 45 or 60 min demonstrated that metabolite production was dependent on time (Figure 5-1).

5.3.2.2 Requirement of NADPH

Incubating ODM with and without $NADP^+$ demonstrated that the production of AM was not entirely dependent on the presence of NADPH. The production of AM in the absence of NADPH was on average approximately 20% of AM production in the presence of NADPH (Figure 5-1).

5.3.2.3 Substrate Concentration Experiment

The incubation of varying concentrations of ODM demonstrated that the production of AM was dependent on ODM concentration (Figure 5-2).

5.3.3 THE METABOLISM OF METOPROLOL

5.3.3.1 Experiments Using Human Liver Microsomes

At 100 μM of MET, the production of ODM correlated with CYP2D6 and CYP2E1 activity. The production of HM and NDM correlated with CYP2D6 activity. The production of AM correlated with CYP2B6 activity (Figure 5-3).

At 3000 μM of MET, the production of ODM correlated with CYP2D6 and CYP2E1 activity. The production of HM and NDM both correlated with CYP3A4 and CYP2B6 activity. The production of AM correlated with CYP3A4 and CYP2B6 activity (Figure 5-4).

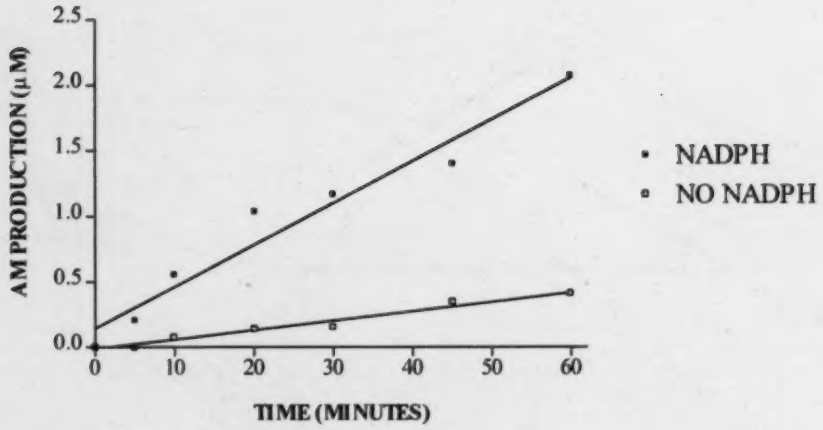

Figure 5-1: The production of AM versus time in the presence and absence of NADPH.

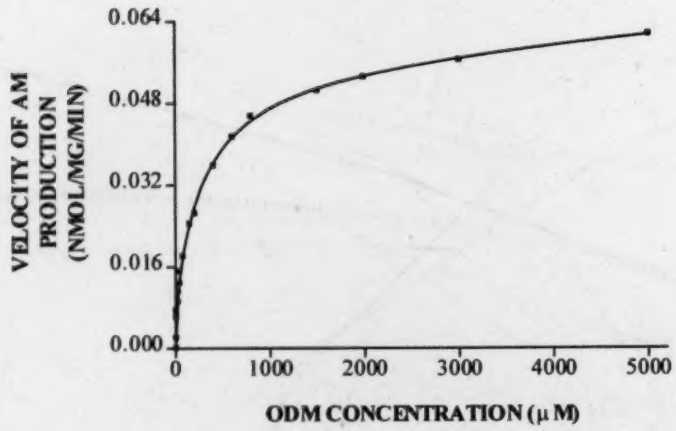

Figure 5-2: The production of AM as a function of ODM concentration.

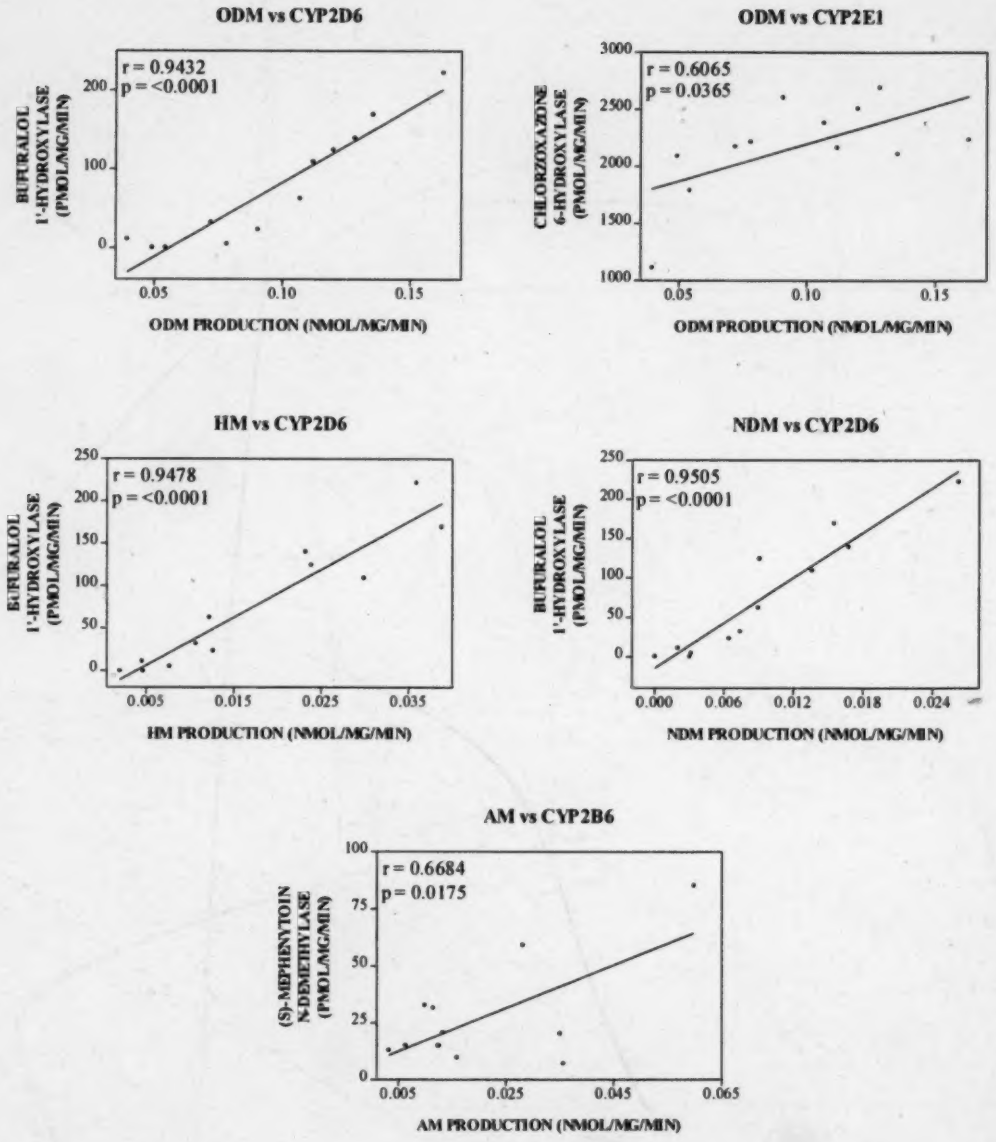

Figure 5-3: Significant correlations resulting from the incubation of 100 μM of MET with human liver microsomes.

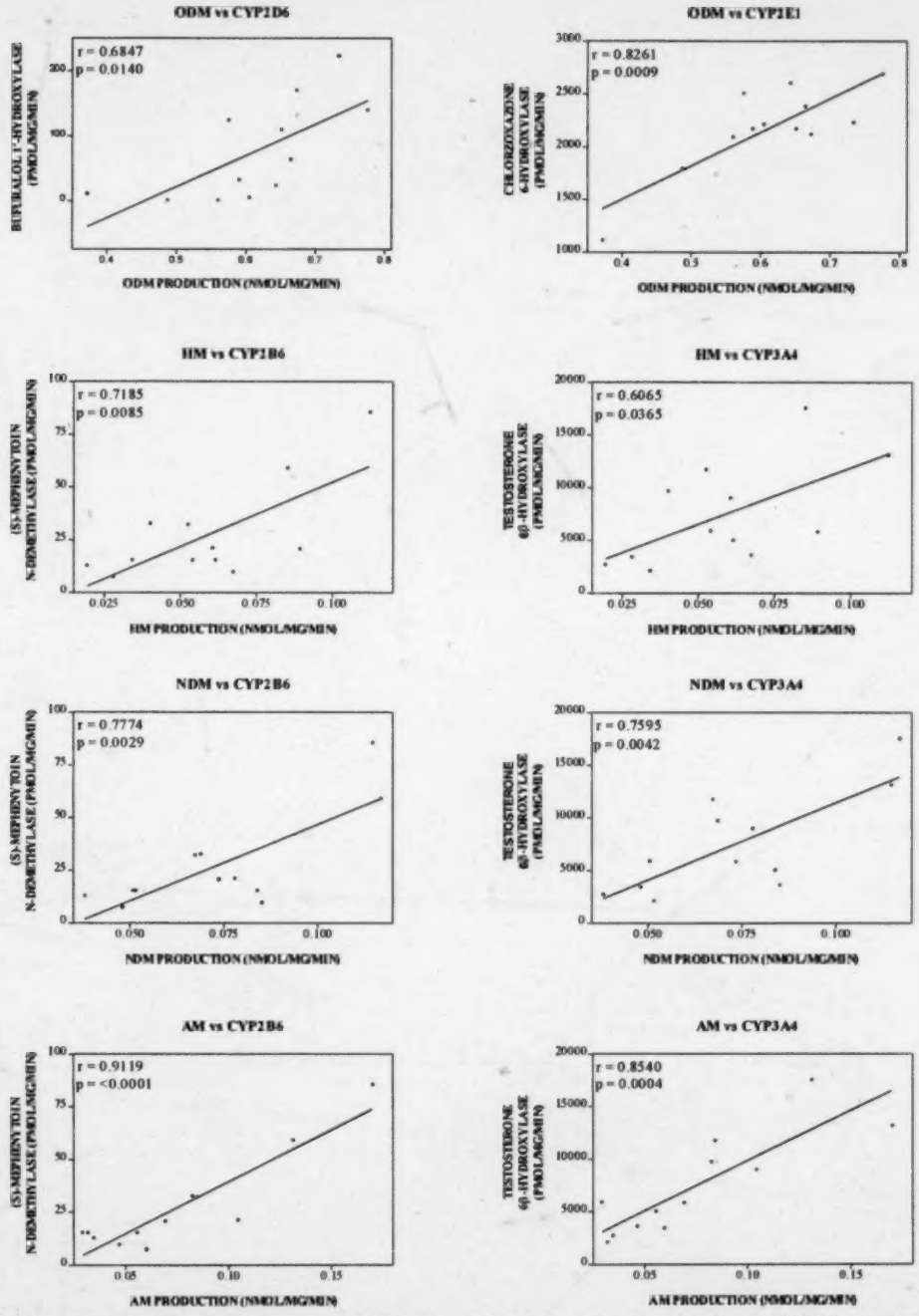

Figure 5-4: Significant correlations resulting from the incubation of 3000 μM of MET with human liver microsomes.

5.3.3.2 Experiments Using Microsomes from Cells Expressing Individual CYP Enzymes

The individual CYP enzymes responsible for the production of ODM were CYP2D6 and CYP2E1. Although CYP3A4 produced a peak at a retention time corresponding to ODM, the chromatography of the peak was poor and not consistent with the chromatography of either the standards or other sample injections. A repeat of that incubation revealed the same chromatography. The production of HM occurred in the incubations with CYP3A4 and CYP2D6. NDM was produced by microsomes expressing CYP3A4, CYP2D6 and CYP2C19. AM was found in the incubations of microsomes expressing CYP3A4 and CYP2D6 (Figure 5-5)

5.3.4 THE METABOLISM OF O-DESMETHYLMETOPROLOL

5.3.4.1 Experiments Using Human Liver Microsomes

The production of AM in the presence of 30 μM of ODM correlated with CYP2D6 activity (Figure 5-6).

5.3.4.2 Experiments Using Microsomes from Cells Expressing Individual CYP Enzymes

The individual CYP enzymes responsible for the production of AM when ODM was used as a substrate were CYP2D6 and CYP3A4 (Figure 5-7).

Table 5-1 summarizes the data from the previous five experiments.

5.4 DISCUSSION

5.4.1 ASSAY CONDITIONS

The assay for the studies involving MET has been discussed previously (Chapter 4). The reason for changing the pH of the mobile phase slightly for the quantitation of AM in studies using ODM as a substrate was to separate AM from an interfering peak.

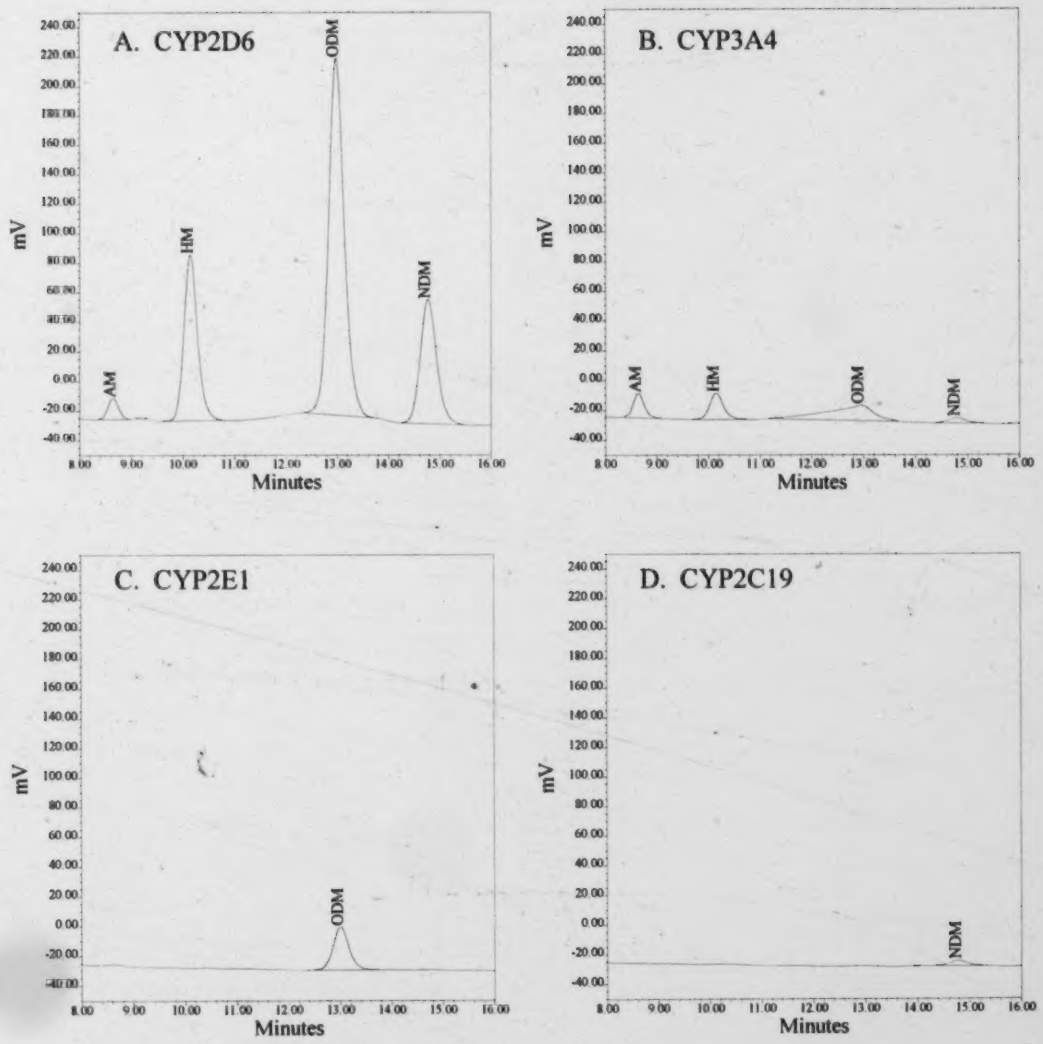

Figure 5-5: Chromatography from the incubations of MET with microsomes expressing A) CYP2D6, B) CYP3A4, C) CYP2E1 or D) CYP2C19.

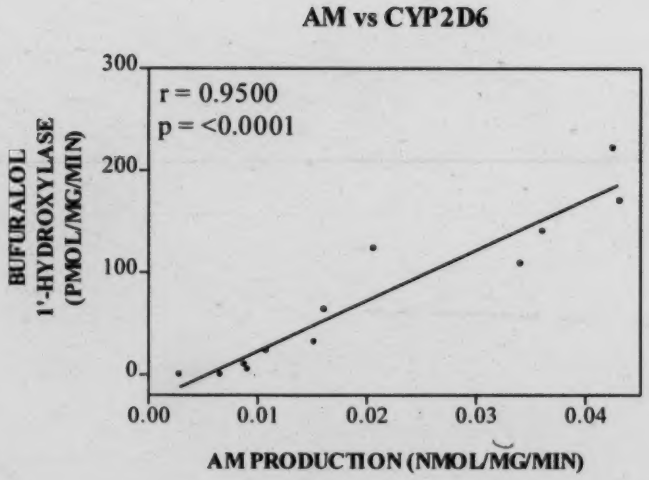

Figure 5-6: Significant correlation resulting from the incubation of 30 μM of ODM with human liver microsomes.

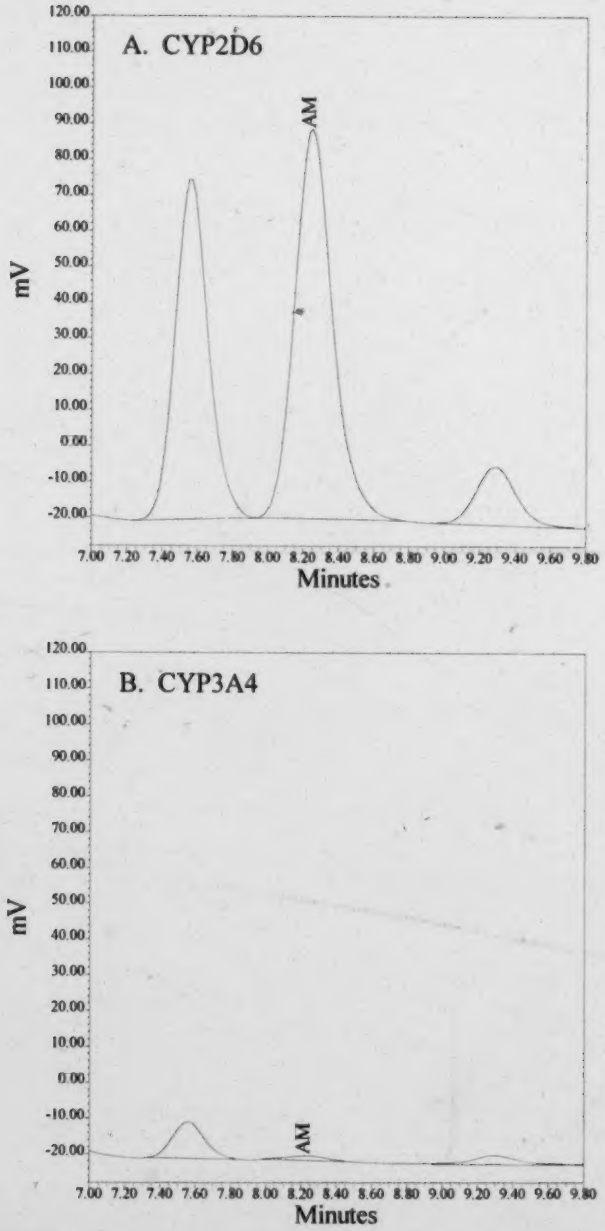

Figure 5-7: Chromatography from the incubations of ODM with microsomes expressing A) CYP2D6 or B) CYP3A4.

Enzyme Preparation	Substrate	Metabolite			
		HM	NDM	ODM	AM
Human Liver Microsomes	100 μM MET	CYP2D6	CYP2D6	CYP2D6 CYP2E1	CYP2B6
	3000 μM MET	CYP3A4 CYP2B6	CYP3A4 CYP2B6	CYP2D6 CYP2E1	CYP3A4 CYP2B6
	30 μM ODM				CYP2D6
Microsomes from cells expressing individual CYP enzymes	200 μM MET	CYP2D6 CYP3A4	CYP3A4 CYP2D6 CYP2C19	CYP2D6 CYP2E1 CYP3A4	CYP2D6 CYP3A4
	200 μM ODM				CYP2D6 CYP3A4

Table 5-1: A summary of the CYP enzymes implicated in the metabolism of MET.

As discussed in Chapter 4, AM was very susceptible to pH changes in the mobile phase. A slight change enabled the separation of AM and the interfering peak.

5.4.2 PRELIMINARY STUDIES

5.4.2.1 Time Course and Substrate Concentration Experiment

The reason for conducting the time course and substrate concentration experiment using ODM as a substrate was to determine if metabolite production was dependent on time and substrate concentration. The experiments were conducted at 30 min to keep conditions consistent with the experiments in which MET was used as the substrate.

5.4.2.2 Requirement of NADPH

The ability of ODM to be metabolized to AM in the absence of NADPH does not negate the involvement of the CYP enzymes in the metabolism of ODM. Although ODM is metabolized in the absence of NADPH, its metabolism is much greater in the presence of that cofactor. It may be possible that the microsomes have enough residual NADPH such that this oxidative reaction can occur.

5.4.3 THE METABOLISM OF METOPROLOL

The decision to conduct the correlation experiments at two different substrate concentrations was simply due to the fact that MET has a low affinity and a high affinity enzyme contributing to its metabolism. The idea was to have conditions that would select for only one of those enzymes in each experiment. Obviously, without conducting in-depth kinetic analysis of each of the livers used, the contribution of each enzyme at each substrate concentration is not known. However, an assumption was made based on the kinetic experiments conducted in Chapter 4 that at 100 μM of MET that there would be a contribution from both enzymes and that at 3000 μM the contribution would be

mainly from the low affinity enzyme. As was apparent from the data, the correlation of enzyme activities to metabolite production did differ slightly between 100 and 3000 μM of MET, supporting the involvement of different enzymes at different substrate concentrations. The major difference between the two experiments was the involvement at higher concentrations of MET, of CYP3A4 in the metabolism of MET to HM, NDM and AM. CYP2B6 was also implicated in the production of HM and NDM.

Incubating MET with the individual CYP enzymes generally supported the findings of the correlation studies. There were some discrepancies, especially with respect to the involvement of CYP2B6. Unfortunately, the involvement of CYP2B6 cannot be entirely discounted based on the results of the experiment using the individual enzymes. The fact remains that the preparation of CYP2B6 used in this study was not co-expressed with cytochrome b_5. It is possible that cytochrome b_5 is necessary for CYP2B6 activity. Regardless, the contribution of CYP2B6 is probably not a major factor in the metabolism of MET since CYP2B6 is not detectable in all human livers and if it is, the highest level present is less than 2% of total CYP (Mimura *et al.*, 1993). Another discrepancy is the involvement of CYP2D6 in the production of AM. It was assumed that AM was the immediate product of ODM. Thus, MET was first metabolized to ODM which was subsequently metabolized to AM. With this assumption, it was reasonable to conclude that the correlation experiments did not have enough power to acknowledge enzymes involved in a two step reaction. CYP2C19 was not implicated in the production of NDM in the correlation experiments. Again, the power of the correlation experiments would seem limited when more than 1 enzyme is involved in one particular metabolic route.

The demonstration of the involvement of CYP3A4 in the metabolism of MET to ODM to AM remains elusive due to the chromatography of the ODM peak when MET was the substrate and the small amount of AM produced when ODM was the substrate. In fact, approximately 10 times more AM was produced from the MET incubation than from the ODM incubation. One possible explanation is that MET is a better substrate than ODM for CYP3A4. When MET is the substrate, it is able to interact with the active site of CYP3A4, and the conversion of MET to AM takes place through a metabolite that is not released from the active site. It is this metabolite, that is neither totally ODM nor AM, that results in the peak with a retention time similar to ODM but has very poor peak shape. This would be slightly different than the situation with CYP2D6. In this case, it seems more likely that the conversion of MET to ODM to AM would take place in a more step-like fashion. One possibility is that MET is converted to ODM in the active site of CYP2D6, and ODM is released and must reorient itself again to be converted to AM. The second possibility is that conversion of MET to ODM to AM takes place without the release of ODM from the active site but any metabolite that is formed do not exist long enough to be visualized on the chromatogram.

The involvement of CYP2D6 in the metabolism of MET to ODM and HM is certainly not a novel finding. However, the elucidation of the involvement of CYP3A4, CYP2C19 and CYP2E1 provides new insights into the metabolism of MET.

5.4.4 THE METABOLISM OF O-DESMETHYLMETOPROLOL

It would seem from the studies described in this chapter that CYP2D6 is involved in the conversion of ODM to AM. Without these studies, the logical assumption would be that this reaction is due to the action of an alcohol dehydrogenase that converts the

alcohol to an aldehyde and an aldehyde dehydrogenase which would in turn convert the aldehyde to an acid. Although the involvement of the CYP enzymes in the conversion of ODM to AM is a novel idea, it is supported by documentation of other alcohols and aldehydes that undergo CYP enzyme oxidation. First, Gibson and Skett (1994), in a textbook on drug metabolism, give the conversion of ethanol to its aldehyde (ethanal = acetaldehyde) as an example of CYP-mediated oxidation. Figure 5-8 shows the proposed mechanism of such a reaction. Gram (1982) also states that the conversion of a primary alcohol to its aldehyde as a result of microsomal oxidation.

Secondly, CYP-mediated conversion of an aldehyde to its acid is demonstrated in several different studies. Kunitoh *et al.* (1997), reported the involvement of CYP2E1 in both ethanol and acetaldehyde oxidation. In mice, Watanabe *et al.* (1991) demonstrated that the conversion of an aldehyde metabolite of marijuana (11-oxo-Δ^8-tetrahydrocannabinol) to its carboxylic acid (Δ^8-tetrahydrocannabinol-11-oic acid) was catalyzed by a member of the CYP2C family. The proposed mechanism for that reaction is shown in Figure 5-9. In addition, CYP1A1 and CYP1A2 seem to be implicated to some extent in the conversion of retinal (an aldehyde) to retinoic acid (Duester, 1996). Watanabe *et al.* (1990) also demonstrated the conversion of a series of aldehydes to their corresponding acids using mice hepatic microsomes. One of the aldehydes used as a substrate in that study was 3-phenylpropionaldehyde, which has a structure similar to the proposed aldehyde intermediate in the conversion of ODM to AM (Figure 5-10).

The involvement of the CYP enzymes in the oxidation of ODM to AM does not negate the possible involvement of alcohol and aldehyde dehydrogenases. It is possible that both systems are functioning in this particular oxidation reaction. Indeed the conversion of retinal to retinoic acid seems to involve both oxidative systems (Duester,

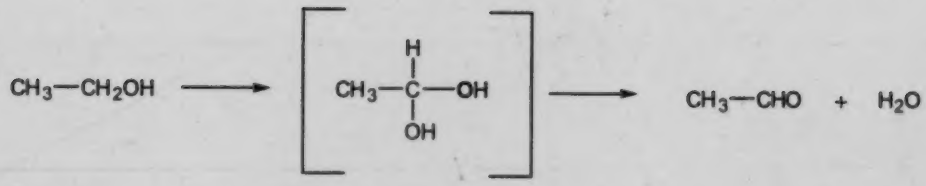

ETHANOL

PROPOSED UNSTABLE INTERMEDIATE

ETHANAL (i.e. acetaldehyde)

Figure 5-8: Proposed mechanism for the CYP-mediated oxidation of ethanol to ethanal (Gibson and Skett, 1994).

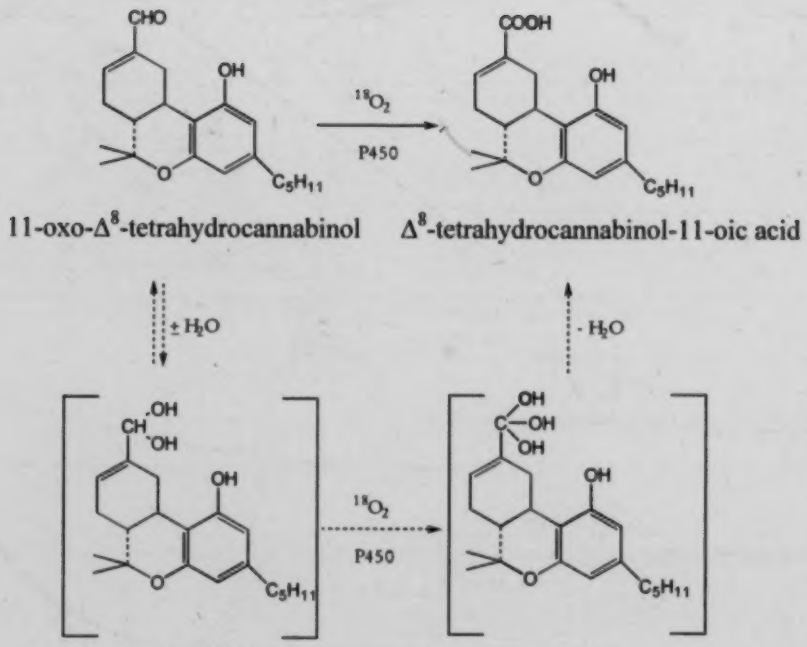

Figure 5-9: Proposed mechanism for the conversion of 11-oxo-Δ^8-tetrahydrocannabinol to Δ^8-tetrahydrocannabinol-11-oic acid (Watanabe *et al.*, 1991).

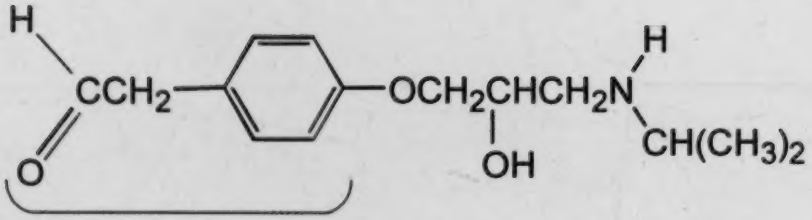

PROPOSED ALDEHYDE INTERMEDIATE

OF

O-DESMETHYLMETOPROLOL

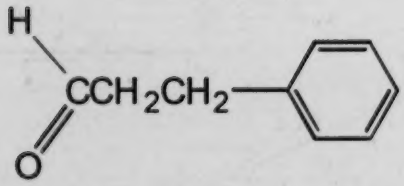

3-PHENYLPROPIONALDEHYDE

Figure 5-10: Comparison of 3-phenylpropionaldehyde (Watanabe *et al.*, 1990) with the proposed aldehyde intermediate in the conversion of ODM to AM.

1996). It is believed that the oxidation of ethanol by CYP-mediated metabolism is of minor importance and that alcohol dehydrogenase accounts for the majority of ethanol metabolism. However, in cases of ethanol induction, the CYP-mediated pathway can account for 80% of ethanol metabolism (Gibson and Skett, 1994). To date, the NAD-dependent aldehyde dehydrogenase system seems to be the principal metabolic pathway by which acetaldehyde is converted to acetate. Incubating rat liver slices with acetaldehyde has shown that there seems to be a low K_m mitochondrial aldehyde dehydrogenase and a low K_m cytosolic aldehyde dehydrogenase that are probably responsible for 60% and 20% of the metabolism of acetaldehyde respectively. The remaining 20% of the metabolism was caused by an undetermined source (Kunitoh *et al.*, 1997). It is therefore possible that ODM is oxidized by both the CYP enzymes and alcohol and aldehyde dehydrogenases. However, these latter enzymes were not studied in the current project.

5.5 REFERENCES

Belpaire FM, Winjnant P, Temmerman A, Rasmussen BB and Brøsen K (1998) The oxidative metabolism of metoprolol in human liver microsomes: inhibition by the selective serotonin reuptake inhibitors. *Eur J Clin Pharmacol* 54: 261-264.

Borg KO, Carlsson E, Hoffmann K-J, Jönsson T-E, Thorin H and Wallin B (1975) Metabolism of metoprolol-(^{3}H) in man, the dog and the rat. *Acta Pharmacol Toxicol* (suppl V): 125-135.

Duester G (1996) Involvement of alcohol dehydrogenase, short-chain dehydrogenase-reductase, aldehyde dehydrogenase and cytochrome P450 in the control of retinoid signalling by activation of retinoic acid synthesis. *Biochemistry* 35: 12221-12227.

Gyllenhaal O and Hoffmann K-J (1984) Simultaneous determination of metoprolol and metabolites in urine by capillary column gas chromatography as oxazolidineone and trimethylsilyl derivatives. *J Chromatogr* 309: 317-328.

Gibson GG and Skett P (1994) in *Introduction to Drug Metabolism, Second Edition*, Blackie Academic and Professional, Glasgow, UK.

Gram TE (1982) Metabolism of drugs. In Craig CR and Stitzel RE (Eds) Modern Pharmacology (pp37-54). Little, Brown and Company, Boston, MA.

Kim M, Shen DD, Eddy AC and Nelson WL (1993) Inhibition of the enantioselective oxidative metabolism of metoprolol by verapamil in human liver microsomes. *Drug Metab Dispos* 21: 309-317.

Kunitoh S, Imaoka S, Hiroi T, Yabusaki Y, Monna T and Funae Y (1997) Acetaldehyde as well as ethanol is metabolized by human CYP2E1. *J Pharmacol Exp Ther* 280: 527-532.

Mimura M, Baba T, Yamazaki H, Ohmori S, Inui Y, Gonzalez F, Guengerich P and Shimada T (1993) Characterization of cytochrome P450 2B6 in human liver microsomes. *Drug Met Dispos* 21: 1048-1056.

Otton SV, Crewe HK, Lennard MS, Tucker GT and Woods HF (1988) Use of quinidine to define the role of the sparteine/debrisoquine cytochrome P450 in metoprolol oxidation by human liver microsomses. *J Pharmacol Exp Ther* 247: 242-247.

Watanabe K, Narimatsu S, Yamamoto I and Yoshimura H (1991) Oxygenation mechanism in conversion of aldehyde to carboxylic acid catalyzed by a cytochrome P-450 isozyme. *J Biol Chem* 266: 2709-2711.

Watanabe K, Narimatsu S, Yamamoto I and Yoshimura H (1990) Hepatic microsomal oxygenation of aldehydes to carboxylic acids. *Biochem Biophys Res Commun* 166: 1308-1312.

Chapter 6: Conclusion

6.1 SUMMARY

The work presented in this thesis demonstrates that both the O-demethylation and α-hydroxylation reactions involved in the metabolism of MET are biphasic. Both CYP2D6 and CYP2E1 are involved in the O-demethylation of MET and CYP2D6 and CYP3A4 are involved in the α-hydroxylation reaction. CYP2D6, CYP2C19 and CYP3A4 catalyzed the N-dealkylation reaction. CYP2D6 and CYP3A4 play a role in the formation of AM. The formation of the acid metabolite of NDM was not studied in the work described herein due to inability to obtain an authentic standard of this metabolite. Whether the majority of this acid metabolite comes directly from MET or comes from the N-dealkylated metabolite was thus not ascertained.

The inhibitory potentials of PAR, FLU and FVX were consistent with other studies which looked at their abilities to inhibit CYP2D6-mediated reactions in that the rank order of potency was PAR and FLU>FVX (Crewe *et al.*, 1992; Belpaire *et al.*, 1998). Based on inhibition of sparteine metabolism (Crewe *et al.*, 1992), the one deviation from the pattern was that of DMI which would have been expected to have an inhibitory potential greater than that of FVX. The results may in fact reflect a true lack of inhibition of MET metabolism. However, as discussed in Chapter 1, there are a number of factors absent in *in vitro* experiments that may be present *in vivo*. The absence of these factors may indeed result in an underestimation of the inhibitory strength of DMI using the present procedures.

With respect to the inhibition of the metabolism of MET by the different antidepressants, the studies in the rat did not mimic the inhibition observed in the studies on human liver microsomes. This work emphasizes the importance of comparing animal

and human systems before using the animal model to study drug metabolism and drug-drug interactions. There are several possible explanations for the discrepancy between the experiments using human liver microsomes and the rat. In addition to possible differences in the enzyme's active site, species differences in the effects of inhibitors may be due to the fact that the activity is catalyzed by different enzymes between species. Species differences in the pharmacokinetics of the inhibitor may also be a contributing factor (Boobis *et al.*, 1990).

In the event that hypertensive individuals need to be prescribed an antidepressant, caution must be exercised to prevent drug-drug interactions from occurring. In the present study it would seem that both FLU and PAR have the potential to inhibit the metabolism of MET and should be avoided.

6.2 LIMITATIONS AND POSSIBLE FUTURE EXPERIMENTS

The rat studies as described in Chapters 2 and 3 used only male rats. Hormonal fluctuations which may affect drug metabolism and thus drug-drug interactions were not taken into account in the present studies. The decision to use only male rats was made in an attempt to obtain a clear picture of possible drug-drug interactions between MET and DMI, FVX or FLU. The inclusion of an extra variable, such as hormonal fluctuations, may have obscured that effect due to increased variance in the sample population since the rapid estrous cycling of female rats (Barker Jørgensen, 1977) would make it difficult to obtain a sample population that would be homogenous with respect to hormone levels. However, it is important to conduct future studies comparing such interactions in male and female rats.

As discussed previously, there are several limitations to conducting *in vitro* experiments and trying to relate them to *in vivo* events. However, these experiments can provide a method by which potentially harmful drug-drug interactions can be identified. Because MET is administered as a racemate, the studies reported in this thesis were conducted using the racemic compound. The effects on the individual enantiomers was not ascertained, although this would be of interest in future studies. However, some of the metabolites retain a chiral centre, and the individual enantiomers of those metabolites are not currently available. In poor metabolizers, it has been shown that the clearance of R-MET was equal to or less than that for S-MET and any differences seen were not as marked as those in extensive metabolizers, in which R-MET was preferentially eliminated (Lennard *et al.*, 1983). Thus, in the event that an extensive metabolizer is phenotypically converted to a poor metabolizer due to the presence of an inhibitor, it is reasonable to assume that stereoselective metabolism becomes less of an issue.

The identity of the low affinity enzyme which contributes to the formation of ODM is thought to be CYP2E1 based on the studies using individually expressed CYP enzymes. Ideally, the inhibition experiments should be repeated using a specific inhibitor of CYP2E1 but currently used inhibitors of CYP2E1 are relatively nonspecific. For example, diethyldithiocarbamate was found to inhibit metabolism mediated by CYP2E1, CYP3A4, CYP1A1, CYP1A2, CYP2A6, CYP2B6, or CYP2C8 (Eagling *et al.*, 1998; Bourrié *et al.*, 1996) and diallyldisulfide inhibited not only CYP2E1 but also CYP2A6, CYP1A2, CYP1A1, CYP2D6 and CYP3A4 (Bourrié *et al.*, 1996). Another possible method involves the use of specific inhibitory antibodies (Bourrié *et al.*, 1996), but this approach is costly.

Also, the inhibition studies described in this thesis assumes competitive inhibition of both the high and low affinity enzymes by FLU, FVX, PAR and DMI. Although, this concept was not proven, previous studies by Crewe *et al.* (1994) has stated that the inhibition of the metabolism of sparteine (a CYP2D6 substrate) by FLU, FVX, PAR and DMI was competitive. Thus, the competitiveness of inhibition of the high affinity enzyme is not in question. However, the nature of the inhibition of these antidepressants on CYP2E1 has not been ascertained. Intuitively, it would seem unlikely that these antidepressants, which are substrates for various other CYP enzymes, would interact with CYP2E1 at a site other than its active site. However, further studies are needed to ascertain the true nature of the inhibition.

6.3 REFERENCES

Belpaire FM, Winjnant P, Temmerman A, Rasmussen BB and Brøsen K (1998) The oxidative metabolism of metoprolol in human liver microsomes: inhibition by the selective serotonin reuptake inhibitors. *Eur J Clin Pharmacol* 54: 261-264.

Boobis AR, Sesardic D, Murray BP, Edwards RJ, Singleton AM, Rich KJ, Murray S, De La Torres R, Segura, Pelkonen O, Pasanen M, Kobayashi S, Zhi-Guang T and Davies DS (1990) Species variation in the response of the cytochrome P-450-dependent monooxygenase system to inducers and inhibitors. *Xenobiotica* 20: 1139-1161.

Bourrié M, Meunier V, Berger Y and Fabre G (1996) Cytochrome P450 isoform inhibitors as a tool for the investigation of metabolic reactions catalyzed by human liver microsomes. *J Pharmacol Exp Ther* 227: 321-332.

Crewe HK, Lennard MS, Tucker GT, Woods FR and Haddock RE (1992) The effect of selective serotonin re-uptake inhibitors on cytochrome P4502D6 (CYP2D6) activity in human liver microsomes. *Br J Clin Pharmac* 34: 262-265.

Eagling VA, Tjia JF and Back DJ (1998) Differential selectivity of cytochrome P450 inhibitors against probe substrates in human and rat liver microsomes. *Br J Pharmacol* 45: 107-114.

Barker Jørgensen C (1977) Reproduction. In Gordon MS (Ed) *Animal Physiology: Principles and Adaptations, Third Edition,* (pp. 636-678) New York, New York, MacMillan Publishing Company, Inc.

Lennard MS, Ticker GT, Silas JH, Freestone S, Ramsay LE and Woods HF (1983) Differential stereoselective metabolism of metoprolol in extensive and poor debrisoquin metabolizers. *Clin Pharmacol Ther* 34: 732-737.